Regulating the Gut Microbiota by Intrinsic and Extrinsic Metabolites

by
Salam M. Habib

School of Human Nutrition, Mcgill University, Montreal
January 2021

A thesis submitted to McGill University
in partial fulfillment of the requirements of the degree
Doctor of Philosophy in Human Nutrition

Table of contents

List of figures

List of tables

Abbreviations

ANOVA	Analysis of variance
Asbt	Apical sodium bile acid transporter
Atf4/6	Activating transcription factor 4/6
AUC	Area under curve
BAM	Bile acid malabsorption
CAR	Constitutive androstane receptor
CD14	Cluster of differentiation 14
CDCA	Chenodeoxycholic acid
DNA	Deoxyribonucleic acid
DKO	Deficient in both Fabp2 and Fabp6
EE	Energy expenditure
ER	Endoplasmic reticulum
Fabps	Fatty acid binding proteins
FXR	Farnesoid X receptor
Gapdh	Glyceraldehyde 3-phosphate dehydrogenase
GC-MS	Gas chromatography mass spectrometry
GIT	Gastrointestinal tract
GLP-1	Glucagon-like peptide-1
GPR41	G-protein coupled receptors
Grp78	Glucose-regulated protein 78kDa
Grp94	Glucose-regulated protein 94kDa
HDHA	7-alpha-hydroxysteroid dehydrogenase
Hprt	Hypoxanthine phosphoribosyl transferase
IgA	Immunoglobulin A
IFNγ	Interferon Gamma
IRE1α	Inositol-requiring enzyme 1 alpha
LFD	Low fat diet
LPS	Lipopolysaccharide
LSD	Least significant difference
LXRα	liver X receptor α
mRNA	Messenger ribonucleic acid
NGS	Next-generation sequencing
NOD	Nucleotide-binding oligomerization domain
OD	Optical density
OGTT	Oral glucose tolerance test
Ostα	Organic solute transporter alpha
PCoA	Principal coordinates analysis
PCR	Polymerase chain reaction
PERK	Protein kinase R-like endoplasmic reticulum kinase
PPP	Purified polyphenolic-rich potato extract

PRPE	Polyphenolic-rich potato extract
PXR	Pregnane X receptor
PYY	Peptide YY
qPCR	Quantitative polymerase chain reaction
ROS	Reactive oxygen species
RQ	Respiratory quotient
rRNA	Ribosomal ribonucleic acid
S1PR2	Sphingosine1-phosphate receptor
SCFAs	Short-chain fatty acids
SGLT-1	Sodium-glucose co-transporter 1
SHIME	Simulator of the Human Intestinal Microbial Ecosystem
sXpb1	Spliced X-box binding protein 1
TCA	Taurocholic acid
TDCA	Taurodeoxycholic acid
TGR5	Takeda G-protein coupled receptor 5
TLRs	Toll-like receptors
TMCA	tauromuricholic acid
TNFα	Tumor necrosis factor alpha
TUDCA	Tauroursodeoxycholic acid
UDCA	Ursodeoxycholic acid
UPR	Unfolded protein response
v/v	Volume by volume
w/v	Weight by volume
VDR	Vitamin D receptor
WSD	Western-style diet
WSD+PPP	Western-style diet with purified polyphenolic-rich potato extract
WSD+PRPE	Western-style diet with polyphenolic-rich potato extract
WT	Wild-type
ZIG	Zero inflated gaussian mixture model
ZILN	Zero inflated log normal mixture model

Abstract

Factors from inside the host (intrinsic factors) or outside the host (extrinsic factors) interact with the gut microbiota and alter the microbiome. Studying these factors provides knowledge on strategies of controlling gut microbiota to improve host health status or prevent disease. In this thesis, the hypothesis that intrinsic metabolites (such as bile acids) and extrinsic metabolites (such as polyphenolic-rich potato extract, PRPE) individually and cooperatively modify gut microbial diversity and composition, and impact the host metabolic status in distinct ways, was tested. Males and females of three mouse genotypes were used in studies: wild-type, *Fabp6*$^{-/-}$ (model of bile acid malabsorption), and *Fabp6*$^{-/-}$;*Fabp2*$^{-/-}$ (model of bile acid and fat malabsorption). In addition, a new *in vitro* gut model was developed to facilitate the study of the gut microbiota in the absence of the host-inherent variables. The elevated concentrations of bile acids in the intestinal lumen of *Fabp6*$^{-/-}$ mice reduced the gut microbial diversity and enriched bile acid tolerant bacteria. On the Western-style diet (WSD; high in saturated fats and refined sugars), *Fabp6*$^{-/-}$ mice displayed sex dimorphic gut microbial dysbiosis, which was associated with a differential predicted enrichment of gut microbial saccharolysis pathways by the two sexes. PRPE supplementation of WSD prevented adiposity, dysbiosis of gut microbiota, and colonocyte endoplasmic reticulum stress that were induced by WSD in wild-type mice. Similarly, feeding PRPE-supplemented WSD to *Fabp6*$^{-/-}$ mice mitigated features of WSD-induced gut microbial dysbiosis, but resulted in greater similarity in the phylum composition of the gut microbiota between male female mice. The combined loss of both Fabp2 and Fabp6 on WSD reduced body weight gain in mice and resulted in a sex dimorphic gut microbial response, enhanced glucose tolerance, and attenuated colonocyte endoplasmic reticulum stress. Together, these results demonstrate the ability of intrinsic and extrinsic metabolites to modify the composition of gut microbiota and alter the metabolic status of the host. In addition, intestinal fatty acid binding proteins appear to be indirectly involved in mediating the sex dimorphic response of the gut microbiota to WSD. This work provides new clues on the importance of gut microbial regulation and emphasizes the need for sex-specific nutritional approaches and guidelines. The knowledge generated by this work will

facilitate strategies for controlling the gut microbial composition for effective control of health and disease.

Résumé

Des facteurs internes à l'hôte (facteurs intrinsèques) ou extérieurs à l'hôte (facteurs extrinsèques) interagissent avec le microbiote intestinal et modifient le microbiome. L'étude de ces facteurs fournit des connaissances sur des stratégies de contrôle du microbiote intestinal afin d'améliorer l'état de santé de l'hôte ou de prévenir la maladie. Cette thèse émet l'hypothèse que les métabolites intrinsèques tels que les acides biliaires et les métabolites extrinsèques tels qu'un extrait de pomme de terre riche en composés polyphénoliques (PRPE) modifient individuellement et en coopération la diversité et la composition microbiennes de l'intestin et ont un impact distinct sur le statut métabolique de l'hôte. Des mâles et des femelles de trois génotypes de souris ont été utilisés dans les études : type sauvage, *Fabp6*$^{-/-}$ (modèle de malabsorption des acides biliaires) et *Fabp6*$^{-/-}$;*Fabp2*$^{-/-}$ (modèle de malabsorption des acides biliaires et des graisses). En outre, un nouveau modèle *in vitro* de l'intestin a été développé pour faciliter l'étude du microbiote intestinal en l'absence de variables inhérentes à l'hôte. Les concentrations élevées d'acides biliaires dans la lumière intestinale des souris *Fabp6*$^{-/-}$ ont réduit la diversité microbienne intestinale et enrichi le milieu en bactéries tolérantes aux acides biliaires. Les souris *Fabp6*$^{-/-}$ nourries au régime alimentaire de type occidental (WSD; riche en graisses saturées et en sucres raffinés) ont présenté une dysbiose microbienne intestinale sexuellement dimorphique, qui peut être associée à un enrichissement différentiel prédite des voies de la saccharolyse microbienne intestinale par les deux sexes. La supplémentation en PRPE du WSD a empêché l'adiposité, la dysbiose du microbiote intestinal et le stress du réticulum endoplasmique des colonocytes induits par le WSD dans les souris de type sauvage. De même, l'alimentation du WSD supplémenté en PRPE aux souris *Fabp6*$^{-/-}$ a atténué les caractéristiques de la dysbiose intestinale induite par le WSD, mais a entraîné une plus grande similitude dans la composition au niveau des embranchements du microbiote intestinal entre les souris mâles et femelles. La perte combinée de Fabp2 et de Fabp6, dans le contexte du WSD, a réduit le gain de poids corporel chez les souris et a entraîné une réponse sexuellement dimorphique du microbiote intestinal, une tolérance accrue au glucose et une atténuation du stress du

réticulum endoplasmique des colonocytes. Ensemble, ces résultats démontrent la capacité des métabolites intrinsèques et extrinsèques d'altérer la composition du microbiote intestinal et de modifier le statut métabolique de l'hôte. De plus, les protéines de liaison aux acides gras intestinales semblent être indirectement impliquées dans la médiation de la réponse sexuellement dimorphique du microbiote intestinal au WSD. Cette thèse fournit de nouveaux indices sur l'importance de la régulation microbienne intestinale et souligne la nécessité d'approches et de directives nutritionnelles spécifiques au sexe. Les connaissances générées par cette thèse faciliteront les stratégies de contrôle de la composition microbienne intestinale pour un contrôle efficace de la santé et des maladies.

Acknowledgments

Firstly, I would like to express my sincere gratitude to my advisor Dr. Luis Agellon for continuous support, patience, and advice. Besides my advisor, I would like to thank the rest of my supervisory committee: Dr. Stan Kubow and Dr. Jeff Xia, for their insightful comments, encouragement, support and thesis review. Similarly, many thanks for my thesis examining committee: Dr. Ben Willing, Dr. Jennifer Ronholm, Dr. Stephanie Chevalier, Dr. Xin Zhao, Dr. Ryan Mailloux and Dr. Ian Strachan for their constructive comments and feedback. Many thanks go to Dr. Linda Wykes, Dr. Raj Duggavathi, and Dr. Vilceu Bordignon who provided me access to their research facilities.

Thanks to my previous and current lab members Dana, Dukgyu, Sherry, Eli, Zeina, Jana, Khadija, Simin, Zhang, Yiheng, and Anikka for sharing all the joy and tough moments during my study. Special thanks to Michele, Kebba, and Baasir from Dr. Kubow's lab for motivating and supporting me all the time. I am grateful for the angels on earth, my dear friends Doaa Taqi and Karina Gutierrez for being there for me.

My profound gratitude goes to my parents for their continuous encouragement, inspiration, and patience. Many thanks to my dear sisters, brothers and extended family for their support. All thanks to my soulmate Saleem and my big girl Lina, this study was not possible without you.

All praise be to you Lord, an abundant beautiful blessed praise, the heavens, and the earth, and all between them be abound with Your praises.

Contribution to original knowledge

- *The characterization of gut microbiota in a model of genetically induced malfunction of intestinal bile acid reclamation system (Fabp6 deficiency).* Bile acid malabsorption in this mouse model caused reduced gut microbial diversity and altered gut microbial composition. Bile acid malabsorption is prevalent in humans; it may be related to ileal resection, Crohn's disease, cystic fibrosis, irritable bowel syndrome and metformin treatment (Hofmann, 1972; O'Brien et al., 1993; Nyhlin et al., 1994; Scarpello et al., 1998; Watson et al., 2015). Since gut microbial metabolism influence host metabolism and, consequently, its health and disease status, the knowledge generated from studying the gut microbiota in this mouse model implies the increased vulnerability of humans with these conditions to environmental perturbations such as imbalanced dietary profiles and uncontrolled exposure to xenobiotics (Chapter 2).

- *The influence of Western-style dietary intervention on the gut microbiota in models of (i) Fabp6 deficiency, and (ii) the genetically induced malfunction of both fat assimilation system and intestinal bile acid reclamation system (combined deficiency of Fabp6 and Fabp2).* This thesis showed distinct gut microbial responses to WSD in these two mouse models and they were associated with enhanced adiposity and improved glucose control in male mice. The fact of the continuous increase in the adoption of WSD worldwide underscores the importance of targeted nutritional intervention and awareness plans in individuals with similar conditions. Documented genetic variations in *FABP6* gene such as T79M mutation, or in *FABP2* gene such as A54T mutation were associated with adiposity and type 2 diabetes (Baier et al., 1995; Kunsan et al., 1999; Fisher et al., 2009). One implication for affected individuals include body weight control, which might not be represented by the conventional energy balance equation, and a modified gut microbial community may underlie resistance to body weight loss or increased risk to diabetes (Chapters 2 and 4).

- *Sex dimorphism in the response of gut microbiota to intrinsic and extrinsic factors.* This thesis has identified several sex dimorphic metabolic phenotypes that were associated with distinct gut microbial communities in male and female mice in response to intrinsic and extrinsic metabolites. The sex dimorphism to metabolic disease risk is evident in human conditions, such as the higher risk of cardiovascular diseases in men than premenopausal women (Nedungadi and Clegg, 2009). Although the sex dimorphism in such conditions is usually attributed to hormonal, genetics and epigenetic factors (Sugiyama and Agellon, 2012), the contribution of gut microbiota to this response is expected and warrants further investigation. In the meantime, it is a necessity to consider biological sex in research and to target both sexes with relevant health and nutritional recommendations (Chapters 2-4).

- *The influence of polyphenolic-rich potato extract (PRPE) supplementation of WSD on gut microbiota.* The thesis has identified the ability of PRPE to prevent gut microbial diversity loss induced by WSD feeding in both wild-type and Fabp6-deficient mice (Chapter 3).

- *The development of a simple, scalable, modular, and feasible in vitro gut model*. The development of this gut model advances gut microbial research by providing a modular system that can be easily adapted and integrated into the study designs to answer questions related to gut microbial responses in the absence of host immune surveillance and under controlled availability of metabolites. It is worthy of mentioning that this model represents one of its kind in North America (Chapter 5).

Contribution of authors

Chapter 1: SMH conceptualized, wrote, and edited the manuscript. LBA was involved in the conception and editing the manuscript.

Chapter 2: SMH designed and conducted the experiments, analyzed the data, and wrote the manuscript. SK provided access to the gas chromatography and edited the manuscript. JX supervised data analysis and edited the manuscript. LBA was involved in the conception of the experimental design and editing the manuscript.

Chapter 3: SMH designed and conducted the experiments, analyzed the data, and wrote the manuscript. SK provided access to the gas chromatography and edited the manuscript. LBA was involved in the conception of the experimental design.

Chapter 4: SMH designed and conducted the experiments, analyzed the data, and wrote the manuscript. LBA was involved in the conception of the experimental design.

Chapter 5: SMH built the model, designed, and conducted evaluation experiments, analyzed the data, and wrote the manuscript. AMS, added the time server, conducted the functionality experiment, helped in evaluation experiments, helped in writing, and editing the manuscript. SK and LBA were involved in the conception, experimental design, interpretation of results and editing of the manuscript.

Chapter 1

Introduction and literature review: The relationship between gut microbial composition and the nutritional status of the host

1.1. Gut microbiota: Background

Microbiota is the assemblage of microorganisms present in a defined environment, whereas microbiome refers to both microorganisms and their genomes (Marchesi and Ravel, 2015). The term was lately coined by Joshua Lederberg (Lederberg and McCray, 2001); however, microorganisms, such as bacteria, have existed billions of years before humans (Brocks et al., 1999). The discovery of bacteria began with the invention of the microscope by Leeuwenhoek in the 1680s (Nagpal et al., 2014), which led to refuting the miasma theory. The proof of the germ theory of disease in1850-80s was provided by Pasteur and Koch (Koch, 1890), who were the first to develop techniques for bacterial culturing. Until recently, advancements regarding knowledge of microbiota was limited to the ability to culture or describe microbiota biochemically. When the Sanger technique of sequencing nucleic acids became available in the 1970s, this allowed the opportunity for discovery of unculturable microbes. Next-generation sequencing (NGS) techniques were developed in 1996 (Mardis, 2008), which enabled researchers to generate massive amounts of data on the phylogeny of microbes and their functional capacities that have revolutionized the related research fields.

The microbiota of the gastrointestinal tracts has attracted extensive research attention, especially, since it comprises more cells than number of cells in a host (Sender et al., 2016). In humans, there are almost 2000 different species of gut bacteria, with 100 times more genes than the human genes (Almeida et al., 2019). In fact, gut microbiota encompasses microorganisms that represent all domains of life, including Archaea, Fungi, Virusobiota, and, the most studied domain, Bacteria. The

dominant bacterial phyla that make up the gut microbial community of humans include: Firmicutes, Bacteroidetes, Actinobacteria, and the minor phyla include: Proteobacteria and Verrucomicrobia (Fig. 1-1) (Human Microbiome Project, 2012; Rosenbaum et al., 2015; Almeida et al., 2019).

Species belonging to the same phylum may vary widely in their genes, and such variations can lead to differing impacts upon host health. To illustrate, *Lactobacillus rhamnosus* belong to the phylum Firmicutes which also comprises “foe” species such as *Clostridium difficile*. *C. difficile* displays aggressive pathogenic behaviors and was responsible for 30,000 deaths in the United States in 2012 (Lessa et al., 2015). The “friendly” probiotic *L. rhamnosus* displays a protective role and shows the ability to attenuate intestinal injury in a colorectal cancer model (Chang et al., 2018).

The complex interaction between host metabolism and gut microbial metabolism is emerging as a mediator of health and disease. Lederberg and McCray (2001) suggested that the integration between metabolic processes and pathways of both the host and its gut microbiota results in a more efficient "co-metabolism", that facilitates the adaptation and evolution. For instance, the gut microbiota helps in facilitating the digestion of macronutrients and generation of energy, enhancing the bioavailability of mineral ions by degrading chelating agents, and producing vitamins and short-chain fatty acids (SCFAs) such as acetate, propionate, and butyrate (Fig. 1-1) (Haros et al., 2009; Bik et al., 2018). From a structural point of view, gut microbiota facilitates the development and maturation of the host immune function by regulating the epithelial barrier proliferation and modulating immune responses such as immunoglobulin A (IgA) and cytokine secretions (Maslowski and Mackay, 2011). In addition, gut microbiota enhances the intestinal capillary density and promotes the development of the vascular network (Hashimoto et al., 1998).

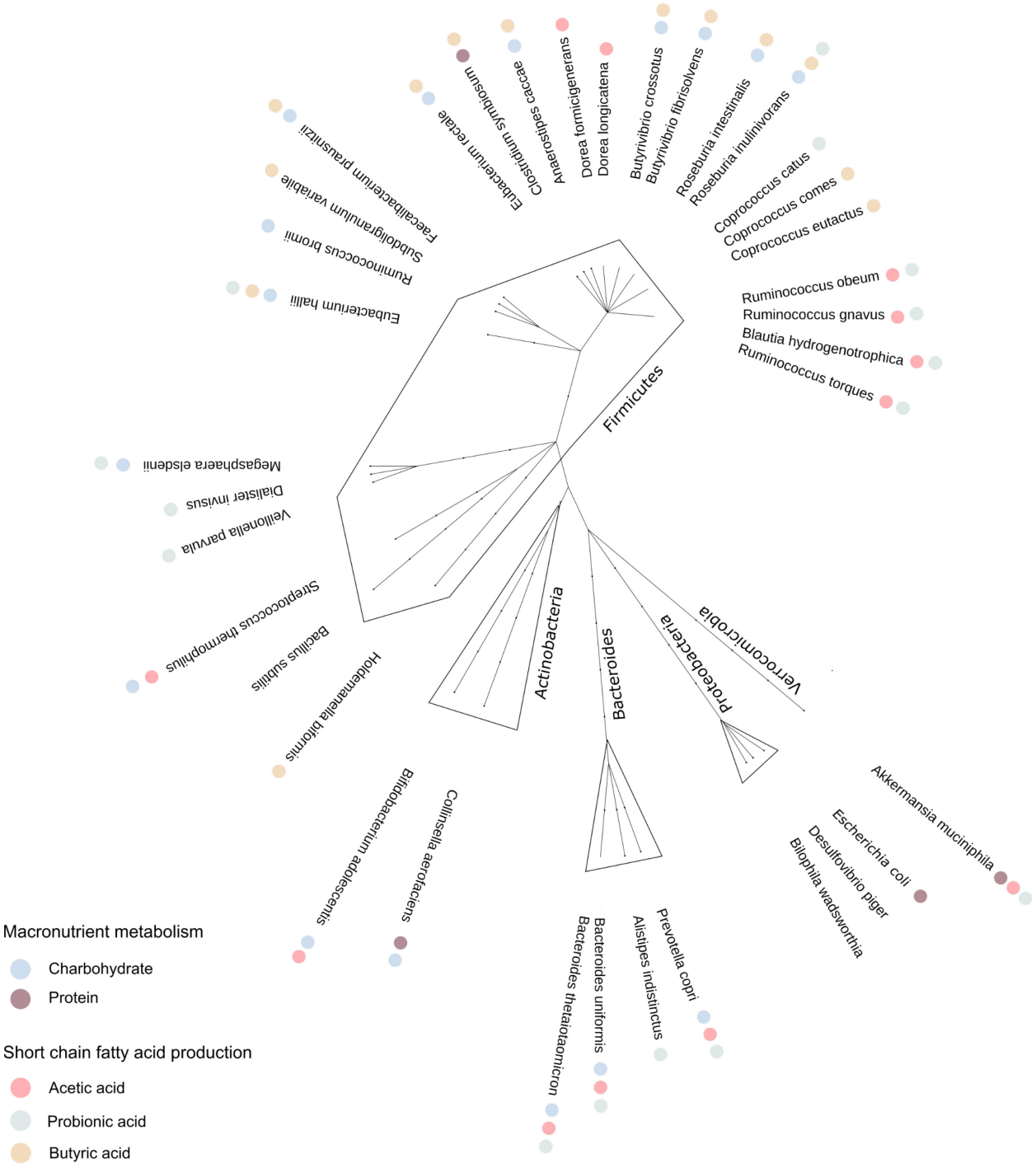

Figure 1-1. Main phyla of the human gut microbiome with selected species of known functions. The tree was generated by PhyloT and visualized by iTOl webtools. Data was curated by Bik et al. 2018.

Since birth, the gut of a newborn is inoculated by the mother's vaginal, skin, and milk microbiota. Thereafter, several factors may alter the gut microbial composition until it reaches a mature stage by adulthood (Arrieta et al., 2014). Dramatic changes in the gut microbial composition and structure, however, may lead to loss of beneficial organisms, overgrowth of harmful organisms, or loss of microbial diversity (DeGruttola et al., 2016). Such changes represent an imbalance in the microbial community and are referred to as dysbiosis. Dysbiosis has been implicated in the pathogenesis of several diseases, including inflammatory bowel diseases, type 1 and 2 diabetes mellitus, cardiovascular diseases, and obesity (Musso et al., 2010; Scaldaferri et al., 2013; Koeth et al., 2013).

1.2. Relationship of gut microbial dysbiosis and obesity

Lean and obese subjects harbor distinct gut microbiota (Maruvada et al., 2017). In comparing the gut microbial composition of obese and lean humans, clinical studies reported differences between obese and lean individuals, with a level of variability. For example, some studies reported a decrease in the gut microbial diversity or an increase in the Firmicutes:Bacteroidetes ratio in obese individuals (Kasai et al., 2015), but other studies reported no difference (Finucane et al., 2014) or even opposite findings (Haro et al., 2016). This variation is likely due to the enormous interpersonal differences in human gut microbial composition, which rendered these studies inadequately powered, or it may be attributed to insufficient consideration of critical clinical characteristics of the subjects (Maruvada et al., 2017). Well-designed animal model studies provide superior control over the above variables. Dysbiosis of obesity in mice is more consistently reported as a decrease in the total gut microbial diversity, increase in Firmicutes, and decrease in Bacteroidetes (Ley et al., 2005; Fleissner et al., 2010; Parks et al., 2013; He et al., 2018), and the same pattern is also evident in non-human primates (Nagpal et al., 2018).

In fact, the use of gnotobiotic animals (germ-free, germ-free inoculated with specific bacterial strains, or germ-free inoculated with human microbiota) is critical to establish a causal relationship between gut microbial dysbiosis and obesity. For

example, fecal transplants from obese mice donor to lean germ-free mice resulted in replication of the obese phenotype by the latter, whereby the gut microbiota was necessary to gain weight on the high fat diet (Turnbaugh et al., 2006). Ridaura et al. (2013) showed that germ-free mice with fecal transplants from twins discordant for obesity reproduced the obesity or leanness phenotype of the corresponding donor. Moreover, co-housing of germ-free mice with obese or lean conventional mice harboring gut microbiota led to a replication of the phenotypes of the cage mates by the germ-free mice (Ridaura et al., 2013). Thus, a specific gut microbial composition is critical to the induction and development of obesity, and the precise characterization of such microbial composition is necessary.

Several mechanisms have been proposed to explain the relationship between gut microbial dysbiosis and obesity. In that regard, there are three major mechanistic categories: (i) energy metabolism; (ii) immune system function; and (iii) altered food intake. Gut microbiota of obese subjects has been suggested to enhance the energy extraction efficiency by facilitating macronutrient degradation such as carbohydrates. Consequently, lower fecal energy content, higher concentrations of cecal SCFAs have been noted in obese compared to lean subjects (Hooper et al., 2001; Turnbaugh et al., 2006). SCFAs can directly serve as an energy substrate, or indirectly by signaling energy metabolism. For example, butyrate is used as a primary energy source of colonocytes (Donohoe et al., 2011), while acetate and propionate induce lipogenesis and gluconeogenesis in the liver (den Besten et al., 2013). In addition, SCFAs can bind specific G-protein coupled receptors (GPR41 and GPR43) in the colon to induce the secretion of gut hormones, such as glucagon-like peptide-1 (GLP-1) and peptide YY (PYY), which stimulate insulin secretion and slow gut motility, respectively (Tolhurst et al., 2012; Psichas et al., 2014).

The gut microbial composition may also determine the efficiency of energy assimilation and storage. For example, when gut microbiota from mice housed at cold temperatures was transplanted into germ-free mice, their energy uptake was induced by increasing intestinal surface area and suppressing enterocyte apoptosis as compared to gut microbiota taken from mice housed at room temperature (Chevalier et

al., 2015). Moreover, enhanced energy storage was noticed in germ-free mice that received fecal gut microbial transplants from free-ranging brown bears during their hibernation in the winter versus summer (Sommer et al., 2016). Similarly, during cold temperatures, voles engaged in huddling (a social behavior of crowding together) exhibited lower resting metabolic rates, less nonshivering thermogenesis, and distinct gut microbial composition compared to separated voles (Zhang et al., 2018). In this experiment, huddling behavior might have promoted gut microbial exchange and energy conservation. Altogether, these examples imply an essential role of the gut microbiota in modulating the host energy metabolism by enhancing the efficiency of energy extraction, assimilation, and storage. However, the identification of triggers that leads to modify the ability of the gut microbiota to metabolize energy is essential and warrants further investigation.

Gut microbiota is also suggested to trigger obesity by altering the immune system function. The gut mucosa encompasses a significant and sophisticated part of the immune system (Tokuhara et al., 2019). It allows for discrimination of commensal from pathogenic microbiota by pattern recognition receptors such as toll-like receptors (TLRs) and nucleotide-binding oligomerization domain (NOD) proteins (O'Hara and Shanahan, 2006). The outer membrane structure of Gram-negative bacteria comprises lipopolysaccharide (LPS), an endotoxin that can cross the gut barrier into the circulatory system and cause endotoxemia (Musso et al., 2010). Endotoxemia provokes the activation and secretion of proinflammatory cytokines mediated by binding of LPS to the TLR4/ (cluster of differentiation 14) CD14 complex, which accordingly affects insulin action. For example, CD14 mutant mice are hypersensitive to insulin, which indicates that CD14 could be a modulator of insulin sensitivity and weight gain (Cani et al., 2007).

On the other hand, Gram negative *Akkermensia muciniphila* is associated with an improved metabolic profile (Plovier et al., 2017). Obesity and type 2 diabetes are associated with a low abundance of *A. muciniphila,* and its administration to mice on a high fat diet reversed endotoxemia and adiposity (Plovier et al., 2017). In contrast to most anti-commensal immune responses that involve the production of IgA antibodies independently of T cells, *A. muciniphila* was shown to induce T cell associated antigen-

specific IgG1 antibodies (Ansaldo et al., 2019). These examples demonstrate the ability of specific gut microbial community members to trigger immune responses that stimulate the development of obesity. Therefore, the identification of biomarker gut microbial species associated with obesity would provide an advantage over gross indicators, such as the ratio of Firmicutes:Bacteroidetes, in defining the mechanistic clues between gut microbial dysbiosis and obesity.

Regulation of the food intake is another mechanism by which gut microbiota can mediate the development of obesity. Microbial metabolites such as SCFAs and neurotransmitters play an essential role in shaping the gut-brain axis (Orellana et al., 2019). As mentioned earlier, SCFAs induce the secretion of GLP-1 and PYY hormones from the intestinal L cells, which selectively express GPR41 and GPR43 receptors. GLP-1 and PYY, can, in turn, bind specific receptors on the arcuate nucleus within the hypothalamus to modify feeding behaviors and food intake (Perry and Wang, 2012). Gut microbiota can also directly produce neurotransmitters or modulate the ability of the host to produce them (Strandwitz, 2018). For instance, most of the serotonin in the body is produced in the gut, and germ-free rodents show significantly lowered serotonin plasma concentrations which were inversely associated with their higher food intake (Wostmann et al., 1983; Lam et al., 2010; Yano et al., 2015). Moreover, the changes in taste, food preferences, and food reward following weight loss surgeries were associated with altered dopamine signaling in the brain and a modified gut microbial composition (Orellana et al., 2019). Taken together, these mechanisms strongly suggest that gut microbiota is involved in regulating the body weight of the host by altering energy homeostasis, immune function, and food intake. Yet, in order to identify how this happens, applying an integrated research approach is necessary to characterize the gut microbiota and to identify the regulated pathways under a properly controlled environment.

1.3. Modulators of the gut microbiota

The question of what constitutes the state of healthy gut microbial composition, i.e., eubiosis, remains unanswered because of the complex interaction between the

host and the environmental factors in driving the gut microbial composition toward eubiosis or dysbiosis (Fig. 1-2). Enormous number of factors may contribute to modifying and remodeling the gut microbiota, however these factors can be divided into two main categories: (a) intrinsic factors, which refer to the host inner natural or constitutional variables; and (b) extrinsic factors, which refer to the outer environmental and ecological variables that originate from outside the host (Table 1-1). The host immune system is amongst the main intrinsic factors that results in the gut microbial selection (Lievin-Le Moal and Servin, 2006; Ley et al., 2006). For example, the two cytokines TNFα and IFNγ were found to highly correlate with gut microbiota compared with other investigated host genetic and environmental factors (Schirmer et al., 2016). Mucus and antimicrobial enzymes such as lysozyme are produced by specialized cells of the intestinal epithelium, such as Goblet and Paneth cells; these peptides can alter the gut microbial composition by inhibiting pathogenic and enriching commensal microbiota (Lievin-Le Moal and Servin, 2006). Furthermore, immune components of mother's milk, such as IgA, allow the maintenance of non-invasive bacteria and promote commensalism in neonates. IgA is also involved in the control of pathobiont and pathogenic microbes by coating their antigens and promoting their excretion (Tsuruta et al., 2009; Belkaid and Hand, 2014). This is particularly significant in the first few months of life, when the ability to produce secretory IgA in the intestine is limited (Palmeira and Carneiro-Sampaio, 2016). Thus, the dynamic homeostasis between host immunity and gut microbiota represent a crucial inherent feature of organisms.

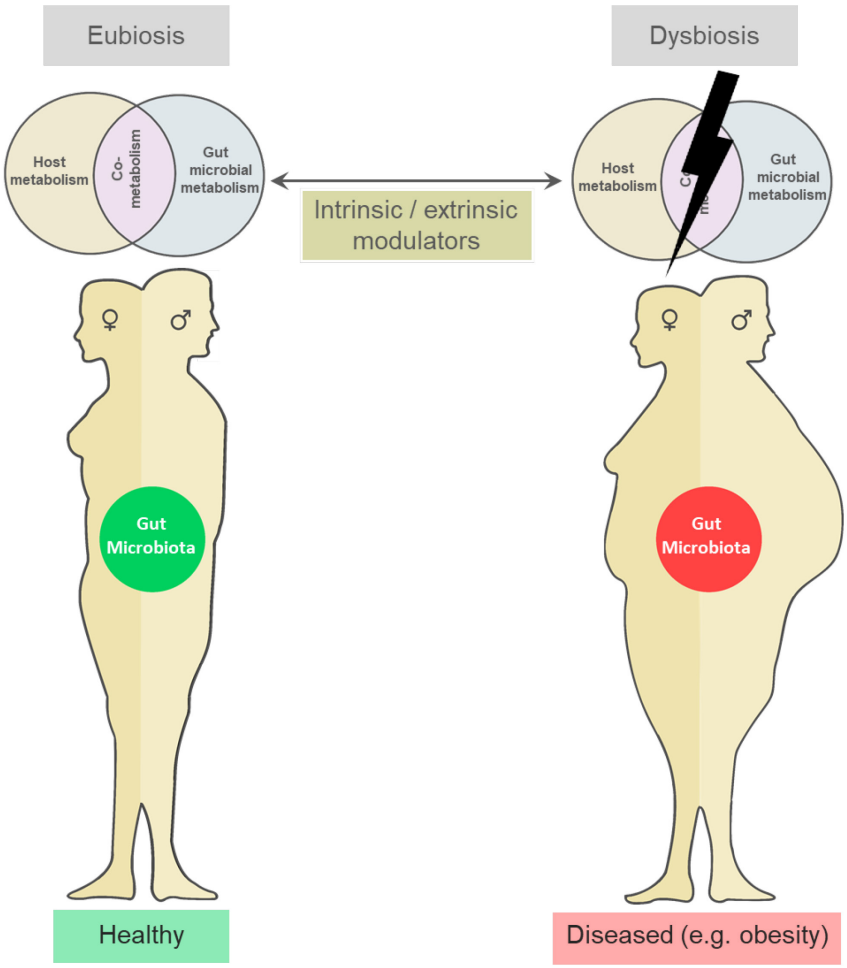

Figure 1-2. Regulating the relationship between gut microbial metabolism and host metabolism by intrinsic and extrinsic factors and the impact on host nutritional status.

Table 1-1. Extrinsic and intrinsic modulators of the gut microbiota.

Category	Modulator (e.g.)	Component (e.g.)
Intrinsic modulators		
	Immunity components	Cytokines
		Antibodies
	Endogenous secretions	Mucin
		Gut enzymes
		Bile acids
	Genetic variations	
	Age	
	Sex	
Extrinsic modulators		
	Dietary components	Nutrients
		Non-nutrients
	Xenobiotics	Antibiotics
		Pesticides
		Pollutants
	Maternal factors	Mode of delivery
		Breastfeeding
	Environmental temperature	

Biological sex is another main intrinsic factor controlling gut microbiota. Differences between males and females in metabolic profile and disease risk are highly influenced by, but not limited to, sex hormones (Sugiyama and Agellon, 2012). Genetic factors, such as those carried on sex chromosomes and epigenetic modifications of the genome also contribute to sex dimorphism in metabolic disease risk (Sugiyama and Agellon, 2012; Chen and Agellon, 2019). For instance, females are generally protected from metabolic syndromes before menopause however, this protection is dramatically lost once menopause occurs (Sugiyama and Agellon, 2012). Gut microbiome may also influence this sex dimorphism, particularly since male and female gut microbial compositions are increasingly appreciated to be different (Mueller et al., 2006; Dominianni et al., 2015; Haro et al., 2016; Takagi et al., 2019). In mice, the analysis of 89 inbred strains demonstrated significant sex differences in the gut microbial composition even at the microbial strain level (Org et al., 2016). Recently, the gut microbiota has been suggested to influence sex maturation (Weger et al., 2019). A metatranscriptomic analysis of germ-free mice versus conventionally raised mice showed feminization of gene expression in the liver and adipose tissue of germ-free male mice, and an attenuation of sex-specific gene expression and metabolic activities in female germ-free mice (Weger et al., 2019). The authors of the latter study pointed out that features of germ-free mice such as reduced growth, increased insulin sensitivity and resistance to diet-induced obesity could be looked at as markers of female metabolism. Together these studies provide insights on the bi-directional relationship between the sex of the host and the gut microbiota. Still, further research is required to study the potential role of sex- specific microbiota in contributing to the sex dimorphic metabolic disease risk.

The genetic makeup, age, and intestinal tract parameters such as lumen pH, and digestive secretions can also influence the gut microbiota (Malo et al., 2010; Yatsunenko et al., 2012). For example, bile acids are amphipathic molecules released into the small intestine to help in lipid digestion and absorption *via* emulsification and micelle formation (Agellon, 2008). Hence, bile acids can also damage bacterial cell membranes by solubilizing membrane phospholipids and integral proteins (Begley et al., 2005). Specific gut bacteria can metabolize bile acids by deconjugation,

hydroxylation, or epimerization activities rendering them less toxic (Ridlon et al., 2014). These processes produce secondary and tertiary bile acids and increase the diversity of the bile acid pool. For instance, the balance of the intestinal bile acid pool, which is implied by the composition of the gut microbiota, determines *C. difficile* spore germination and controls the clinical outcome of the infection (Britton and Young, 2012). Certain genetic variations and dietary components have been long recognized to induce bile acid excretion (Kay, 1981; Oelkers et al., 1997). However, how increased bile acid excretion influence the gut microbial community and the subsequent effects on host health status requires more investigation.

Extrinsic factors involved in the modification of the gut microbiota include a wide range of environmental variables, such as maternal factors, exposure to fever, illnesses, hospitalization, traveling and the use of antibiotics (Table 1-1) (Spor et al., 2011; Cho et al., 2012; Biedermann et al., 2013; Sofi et al., 2013). Among the extrinsic factors, the role of both diet patterns and dietary components is dominant and well-established in both animal models and humans. For example, Zhang et al. (2009) assessed the contributions of host genetics and diet in shaping the gut microbiota and the associated metabolic syndrome phenotypes in mice. They found that diet explained 57% of the total variability in gut microbiota whereas genetic variations accounted for no more than 12% (Zhang et al., 2009). In a transgenic mouse model susceptible to Crohn's disease, Martinez-Medina et al. (2013) showed that the Western-style diet (WSD; high in saturated fat and simple sugars (Chen et al., 2018) induced inflammation associated with a change in gut microbial composition, which was characterized by decreased total abundance of bacteria, increased Bacteroidetes phyla, and in particular, a high increase in the amounts of *E. coli* (Martinez-Medina et al., 2013). Parks et al. (2013) found that mice fed WSD had a greater abundance of order Clostridales and a lower abundance of Bacteroidetes compared to mice on a chow diet (Parks et al., 2013). Using metaproteome and metabolome analyses, Daniel et al. (2013) showed that, in addition to modulating the gut microbial composition, the high fat diet influenced hormonal and anti-microbial networks, bile acid and bilirubin metabolism and shifted the metabolic activity toward simple sugar catabolism (Daniel et al., 2013).

The above studies provide insights on the importance of diet in regulating the gut microbiota and, consequently, the host health outcomes.

In addition to nutrients, the diet also contains non-nutrient components that might have profound effects on gut microbiota (Chen et al., 2018). For example, plant polyphenols represent a group of bioactive food components that have beneficial effects on human health (Manach et al., 2004). The intake of polyphenols occurs by ingesting foods of plant origin, including a wide array of fruits, vegetables, and whole-grain cereals. Several studies have explored the effect of various polyphenolic compounds on gut microbiota by their potential bacteriostatic, bactericidal or prebiotic activity (Nohynek et al., 2006; Hervert-Hernandez et al., 2009; Etxeberria et al., 2013; Marin et al., 2015). In this context, investigations have been carried out on polyphenols from fruits, tea phenolics, resveratrol extracted from grapes, pomegranate peel phenolic extracts, blueberry water soluble extracts, and polyphenolic compounds from kiwi fruit. Consistently, plant polyphenols reduced the viability and abundance of tested microbial species but enhanced probiotic species, such as *Lactobacillus* and Bifidobacteria (Lee et al., 2006; Parkar et al., 2008; Larrosa et al., 2009; Molan et al., 2009; Bialonska et al., 2010; Neyrinck et al., 2013; Ansell et al., 2013). The effect of plant polyphenols on the enhancement of these probiotic species is largely dependent on the type of polyphenol and the dose used (Gwiazdowska et al., 2015; Burgos-Edwards et al., 2020). Gut microbiota is capable of hydrolyzing many complex polyphenols into smaller phenolic acids, which can increase their absorption and bioavailability (Del Rio et al., 2013; Kawabata et al., 2019). Some studies have pointed out the superior bioactivity of polyphenolic microbial catabolites over their parent compounds. For example, Verzelloni et al. (2011) have found that gut microbial generated polyphenolic catabolites from ellagitannin and chlorogenic acid were effective in counteracting protein glycation and neurodegeneration *in vitro* (Verzelloni et al., 2011). However, inter-individual variability in the gut microbial response to the intake of plant polyphenols have also been reported (Rafii et al., 2003; Bode et al., 2013; Guglielmetti et al., 2013). Such variability might be attributed to a variable polyphenolic composition of different extracts, other non-polyphenolic components of

the extract, and the interaction with host factors that might have not been accounted for in the study designs.

1.4. Modeling and profiling the gut microbiome

Due to the complex nature of interaction between the host and gut microbiota, and the importance of this relationship in influencing the health status of the host, it is necessary to apply a framework of research that accounts for each part separately with appropriate control. Various animal models have been used in gut microbial research such as Hawaiian bobtailed squids, fruit flies, zebrafish, and mice (Kostic et al., 2013). Mouse models have attracted particular attention in this regard due to their homologies with humans at both genetic (almost 90% of mice genes are shared with humans) (Waterston et al., 2002) and gut microbial levels (sharing the main phyla and families). In addition, mice are particularly amenable for gut microbial research due to their ease of maintenance as well as amenable environment manipulations, including housing, light-dark cycles, and diet (Kostic et al., 2013). Comparing gnotobiotic mice versus traditionally raised mice (conventional mice) provides significant insights on the specific role gut microbiota plays toward host metabolism. Mice and humans, however, differ in aspects related to their gastrointestinal tract physiology and dietary patterns. One difference in the gastrointestinal tract is the existence of non-glandular forestomach in mice that is not present in humans. The function of the forestomach is to store food and it is characterized by high pH (i.e., 3-4) (Ghoshal and Bal, 1989). Differences in dietary patterns include the continuous food intake pattern in mice, particularly at night when they are most active. In addition, coprophagy (re-ingesting their stools) and the “mucus-trap” (a mixture of microbiota and mucus can be transferred back from the colon to the cecum) do not normally occur in humans (Hugenholtz and de Vos, 2018). When these differences are accounted for, mice can be an instrumental model to study the human-microbial metabolic interactions.

On the other hand, the use of *in vitro* gut models improves the understanding of gut microbial functions outside the host environment. For example, characterizing the competitive fitness of pathogenic *C. difficile* strains *in vitro* vastly aided in the discovery of their enhanced virulence on the sugar trehalose (Robinson et al., 2014; Collins et al., 2018). Several *in vitro* gut model systems are currently in use (Molly et al., 1993; Tanner et al., 2014; Williams et al., 2015); although, these systems are not readily available due to high capital costs and complicated operational modes. There is a need for the development of feasible and dynamic *in vitro* gut models to facilitate investigating the complex gut microbiome-host interaction.

Next-generation sequencing (NGS) is indispensable in characterizing the gut microbial composition and the encoded microbial functions. NGS is more efficient, easier to carry out, and less expensive compared to traditional Sanger sequencing. For example, the bridge clonal amplification of nucleic acid sequences coupled with the Solexa sequencing-by-synthesis in Illumina Mi-seq technology allows for 99.9% accuracy of over 50 million reads with high quality within almost two days (Illumina, 2019). By multiplexing samples in one run, the cost of amplicon sequencing, such as the phylogenic marker 16S rRNA gene, can be less than $20 per sample. A drawback of this technology is its limited read length (300 bp maximum), which can be a challenge for data analyses that aims to elucidate metagenomic and metatranscriptomic sequences or to construct full genomes. Recent developments in sequencing technologies pioneered by Pacbio and Nanopore attracted wide attention due to their extremely long read length (>10 Kbp) which facilitates genome construction (Song et al., 2018; McNaughton et al., 2019).

With the continuous improvements in both yield and accuracy of NGS, there is a continuous generation of big data that requires analysis. Sequence data analysis is a long and multi-step process. It starts with quality check and filtering out low-quality reads, followed by sequence annotation and alignment against reference databases. Common software tools used for this regard include MG-Rast, Mothur, and Qiime

(Plummer and Twin, 2015). This is usually followed by data visualization and statistical analysis to produce meaningful results. Several R packages have been recently developed to visualize and statistically analyze microbiome data. Examples include phyloseq, vegan, and deseq2 packages (McMurdie and Holmes, 2013; Love et al., 2014; Oksanen et al., 2016). MicrobiomeAnalyst is a new web-tool that comprehensively combines the available tools and appropriate statistical methods developed to analyze microbiome data (Dhariwal et al., 2017). Currently, MicrobiomeAnalyst includes four modules: (i) Marker Data Profiling module which offers microbial community profiling, comparative and functional analysis; (ii) Shotgun Data Profiling module provides an exploratory window of shotgun metagenomics and metatranscriptomics data by functional and metabolic network visualization; (iii) Taxon Set Enrichment Analysis module helps interpret taxonomic signatures of the microbiome; and (iv) Projection with Public Data module which allows the comparison of the data with public data sets for pattern discovery and biological insights (Dhariwal et al., 2017). The use of MicrobiomeAnalyst significantly simplifies processing microbial sequencing data and reduces the time of data analysis.

1.5. Rationale and objectives

Over the last several decades, the prevalence of acquired metabolic syndromes including obesity, diabetes, fatty liver and cardiovascular diseases has increased globally (GBD 2015 Obesity Collaborators, 2017; GBD 2017 Risk Factor Collaborator, 2018; Saeedi et al., 2019). This increase was associated with a wave of nutritional transition from traditional to modern diets, therefore it has been proposed that the development of acquired metabolic syndromes is induced by dysregulation of nutrient metabolism and cellular function (Phillips et al., 2010; Sugiyama and Agellon, 2012). Nutrient metabolism deals with sensing, assimilation, trafficking, and processing of food components to provide the required energy and metabolites for optimal cellular function. It is evident that both extrinsic and intrinsic factors are involved in regulating this process.

Extrinsic factors originate from outside the body such as environmental elements, compounds that are present in food, which is comprised of both nutrient and non-nutrient components, as well as xenobiotics. Nutrients are essential for proper metabolism and cell function; however, excess, or sub-optimal nutrient intake induce detrimental impact on nutrient metabolism. For example, excess consumption of saturated fats and refined sugars, a characteristic of the modern Western-style diets (WSD), is correlated with metabolic dysregulations such as increased adiposity and insulin resistance (Lutsey et al., 2008; Drake et al., 2018).

Intrinsic factors include physiological components and genetic traits that characterize an organism, such as internal metabolites, genetic variations, and sex. For example, bile acids are synthesized in the liver from cholesterol, secreted into the small intestine to facilitate lipid digestion, then reclaimed in the ileum to be reused. Individuals with variations in genes that encode specific bile acid transporters in the intestine show primary bile acid malabsorption (BAM) (Oelkers et al., 1997). BAM is a gastrointestinal condition characterized by excessive amounts of bile acids passed into the colon, where it causes chronic fatty diarrhea and influence the efficiency of nutrient assimilation. Similarly, determinants of sex such as sex-specific genetic factors and hormones

underly the sex differences in gene expression and nutrient metabolism. For example, although males and females carry a shared genome, more than 1000 liver genes of men and women are sex-biased in expression, with the top biological pathways involved in lipid metabolism (Zhang et al., 2011). Indeed, sex-biased gene expression and differences in nutrient metabolism between the two sexes were detected in many tissues and among various animal species (Freire et al., 2011; Melé et al., 2015; Link and Reue, 2017; Naqvi et al., 2019). Such differences are suggested to trigger distinct susceptibility to acquired metabolic syndromes in males and females, which denotes the need to consider both sexes independently in all relevant research efforts.

A wide range of studies have investigated the impact of either an extrinsic or an intrinsic factor on a specific metabolic pathway; however, the impact of these factors is rarely exclusive, and a cooperative interactive relationship between intrinsic and extrinsic factors is more physiologically relevant. For example, in mice, genetic reprogramming of the intestinal fatty acid binding protein 6 (Fabp6) results in malabsorption of the intrinsic metabolites bile acids (Praslickova et al., 2012). Although bile acids are essential for efficient absorption of dietary fat, BAM was not associated with fat malabsorption on low fat diets in some species such as mice (Dawson et al., 2003). In the manuscript presented in **Appendix I**, I showed that by increasing the intake of extrinsic dietary fats using a high fat diet, such as the WSD, BAM in Fabp6 mouse model resulted in fat malabsorption. This study represents an example of the interaction between intrinsic and extrinsic factors in regulating nutrient metabolism and influencing the development of pathological conditions. Interestingly, this study also revealed unique characteristics of the bile acid profiles of Fabp6-deficent mice fed WSD. These characteristics implied gut microbial modulation in Fabp6-deficent mice, which was verified using a basic qPCR assay (**Appendix I**).

Indeed, the impact of gut microbiota on host nutrient metabolism and cellular function is increasingly appreciated. Gut microbiota include species from all domains of life; however, the domain of Bacteria has been the most investigated. More than 2000 bacterial species were detected in the human gastrointestinal tract (GIT) with over than 3 million genes (Sender et al., 2016; Almeida et al., 2019), which are proposed to

provide the host with the ability to perform additional metabolic, structural and protective functions. The integration between host metabolism and gut microbial metabolism results in a more efficient co-metabolism that enhances adaptation and evolution (Hashimoto et al., 1998; Lederberg and McCray, 2001; Maslowski and Mackay, 2011). For example, human GIT is incapable of digesting dietary fibers of plant sources, but gut microbiota has the ability to ferment these fibers for nutrients and energy. Fermentation products such as short chain fatty acids (SCFAs), after being absorbed in the large intestine, provide the host with a source of energy and regulate fundamental metabolic processes such as insulin secretion and appetite stimulation (Tolhurst et al., 2012; Perry and Wang, 2012; Psichas et al., 2014).

Importantly, abnormal changes in the gut microbial composition and diversity are implicated in altering the host-gut microbial co-metabolism. These alterations in the gut microbial ecosystem have been indicated to contribute to dysregulation in nutrient metabolism and cellular function and triggering the pathogenesis of several acquired metabolic syndromes (Musso et al., 2010; Scaldaferri et al., 2013; Koeth et al., 2013; DeGruttola et al., 2016). It is unknown how intrinsic and extrinsic factors regulate host-gut microbial co-metabolism and influence the risk of acquired metabolic syndromes. Herein, I addressed the central question in terms of the impact of intrinsic and extrinsic factors, independently and cooperatively, on the gut microbiota and the associated host metabolic status. **The overall thesis hypothesis** is that intrinsic factors (e.g. bile acids, genetic variations, and sex) and extrinsic factors (e.g. plant metabolites and dietary fat) individually and cooperatively modify the gut microbial characteristics (e.g. diversity and composition) and modulate metabolic activity and the risk to acquired metabolic syndromes (e.g. obesity and diabetes). The following **sub-hypotheses** were tested:

i. The increased luminal intestinal concentration of bile acids in Fabp6-deficient mouse model reduces the gut microbial diversity, enriches bile acid metabolizing bacterial species, and is associated with sex-specific adiposity and glucose tolerance.
ii. The consumption of a WSD supplemented with polyphenolic-rich potato extract (PRPE) in mice prevents WSD-induced loss of gut microbial diversity, enriches

probiotic species, and is associated with sex-specific prevention of adiposity and colonocyte endoplasmic reticular stress.

iii. The combined deficiency of Fabp6 and Fabp2 in mice enriches the gut microbial species capable of metabolizing increased bile acids and dietary fat concentrations and is associated with sex-specific adiposity, glucose tolerance and colonocyte endoplasmic reticular stress.

Bile acids are cytotoxic to a wide range of bacteria. Based on their concentration, bile acids act on the microbial cellular membrane by either modifying its permeability and fluidity leading to altered protein signaling and DNA damage, or by dissolving its lipids and causing cell content leakage and cell death (Begley et al., 2005). However, gut microbes differ in their tolerance to bile acids, a property that depends on their ability to biotransform bile acids to less toxic and soluble forms. In **Chapter 2** of this thesis, Fabp6-deficient mice were used as a model of bile acid malabsorption (Praslickova et al., 2012). Fatty acid binding proteins (Fabps) represent a family of intracellular lipid binding proteins which bind a variety of hydrophobic compounds, with preference to bile and fatty acids (Agellon et al., 2002; Labonté et al., 2003). Fabp6 is a key component of the ileal enterocyte bile acid reclamation system, together with the apical sodium bile acid transporter (Asbt), and the basolateral organic solute transporter alpha (Ostα) (Dawson et al., 2003; Ballatori et al., 2008; Praslickova et al., 2012). Besides their BAM phenotype (Praslickova et al., 2012), on high fat diets, such as the WSD, Fabp6-deficenct mice show fat malabsorption and, interestingly, males but not females gain excess adiposity (Appendix I). The exposure to elevated concentrations of bile acids in this mouse model is expected to disrupt the normal gut microbial structure. Therefore, the objective of the study presented in **Chapter 2** was (i) was to characterize the changes in the gut microbiota of *Fabp6*$^{-/-}$ mice challenged with WSD and to identify the nature of the associated metabolic dysfunction.

Diet has a dominant role in modifying the gut microbiota over many other extrinsic factors. In addition to its nutrient components, diet also contains non-nutrient components that may impact on the gut microbiota (Chen et al., 2018). Previously phenolic-rich potato extract (PRPE) was shown to reduce body weight gain and improve

glucose tolerance of mice on a high-fat diet (Kubow et al., 2014). Since polyphenols are poorly absorbed in the small intestine (Williamson and Manach, 2005), they come into direct contact with the gut microbiota. Plant polyphenols may act as prebiotics and enhance the growth of some bacterial species, or act as antibacterial compounds and be harmful to other bacteria species (Nohynek et al., 2006; Hervert-Hernandez et al., 2009; Bialonska et al., 2010). Therefore, the objective of the study presented in **Chapter 3** was to (ii) to evaluate if the ability of PRPE to reduce the body weight gain of mice on a high fat diet was associated with remodeling of the gut microbiota and modification of metabolic functions in the host.

Dietary fats are digested and absorbed efficiently in the small intestine. However, the deficiency of Fabp2 in mice has been shown to cause fat malabsorption. Similar to Fabp6-deficient mice, Fabp2-deficient mice exhibit sex dimorphic response to high fat diet feeding (Vassileva et al., 2000; Agellon et al., 2002; Agellon et al., 2007). In addition to the hormonal, genetic and epigenetic factors (Sugiyama and Agellon, 2012), gut microbiota may be involved in driving sex differences in lipid metabolism. Interestingly, a mouse model deficient in both Fabp2 and Fabp6 showed increase in gene expression programs related to fatty acid and lipoprotein metabolism in the small intestine compared to a mouse model deficient in either Fabp2 or Fabp6 (Chen and Agellon, 2019). Despite the high prevalence of conditions associated with bile acid malabsorption (Wedlake et al., 2009), and the fact that bile acid malabsorption induces fat malabsorption (Ung et al., 2000), the impact of concurrent bile acid malabsorption and fat malabsorption on the gut microbiota and host metabolic response to dietary perturbations is unknown. The mouse model of the genetically induced deficiency for both Fabp2 and Fabp6 represents a key opportunity to investigate both bile acid malabsorption and fat malabsorption within the same animal model. Therefore, the objective of the study presented in **Chapter 4** was (iii) to identify the gut microbial modification in response to combined deficiency of Fabp2 and Fabp6 and to determine if the loss of these intestinal fatty acid binding proteins influence the response of the gut microbiota to diet.

The complex integration between host metabolism and gut microbial metabolism may restrain the determination of the specific impact of intrinsic and extrinsic factors on gut microbiota. This issue can be accounted for by applying an integrated gut microbial research approach where both *in vivo* and *in vitro* models are used. Several *in vitro* gut models are currently available. Based on their design, most *in vitro* gut models represent either batch or continuous culture designs. The frequency a culture is recycled is usually fixed; such as in the semi-continuous model EnteroMix (Makivuokko and Nurminen, 2006), or the continuous fixed flow rate model the Simulator of the Human Intestinal Microbial Ecosystem (SHIME) (Molly et al., 1993). A number of *in vitro* gut models have been developed and accustomed to simulate particular conditions or digestive tracts of animals, such as that of swine or chicken (Tanner et al., 2014; Card et al., 2017). These models usually occupy large laboratory space footprints and are typically complex and not user-friendly (Minekus et al., 1999; Payne et al., 2012; von Martels et al., 2017). The objective of the study presented in **Chapter 5** was (iv) to develop a modular, scalable, and dynamic *in vitro* gut model to facilitate studying the gut microbiota in the absence of the host inherent variables.

1.6. References

Agellon, L.B. (2008). Metabolism and function of bile acids. In D.E. Vance & J.E. Vance (Eds.), *Biochemistry of lipids, lipoproteins and membranes (5th edition)* (Vol. 36, pp. 423-440). San Diego: Elsevier.

Agellon, L.B., Drozdowski, L., Li, L.*, et al.* (2007). Loss of intestinal fatty acid binding protein increases the susceptibility of male mice to high fat diet-induced fatty liver. *Biochim Biophys Acta, 1771* (10), 1283-1288.

Agellon, L.B., Toth, M.J. and Thomson, A.B. (2002). Intracellular lipid binding proteins of the small intestine. *Mol Cell Biochem, 239* (1-2), 79-82.

Almeida, A., Mitchell, A.L., Boland, M.*, et al.* (2019). A new genomic blueprint of the human gut microbiota. *Nature, 568* (7753), 499-504.

Ansaldo, E., Slayden, L.C., Ching, K.L.*, et al.* (2019). *Akkermansia muciniphila* induces intestinal adaptive immune responses during homeostasis. *Science, 364* (6446), 1179.

Ansell, J., Parkar, S., Paturi, G.*, et al.* (2013). Modification of the colonic microbiota. *Adv Food Nutr Res, 68*, 205-217.

Arrieta, M.C., Stiemsma, L.T., Amenyogbe, N.*, et al.* (2014). The intestinal microbiome in early life: Health and disease. *Front Immunol, 5*, 427.

Baier, L.J., Sacchettini, J.C., Knowler, W.C.*, et al.* (1995). An amino acid substitution in the human intestinal fatty acid binding protein is associated with increased fatty acid binding, increased fat oxidation, and insulin resistance. *J Clin Invest, 95* (3), 1281-1287.

Ballatori, N., Fang, F., Christian, W.V.*, et al.* (2008). Ostα-Ostβ is required for bile acid and conjugated steroid disposition in the intestine, kidney, and liver. *Am J Physiol Gastrointest Liver Physiol, 295* (1), G179-G186.

Begley, M., Gahan, C.G. and Hill, C. (2005). The interaction between bacteria and bile. *FEMS Microbiol Rev, 29* (4), 625-651.

Belkaid, Y. and Hand, Timothy W. (2014). Role of the microbiota in immunity and inflammation. *Cell, 157* (1), 121-141.

Bialonska, D., Ramnani, P., Kasimsetty, S.G.*, et al.* (2010). The influence of pomegranate by-product and punicalagins on selected groups of human intestinal microbiota. *Int J Food Microbiol, 140* (2-3), 175-182.

Biedermann, L., Zeitz, J., Mwinyi, J.*, et al.* (2013). Smoking cessation induces profound changes in the composition of the intestinal microbiota in humans. *PLoS One, 8* (3), e59260.

Bik, E.M., Ugalde, J.A., Cousins, J.*, et al.* (2018). Microbial biotransformations in the human distal gut. *Br J Pharmacol, 175* (24), 4404-4414.

Bode, L.M., Bunzel, D., Huch, M.*, et al.* (2013). In vivo and in vitro metabolism of trans-resveratrol by human gut microbiota. *Am J Clin Nutr, 97* (2), 295-309.

Britton, R.A. and Young, V.B. (2012). Interaction between the intestinal microbiota and host in *Clostridium difficile* colonization resistance. *Trends Microbiol, 20* (7), 313-319.

Brocks, J.J., Logan, G.A., Buick, R.*, et al.* (1999). Archean molecular fossils and the early rise of eukaryotes. *Science, 285* (5430), 1033-1036.

Burgos-Edwards, A., Fernández-Romero, A., Carmona, M.*, et al.* (2020). Effects of gastrointestinal digested polyphenolic enriched extracts of Chilean currants (Ribes magellanicum and Ribes punctatum) on in vitro fecal microbiota. *Food Res Int, 129*, 108848.

Cani, P.D., Amar, J., Iglesias, M.A.*, et al.* (2007). Metabolic endotoxemia initiates obesity and insulin resistance. *Diabetes, 56* (7), 1761-1772.

Card, R.M., Cawthraw, S.A., Nunez-Garcia, J.*, et al.* (2017). An in vitro chicken gut model demonstrates transfer of a multidrug resistance plasmid from Salmonella to commensal *Escherichia coli*. *mBio, 8* (4).

Chang, C.-W., Liu, C.-Y., Lee, H.-C.*, et al.* (2018). *Lactobacillus casei* variety rhamnosus probiotic preventively attenuates 5-fluorouracil/oxaliplatin-induced intestinal injury in a syngeneic colorectal cancer model. *Front Microbiol, 9* (983).

Chen, Y. and Agellon, L.B. (2019). Distinct alteration of gene expression programs in the small intestine of male and female mice in response to ablation of intestinal fabp genes. *Genes (Basel), 11* (8), 943.

Chen, Y., Michalak, M. and Agellon, L.B. (2018). Importance of nutrients and nutrient metabolism on human health. *Yale J Biol Med, 91* (2), 95-103.

Chevalier, C., Stojanovic, O., Colin, D.J.*, et al.* (2015). Gut microbiota orchestrates energy homeostasis during cold. *Cell, 163* (6), 1360-1374.

Cho, I., Yamanishi, S., Cox, L.*, et al.* (2012). Antibiotics in early life alter the murine colonic microbiome and adiposity. *Nature, 488* (7413), 621-626.

Collins, J., Robinson, C., Danhof, H.*, et al.* (2018). Dietary trehalose enhances virulence of epidemic *Clostridium difficile*. *Nature, 553* (7688), 291-294.

Daniel, H., Gholami, A.M., Berry, D.*, et al.* (2013). High-fat diet alters gut microbiota physiology in mice. *ISME J, 8* (2), 295-308.

Dawson, P.A., Haywood, J., Craddock, A.L.*, et al.* (2003). Targeted deletion of the ileal bile acid transporter eliminates enterohepatic cycling of bile acids in mice. *J Biol Chem, 278* (36), 33920-33927.

DeGruttola, A.K., Low, D., Mizoguchi, A.*, et al.* (2016). Current understanding of dysbiosis in disease in human and animal models. *J Inflamm Bowel Dis Disord, 22* (5), 1137-1150.

Del Rio, D., Rodriguez-Mateos, A., Spencer, J.P.*, et al.* (2013). Dietary polyphenolics in human health: Structures, bioavailability, and evidence of protective effects against chronic diseases. *Antioxid Redox Signal, 18* (14), 1818-1892.

den Besten, G., Lange, K., Havinga, R.*, et al.* (2013). Gut-derived short-chain fatty acids are vividly assimilated into host carbohydrates and lipids. *Am J Physiol Gastrointest Liver Physiol, 305* (12), G900-910.

Dhariwal, A., Chong, J., Habib, S.*, et al.* (2017). Microbiomeanalyst - A web-based tool for comprehensive statistical, visual and meta-analysis of microbiome data *Nucleic Acids Res, 45* (W1), W180–W188.

Dominianni, C., Sinha, R., Goedert, J.J.*, et al.* (2015). Sex, body mass index, and dietary fiber intake influence the human gut microbiome. *PLoS One, 10* (4), e0124599.

Donohoe, D.R., Garge, N., Zhang, X.*, et al.* (2011). The microbiome and butyrate regulate energy metabolism and autophagy in the mammalian colon. *Cell Metab, 13* (5), 517-526.

Drake, I., Sonestedt, E., Ericson, U.*, et al.* (2018). A Western dietary pattern is prospectively associated with cardio-metabolic traits and incidence of the metabolic syndrome. *Br J Nutr, 119* (10), 1168-1176.

Etxeberria, U., Fernandez-Quintela, A., Milagro, F.I.*, et al.* (2013). Impact of polyphenols and polyphenol-rich dietary sources on gut microbiota composition. *J Agric Food Chem, 61* (40), 9517-9533.

Finucane, M.M., Sharpton, T.J., Laurent, T.J.*, et al.* (2014). A taxonomic signature of obesity in the microbiome? Getting to the guts of the matter. *PLoS One, 9* (1), e84689.

Fisher, E., Grallert, H., Klapper, M.*, et al.* (2009). Evidence for the Thr79Met polymorphism of the ileal fatty acid binding protein (FABP6) to be associated with type 2 diabetes in obese individuals. *Mol Genet Metab, 98* (4), 400-405.

Fleissner, C.K., Huebel, N., Abd El-Bary, M.M.*, et al.* (2010). Absence of intestinal microbiota does not protect mice from diet-induced obesity. *Br J Nutr, 104* (6), 919-929.

Freire, A.C., Basit, A.W., Choudhary, R.*, et al.* (2011). Does sex matter? The influence of gender on gastrointestinal physiology and drug delivery. *Int J Pharm, 415* (1-2), 15-28.

GBD 2015 Obesity Collaborators. (2017). Health effects of overweight and obesity in 195 countries over 25 years. *New Engl J Med, 377* (1), 13-27.

GBD 2017 Risk Factor Collaborator. (2018). Global, regional, and national comparative risk assessment of 84 behavioural, environmental and occupational, and metabolic risks or clusters of risks for 195 countries and territories, 1990-2017: A systematic analysis for the Global Burden of Disease Study 2017. *Lancet, 392* (10159), 1923-1994.

Ghoshal, N.G. and Bal, H.S. (1989). Comparative morphology of the stomach of some laboratory mammals. *Lab Anim, 23* (1), 21-29.

Guglielmetti, S., Fracassetti, D., Taverniti, V.*, et al.* (2013). Differential modulation of human intestinal bifidobacterium populations after consumption of a wild blueberry (*Vaccinium angustifolium*) drink. *J Agric Food Chem, 61* (34), 8134-8140.

Gwiazdowska, D., Juś, K., Jasnowska, J.*, et al.* (2015). The impact of polyphenols on Bifidobacterium growth. *Acta Biochim Pol, 62*, 895–901.

Haro, C., Rangel-Zuniga, O.A., Alcala-Diaz, J.F.*, et al.* (2016). Intestinal microbiota is influenced by gender and body mass index. *PLoS One, 11* (5), e0154090.

Haros, M., Carlsson, N.G., Almgren, A.*, et al.* (2009). Phytate degradation by human gut isolated *Bifidobacterium pseudocatenulatum* ATCC27919 and its probiotic potential. *Int J Food Microbiol, 135* (1), 7-14.

Hashimoto, H., Ishikawa, H. and Kusakabe, M. (1998). Simultaneous observation of capillary nets and tenascin in intestinal villi. *Anat Rec, 250* (4), 488-492.

He, C., Cheng, D., Peng, C.*, et al.* (2018). High-fat diet induces dysbiosis of gastric microbiota prior to gut microbiota in association with metabolic disorders in mice. *Front Microbiol, 9* (9), 639.

Hervert-Hernandez, D., Pintado, C., Rotger, R.*, et al.* (2009). Stimulatory role of grape pomace polyphenols on *Lactobacillus acidophilus* growth. *Int J Food Microbiol, 136* (1), 119-122.

Hofmann, A.F. (1972). Bile acid malabsorption caused by ileal resection. *Arch Intern Med, 130* (4), 597-605.

Hooper, L.V., Wong, M.H., Thelin, A.*, et al.* (2001). Molecular analysis of commensal host-microbial relationships in the intestine. *Science, 291* (5505), 881-884.

Hugenholtz, F. and de Vos, W.M. (2018). Mouse models for human intestinal microbiota research: A critical evaluation. *Cell Mol Life Sci, 75* (1), 149-160.

Human Microbiome Project. (2012). Structure, function and diversity of the healthy human microbiome. *Nature, 486* (7402), 207-214.

Illumina. (2019). Specifications for the MiSeq system. Retrieved from https://www.illumina.com/systems/sequencing-platforms/miseq/specifications.html

Kasai, C., Sugimoto, K., Moritani, I.*, et al.* (2015). Comparison of the gut microbiota composition between obese and non-obese individuals in a Japanese population, as analyzed by terminal restriction fragment length polymorphism and next-generation sequencing. *BMC Gastroenterol, 15*, 100.

Kawabata, K., Yoshioka, Y. and Terao, J. (2019). Role of intestinal microbiota in the bioavailability and physiological functions of dietary polyphenols. *Molecules, 24* (2).

Kay, R.M. (1981). Effects of diet on the fecal excretion and bacterial modification of acidic and neutral steroids, and implications for colon carcinogenesis. *Cancer Res, 41*, 3774-3777.

Koch, R. (1890). An address on bacteriological research. *Br Med J, 2* (1546), 380-383.

Koeth, R.A., Wang, Z., Levison, B.S.*, et al.* (2013). Intestinal microbiota metabolism of L-carnitine, a nutrient in red meat, promotes atherosclerosis. *Nat Med, 19* (5), 576-585.

Kostic, A.D., Howitt, M.R. and Garrett, W.S. (2013). Exploring host–microbiota interactions in animal models and humans. *Genes Dev, 27* (7), 701-718.

Kubow, S., Hobson, L., Iskandar, M.M.*, et al.* (2014). Extract of Irish potatoes (*Solanum tuberosum* L.) decreases body weight gain and adiposity and improves glucose control in the mouse model of diet-induced obesity. *Mol Nutr Food Res, 58* (11), 2235-2238.

Kunsan, X., Taisan, Z., Weiping, J.*, et al.* (1999). The association of Ala54Thr variant of intestinal fatty acid binding protein gene with general and regional adipose tissue depots. *Chin Med Sci J, 14* (1), 46-51.

Labonté, E.D., Li, Q., Kay, C.M.*, et al.* (2003). The relative ligand binding preference of the murine ileal lipid binding protein. *Protein Expr Purif, 28* (1), 25-33.

Lam, D.D., Garfield, A.S., Marston, O.J.*, et al.* (2010). Brain serotonin system in the coordination of food intake and body weight. *Pharmacol Biochem Behav, 97* (1), 84-91.

Larrosa, M., Yanez-Gascon, M.J., Selma, M.V.*, et al.* (2009). Effect of a low dose of dietary resveratrol on colon microbiota, inflammation and tissue damage in a DSS-induced colitis rat model. *J Agric Food Chem, 57* (6), 2211-2220.

Lederberg, J. and McCray, A.T.J. (2001). Ome sweet omics - A genealogical treasury of words. *Scientist, 15* (7), 8.

Lee, H.C., Jenner, A.M., Low, C.S.*, et al.* (2006). Effect of tea phenolics and their aromatic fecal bacterial metabolites on intestinal microbiota. *Res Microbiol, 157* (9), 876-884.

Lessa, F.C., Mu, Y., Bamberg, W.M.*, et al.* (2015). Burden of *Clostridium difficile* infection in the United States. *New Engl J Med, 372* (9), 825-834.

Ley, R.E., Backhed, F., Turnbaugh, P.*, et al.* (2005). Obesity alters gut microbial ecology. *Proc Natl Acad Sci USA, 102* (31), 11070-11075.

Ley, R.E., Peterson, D.A. and Gordon, J.I. (2006). Ecological and evolutionary forces shaping microbial diversity in the human intestine. *Cell, 124* (4), 837-848.

Lievin-Le Moal, V. and Servin, A.L. (2006). The front line of enteric host defense against unwelcome intrusion of harmful microorganisms: Mucins, antimicrobial peptides, and microbiota. *Clin Microbiol Rev, 19* (2), 315-337.

Link, J.C. and Reue, K. (2017). Genetic basis for sex differences in obesity and lipid metabolism. *Annu Rev Nutr, 37*, 225-245.

Love, M.I., Huber, W. and Anders, S. (2014). Moderated estimation of fold change and dispersion for RNA-seq data with DESeq2. *Genome Biol, 15*, 550.

Lutsey, P.L., Steffen, L.M. and Stevens, J. (2008). Dietary intake and the development of the metabolic syndrome: The atherosclerosis risk in communities study. *Circulation, 117* (6), 754-761.

Makivuokko, H. and Nurminen, P. (2006). In vitro methods to model the gastrointestinal tract. In A. Ouwehand & E. Vaughan (Eds.), *Gastrointestinal microbiology*. Boca Raton, FL: Taylor & Francis Group.

Malo, M.S., Alam, S.N., Mostafa, G.*, et al.* (2010). Intestinal alkaline phosphatase preserves the normal homeostasis of gut microbiota. *Gut, 59* (11), 1476-1484.

Manach, C., Scalbert, A., Morand, C.*, et al.* (2004). Polyphenols: Food sources and bioavailability. *Am J Clin Nutr, 79* (5), 727-747.

Marchesi, J.R. and Ravel, J. (2015). The vocabulary of microbiome research: A proposal. *Microbiome, 3*, 31-31.

Mardis, E.R. (2008). The impact of next-generation sequencing technology on genetics. *Trends Genet, 24* (3), 133-141.

Marin, L., Miguelez, E.M., Villar, C.J.*, et al.* (2015). Bioavailability of dietary polyphenols and gut microbiota metabolism: Antimicrobial properties. *Biomed Res Int, 2015*, 905215.

Martinez-Medina, M., Denizot, J., Dreux, N.*, et al.* (2013). Western diet induces dysbiosis with increased *E. Coli* in CEABAC10 mice, alters host barrier function favouring AIEC colonisation. *Gut, 63* (1), 116-124.

Maruvada, P., Leone, V., Kaplan, L.M.*, et al.* (2017). The human microbiome and obesity: Moving beyond associations. *Cell Host Microbe, 22* (5), 589-599.

Maslowski, K.M. and Mackay, C.R. (2011). Diet, gut microbiota and immune responses. *Nat Immunol, 12* (1), 5-9.

McMurdie, P.J. and Holmes, S. (2013). Phyloseq: An R package for reproducible interactive analysis and graphics of microbiome census data. *PLoS One, 8* (4), e61217.

McNaughton, A.L., Roberts, H.E., Bonsall, D.*, et al.* (2019). Illumina and Nanopore methods for whole genome sequencing of hepatitis B virus (HBV). *Sci Rep, 9* (1), 7081-7081.

Melé, M., Ferreira, P.G., Reverter, F.*, et al.* (2015). The human transcriptome across tissues and individuals. *Science, 348* (6235), 660.

Minekus, M., Smeets-Peeters, M., Havenaar, R.*, et al.* (1999). A computer-controlled system to simulate conditions of the large intestine with peristaltic mixing, water absorption and absorption of fermentation products. *Appl Microbiol Biotechnol, 53* (1), 108-114.

Molan, A., Lila, M., Mawson, J.*, et al.* (2009). In vitro and in vivo evaluation of the prebiotic activity of water-soluble blueberry extracts. *World J Microbiol Biotechnol, 25* (7), 1243-1249.

Molly, K., Vande Woestyne, M. and Verstraete, W. (1993). Development of a 5-step multi-chamber reactor as a simulation of the human intestinal microbial ecosystem. *Appl Microbiol Biotechnol, 39* (2), 254-258.

Mueller, S., Saunier, K., Hanisch, C.*, et al.* (2006). Differences in fecal microbiota in different european study populations in relation to age, gender, and country: A cross-sectional study. *Appl Environ Microbiol, 72* (2), 1027-1033.

Musso, G., Gambino, R. and Cassader, M. (2010). Obesity, diabetes, and gut microbiota: The hygiene hypothesis expanded? *Diabetes Care, 33* (10), 2277-2284.

Nagpal, R., Shively, C.A., Appt, S.A.*, et al.* (2018). Gut microbiome composition in non-human primates consuming a Western or Mediterranean diet. *Front Nutr, 5*, 28-28.

Nagpal, R., Yadav, H. and Marotta, F. (2014). Gut microbiota: The next-gen frontier in preventive and therapeutic medicine? *Front Med, 1*, 15.

Naqvi, S., Godfrey, A.K., Hughes, J.F.*, et al.* (2019). Conservation, acquisition, and functional impact of sex-biased gene expression in mammals. *Science, 365* (6450), eaaw7317.

Nedungadi, T.P. and Clegg, D.J. (2009). Sexual dimorphism in body fat distribution and risk for cardiovascular diseases. *J Cardiovasc Transl Res, 2* (3), 321-327.

Neyrinck, A.M., Van Hee, V.F., Bindels, L.B.*, et al.* (2013). Polyphenol-rich extract of pomegranate peel alleviates tissue inflammation and hypercholesterolaemia in high-fat diet-induced obese mice: Potential implication of the gut microbiota. *Br J Nutr, 109* (5), 802-809.

Nohynek, L.J., Alakomi, H.L., Kahkonen, M.P.*, et al.* (2006). Berry phenolics: Antimicrobial properties and mechanisms of action against severe human pathogens. *Nutr Cancer, 54* (1), 18-32.

Nyhlin, H., Merrick, M.V. and Eastwood, M.A. (1994). Bile acid malabsorption in Crohn's disease and indications for its assessment using SeHCAT. *Gut, 35* (1), 90-93.

O'Brien, S., Mulcahy, H., Fenlon, H.*, et al.* (1993). Intestinal bile acid malabsorption in cystic fibrosis. *Gut, 34* (8), 1137-1141.

O'Hara, A.M. and Shanahan, F. (2006). The gut flora as a forgotten organ. *EMBO Rep, 7* (7), 688-693.

Oelkers, P., Kirby, L.C., Heubi, J.E.*, et al.* (1997). Primary bile acid malabsorption caused by mutations in the ileal sodium-dependent bile acid transporter gene (SLC10A2). *J Clin Invest, 99* (8), 1880-1887.

Oksanen, J., Blanchet, F.G., Kindt, R.*, et al.* (2016). Vegan: Community ecology package (Version 2.4-3.). Retrieved from https://github.com/vegandevs/vegan

Orellana, E.R., Covasa, M. and Hajnal, A. (2019). Neuro-hormonal mechanisms underlying changes in reward related behaviors following weight loss surgery: Potential pharmacological targets. *Biochem Pharmacol, 164*, 106-114.

Org, E., Mehrabian, M., Parks, B.W.*, et al.* (2016). Sex differences and hormonal effects on gut microbiota composition in mice. *Gut Microbes, 7* (4), 313-322.

Palmeira, P. and Carneiro-Sampaio, M. (2016). Immunology of breast milk. *Rev Assoc Med Bras, 62* (6), 584-593.

Parkar, S.G., Stevenson, D.E. and Skinner, M.A. (2008). The potential influence of fruit polyphenols on colonic microflora and human gut health. *Int J Food Microbiol, 124* (3), 295-298.

Parks, Brian W., Nam, E., Org, E.*, et al.* (2013). Genetic control of obesity and gut microbiota composition in response to high-fat, high-sucrose diet in mice. *Cell Metab, 17* (1), 141-152.

Payne, A.N., Zihler, A., Chassard, C.*, et al.* (2012). Advances and perspectives in *in vitro* human gut fermentation modeling. *Trends Biotechnol, 30* (1), 17-25.

Perry, B. and Wang, Y. (2012). Appetite regulation and weight control: The role of gut hormones. *Nutr Diabetes, 2*, e26.

Phillips, C.M., Goumidi, L., Bertrais, S.*, et al.* (2010). Gene-nutrient interactions with dietary fat modulate the association between genetic variation of the acsl1 gene and metabolic syndrome. *J Lipid Res, 51* (7), 1793-1800.

Plovier, H., Everard, A., Druart, C.*, et al.* (2017). A purified membrane protein from *Akkermansia muciniphila* or the pasteurized bacterium improves metabolism in obese and diabetic mice. *Nat Med, 23* (1), 107-113.

Plummer, E. and Twin, J. (2015). A comparison of three bioinformatics pipelines for the analysis of preterm gut microbiota using 16S rRNA gene sequencing data. *J Proteomics Bioinform, 8* (12), 283-291.

Praslickova, D., Torchia, E.C., Sugiyama, M.G.*, et al.* (2012). The ileal lipid binding protein is required for efficient absorption and transport of bile acids in the distal portion of the murine small intestine. *PLoS One, 7* (12), 1.

Psichas, A., Sleeth, M.L., Murphy, K.G.*, et al.* (2014). The short chain fatty acid propionate stimulates GLP-1 and PYY secretion via free fatty acid receptor 2 in rodents. *Int J Obesity, 39*, 424.

Rafii, F., Davis, C., Park, M.*, et al.* (2003). Variations in metabolism of the soy isoflavonoid daidzein by human intestinal microfloras from different individuals. *Arch Microbiol, 180* (1), 11-16.

Ridaura, V.K., Faith, J.J., Rey, F.E.*, et al.* (2013). Gut microbiota from twins discordant for obesity modulate metabolism in mice. *Science, 341* (6150), 1241214.

Ridlon, J.M., Kang, D.J., Hylemon, P.B.*, et al.* (2014). Bile acids and the gut microbiome. *Curr Opin Gastroenterol, 30* (3), 332-338.

Robinson, C.D., Auchtung, J.M., Collins, J.*, et al.* (2014). Epidemic *Clostridium difficile* strains demonstrate increased competitive fitness compared to nonepidemic isolates. *Infect Immun, 82* (7), 2815-2825.

Rosenbaum, M., Knight, R. and Leibel, R.L. (2015). The gut microbiota in human energy homeostasis and obesity. *Trends Endocrinol Metab, 26* (9), 493-501.

Saeedi, P., Petersohn, I., Salpea, P.*, et al.* (2019). Global and regional diabetes prevalence estimates for 2019 and projections for 2030 and 2045: Results from the International Diabetes Federation Diabetes Atlas, 9th edition. *Diabetes Res Clin Pract, 157*, 107843.

Scaldaferri, F., Gerardi, V., Lopetuso, L.R.*, et al.* (2013). Gut microbial flora, prebiotics, and probiotics in IBD: Their current usage and utility. *Biomed Res Int, 2013*, 435268.

Scarpello, J.H., Hodgson, E. and Howlett, H.C. (1998). Effect of metformin on bile salt circulation and intestinal motility in type 2 diabetes mellitus. *Diabet Med, 15* (8), 651-656.

Schirmer, M., Smeekens, S.P., Vlamakis, H.*, et al.* (2016). Linking the human gut microbiome to inflammatory cytokine production capacity. *Cell, 167* (4), 1125-1136.e1128.

Sender, R., Fuchs, S. and Milo, R. (2016). Revised estimates for the number of human and bacteria cells in the body. *PLoS Biol, 14* (8), e1002533.

Sofi, M.H., Gudi, R.R., Karumuthil-Melethil, S.*, et al.* (2013). pH of drinking water influences the composition of gut microbiome and type 1 diabetes incidence. *Diabetes, 63* (2), 632–644.

Sommer, F., Ståhlman, M., Ilkayeva, O.*, et al.* (2016). The gut microbiota modulates energy metabolism in the hibernating brown bear *Ursus arctos*. *Cell Rep, 14* (7), 1655-1661.

Song, E.J., Lee, E.S. and Nam, Y.D. (2018). Progress of analytical tools and techniques for human gut microbiome research. *J Microbiol, 56* (10), 693-705.

Spor, A., Koren, O. and Ley, R. (2011). Unravelling the effects of the environment and host genotype on the gut microbiome. *Nat Rev Microbiol, 9* (4), 279-290.

Strandwitz, P. (2018). Neurotransmitter modulation by the gut microbiota. *Brain Res, 1693*, 128-133.

Sugiyama, M.G. and Agellon, L.B. (2012). Sex differences in lipid metabolism and metabolic disease risk. *Biochem Cell Biol, 90* (2), 124-141.

Takagi, T., Naito, Y., Inoue, R.*, et al.* (2019). Differences in gut microbiota associated with age, sex, and stool consistency in healthy Japanese subjects. *J Gastroenterol, 54* (1), 53-63.

Tanner, S.A., Zihler Berner, A., Rigozzi, E.*, et al.* (2014). In vitro continuous fermentation model (PolyFermS) of the swine proximal colon for simultaneous testing on the same gut microbiota. *PLoS One, 9* (4), e94123.

Tokuhara, D., Kurashima, Y., Kamioka, M.*, et al.* (2019). A comprehensive understanding of the gut mucosal immune system in allergic inflammation. *Allergol Int, 68* (1), 17-25.

Tolhurst, G., Heffron, H., Lam, Y.S.*, et al.* (2012). Short-chain fatty acids stimulate glucagon-like peptide-1 secretion via the G-protein-coupled receptor FFAR2. *Diabetes, 61* (2), 364-371.

Tsuruta, T., Inoue, R., Nojima, I.*, et al.* (2009). The amount of secreted IgA may not determine the secretory IgA coating ratio of gastrointestinal bacteria. *FEMS Immunol Med Microbiol, 56* (2), 185-189.

Turnbaugh, P.J., Ley, R.E., Mahowald, M.A.*, et al.* (2006). An obesity-associated gut microbiome with increased capacity for energy harvest. *Nature, 444* (7122), 1027-1131.

Ung, K.A., Kilander, A.F., Lindgren, A.*, et al.* (2000). Impact of bile acid malabsorption on steatorrhoea and symptoms in patients with chronic diarrhoea. *Eur J Gastroenterol Hepatol, 12* (5), 541-547.

Vassileva, G., Huwyler, L., Poirier, K.*, et al.* (2000). The intestinal fatty acid binding protein is not essential for dietary fat absorption in mice. *FASEB J, 14* (13), 2040-2046.

Verzelloni, E., Pellacani, C., Tagliazucchi, D.*, et al.* (2011). Antiglycative and neuroprotective activity of colon-derived polyphenol catabolites. *Mol Nutr Food Res, 55* (S1), S35-S43.

von Martels, J.Z.H., Sadaghian Sadabad, M., Bourgonje, A.R.*, et al.* (2017). The role of gut microbiota in health and disease: In vitro modeling of host-microbe interactions at the aerobe-anaerobe interphase of the human gut. *Anaerobe, 44* (Supplement C), 3-12.

Waterston, R.H., Lindblad-Toh, K., Birney, E.*, et al.* (2002). Initial sequencing and comparative analysis of the mouse genome. *Nature, 420* (6915), 520-562.

Watson, L., Lalji, A., Bodla, S.*, et al.* (2015). Management of bile acid malabsorption using low-fat dietary interventions: A useful strategy applicable to some patients with diarrhoea-predominant irritable bowel syndrome? *Clin Med, 15* (6), 536-540.

Wedlake, L., A'Hern, R., Russell, D.*, et al.* (2009). Systematic review: The prevalence of idiopathic bile acid malabsorption as diagnosed by SeHCAT scanning in patients with diarrhoea-predominant irritable bowel syndrome. *Aliment Pharmacol Ther, 30* (7), 707-717.

Weger, B.D., Gobet, C., Yeung, J.*, et al.* (2019). The mouse microbiome is required for sex-specific diurnal rhythms of gene expression and metabolism. *Cell Metab, 29* (2), 362-382.e368.

Williams, C.F., Walton, G.E., Jiang, L.*, et al.* (2015). Comparative analysis of intestinal tract models. *Annu Rev Food Sci Technol, 6*, 329-350.

Williamson, G. and Manach, C. (2005). Bioavailability and bioefficacy of polyphenols in humans. II. Review of 93 intervention studies. *Am J Clin Nutr, 81* (1 Suppl), 243s-255s.

Wostmann, B.S., Larkin, C., Moriarty, A.*, et al.* (1983). Dietary intake, energy metabolism, and excretory losses of adult male germ-free Wistar rats. *Lab Anim Sci, 33* (1), 46-50.

Yano, Jessica M., Yu, K., Donaldson, Gregory P.*, et al.* (2015). Indigenous bacteria from the gut microbiota regulate host serotonin biosynthesis. *Cell, 161* (2), 264-276.

Yatsunenko, T., Rey, F.E., Manary, M.J.*, et al.* (2012). Human gut microbiome viewed across age and geography. *Nature, 486* (7402), 222-227.

Zhang, C., Zhang, M., Wang, S.*, et al.* (2009). Interactions between gut microbiota, host genetics and diet relevant to development of metabolic syndromes in mice. *ISME J, 4* (2), 232-241.

Zhang, X.-Y., Sukhchuluun, G., Bo, T.-B.*, et al.* (2018). Huddling remodels gut microbiota to reduce energy requirements in a small mammal species during cold exposure. *Microbiome, 6* (1), 103.

Zhang, Y., Klein, K., Sugathan, A.*, et al.* (2011). Transcriptional profiling of human liver identifies sex-biased genes associated with polygenic dyslipidemia and coronary artery disease. *PLoS One, 6* (8), e23506-e23506.

Connecting statement to Chapter 2

In Chapter 1, I reviewed the major intrinsic and extrinsic factors that regulate the gut microbiota, and the growing evidence of the relationship between the gut microbiota and acquired metabolic disorders such as obesity. In Chapter 2, I investigate the regulation of the gut microbiota by bile acids, an example of an intrinsic metabolite. Bile acids are synthesized by the liver and secreted into the small intestine to aid in lipid digestion and absorption (Agellon, 2008). The majority of bile acids are recovered in the distal small intestine through an active bile acid reclamation system of ileal enterocytes (Zwicker and Agellon, 2013). Fatty acid binding proteins (Fabps) make up a family of intracellular lipid binding proteins which bind hydrophobic compounds such as fatty acids, bile acids and other small hydrophobic compounds (Agellon et al., 2002). Specifically, fatty acid binding protein 6 (Fabp6) is a key component of the bile acid reclamation system, and its deficiency in mice induces bile acid malabsorption (Praslickova et al., 2012). Bile acid malabsorption increases bile acid concentration in the intestinal lumen, and thus influences the gut microbiota due to the detergent-like properties of bile acids (Begley et al., 2005). The availability of *Fabp6*$^{-/-}$ mice was fortunate for this study. Furthermore, bile acid malabsorption exhibited by these mice is a convenient model of clinical bile acid malabsorption. Yet, the response of the gut microbiota to excess luminal bile acid concentrations, such as in the case of genetically induced malfunction of the bile acid reclamation system, has not been studied comprehensively and thus warrants further investigation.

Our previous studies on the *Fabp6*$^{-/-}$ mouse model showed that bile acid malabsorption causes fat malabsorption (Appendix I). Combined with this finding, *Fabp6*$^{-/-}$ mice displayed sex dimorphic metabolic response to the Western-style diet (WSD) feeding (Appendix I). The aim of the study described in Chapter 2 was to characterize the changes in gut microbiota of *Fabp6*$^{-/-}$ mice challenged with the WSD and to identify the nature of the associated metabolic dysfunction.

Chapter 2

Bile acid malabsorption induces sex dimorphic gut microbial dysbiosis in fatty acid binding protein 6 (Fabp6)-deficient mice

Salam M. Habib[1], Stan Kubow[1], Jianguo Xia[2,3,4,5], Luis B. Agellon[1*]

[1]School of Human Nutrition, [2]Institute of Parasitology, [3]Department of Animal Science, [4]Department of Microbiology and Immunology, [5]Microbiome and Disease Tolerance Center, McGill University, Quebec, Canada.

*Corresponding author at: McGill University School of Human Nutrition, 21111 Lakeshore Road, Ste. Anne de Bellevue, QC H9X 3V9 Canada

Email: luis.agellon@mcgill.ca (L.B. Agellon)

Author contribution: SMH designed and conducted the experiments, analyzed the data, and wrote the manuscript. SK provided access to the gas chromatography and edited the manuscript. JX supervised data analysis and edited the manuscript. LBA was involved in the conception of the experimental design and editing the manuscript.

A version of this manuscript is in preparation for submission to Microorganisms journal.

Abstract

Background: Fabp6 is an abundant cytoplasmic protein that facilitates intracellular transport of bile acids in ileal enterocytes. The loss of Fabp6 causes a defect in bile acid reabsorption in the ileum and results in excessive amounts of bile acids to be passed to the colon. The gut microbiota, a majority of which resides in the colon, is postulated to be a key modulator of the health status of the host. Bile acids impose bacteriostatic and bactericidal actions on a broad range of bacteria; in contrast, the enrichment of particular types of bacteria is made feasible by bile acids. The objective of this study was to determine the changes in the gut microbiota in response to excess luminal concentrations of bile acids in the intestines as a result of Fabp6 deficiency and the association of these modifications with induction of adiposity in mice. **Methods:** Male and female wild-type and *Fabp6*$^{-/-}$ mice were fed either low fat diet (LFD) or Western-style diet (WSD) for 10 weeks. At the end of the controlled feeding period, the bacterial composition of the gut microbiota was assessed by 16S rRNA gene amplicon sequencing of DNA from mouse stool samples. Plasma short-chain fatty acids (SCFAs) and oral glucose tolerance were also measured. **Results:** WSD feeding reduced the gut microbial richness and diversity profiles in both male and female wild-type mice, however, Fabp6 deficiency prevented gut microbial richness and diversity loss in response to WSD in male mice but not female. *Fabp6*$^{-/-}$ mice on WSD showed enrichment of the Lactobacillaceae family, similarly this enrichment was more prominent in male compared to female mice. The gut microbiota of male *Fabp6*$^{-/-}$ mice on WSD showed a higher predicted preference to saccharolysis over proteolysis for SCFAs-production. In wild-type mice, WSD reduced plasma SCFAs in males and induced glucose intolerance in both sexes. Interestingly, superior concentrations of plasma SCFAs and improved glucose tolerance were observed in male *Fabp6*$^{-/-}$ mice compared to their female counterparts on WSD. **Conclusions:** Fabp6 deficiency induces sex dimorphic remodeling of the gut microbiome in response to WSD feeding. The change in the gut microbial composition of male Fabp6-deficient mice on WSD may be associated with differential capacity for saccharolysis and bile acid metabolism which warrants further investigation.

2.1. Introduction

Fatty acid binding protein 6 (Fabp6; also known as ileal lipid binding protein, ileal bile acid binding protein and gastrotropin) is a 14 kDa abundant cytoplasmic protein found in ileal enterocytes. It belongs to the family of intracellular lipid binding proteins, which binds hydrophobic compounds such as fatty acids, cholesterol, some vitamins, and bile acids (Agellon et al., 2002). This family is conserved among various animal species (Gantz et al., 1989; Kanda et al., 1991; Kramer et al., 1993), and its member proteins share a common tertiary structure composed of two orthogonal antiparallel β-sheets that form a barrel-like shape and a helix-loop-helix on top of the barrel (Kramer et al., 2001; Horváth et al., 2016). In Fabp6, a specific gap between the β-strands H and G allows for extra flexibility of structure and larger binding cavity, which increases Fabp6 affinity to bulky and rigid hydrophobic compounds such as bile acids (Besnard et al., 2002; Tochtrop et al., 2003). Fabp6 participates in the intracellular trafficking of bile acids and aids in their recovery from the intestinal lumen (Praslickova et al., 2012). In addition to the Fabp6, the ileal bile acid recovery system also includes the apical sodium bile acid transporter (Asbt), and the organic solute transporter alpha (Ostα) which control the traffic of bile acids into and out of the enterocyte, respectively (Zwicker and Agellon, 2013). Murine Fabp6 binds both conjugated and unconjugated bile acids with higher preference to taurine/glycine-conjugated, doubly hydroxylated bile acids, such as β-muricholic acid and chenodeoxycholic acids (Labonté et al., 2003). The loss of functional Fabp6 in mice results in bile acid malabsorption, which is characterized by excessive amounts of bile acids passed to the colon (Praslickova et al., 2012).

Bile acids are a significant challenge to a wide range of gut microbes. Bile acids possess a detergent activity due to their amphipathic structure (Agellon, 2008). At critical micellar concentrations, bile acids can dissolve microbial cell membrane lipids and cause loss of cellular integrity, leading to leakage of cell contents and cell death. At sub-micellar concentrations, bile acids can modify microbial cell membrane permeability and fluidity, modulate activity of signaling proteins, induce DNA damage, and trigger protein denaturation (Begley et al., 2005).

Gut microbial species differ in their tolerance to bile acids. For example, due to differences in their cell wall structure, Gram-negative bacteria are more resistant to bile acids compared to Gram-positive bacteria. Some Gram-negative bacteria are even able to colonize the gallbladder where bile acids concentrations are extremely high (Crawford et al., 2010). Tolerance to bile acids is explained by the ability of bacteria to biotransform bile acids into forms of lower toxicity and solubility (Ridlon et al., 2014). Primary bile acids are biotransformed by gut microbiota in several ways, including deconjugation (removal of the amino acid side chain), epimerization of the hydroxyl groups attached to carbon atoms of the steroid moiety, and dehydroxylation of the steroid moiety. Biotransformed bile acids have higher potential to passive reabsorption by intestine, and may have additional biological activities on the host (Ridlon et al., 2006; Enright et al., 2018). Interestingly, the ability of some gastrointestinal pathogens to colonize and cause gastrointestinal infection is influenced by the balance between primary and secondary bile acid levels (Britton and Young, 2012). Hence, the exposure to excess bile acids in the gut is expected to modify the structure and composition of the gut microbial community.

In a previous study, bile acid malabsorption in Fabp6-deficient (*Fabp6*$^{-/-}$) mice was shown to also cause intestinal fat malabsorption (Appendix I). However, on Western-style diet (WSD), these mice showed comparable adiposity degree to normal mice without an increase in food intake. This enhancement of adiposity was particularly evident in male mice (Appendix I). The objective of the present study was to determine the nature of the modifications of the gut microbial community when exposed to elevated levels of luminal bile acids as a result of Fabp6 deficiency in mice and whether this modification is associated with enhanced adiposity.

2.2. Materials and methods

Mice and diets

C57BL/6J mice (Jackson Laboratory, Bar Harbor, Maine, USA) were crossed to *Fabp6*$^{-/-}$ mice (Praslickova et al., 2012), heterozygotes of F1 generation were then inbred in harem scheme to yield *Fabp6*$^{+/+}$ (Wild-type) and *Fabp6*$^{-/-}$ mice which were

used in this study. At three weeks of age, mice were weaned (n ≤ 5 mice per cage) and their genotypes were confirmed by PCR as described previously (Appendix I). Mice of wild-type and *Fabp6*$^{-/-}$ genotypes were then separated and heterozygotes were euthanized. Mice were maintained in a climate-controlled facility with a 12-h light/dark photoperiod, and on the Teklad 2020X diet (Teklad-Envigo, Lachine, QC). Age matched, wild-type and *Fabp6*$^{-/-}$ sibling mice (n = 5-6 mice per treatment housed in 3-5 cages per treatment; males and females in separate groups) were placed on WSD (D12079B, Research Diets, New Brunswick, NJ) or maintained on Teklad 2020X, which was used as a reference low fat diet (LFD) for 10 weeks. During this period, mice had free access to food and water. At the end of the controlled diet period, stool samples from each mouse were collected and mice were fasted for 16 h prior isoflurane/CO_2 euthanasia, which was followed by total blood collection through cardiac puncture. Collected stools and plasma were stored at -70°C until analyzed. The use of animals was approved by the animal care and use committee at McGill University in concordance with the Canadian Council on Animal Care.

DNA extraction and sequencing

DNA was extracted from mouse stool samples using Maxwell16 Tissue DNA Purification Kit (Promega Co., Madison, WI, USA) preceded with lysozyme incubation step to facilitate the extraction of DNA from Gram-positive bacteria (Wierczorek and Schagat, 2007). Extracted DNA samples were quality checked by gel electrophoresis and quantified using Qubit fluorometer 2.0 (Thermo Fisher Scientific, Waltham, USA). Library preparation and amplicon sequencing were performed at Génome Québec Innovation Centre, Montréal, Canada. Briefly, hypervariable region V3-V4 region of the 16S rRNA gene was amplified by PCR using specifically tagged primers: 338F-CS1: ACACTGACGACATGGTTCTACAACTCCTACGGGAGGCAGCAG, and 806R-CS2: TACGGTAGCAGAGACTTGGTCTGGACTACHVGGGTWTCTAAT. This was followed by a second PCR step where barcodes and Illumina adaptors were appended. Equal amounts of each sample were added to form a pool, which was purified with Agencourt AMPure beads (Beckman Coulter Canada Inc., Mississauga, ON, Canada), quantified using Kapa Illumina GA with Revised Primers-SYBR Fast Universal kit (Kapa

Biosystems Inc., Wilmington, MA, USA), and the average fragment size was determined using a LabChip GX (PerkinElmer, Waltham, MA, USA) instrument. Before sequencing, 25% of Phix control library was spiked into the amplicon pool (at a final concentration of 4pM) to improve the unbalanced base composition. Amplicon pool was loaded to the flow cell and sequenced for 500 cycles using 250bp paired end MiSeq Illumina platform (Miseq v2 Reagent Kit, Illumina, San Diego, CA).

Bioinformatics

Sequence pre-processing: 16S rRNA gene amplicon reads obtained from Illumina in demultiplexed FASTQ format were uploaded to supercluster Cedar of WestGrid and Compute Canada where bioinformatic analyses were performed. First, reads were quality inspected using FastQC v.0.11.8 (Andrews, 2010), then, primer sequences were trimmed using Cutadapt v.1.10 (Martin, 2011), next, reads were imported as a Quantitative Insights Into Microbial Ecology 2 artifact (QIIME 2).

Resolving sequence variants: The workflow of QIIME2 v.2019.1.0 (Bolyen et al., 2019) was followed for resolving sequence variants and their identification as described in Microbiome Helper pipeline v.2.0 (Comeau et al., 2017). Briefly, forward and reverse reads were joined by VSEARCH v.2.12.0 (Rognes et al., 2016), low-quality joined reads and chimeric sequences were filtered out using q2-quality-filter plugin of QIIME2 (Bokulich et al., 2013) and UCHIME algorithm (Edgar et al., 2011), respectively. Deblur algorithm v.1.1.0 (Amir et al., 2017) was used to resolve the amplicon sequence variants (ASVs) (Callahan et al., 2017). Taxonomy was assigned to ASVs using q2-feature-classifier of QIIME2 (Bokulich et al., 2018) based on a 338F/806R amplicon specific (Werner et al., 2012) pre-trained sklearn (Pedregosa et al., 2011) Naïve Bayesian classifier against SILVA v.132 reference release (Yilmaz et al., 2013) with 99% confidence level. Finally, the ASV table and taxonomy data were exported from QIIME2 in biom format (McDonald et al., 2012) and converted to .tsv format for visualization and statistical analysis.

Data decontamination: Prior to visualization and statistics, ASVs were filtered to remove taxa present in only one sample (minimal filtration), taxa with low count (10% of

samples each contain ≥ 1 read), and taxa with low variance (10% of lowest variance taxa based on inter-quantile range) using SanityCheckData, ApplyAbundunceFilter, and ApplyVarianceFilter functions of MicrobiomeAnalyst, respectively (Dhariwal et al., 2017). Samples were confirmed to have a minimum of 2000 reads each, and a difference in sequencing depth of <10x.

α- and β-diversity: Taxonomic richness, estimated by Chao1 index, and diversity estimated by Shannon's diversity index (*H*) which accounts for both species richness and evenness were calculated for ASV data with minimal filtration applied using phyloseq R package v.1.32.0 (McMurdie and Holmes, 2013) implemented by MicrobiomeAnalyst (Dhariwal et al., 2017). In addition, the rarefaction curves and Good's coverage based on unfiltered ASV data were calculated (Appendix II). To investigate the differences in taxa among experimental groups (β-diversity) principal coordinate analysis (PCoA) was calculated using Bray-Curtis dissimilarity metric at the species level with phyloseq R package v.1.32.0 (McMurdie and Holmes, 2013) implemented by MicrobiomeAnalyst (Dhariwal et al., 2017).

Heatmap clustering and microbial composition: ASVs with abundance greater than 100 were clustered by Ward algorithm based on Euclidean distance measure and visualized in a heatmap using ggplot2 v.3.3.2 (Wickham, 2016) and viridis v.0.5.1 (Garnier, 2018) as implemented by MicrobiomeAnalyst (Dhariwal et al., 2017). The relative abundance of the gut microbial families, and the corresponding phyla were exported from MicrobiomeAnalyst and visualized in pie plot using GraphPad Prism v.8.2.1 (GraphPad Software Inc., CA, USA).

Metabolic potential of the gut microbiota: The genes present in the gut microbial community (i.e. metagenomes) were inferred from the 16S rRNA gene data using Tax4Fun R package v.0.3.1 (Asshauer et al., 2015) against SILVA v.123 reference release and based on precalculated metabolic reference profiles from the Kyoto Encyclopedia of Genes and Genomes (KEGG) (Kanehisa and Goto, 2000). The produced KEGG ortholog (KO) table was then analyzed using the Shotgun data profiling module of MicrobiomeAnalyst (Dhariwal et al., 2017). Briefly, KO entries were

filtered to remove low count entries (20% of samples each contain ≥ 4 hits), and low variance entries (10% of lowest variance entries based on inter-quantile range) using ApplyAbundunceFilter, and ApplyVarianceFilter functions of MicrobiomeAnalyst (Dhariwal et al., 2017), respectively. Then, KO entries were scaled by cumulative sum scaling and the total hits of KEGG metabolism of macromolecules, or KEGG pathways involved in SCFA and secondary bile acid biosynthesis were compared between genotypes. The targeted pathways are outlined in Appendix II.

Short-chain fatty acids

Plasma samples were mixed 1:2 with methanol (GC grade) and centrifuged at 14,000 g for 60 min. One microliter of supernatant was injected into an Agilent gas chromatograph system 7890A, with flame ionization detector (Agilent Technologies, Wilmington, DE, USA). Short-chain fatty acids *(*SCFAs) were separated on a 19091N-133 Agilent capillary column. Helium was used as the carrier gas at a flow rate of 1.0 mL/min. Oven temperature was set to 100 °C for 10 min and gradually increased over 25 min to reach 220 °C. SCFAs standard solution (Supelco, cat.46975-U, Bellefonte, PA, USA) was used for peak identification.

Oral glucose tolerance test

Mice were fasted for four hours to prevent weight loss and minimize discomfort for the mice (Heijboer et al., 2005; Jensen et al., 2013). Glucose (2 g/kg body weight) was administered by oral gavage. Blood samples were collected from the tail vein for baseline and glucose monitoring over 2 h using OneTouch UltraMini glucometer (LifeScan Inc., Milpitas, CA, USA).

Statistical analysis

Statistics were performed with GraphPad Prism v.8.2.1 (GraphPad Software Inc., CA, USA) and RStudio v.1.1.463 with R v.3.5.2 and 4.0 (R Core Team, 2020). All statistical analyses were applied to male and female mice separately. Normality of the data was evaluated using Shapiro-Wilk test. The details of the statistical tests are provided in the figure legends. Data is presented as mean ± SEM unless otherwise indicated. Means denoted by (*) symbol or different superscript letters indicate a

significant difference by unpaired student's *t*-test, or one-way ANOVA accompanied with Fisher's LSD test, respectively, unless stated otherwise. The differences were considered significant when $p<0.05$.

Permutational analysis of variance (PERMANOVA) for PCoA was calculated using Adonis function of VEGAN package v.2.5-6 (Dixon, 2003). Pairwise PERMANOVAs with FDR correction were calculated using RVAideMemoire package v.0.9-75 (Hervé, 2020). The ellipses of PCoA were plotted using ggplot2 package v.3.3.2 (Wickham, 2016) and indicate 95% level of confidence based on *t* distribution.

For the indicator taxa (biomarker) analysis, gut microbial genera estimated by the LefSe model (Segata et al., 2011) were used to predict classifier taxa. To evaluate the differential abundance of the estimated genera between genotypes a number of statistical models were applied (Mann-Whitney *U*-test of R base, Zero inflated gaussian mixture (ZIG) and Zero inflated log normal mixture (ZILN) of MetagenomeSeq v.3.11 (Paulson et al., 2013), EdgeR v.3.9 (Robinson et al., 2010), and DESeq2 v.3.11 (Love et al., 2014). For stringency, $p<0.05$ in two or more of these tests were considered significant.

2.3. Results

2.3.1. Modification of the gut microbial diversity by Fabp6 deficiency is influenced by mice sex and diet

Fabp6$^{-/-}$ mice exhibited changes in Firmicutes:Bacteroidetes ratio as shown by quantitative PCR assays (Appendix I). To characterize the gut microbial changes in *Fabp6*$^{-/-}$ mice at a higher resolution we sequenced the phylogenetic marker gene encoding 16S rRNA. First, both taxonomic richness estimated by Chao1 index, and diversity represented by Shannon's index were investigated (Shannon, 1948; Chao, 1984). On LFD, Fabp6 deficiency reduced the taxonomic richness of the gut microbial community in male *Fabp6*$^{-/-}$ mice, but not in female *Fabp6*$^{-/-}$ mice compared to their respective wild-type counterparts (Fig. 2-1A and Fig. 2-1B). Both male and female wild-type mice showed lower taxonomic richness and diversity in their gut microbial

community on WSD compared to LFD (Fig. 2-1A and Fig. 2-1B). Female *Fabp6*$^{-/-}$ mice also showed lower gut microbial richness and diversity on WSD compared to LFD (Fig. 2-1A and 2-1B). The lower gut microbial richness in response to Fabp6-deficiency or WSD feeding is unlikely due to sequencing depth, as the average Good's coverage of samples was 99.8% ± 0.09 (mean ± SD) with a lowest value of 99.5% (Appendix II). Interestingly, only male *Fabp6*$^{-/-}$ mice exhibited similar gut microbial richness and diversity on both diets and showed higher gut microbial diversity compared to their wild-type counterparts on WSD (Fig. 2-1A and Fig. 2-1B). Thus, the response of gut microbial α-diversity to WSD in mice is influenced by their Fabp6 genotype and sex.

To estimate the β-diversity of gut microbial communities of mice, principal coordinate analysis (PCoA) was used to plot Bray Curtis distances between samples. Both male and female *Fabp6*$^{-/-}$ mice showed similar patterns of sample distribution to their wild-type counterparts on LFD (Males: Fig. 2-2A, left; females: Fig. 2-2A, right). WSD induced further separation of *Fabp6*$^{-/-}$ mice samples from their wild-type counterparts, a pattern that was more evident in male compared to female mice (Males: Fig. 2-2A, left; females: Fig. 2-2A, right). Similarly, only male *Fabp6*$^{-/-}$ mice, but not female, showed a distinct heatmap clustering pattern of species abundance compared to their wild-type counterparts on WSD (Males: Fig. 2-2B, left; females: Fig. 2-2B, right). Thus, Fabp6 deficiency results in a unique pattern of gut microbiota in male mice on WSD.

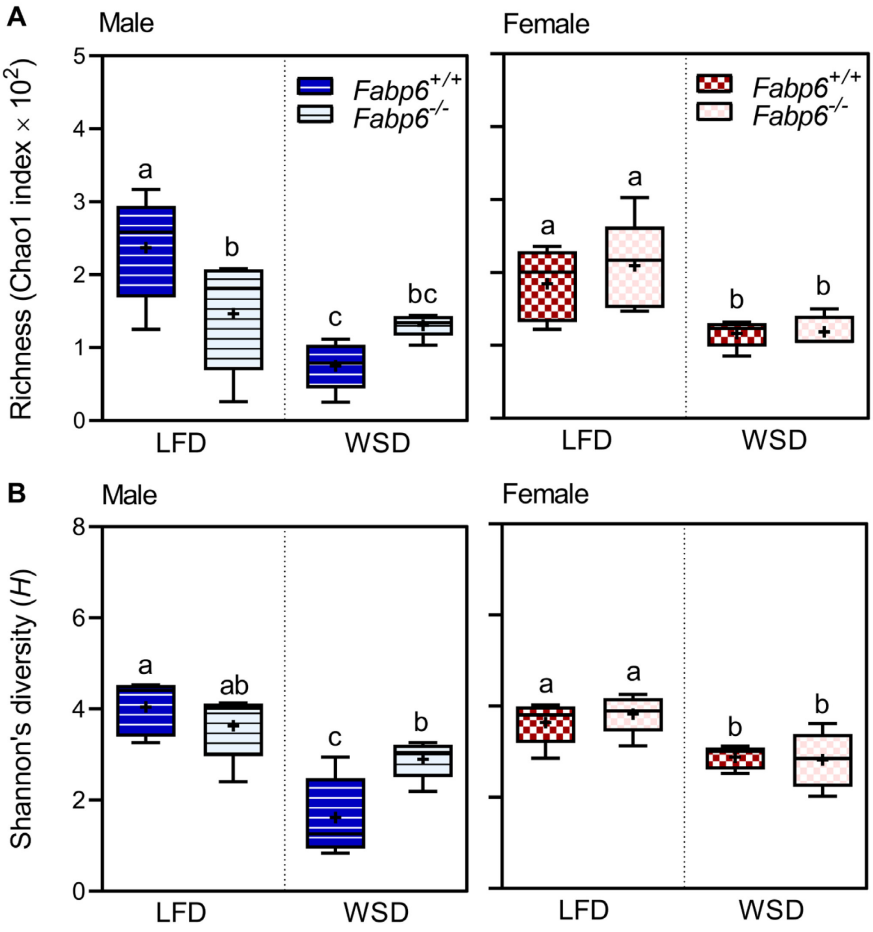

Figure 2-1. Sex dimorphic gut microbial α-diversity in response to Fabp6-deficency. (A) Chao1 index represents gut microbial richness, (B) Shannon's diversity (*H*) index accounts for gut microbial richness and evenness; (n=5), (+) represent mean and whiskers represent range, means denoted by different letters indicate a significant difference (p<0.05) by one-way ANOVA accompanied with Fisher's LSD test, males and females analyzed in separate models. Dark and light bars indicate *Fabp6*$^{+/+}$ and *Fabp6*$^{-/-}$ mice, respectively. Blue and red indicate male and female mice, respectively. LFD: low fat diet, WSD: Western-style diet.

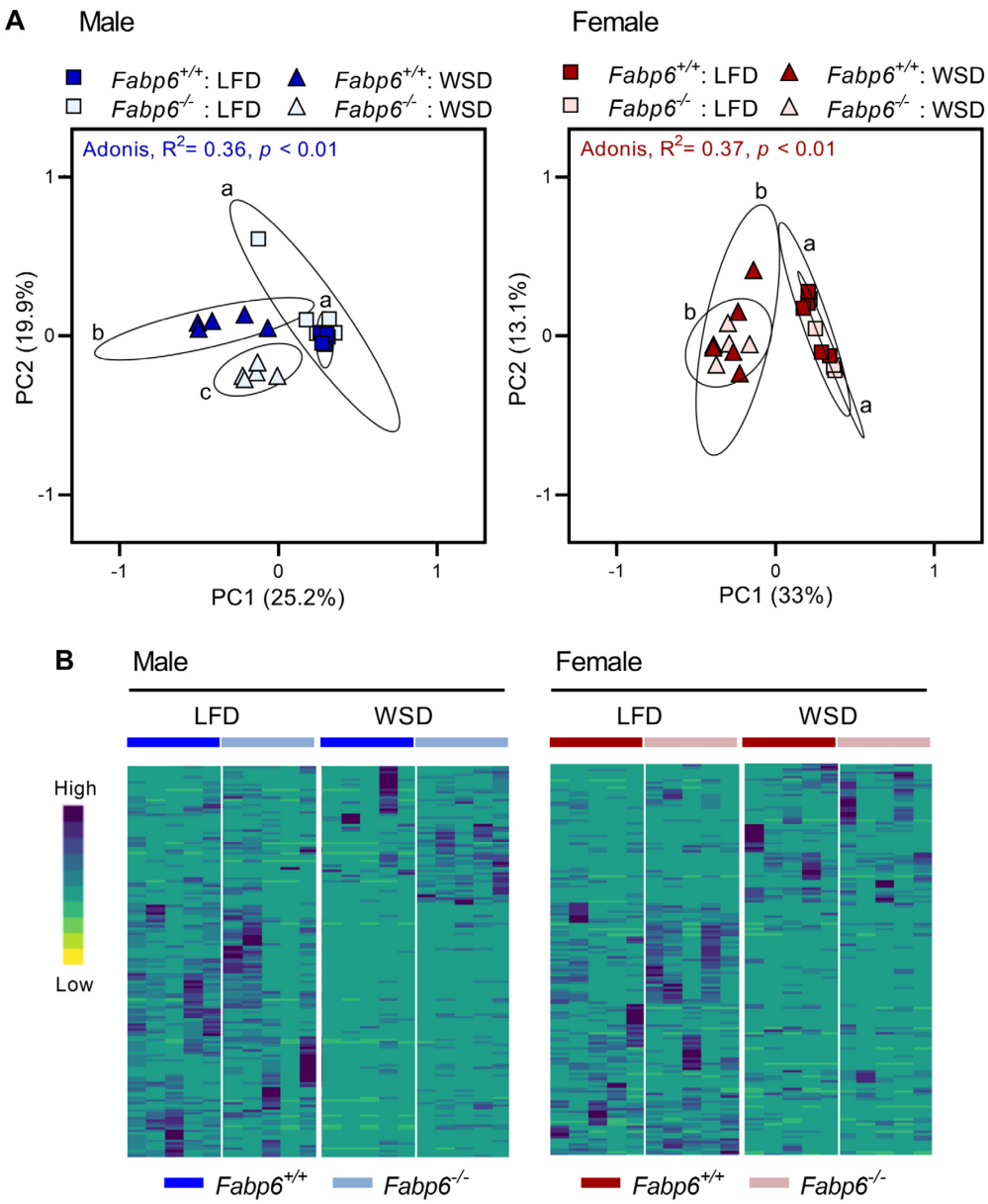

2-2. Distinct male and female gut microbial responses to Fabp6-deficency and WSD. (A) Principal coordinate analysis of gut microbial samples of male and female mice on LFD and WSD, sample clusters denoted by different letters indicate significant clustering (p<0.05) by Adonis PERMANOVA accompanied with FDR corrected pairwise comparisons, ellipses indicate 95% level of confidence assuming *t* distribution (n=5). Males and females analyzed in separate models. (B) Heatmap of gut microbial species abundance, Ward algorithm clustering based on Euclidean distance measure (n=5). Square and tringle symbols represent LFD and WSD, respectively. Dark and light colors indicate *Fabp6*$^{+/+}$ and *Fabp6*$^{-/-}$ mice, respectively. Blue and red indicate male and female mice, respectively. Fabp6: Fatty acid binding protein 6, PC: principal coordinate, LFD: low fat diet, WSD: Western-style diet.

2.3.2. Distinct gut microbial dysbiosis in male Fabp6$^{-/-}$ mice fed WSD

To gain further insights of the distinctive pattern of gut microbiota of *Fabp6*$^{-/-}$ mice, the proportions of gut microbiota at the phylum, family, and genus levels were examined. At the phylum level, compared to their wild-type counterparts, male *Fabp6*$^{-/-}$ mice showed higher Firmicutes:Bacteroidetes ratio, while female *Fabp6*$^{-/-}$ mice showed lower Firmicutes:Bacteroidetes ratio on LFD (Males: Fig. 2-3A, top; females: Fig. 2-3B, top). Mice of both sexes and genotypes showed higher Firmicutes: Bacteroides ratio on WSD compared to mice on LFD (Males: Fig. 2-3A; females: Fig. 2-3B). Male *Fabp6*$^{-/-}$ mice on WSD, but not female, showed higher Bacteroidetes and lower Proteobacteria compared to their wild-type counterparts on the same diet (Males: Fig. 2-3A bottom; females: Fig. 2-3B bottom).

At the family level, male and female *Fabp6*$^{-/-}$ mice showed different patterns of abundant families of gut microbiota on LFD. For example, compared to their respective wild-type counterparts, male *Fabp6*$^{-/-}$ mice showed a sex-specific increase in the family Erysipelotrichaceae, while female *Fabp6*$^{-/-}$ mice showed a sex-specific increase in the family Rikenellaceae (Males: Fig. 2-3A, top; females: Fig. 2-3B, top). The proportions of Bacteroidaceae, Lachnospiraceae, and Muribaculaceae, the main families of gut microbiota of mice on LFD, were similar between *Fabp6*$^{-/-}$ and wild-type mice in both males and females (Males: Fig. 2-3A, top; females: Fig. 2-3B, top). WSD induced the expansion of Peptostreptococcaceae and Enterococcaceae in male but not in female wild-type mice, this effect was absent in male *Fabp6*$^{-/-}$ mice on the same diet (Males: Fig. 2-3A, bottom; females: Fig. 2-3B, bottom). Remarkably, both male and female *Fabp6*$^{-/-}$ mice had higher proportions of Lactobacillaceae on WSD compared to their wild-type counterparts. This increase of Lactobacillaceae was prominent in male compared to female *Fabp6*$^{-/-}$ mice (Males: Fig. 2-3A, bottom; females: Fig. 2-3B, bottom). Based on these results, Fabp6 deficiency induced sex dimorphic gut microbial dysbiosis and altered the gut microbial response to the WSD.

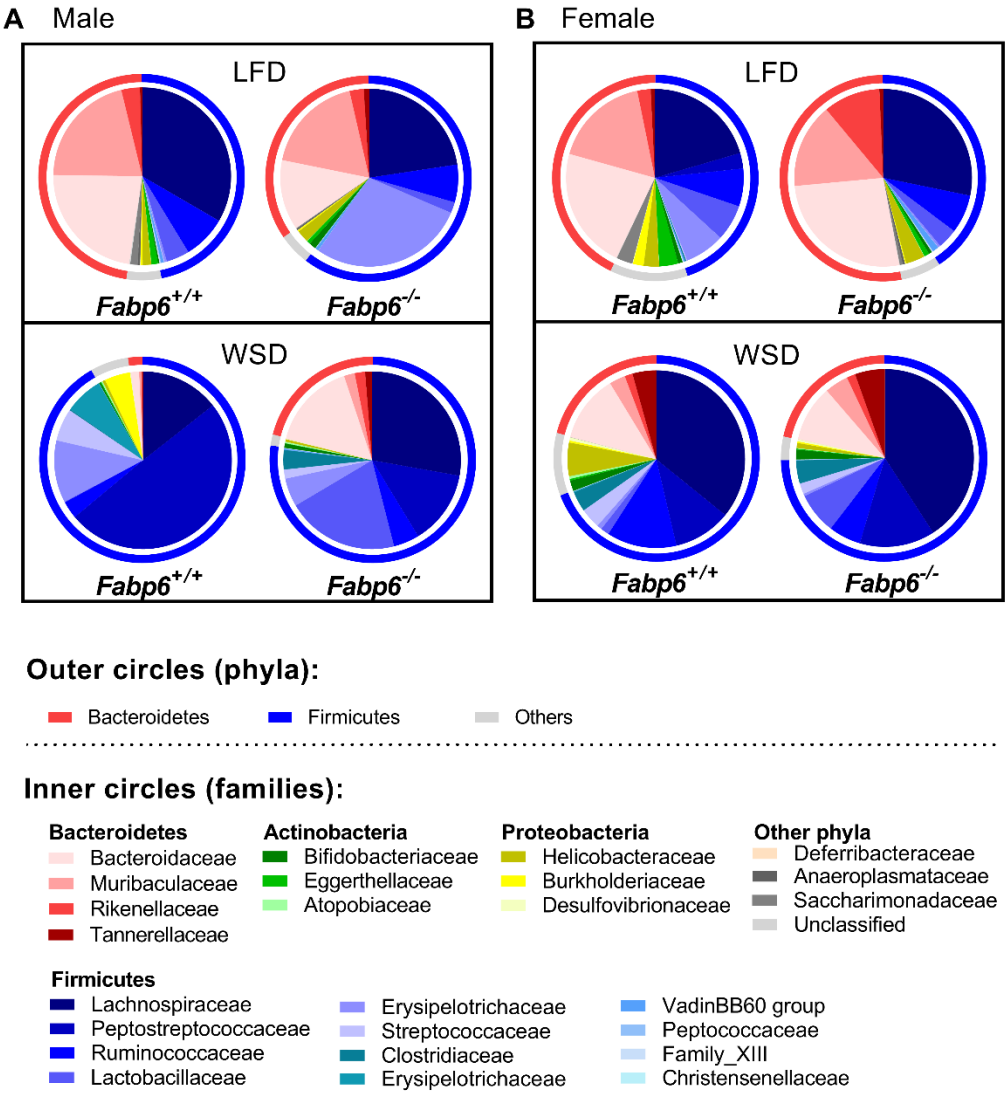

Figure 2-3. Sex dimorphic gut microbial dysbiosis in *Fabp6*$^{-/-}$ mice in response to WSD. (A) Male and (B) female. Outer circles represent relative abundance of the gut microbiota at the phylum level, inner circles represent relative abundance of the gut microbiota at the family level. n=5 mice per group. Fabp6: Fatty acid binding protein 6, LFD: low fat diet, WSD: Western-style diet.

Next, we used the LefSe model to compare the gut microbial composition and discover candidate classifier taxa at the genus level. A set of statistical tests were used to identify the differentially abundant classifier taxa (Dhariwal et al., 2017). On LFD, lower number of candidate classifiers were discovered in *Fabp6*$^{-/-}$ mice compared to their wild-type counterparts in both males and females (Males: Fig. 2-4A; females: Fig. 2-4B). *Angelakisella*, was the only differentially abundant gut microbial classifier of male *Fabp6*$^{-/-}$ mice, which was not shared with their female counterparts, whose gut microbiota were characterized by differential abundance of each of *Allstipes*, *Anaerotruncus* and *Butyricicoccus* (Males: Fig. 2-4A; Females: Fig. 2-4B). On WSD, higher number of candidate classifiers were discovered in male *Fabp6*$^{-/-}$ mice compared to their wild-type counterparts, while similar number of candidate classifiers were discovered in both female *Fabp6*$^{-/-}$ mice and their wild-type counterparts (Males: Fig. 2-5A; females: Fig. 2-5B). Eleven gut microbial classifiers of male *Fabp6*$^{-/-}$ mice were differentially abundant compared to their wild-type counterparts, these include for example *Bacteroides* and *Lactobacillus* (Fig. 2-5A). Only *Faecalibacterium_UBA1819* was differentially abundant classifier of female *Fabp6*$^{-/-}$ mice gut microbiota on WSD (Fig. 2-5B). Thus, Fabp6 deficiency and WSD together induce distinct genus composition among the gut microbial communities of male and female mice.

2.3.3. Higher predicted capacity to produce SCFAs by saccharolysis and metabolize bile acids in of male Fabp6$^{-/-}$ *mice fed WSD*

Next, encoded metabolic capacities of the gut microbial communities of mice were predicted based on their 16S rRNA sequences using Tax4Fun R package (Asshauer et al., 2015). On LFD, the gut microbiota of male *Fabp6*$^{-/-}$ mice were predicted to have lower proportions of genes involved in metabolizing carbohydrates (Fig. 2-6A, left), while that of female *Fabp6*$^{-/-}$ mice were predicted to have higher proportions of genes involved in metabolizing each of the macronutrients compared to their respective wild-type counterparts (Fig. 2-6A, right). Conversely, on WSD, the gut microbiota of male *Fabp6*$^{-/-}$ mice were predicted to have higher proportions of genes involved in metabolizing carbohydrates and lipids compared to that of their wild-type counterparts, while no difference was found in females (Fig. 2-6B).

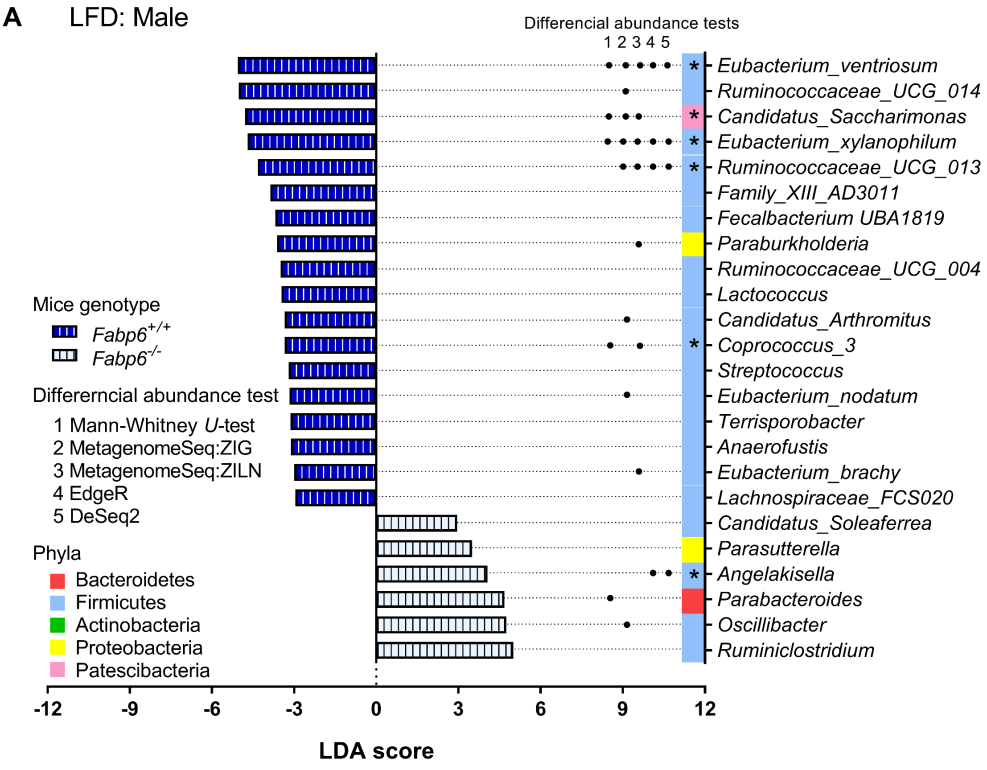
A
LFD: Male
Differencial abundance tests
1 2 3 4 5
Eubacterium_ventriosum
Ruminococcaceae_UCG_014
Candidatus_Saccharimonas
Eubacterium_xylanophilum
Ruminococcaceae_UCG_013
Family_XIII_AD3011
Fecalbacterium UBA1819
Paraburkholderia
Ruminococcaceae_UCG_004
Lactococcus
Candidatus_Arthromitus
Coprococcus_3
Streptococcus
Eubacterium_nodatum
Terrisporobacter
Anaerofustis
Eubacterium_brachy
Lachnospiraceae_FCS020
Candidatus_Soleaferrea
Parasutterella
Angelakisella
Parabacteroides
Oscillibacter
Ruminiclostridium
Mice genotype
Fabp6+/+
Fabp6-/-
Differerncial abundance test
1 Mann-Whitney U-test
2 MetagenomeSeq:ZIG
3 MetagenomeSeq:ZILN
4 EdgeR
5 DeSeq2
Phyla
Bacteroidetes
Firmicutes
Actinobacteria
Proteobacteria
Patescibacteria
-12 -9 -6 -3 0 3 6 9 12
LDA score

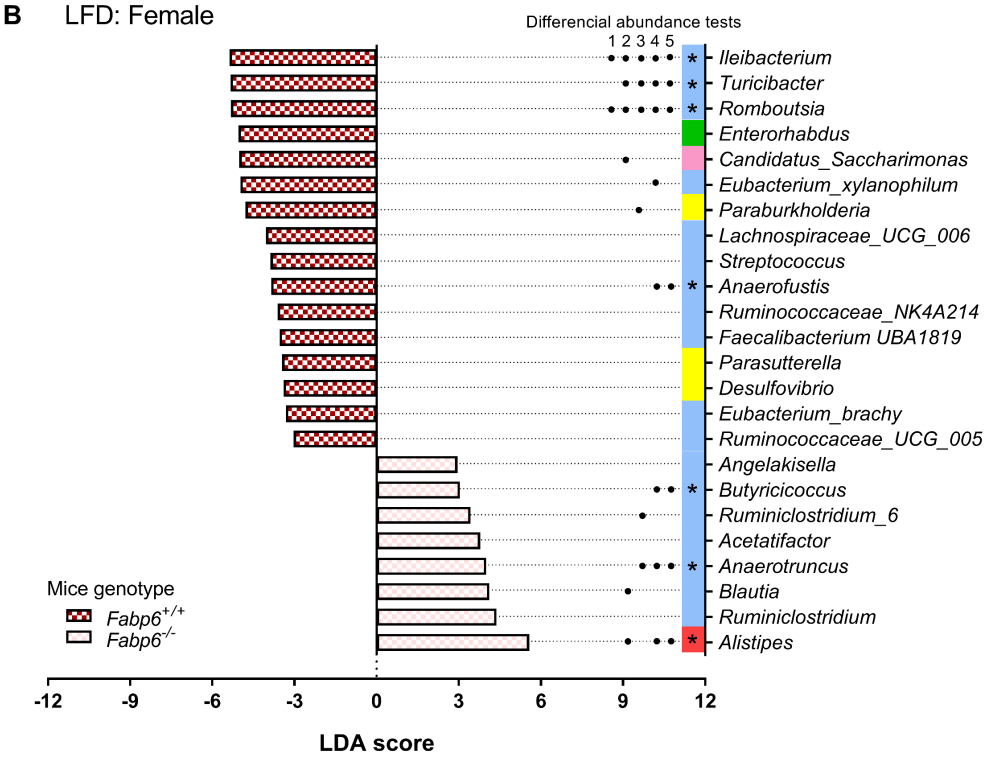
B
LFD: Female
Differencial abundance tests
1 2 3 4 5
Ileibacterium
Turicibacter
Romboutsia
Enterorhabdus
Candidatus_Saccharimonas
Eubacterium_xylanophilum
Paraburkholderia
Lachnospiraceae_UCG_006
Streptococcus
Anaerofustis
Ruminococcaceae_NK4A214
Faecalibacterium UBA1819
Parasutterella
Desulfovibrio
Eubacterium_brachy
Ruminococcaceae_UCG_005
Angelakisella
Butyricicoccus
Ruminiclostridium_6
Acetatifactor
Anaerotruncus
Blautia
Ruminiclostridium
Alistipes
Mice genotype
Fabp6+/+
Fabp6-/-
-12 -9 -6 -3 0 3 6 9 12
LDA score

Figure 2-4. Differential analysis of classifier genera discovered by LefSe model in LFD-fed mice. (A) Male, (B) female. n=5 mice per group. Dark and light bars indicate *Fabp6*$^{+/+}$ and *Fabp6*$^{-/-}$ mice, respectively. Blue and red indicate male and female mice respectively, (●) indicate $p<0.05$, (*) indicate 2 or more statistical tests with $p<0.05$. LDA: Linear discriminant analysis score, Fabp6: Fatty acid binding protein 6, LFD: low fat diet.

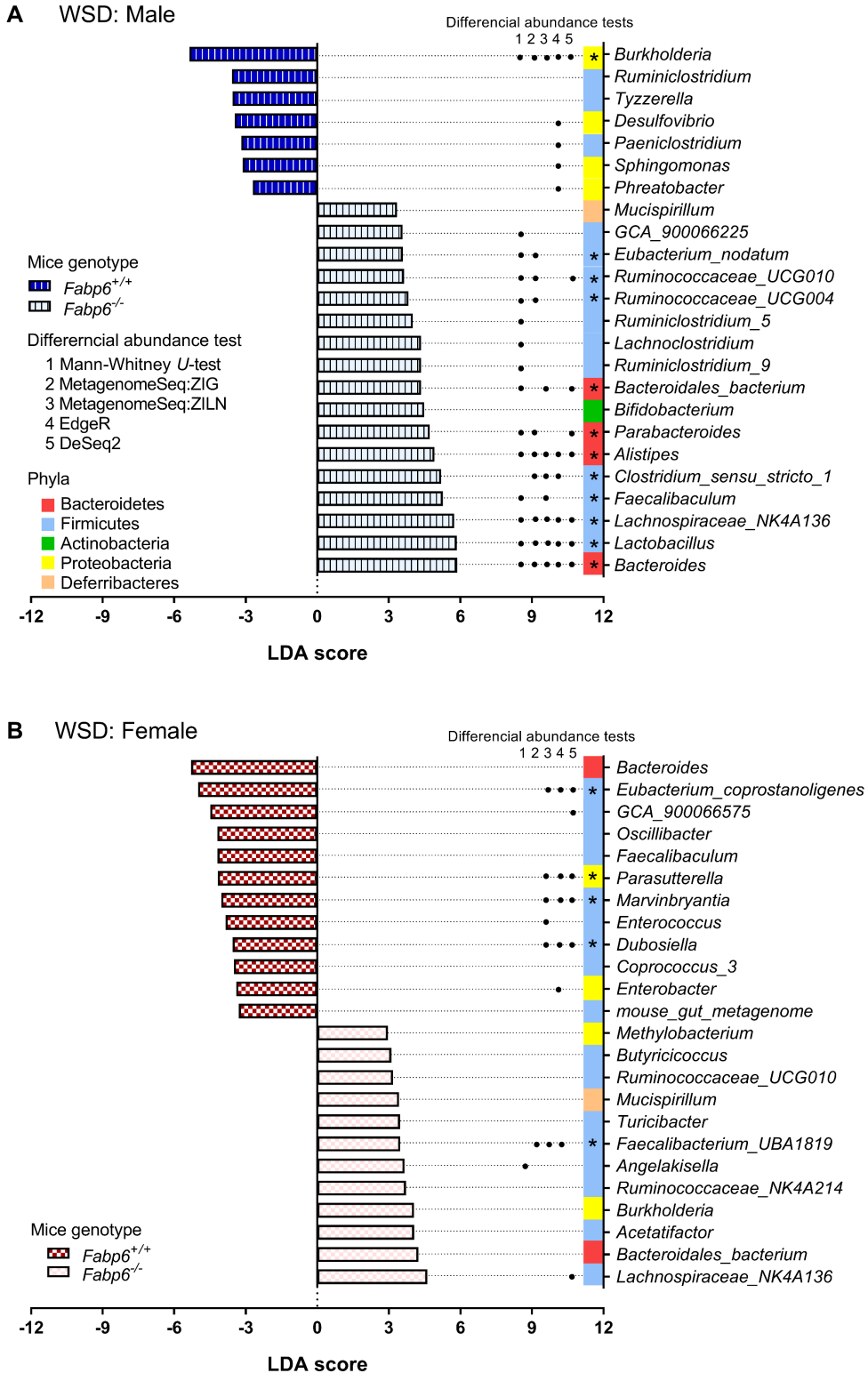
A
WSD: Male
Differencial abundance tests
1 2 3 4 5
Burkholderia
Ruminiclostridium
Tyzzerella
Desulfovibrio
Paeniclostridium
Sphingomonas
Phreatobacter
Mucispirillum
GCA_900066225
Eubacterium_nodatum
Ruminococcaceae_UCG010
Ruminococcaceae_UCG004
Ruminiclostridium_5
Lachnoclostridium
Ruminiclostridium_9
Bacteroidales_bacterium
Bifidobacterium
Parabacteroides
Alistipes
Clostridium_sensu_stricto_1
Faecalibaculum
Lachnospiraceae_NK4A136
Lactobacillus
Bacteroides
Mice genotype
Fabp6+/+
Fabp6-/-
Differerncial abundance test
1 Mann-Whitney U-test
2 MetagenomeSeq:ZIG
3 MetagenomeSeq:ZILN
4 EdgeR
5 DeSeq2
Phyla
Bacteroidetes
Firmicutes
Actinobacteria
Proteobacteria
Deferribacteres
-12 -9 -6 -3 0 3 6 9 12
LDA score
B
WSD: Female
Differencial abundance tests
1 2 3 4 5
Bacteroides
Eubacterium_coprostanoligenes
GCA_900066575
Oscillibacter
Faecalibaculum
Parasutterella
Marvinbryantia
Enterococcus
Dubosiella
Coprococcus_3
Enterobacter
mouse_gut_metagenome
Methylobacterium
Butyricicoccus
Ruminococcaceae_UCG010
Mucispirillum
Turicibacter
Faecalibacterium_UBA1819
Angelakisella
Ruminococcaceae_NK4A214
Burkholderia
Acetatifactor
Bacteroidales_bacterium
Lachnospiraceae_NK4A136
Mice genotype
Fabp6+/+
Fabp6-/-
-12 -9 -6 -3 0 3 6 9 12
LDA score

Figure 2-5. Differential analysis of classifier genera discovered by LefSe model in WSD-fed mice. (A) Male, (B) female. n=5 mice per group. Dark and light bars indicate *Fabp6*$^{+/+}$ and *Fabp6*$^{-/-}$ mice, respectively. Blue and red indicate male and female mice respectively, (●) indicate $p<0.05$, (*) indicate 2 or more statistical tests with $p<0.05$. LDA: Linear discriminant analysis score, Fabp6: Fatty acid binding protein 6, WSD: Western-style diet.

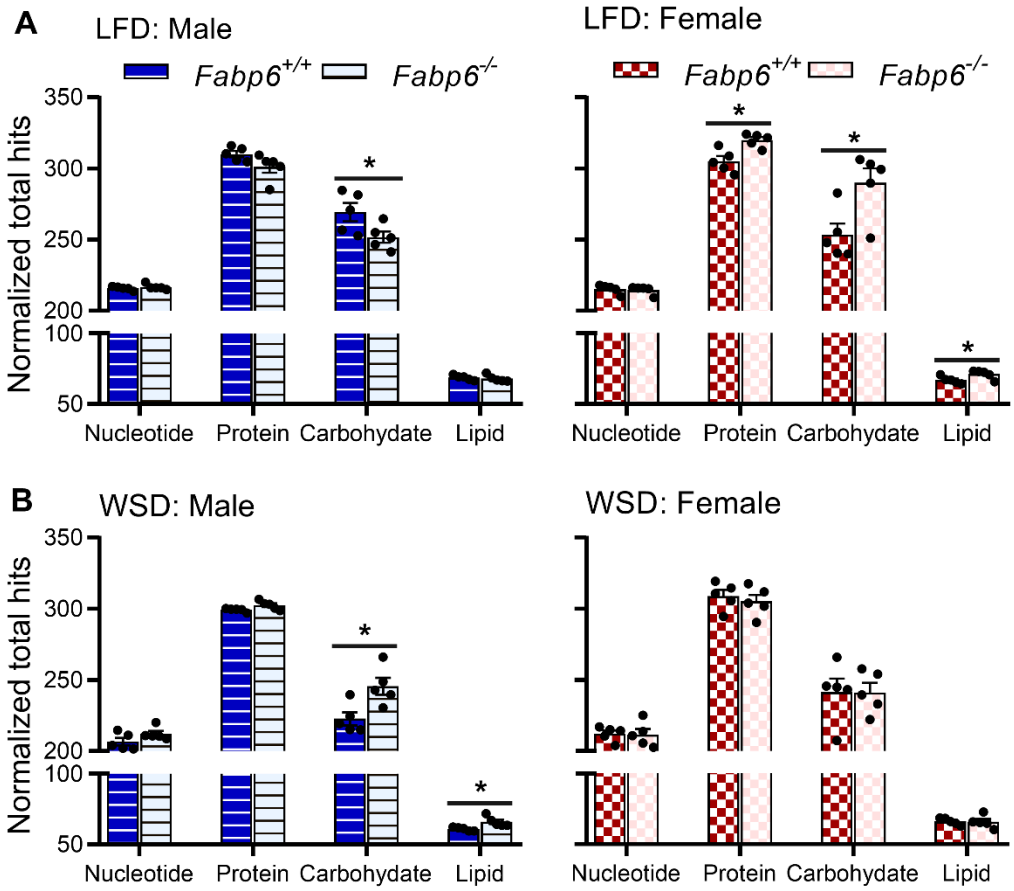

Figure 2-6. Fabp6 deficiency alters the gut microbiome ability to metabolize macronutrients. Normalized total hits of gut microbial genes inferred from 16S rRNA gene data and pinned to macromolecule metabolism of male and female mice fed (A) LFD, and (B) WSD, mean ± SEM (n=5), means denoted by (*) indicate a significant difference (p<0.05) by unpaired t test. Dark and light bars indicate *Fabp6*$^{+/+}$ and *Fabp6*$^{-/-}$ mice, respectively. Blue and red indicate male and female mice, respectively. Fabp6: Fatty acid binding protein 6, LFD: low fat diet, WSD: Western-style diet.

SCFAs are common products of gut microbial catabolism of carbohydrate and protein, and these abundant microbial metabolites represent a source of energy for the host. Using Tax4Fun package, the capacity of the gut microbiome to produce SCFAs by saccharolysis or proteolysis were predicted. On LFD, the gut microbiome of both male and female *Fabp6*$^{-/-}$ mice have the genetic ability to produce SCFAs by both saccharolysis and proteolysis without a specific preference (Fig. 2-7A). On WSD, the gut microbiome of male *Fabp6*$^{-/-}$ mice, but not female, showed higher proportions of genes involved in SCFAs production by saccharolysis over proteolysis compared to that of their wild-type counterparts (Fig. 2-7B). Thus, the enrichment of gut microbial species with preference to saccharolysis in Fabp6-deficient mice appears to be influenced by the sex and diet.

Bile salt hydrolases (BSH) catalyze the deconjugation of bile acids from taurine or glycine, while 7α-hydroxysteroid dehydrogenase (HDHA) catalyzes the oxidation of 7α-hydroxyl group of primary bile acids to produce secondary bile acids. On WSD, male wild-type mice, but not females, showed lower predicted abundance of the gut microbial *bsh* compared to their counterparts on LFD (Males: Fig. 2-7C, left; females: Fig. 2-7C, right). Conversely, male *Fabp6*$^{-/-}$ mice showed similar predicted abundance of the gut microbial *bsh* on both diets, while female *Fabp6*$^{-/-}$ mice on WSD showed lower predicted abundance of the gut microbial *bsh* compared to their counterparts on LFD (Males: Fig. 2-7C, left; females: Fig. 2-7C, right). Although significance was not reached, only male *Fabp6*$^{-/-}$ mice showed higher predicted abundance of the gut microbial *HdhA* compared to their wild-type mice on both diets (Fig. 2-7C, left). Thus, male *Fabp6*$^{-/-}$ mice are predicted to have enhanced ability to metabolize bile acids on WSD.

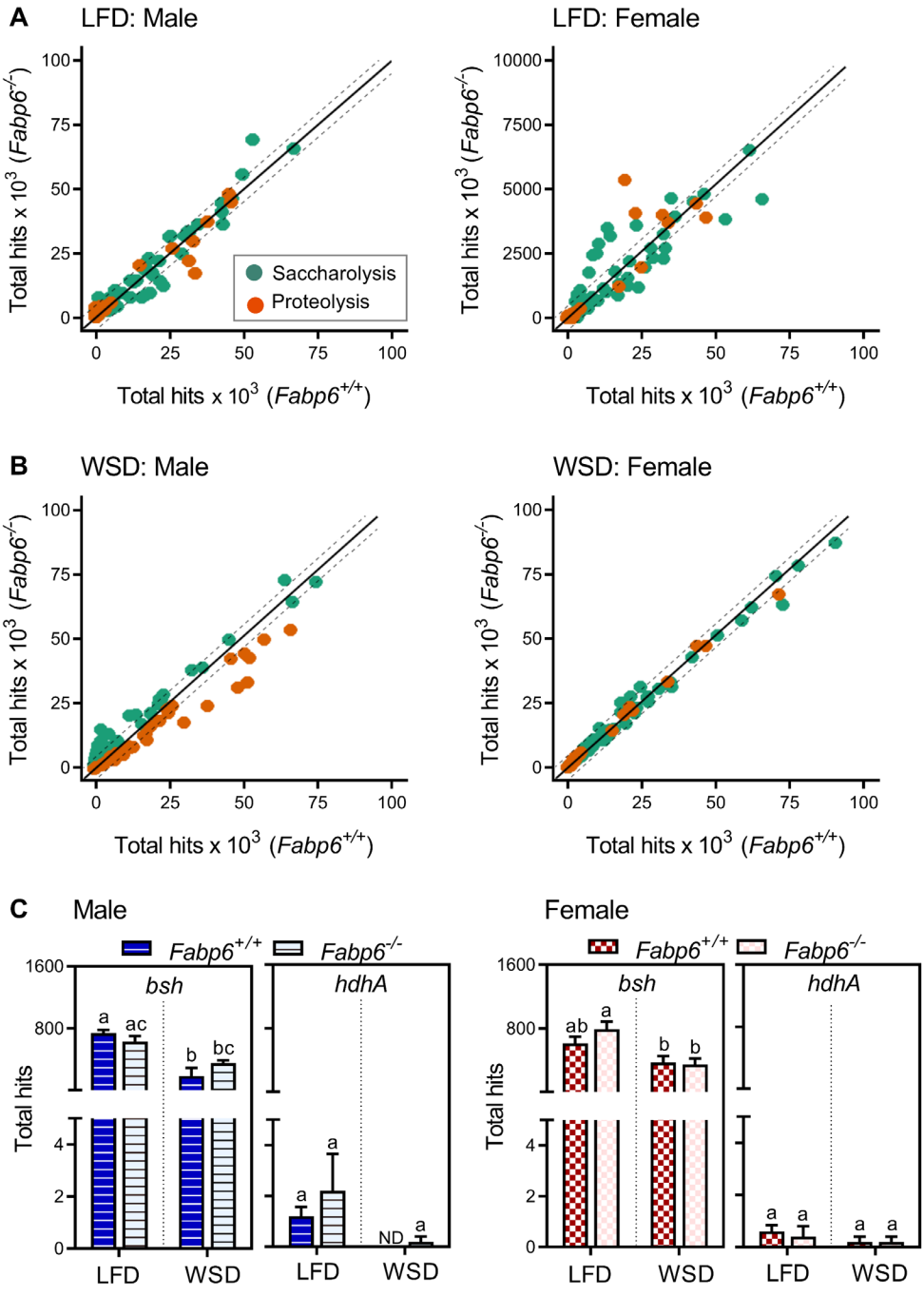
A
LFD: Male
LFD: Female
Total hits x 10^3 (Fabp6^-/-)
Total hits x 10^3 (Fabp6^+/+)
Saccharolysis
Proteolysis
B
WSD: Male
WSD: Female
C
Male
Female
Fabp6^+/+
Fabp6^-/-
bsh
hdhA
Total hits
LFD
WSD
ND

Figure 2-7. Higher predicted capacity to produce SCFAs by saccharolysis and metabolize bile acids by the gut microbiota of male *Fabp6*$^{-/-}$ mice on WSD. Predicted abundance of genes involved in SCFAs production of the gut microbiome of mice on (A) LFD and (B) WSD. (C) Predicted abundance of genes involved in bile acid metabolism of the gut microbiome of male and female mice, mean ± SEM (n=5), means denoted by different letters indicate a significant difference (p<0.05) by Kruskal-Wallis test accompanied with Dunn's test, males and females analyzed in separate models. Green and orange circles indicate genes involved in saccharolysis, and proteolysis, respectively. Dark and light colors indicate *Fabp6*$^{+/+}$ mice and *Fabp6*$^{-/-}$ mice, respectively. Blue and red indicate male and female mice, respectively. Fabp6: Fatty acid binding protein 6, SCFAs: Short-chain fatty acids, bsh: Bile salt hydrolase, hdhA: 7α-hydroxysteroid dehydrogenase, LFD: low fat diet, WSD: Western-style diet.

2.3.4. Increased plasma SCFAs and improved glucose tolerance in male Fabp6$^{-/-}$ mice fed WSD

To determine whether the higher predicted gut microbial capacity of male *Fabp6*$^{-/-}$ mice fed WSD to produce SCFAs by saccharolysis is associated with altered concentration of SCFAs in blood, plasma SCFAs were measured. On LFD, compared to their respective wild-type counterparts, male, but not female *Fabp6*$^{-/-}$ mice showed lower total plasma SCFAs concentration (Fig. 2-8A, left). While the consumption of WSD was associated with reduced plasma SCFAs concentration in male wildtype mice, it was associated with higher plasma SCFAs in male *Fabp6*$^{-/-}$ mice on WSD compared to their counterparts on the LFD (Fig. 2-8A, left). These changes in total plasma SCFAs were particularly associated with the changes in plasma acetic acid concentrations (Fig. 2-8A, left). No difference in plasma SCFAs concentration was noticed between female *Fabp6*$^{-/-}$ mice and their wildtype counterparts on both diets (Fig. 2-8A, right).

In addition to being utilized as nutrient substrates, SCFAs and other gut microbial metabolites, such as secondary bile acids, may influence glucose metabolism by activating specific G-protein coupled receptors to induce insulin secretion (Duran-Sandoval et al., 2004; Tolhurst et al., 2012; Psichas et al., 2014; Sanna et al., 2019). To determine if Fabp6 deficiency is associated with modified glucose tolerance, oral glucose tolerance test was performed. On LFD, male and female *Fabp6*$^{-/-}$ mice showed similar fasting blood glucose levels compared to their respective wild-type counterparts, but only male mice showed lower blood glucose levels over 2 hours following the oral glucose challenge compared to their wild-type counterparts (Fig. 2-8B). On WSD, both male and female *Fabp6*$^{-/-}$ mice showed lower fasting blood glucose concentrations compared to their wild-type counterparts. Although values did not reach statistical significance, only male *Fabp6*$^{-/-}$ mice showed lower blood glucose concentrations over 2 h following a glucose challenge (Fig. 2-8C). Therefore, the deficiency of Fabp6 may be associated with improved glucose tolerance in male mice fed the WSD.

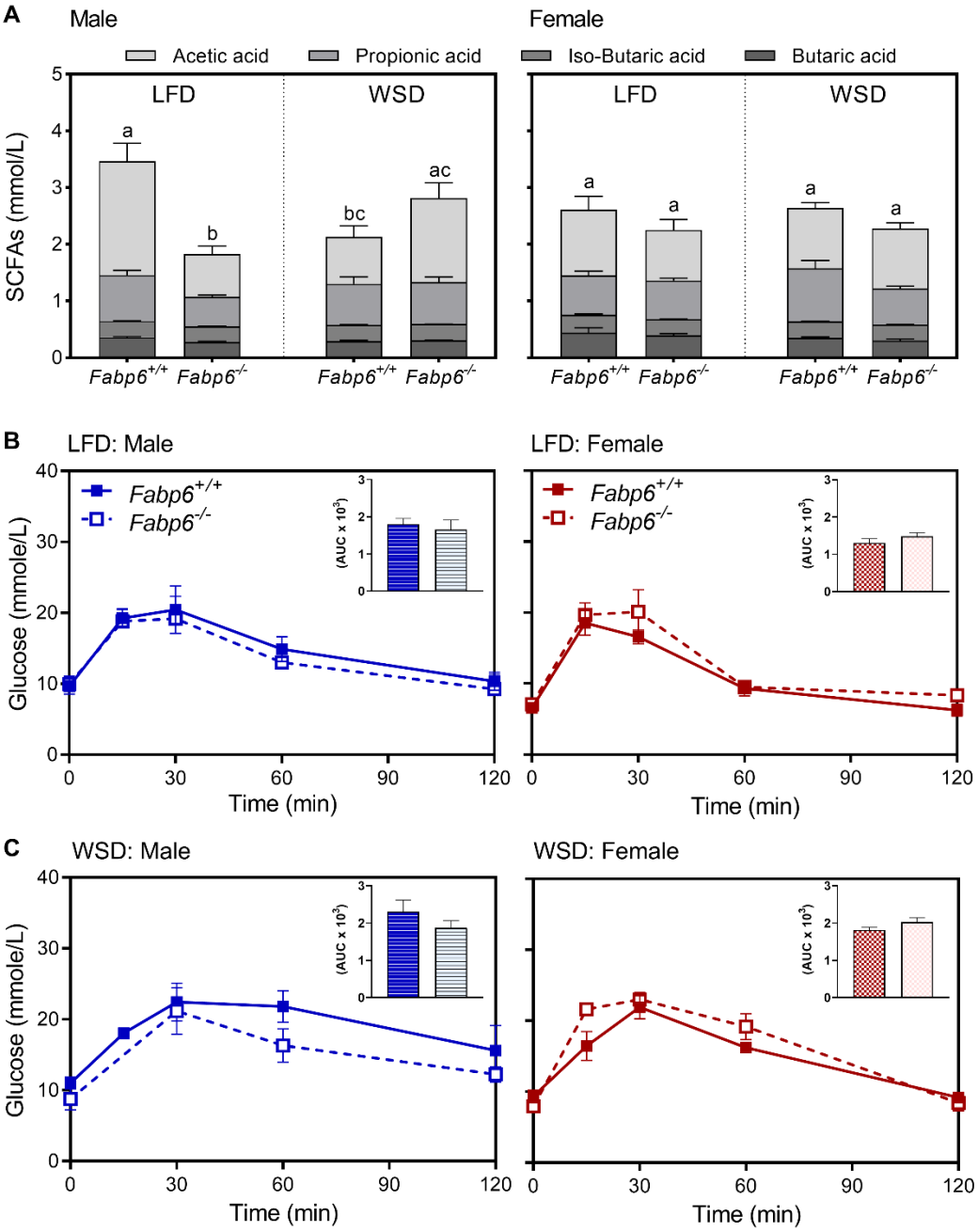

Figure 2-8. Increased plasma SCFAs and improved glucose tolerance in male *Fabp6*$^{-/-}$ mice on WSD. (A) Plasma SCFAs, mean ± SEM (n=4-6), means denoted by different letters indicate a significant difference (p<0.05) by one-way ANOVA accompanied with Fisher's LSD test, males and females analyzed in separate models, (B and C) blood glucose levels during oral glucose tolerance test (OGTT) of mice on LFD and WSD, respectively, insets represent area under the curve (AUC), mean ± SEM (n=3-5), means were compared by unpaired *t* test. Dark color and solid line indicate wildtype mice, light color and dashed lines indicate *Fabp6*$^{-/-}$ mice. Blue and red indicate male and female mice, respectively. Fabp6: Fatty acid binding protein 6, SCFAs: Short chain fatty acids, LFD: low fat diet, WSD: Western-style diet.

2.4. Discussion

The gut microbial composition is vulnerable to modification by various intrinsic factors provided by the host and by extrinsic factors that originate from the diet. Bile acids secreted into the gut help in the digestion and absorption of lipids, but may also induce gut microbial modification due to their bactericidal and bacteriostatic effects (Agellon, 2008). In previous studies, the deficiency of Fabp6 induced bile malabsorption in mice (Praslickova et al., 2012), and male *Fabp6*$^{-/-}$ mice exhibited a state of unexplained adiposity on WSD (Appendix I). In the present study, both wild-type and *Fabp6*$^{-/-}$ mice were produced by inbreeding of *Fabp6*$^{+/-}$ mice to ensure vertical transmission of gut microbiota from the dams (Hufeldt et al., 2010; Moeller et al., 2018). This allowed for the inoculation of all progeny, including males and females of all possible *Fabp6* genotypes, with the same microbiota.

The results of this study showed that the gut microbial response to Fabp6 deficiency was influenced by both the sex of mice and their diet. In particular, male *Fabp6*$^{-/-}$ mice on WSD, exclusively exhibited gut microbial dysbiosis characterized by greater Firmicutes:Bacteroidetes ratio, increased gut microbial diversity, and significantly enriched Lactobacillaceae family. The greater Firmicutes:Bacteroidetes ratio in male *Fabp6*$^{-/-}$ mice was consistent with that observed in male rats fed cholic acid-supplemented diet (Islam et al., 2011). In addition, the increased gut microbial diversity may be attributed to the lower level of bile malabsorption in male *Fabp6*$^{-/-}$ mice compared to female (Praslickova et al., 2012). The high sugar content (35% w/w) of WSD compared to that of the LFD used in this study may have provided an extra nutrient source for certain gut microbial species and consequently promoted adiposity. For example, some species of *Lactobacillus* can utilize both sucrose and fructose sugars (Srinivas et al., 1990), while other *Lactobacillus* spp. are even more efficient in utilizing pentose sugars than hexose sugars (Andreevskaya et al., 2016).

The proportions of major bacterial families were stable in response to Fabp6 deficiency. This was an expected finding since bile acids are continuously secreted into the gastrointestinal tract and in order to overcome the bacteriostatic and bactericidal

activities of bile acids, commensal bacteria must activate relevant resistance mechanisms, such as the activation of stress response genes, efflux pumps, and detoxification systems (Begley et al., 2005). Bile salt hydrolases reduce the toxicity of bile acids by hydrolyzing the bond between bile acids and their amino acid conjugates, rendering the bile acids less polar. In this study, the predicted gut microbial *bsh* abundance was influenced by both the sex and diet of mice and was associated with the gut microbial diversity. This is in concert with the fact that *bsh* is widely abundant and broadly distributed in the gut microbiota (Jones et al., 2008). The disruption of major families may allow minor gut microbial families to vastly increase in response to Fabp6 deficiency and these minor families appear to be enriched by higher concentrations of bile acids in the large intestine. This may be attributable to the possession of resistance mechanisms, such as 7α-dehydroxylation activity (Ridlon et al., 2014), or virulence factors such as type VI secretion system (Sana et al., 2017), which are less commonly distributed among the gut microbiota.

An interesting finding of this study was the exceptional increase of gut microbial species that are known to efficiently metabolize carbohydrates over proteins for SCFAs-production in male *Fabp6*$^{-/-}$ fed the WSD. Gut microbial proteolysis is increased in the distal parts of the colon and with longer intestinal transit times (Macfarlane and Macfarlane, 2003). Bile acid malabsorption is usually accompanied by shorter intestinal transit times, which might explain, in part, the lower probability of proteolysis in male *Fabp6*$^{-/-}$ mice. Moreover, refined sugars, which is a significant component of WSD, may represent an important substrate for SCFAs production (Mortensen et al., 1990) and thus prevent colonization of the colon by protein-catabolizing microbiota (Townsend et al., 2019). The higher levels of SCFAs in the plasma of male *Fabp6*$^{-/-}$ mice on WSD were consistent with their distinctly enriched SCFAs producing genera discovered by the LefSe model. In fact, species of *Bacteroides*, *Lactobacillus, Lachnospiraceae* and *Ruminococcaceae* are producers of acetic acid, while species of *Clostridium, Faecalibacterium* and *Eubacterium* are main producers of propionic and butyric acids (Louis and Flint, 2009; Biddle et al., 2013; Bik et al., 2018) This was also consistent with their distinct enrichment of saccharolysis pathways inferred by Tax4Fun analysis. These results may suggest enhanced carbohydrate and sugar fermentation in these mice.

However, a comprehensive assessment of energy balance including digestibility and fecal energy density is needed in order to evaluate if it is associated with enhanced energy extraction and promotes adiposity.

Although male *Fabp6*$^{-/-}$ mice on WSD showed enhanced adiposity, they unexpectedly displayed improved glucose tolerance. This may be attributable to the fact that in addition to serving as energy substrates and promoting lipogenesis and gluconeogenesis, SCFAs also act to modulate glucose homeostasis. SCFAs bind specific G-protein coupled receptors in the colonic enterocytes which promotes GLP-1 secretion. Higher GLP-1 levels in the circulation induce pancreatic insulin production and secretion. In turn, improved induction of insulin secretion following meal ingestion is associated with enhanced glucose tolerance (Tolhurst et al., 2012; Psichas et al., 2014). Moreover, glucose homeostasis is also regulated by bile acids through binding to farnesoid X receptor (FXR) or Takeda G protein receptor 5 (TGR5) in different tissues (Duran-Sandoval et al., 2004). For example, the activation of FXR reduces gluconeogenesis in liver and induces insulin secretion in pancreatic β cells, whereas the activation of TGR5 stimulates the production of GLP-1 in colonic L cells and increases energy expenditure in skeletal muscles and brown adipose tissue (Shapiro et al., 2018). Together, the enhanced predicted ability of male *Fabp6*$^{-/-}$ mice on WSD to metabolize bile acids and the previous finding that the bile acid profile of male *Fabp6*$^{-/-}$ mice on WSD is characterized by a greater taurocholic acid: tauromuricholic acid ratio (Appendix I) and indicated the likelihood of improved glucose metabolism regulation by Fabp6 deficiency. Combined, the alteration of SCFAs and bile acids profiles in male *Fabp6*$^{-/-}$ mice on WSD may positively impact their glucose tolerance.

This study is limited by the small number of mice and the cohousing of some of the replicates during the controlled feeding period. A replication of the experiment with a larger number of mice and more cage replicates per treatment would improve the robustness of the results. In addition, the use of fecal microbiota transplantation in germ-free mice would help in establishing a causal relationship between the modulated gut microbiota of Fabp6-deficient mice and the observed phenotypes. Bearing that in mind, the gut microbial modifications in response to Fabp6 deficiency in mice may

imply increased vulnerability of individuals with clinical conditions associated with bile acid malabsorption, such as cystic fibrosis, ileal resection, and inflammatory bowel diseases (Wedlake et al., 2009) to environmental perturbations such as imbalanced dietary profiles and uncontrolled exposure to xenobiotics. Obesity in some of these conditions (Nic Suibhne et al., 2013; Singh et al., 2017) may be triggered by remodeling of gut microbial composition following the exposure to excess levels of bile acids. Furthermore, individuals with genetic variations in *FABP6* gene that may induce malfunction in the Fabp6 protein, such as T79M mutation were found to be protected from type 2 diabetes despite being obese (Fisher et al., 2009). Thus, the direct contribution of the gut microbial composition to these phenotypes requires further investigation.

Collectively, this study demonstrated that the gut microbial composition in male Fabp6-deficient mice was associated with their enhanced adiposity. Excess exposure to bile acids in this mouse model promoted a shift in the gut microbial composition toward microbial species efficient in SCFAs production and bile acid metabolism. Future work is needed to establish whether this gut microbial shift is involved in enhancing energy extraction and improving glucose tolerance.

Acknowledgment

This study was supported by grants (to LBA) from the Natural Sciences and Engineering Research Council of Canada. The data analysis was enabled in part by support provided by WestGrid (www.westgrid.ca) and Compute Canada Calcul Canada (www.computecanada.ca).

2.5. References

Agellon, L.B. (2008). Metabolism and function of bile acids. In D.E. Vance & J.E. Vance (Eds.), *Biochemistry of lipids, lipoproteins and membranes (5th edition)* (Vol. 36, pp. 423-440). San Diego: Elsevier.

Agellon, L.B., Toth, M.J. and Thomson, A.B. (2002). Intracellular lipid binding proteins of the small intestine. *Mol Cell Biochem, 239* (1-2), 79-82.

Amir, A., McDonald, D., Navas-Molina, J.A.*, et al.* (2017). Deblur rapidly resolves single-nucleotide community sequence patterns. *mSystems, 2* (2), e00191-00116.

Andreevskaya, M., Johansson, P., Jääskeläinen, E.*, et al.* (2016). *Lactobacillus oligofermentans* glucose, ribose and xylose transcriptomes show higher similarity between glucose and xylose catabolism-induced responses in the early exponential growth phase. *BMC Genomics, 17*, 539-539.

Andrews, S. (2010). FastQC: A quality control tool for high throughput sequence data. Retrieved from http://www.bioinformatics.babraham.ac.uk/projects/fastqc/

Asshauer, K.P., Wemheuer, B., Daniel, R.*, et al.* (2015). Tax4Fun: Predicting functional profiles from metagenomic 16S rRNA data. *Bioinformatics, 31* (17), 2882-2884.

Begley, M., Gahan, C.G. and Hill, C. (2005). The interaction between bacteria and bile. *FEMS Microbiol Rev, 29* (4), 625-651.

Besnard, P., Niot, I., Poirier, H.*, et al.* (2002). New insights into the fatty acid-binding protein (FABP) family in the small intestine. *Mol Cell Biochem, 239* (1-2), 139-147.

Biddle, A., Stewart, L., Blanchard, J.*, et al.* (2013). Untangling the genetic basis of fibrolytic specialization by lachnospiraceae and ruminococcaceae in diverse gut communities. *Diversity, 5*, 627-640.

Bik, E.M., Ugalde, J.A., Cousins, J.*, et al.* (2018). Microbial biotransformations in the human distal gut. *Br J Pharmacol, 175* (24), 4404-4414.

Bokulich, N.A., Kaehler, B.D., Rideout, J.R.*, et al.* (2018). Optimizing taxonomic classification of marker-gene amplicon sequences with QIIME 2's q2-feature-classifier plugin. *Microbiome, 6* (1), 90.

Bokulich, N.A., Subramanian, S., Faith, J.J.*, et al.* (2013). Quality-filtering vastly improves diversity estimates from illumina amplicon sequencing. *Nat Methods, 10* (1), 57-59.

Bolyen, E., Rideout, J.R., Dillon, M.R.*, et al.* (2019). Reproducible, interactive, scalable and extensible microbiome data science using QIIME 2. *Nat Biotechnol, 37* (8), 852-857.

Britton, R.A. and Young, V.B. (2012). Interaction between the intestinal microbiota and host in *Clostridium difficile* colonization resistance. *Trends Microbiol, 20* (7), 313-319.

Callahan, B.J., McMurdie, P.J. and Holmes, S.P. (2017). Exact sequence variants should replace operational taxonomic units in marker-gene data analysis. *ISME J, 11*, 2639.

Chao, A. (1984). Nonparametric estimation of the number of classes in a population. *Scand J Stat, 11* (4), 265-270.

Comeau, A.M., Douglas, G.M. and Langille, M.G.I. (2017). Microbiome helper: A custom and streamlined workflow for microbiome research. *mSystems, 2* (1), e00127-00116.

Crawford, R.W., Rosales-Reyes, R., Ramirez-Aguilar Mde, L.*, et al.* (2010). Gallstones play a significant role in *Salmonella* spp gallbladder colonization and carriage. *Proc Natl Acad Sci USA, 107* (9), 4353-4358.

Dhariwal, A., Chong, J., Habib, S.*, et al.* (2017). Microbiomeanalyst - A web-based tool for comprehensive statistical, visual and meta-analysis of microbiome data *Nucleic Acids Res, 45* (W1), W180–W188.

Dixon, P. (2003). Vegan, a package of R functions for community ecology. *Journal of Vegetation Science, 14* (6), 927-930.

Duran-Sandoval, D., Mautino, G., Martin, G.*, et al.* (2004). Glucose regulates the expression of the farnesoid X receptor in liver. *Diabetes, 53* (4), 890.

Edgar, R.C., Haas, B.J., Clemente, J.C.*, et al.* (2011). UCHIME improves sensitivity and speed of chimera detection. *Bioinformatics, 27* (16), 2194-2200.

Enright, E.F., Griffin, B.T., Gahan, C.G.M., *et al.* (2018). Microbiome-mediated bile acid modification: Role in intestinal drug absorption and metabolism. *Pharmacol Res, 133*, 170-186.

Fisher, E., Grallert, H., Klapper, M., *et al.* (2009). Evidence for the Thr79Met polymorphism of the ileal fatty acid binding protein (FABP6) to be associated with type 2 diabetes in obese individuals. *Mol Genet Metab, 98* (4), 400-405.

Gantz, I., Nothwehr, S.F., Lucey, M., *et al.* (1989). Gastrotropin: Not an enterooxyntin but a member of a family of cytoplasmic hydrophobic ligand binding proteins. *J Biol Chem, 264* (34), 20248-20254.

Garnier, S. (2018). Viridis: Default color maps from 'matplotlib': R package version 0.5.1. Retrieved from https://CRAN.R-project.org/package=viridis

Heijboer, A.C., Donga, E., Voshol, P.J., *et al.* (2005). Sixteen hours of fasting differentially affects hepatic and muscle insulin sensitivity in mice. *J Lipid Res, 46* (3), 582-588.

Hervé, M. (2020). RVAideMemoire: Testing and plotting procedures for biostatistics: R package version 0.9-75. Retrieved from https://CRAN.R-project.org/package=RVAideMemoire

Horváth, G., Bencsura, Á., Simon, Á., *et al.* (2016). Structural determinants of ligand binding in the ternary complex of human ileal bile acid binding protein with glycocholate and glycochenodeoxycholate obtained from solution NMR. *FEBS J, 283* (3), 541-555.

Hufeldt, M.R., Nielsen, D.S., Vogensen, F.K., *et al.* (2010). Family relationship of female breeders reduce the systematic inter-individual variation in the gut microbiota of inbred laboratory mice. *Lab Anim, 44* (4), 283-289.

Islam, K.B.M.S., Fukiya, S., Hagio, M., *et al.* (2011). Bile acid is a host factor that regulates the composition of the cecal microbiota in rats. *Gastroenterology, 141* (5), 1773-1781.

Jensen, T.L., Kiersgaard, M.K., Sørensen, D.B., *et al.* (2013). Fasting of mice: A review. *Lab Anim, 47* (4), 225-240.

Jones, B.V., Begley, M., Hill, C.*, et al.* (2008). Functional and comparative metagenomic analysis of bile salt hydrolase activity in the human gut microbiome. *Proc Natl Acad Sci USA, 105* (36), 13580-13585.

Kanda, T., Odani, S., Tomoi, M.*, et al.* (1991). Primary structure of a 15-kDa protein from rat intestinal epithelium. *Eur J Biochem, 197* (3), 759-769.

Kanehisa, M. and Goto, S. (2000). KEGG: Kyoto encyclopedia of genes and genomes. *Nucleic Acids Res, 28* (1), 27-30.

Kramer, W., Girbig, F., Gutjahr, U.*, et al.* (1993). Intestinal bile acid absorption. Na^+-dependent bile acid transport activity in rabbit small intestine correlates with the coexpression of an integral 93-kDa and a peripheral 14-kDa bile acid-binding membrane protein along the duodenum-ileum axis. *J Biol Chem, 268* (24), 18035-18046.

Kramer, W., Sauber, K., Baringhaus, K.H.*, et al.* (2001). Identification of the bile acid-binding site of the ileal lipid-binding protein by photoaffinity labeling, matrix-assisted laser desorption ionization-mass spectrometry, and NMR structure. *J Biol Chem, 276* (10), 7291-7301.

Labonté, E.D., Li, Q., Kay, C.M.*, et al.* (2003). The relative ligand binding preference of the murine ileal lipid binding protein. *Protein Expr Purif, 28* (1), 25-33.

Louis, P. and Flint, H.J. (2009). Diversity, metabolism and microbial ecology of butyrate-producing bacteria from the human large intestine. *FEMS Microbiol Lett, 294* (1), 1-8.

Love, M.I., Huber, W. and Anders, S. (2014). Moderated estimation of fold change and dispersion for RNA-seq data with DESeq2. *Genome Biol, 15*, 550.

Macfarlane, S. and Macfarlane, G.T. (2003). Regulation of short-chain fatty acid production. *Proc Nutr Soc, 62* (1), 67-72.

Martin, M. (2011). Cutadapt removes adapter sequences from high-throughput sequencing reads. *EMBnet J, 17* (1), 10-12.

McDonald, D., Clemente, J., Kuczynski, J.*, et al.* (2012). The Biological Observation Matrix (BIOM) format or: How I learned to stop worrying and love the ome-ome. *GigaScience, 1*, 7.

McMurdie, P.J. and Holmes, S. (2013). Phyloseq: An R package for reproducible interactive analysis and graphics of microbiome census data. *PLoS One, 8* (4), e61217.

Moeller, A.H., Suzuki, T.A., Phifer-Rixey, M.*, et al.* (2018). Transmission modes of the mammalian gut microbiota. *Science, 362* (6413), 453-457.

Mortensen, P.B., Holtug, K., Bonnen, H.*, et al.* (1990). The degradation of amino acids, proteins, and blood to short-chain fatty acids in colon is prevented by lactulose. *Gastroenterology, 98* (2), 353-360.

Nic Suibhne, T., Raftery, T.C., McMahon, O.*, et al.* (2013). High prevalence of overweight and obesity in adults with Crohn's disease: Associations with disease and lifestyle factors. *J Crohns Colitis, 7* (7), e241-e248.

Paulson, J.N., Stine, O.C., Bravo, H.C.*, et al.* (2013). Differential abundance analysis for microbial marker-gene surveys. *Nat Methods, 10*, 1200.

Pedregosa, F., Varoquaux, G., Gramfort, A.*, et al.* (2011). Scikit-learn: Machine learning in python. *J. Mach. Learn. Res., 12*, 2825–2830.

Praslickova, D., Torchia, E.C., Sugiyama, M.G.*, et al.* (2012). The ileal lipid binding protein is required for efficient absorption and transport of bile acids in the distal portion of the murine small intestine. *PLoS One, 7* (12), 1.

Psichas, A., Sleeth, M.L., Murphy, K.G.*, et al.* (2014). The short chain fatty acid propionate stimulates GLP-1 and PYY secretion via free fatty acid receptor 2 in rodents. *Int J Obesity, 39*, 424.

R Core Team. (2020). R: A language and environment for statistical computing. Vienna, Austria: R Foundation for Statistical Computing. Retrieved from https://www.R-project.org/

Ridlon, J.M., Kang, D.J. and Hylemon, P.B. (2006). Bile salt biotransformations by human intestinal bacteria. *J Lipid Res, 47* (2), 241-259.

Ridlon, J.M., Kang, D.J., Hylemon, P.B.*, et al.* (2014). Bile acids and the gut microbiome. *Curr Opin Gastroenterol, 30* (3), 332-338.

Robinson, M.D., McCarthy, D.J. and Smyth, G.K. (2010). EdgeR: A Bioconductor package for differential expression analysis of digital gene expression data. *Bioinformatics, 26* (1), 139-140.

Rognes, T., Flouri, T., Nichols, B.*, et al.* (2016). VSEARCH: A versatile open source tool for metagenomics. *PeerJ, 4*, e2584-e2584.

Sana, T.G., Lugo, K.A. and Monack, D.M. (2017). T6SS: The bacterial "fight club" in the host gut. *PLoS Path, 13* (6), e1006325.

Sanna, S., van Zuydam, N.R., Mahajan, A.*, et al.* (2019). Causal relationships among the gut microbiome, short-chain fatty acids and metabolic diseases. *Nat Genet, 51* (4), 600-605.

Segata, N., Izard, J., Waldron, L.*, et al.* (2011). Metagenomic biomarker discovery and explanation. *Genome Biol, 12* (6), R60.

Shannon, C.E. (1948). A mathematical theory of communication. *Bell Syst Tech J, 27* (3), 379-423.

Shapiro, H., Kolodziejczyk, A.A., Halstuch, D.*, et al.* (2018). Bile acids in glucose metabolism in health and disease. *J Exp Med, 215* (2), 383–396.

Singh, S., Dulai, P.S., Zarrinpar, A.*, et al.* (2017). Obesity in IBD: Epidemiology, pathogenesis, disease course and treatment outcomes. *Nat Rev Gastroenterol Hepatol, 14* (2), 110-121.

Srinivas, D., Mital, B.K. and Garg, S.K. (1990). Utilization of sugars by *Lactobacillus acidophilus* strains. *Int J Food Microbiol, 10* (1), 51-57.

Tochtrop, G.P., Bruns, J.L., Tang, C.*, et al.* (2003). Steroid ring hydroxylation patterns govern cooperativity in human bile acid binding protein. *Biochemistry, 42* (40), 11561-11567.

Tolhurst, G., Heffron, H., Lam, Y.S.*, et al.* (2012). Short-chain fatty acids stimulate glucagon-like peptide-1 secretion via the G-protein-coupled receptor FFAR2. *Diabetes, 61* (2), 364-371.

Townsend, G.E., Han, W., Schwalm, N.D.*, et al.* (2019). Dietary sugar silences a colonization factor in a mammalian gut symbiont. *Proc Natl Acad Sci USA, 116* (1), 233.

Wedlake, L., A'Hern, R., Russell, D.*, et al.* (2009). Systematic review: The prevalence of idiopathic bile acid malabsorption as diagnosed by SeHCAT scanning in patients with diarrhoea-predominant irritable bowel syndrome. *Aliment Pharmacol Ther, 30* (7), 707-717.

Werner, J.J., Koren, O., Hugenholtz, P.*, et al.* (2012). Impact of training sets on classification of high-throughput bacterial 16s rRNA gene surveys. *ISME J, 6* (1), 94-103.

Wickham, H. (2016). *ggplot2: Elegant graphics for data analysis*: Springer-Verlag New York. Retrieved from https://ggplot2.tidyverse.org

Wierczorek, D. and Schagat, T. (2007). Purification of genomic DNA from mouse feces using the Maxwell® 16 system. Retrieved from https://www.promega.ca/resources/pubhub/enotes/purification-of-genomic-dna-from-mouse-feces-using-the-maxwell-16-system/

Yilmaz, P., Parfrey, L.W., Yarza, P.*, et al.* (2013). The SILVA and "all-species living tree project (LTP)" taxonomic frameworks. *Nucleic Acids Res, 42* (D1), D643-D648.

Zwicker, B.L. and Agellon, L.B. (2013). Transport and biological activities of bile acids. *Int J Biochem Cell Biol, 45* (7), 1389-1398.

Connecting statement to Chapter 3

In Chapter 2, I showed that an intrinsic metabolite, such as bile acids, induced gut microbial dysbiosis distinctly in male and female Fabp6-deficient mice, which was predicted to be associated with differential genetic capacity to carbohydrate and bile acid metabolism by the two sexes. In Chapter 3, I investigate the ability of extrinsic metabolites, such as plant-derived polyphenolic compounds, to modify the gut microbial composition and alter the metabolic status of the host. Diet is the major source of extrinsic factors that enters the host. Recent studies show that different dietary patterns distinctly impact both the composition of the gut microbiota and the host health status (Nagpal et al., 2018a). For example, plant-based diets, such as the Mediterranean diet, are associated with gut microbial eubiosis and lower risk to metabolic disorders (Singh et al., 2017), while plant-scarce diets, such as the WSD, induce gut microbial dysbiosis and metabolic disorders (Chen et al., 2018). However, the human digestive system is not efficient in processing complex plant metabolites such as plant fibers, natural gum, phytosterols and polyphenols. As a result, these compounds are excreted out of the body *via* the colon where they interact with the gut microbiota.

A previous study by our research group described the ability of polyphenolic-rich potato extract (PRPE) to improve several metabolic parameters in mice fed an obesity-inducing high fat diet (Kubow et al., 2014). The aim of the study described in Chapter 3 was to evaluate if the ability of PRPE to reduce the body weight gain of mice on a high fat diet was associated with remodeling of the gut microbiota and modification of metabolic functions in the host.

Chapter 3

Polyphenolic-rich potato extract prevents adiposity and gut microbial dysbiosis induced by the Western-style diet in mice

Salam M. Habib, Stan Kubow, Luis B. Agellon*

School of Human Nutrition, McGill University, QC, Canada

*Corresponding author at: McGill University School of Human Nutrition, 21111 Lakeshore Road, Ste. Anne de Bellevue, QC H9X 3V9 Canada

Email: luis.agellon@mcgill.ca (L.B. Agellon)

Author contribution: SMH designed and conducted the experiments, analyzed the data, and wrote the manuscript. SK provided access to the gas chromatography and edited the manuscript. LBA was involved in the conception of the experimental design.

A version of this manuscript is in preparation for submission to the journal Gut Microbes.

Abstract

Background: The widespread adoption of Western-style diet (WSD) is paralleled by an increased risk of acquired metabolic syndromes worldwide. WSD is associated with gut microbial dysbiosis, and its components, notably saturated fatty acids and refined sugars, induce cellular stress. A polyphenol-rich potato extract (PRPE) was previously shown to reduce body weight gain in mice, and a synthetic polyphenol mixture that mimic the major composition of polyphenols in PRPE alters gut microbial short-chain fatty acid (SCFAs) metabolism *in vitro*. **Objective:** The purpose of this study was to determine if the ability of PRPE to reduce adiposity in mice fed a high fat diet was associated with remodeling of the gut microbial composition. **Methods:** C57BL/6J mice of both sexes were fed WSD with or without PRPE supplementation for 7 weeks. Energy metabolism was evaluated using indirect calorimetry. Gut microbial composition was assayed by sequencing the full 16S rRNA gene of DNA extracted from stool samples. SCFAs in plasma were characterized and quantitated by gas chromatography. Markers of unfolded protein response (UPR) were assayed by qPCR of RNA extracted from colons. **Results:** WSD feeding reduced the diversity of the gut microbial community which was associated with increased adiposity. In contrast, PRPE supplementation of WSD increased the diversity of the gut microbiota and reduced body weight gain in a sex dimorphic manner. PRPE supplementation prevented the reduction in energy expenditure induced by WSD in both male and female mice. In male mice, PRPE supplementation prevented both the reduction in plasma SCFAs concentration, and the appearance of UPR activation markers in the large intestine of male mice induced by WSD feeding. **Conclusions:** PRPE supplementation of WSD counteracted the effects of WSD feeding on adiposity and gut microbial dysbiosis.

3.1. Introduction

Polyphenolic compounds form a major part of the non-nutrient component of a healthy human diet (Chen et al., 2018). Plants generally produce polyphenolic compounds to protect them from oxidation induced by ultraviolet radiation or against pathogen infections (Manach et al., 2004). Consumption of certain polyphenolic extracts and foods rich in polyphenols has been linked with favorable health outcomes (Kim et al., 2016; Tresserra-Rimbau et al., 2016; Lee et al., 2017; Serino and Salazar, 2018; Freyssin et al., 2018; Dhouafli et al., 2018; Castro-Barquero et al., 2018), including improvement of glycemic control and prevention of the early onset of diabetes (Kim et al., 2016; Tresserra-Rimbau et al., 2016), protection against vascular inflammation and cardiovascular disease (Serino and Salazar, 2018), promotion of proteostasis in neurodegenerative diseases (Freyssin et al., 2018; Dhouafli et al., 2018), and prevention of obesity (Lee et al., 2017; Castro-Barquero et al., 2018). Therefore, there is growing interest in studying the mechanisms of action of various polyphenolic extracts and supplements.

Dietary polyphenols are poorly absorbed in the small intestine and are therefore available to interact with gut microbiota (Williamson and Manach, 2005). The latter hydrolyzes and breaks down complex polyphenolic compounds into smaller phenolic acids, increasing their bioavailability and bioactivity (Del Rio et al., 2013; Kawabata et al., 2019). Polyphenols can also act as prebiotics as they are a nutrient source for some classes of gut microbiota and enhance their growth (Hervert-Hernandez et al., 2009; Bialonska et al., 2010; Etxeberria et al., 2013), whereas for other classes of gut microbiota polyphenols pose a potential stress due to their antibacterial properties and thus reduce their colonization ability (Nohynek et al., 2006; Marin et al., 2015). The above examples illustrate the ability of polyphenols to modulate the gut microbial composition.

Globalization and economic development have promoted a nutrition transition and adoption of the Western-style diet (WSD) in many nations (Popkin, 2001). WSD is characterized by foods with high energy density and low nutrient diversity, such as

processed food products (Chen et al., 2018). The consumption of WSD is associated with increased risk of developing acquired metabolic syndromes including obesity, cardiovascular diseases and colonic disorders (Chen et al., 2018). Components of WSD, notably saturated fatty acids and refined sugars, induce the loss of cellular homeostasis and the activation of cellular stress coping mechanisms such as the unfolded protein response (UPR) (Groenendyk et al., 2013; Pardo et al., 2015; Shah et al., 2017). The ability of polyphenols to reduce endoplasmic reticulum stress might be mediated through the gut microbiota (Suganya et al., 2016; Wang et al., 2018). In a previous study, we showed that a polyphenolic-rich potato extract (PRPE) prevented body weight gain in mice fed an obesity-inducing high fat diet (Kubow et al., 2014). In addition, synthetic polyphenol mixtures that mimic polyphenol profile of PRPE were able to alter short-chain fatty acids (SCFAs) production of cultured fecal microbiota in an *in vitro* gastrointestinal model (Sadeghi Ekbatan et al., 2016). The objective of this study was to determine if the ability of PRPE to reduce the body weight gain on a high fat diet was associated with favorable remodeling of the gut microbial composition and improvement of metabolic function in the host.

3.2. Materials and methods

Mice and diets

In the first experiment, eight weeks old C57BL/6J male and female mice were obtained in one batch from Jackson Labs (Bar Harbor, Maine, USA). Mice were acclimated for two weeks and housed n=5 mice per cage. In the second experiment, *Fabp6*$^{+/+}$ and *Fabp6*$^{-/-}$ and mice were produced as described previously in Chapter 2. Briefly, heterozygote *Fabp6* mice were inbred to yield *Fabp6*$^{+/+}$ and *Fabp6*$^{-/-}$ mice for this experiment. The produced mice were genotyped at three weeks of age as described in (Appendix I). *Fabp6*$^{+/+}$ and *Fabp6*$^{-/-}$ (n=3-6 mice per treatment) were housed in 2-3 cages per treatment and *Fabp6*$^{+/+}$ *and Fabp6*$^{-/-}$ mice in different cages. All mice were maintained on Teklad 2020X diet (Teklad-Envigo, Lachine, QC), in a climate-controlled facility with a 12-h light/dark photoperiod.

During the controlled feeding experiments, mice were either maintained on the Teklad 2020X diet (Teklad-Envigo, Lachine, QC), which is a low fat diet (LFD), or placed on either WSD (D12079B, Research Diets, New Brunswick, NJ), WSD supplemented with PRPE (WSD+PRPE), or WSD supplemented with purified polyphenols of potato (WSD+PPP). Mice had *ad libitum* access to the diets for 7 weeks. PRPE was extracted from Russet Burbank potato cultivar by POS Bio-Sciences, Saskatoon, Canada as described previously (Kubow et al., 2014). PPP was extracted from the same potato cultivar, Russet Burbank, by CÉPROCQ, Montreal, Canada. Briefly, the methanolic extract of PRPE was passed on a stationary C18 phase, washed twice with water, eluted with acidified methanol and freeze-dried to produce the PPP extract. The dosage of polyphenolic extract used in WSD supplementation was matched with the dosage described earlier (Kubow et al., 2014), which corresponds to 200 mg chlorogenic acid and 6 mg ferulic acid per kg of WSD (Kubow et al., 2014). To ensure the above ratio of chlorogenic acid: ferulic acid in the polyphenolic extract was matched, synthetic chlorogenic acid and ferulic acid (Sigma-Aldrich Co., MO, USA) were added to maintain the same ratio. At the end of the controlled feeding experiments, stool samples were collected from each mouse, then mice were fasted 16 h prior to isoflurane/CO_2 euthanasia and total blood collection by cardiac puncture. Stool, plasma and tissue samples were stored at -70°C until analyzed. The use of animals in this study was approved by the animal care and use committee at McGill in compliance with the policies of the Canadian Council on Animal Care.

Indirect Calorimetry

Mice physical activity, respiratory quotient, energy expenditure and food intake were estimated using the Oxylet Metabolic Monitoring System (Panlab-Harvard Apparatus, Barcelona, Spain) as described in Appendix I. Briefly, in the last week of the controlled feeding period, 3 mice from each group were individually housed in the Physiocage apparatus and monitored for 3 days, then returned to the original housing. Data was simultaneously saved to a connected computer.

DNA extraction

DNA was extracted from mouse stool samples, previously stored at -70°C, using the protocol described by Tsai and Olson (Tsai and Olson, 1992). This was preceded with a bead beating step for 30 seconds using a Mini-Beadbeater apparatus (BioSpec Products, Bartlesville, Oklahoma, USA) and 1 mm zirconia beads to maximize the DNA extraction. The final DNA suspensions were further purified by running through GeneJET DNA purification columns (Thermo Scientific, ON, Canada). The extracted DNA was evaluated for quality by gel electrophoresis and quantified spectrophotometrically by measuring the absorbance at 260 nm.

Library preparation

The extracted DNA (1 µg) was used to amplify the full 16S rRNA gene by polymerase chain reaction (PCR) using previously described primers (Klindworth et al., 2012) (Appendix II). Each primer was tagged with a specific 12 bp barcode as previously described (Srivathsan et al., 2018) to allow sample dual multiplexing, the sequences of the barcodes are shown in Appendix II. Amplicons were purified with homemade solid phase reversible immobilization (SPRI) bead mix as described earlier (Jolivet and Foley, 2015). DNA concentration was measured by Qubit fluorometer 2.0 (Thermo Fisher Scientific, Waltham, USA). An amount of 300 ng of the pooled amplicons were used for MinION library preparation by SQK-LSK109 ligation kit (Oxford Nanopore Technologies, New York, USA) mixed with 1 µl internal control DNA (DNA CS provided in the same kit) following the guidelines of the corresponding Nanopore kit protocol (v.109, rev_C). Briefly, DNA templates were repaired and end-prepared using the NEBNext FFPE DNA Repair and NEBNext Ultra II End Repair/dA-Tailing modules, respectively (NEB, Whitby, Ontario, Canada), followed with product clean-up using 1:1 SPRI bead mix. Next, these templates were ligated with the adapter mix (AMX) in (LNB) ligation buffer from the same kit (Oxford Nanopore Technologies, New York, USA) using NEBNext Quick T4 DNA Ligase (NEB, Whitby, Ontario, Canada), then cleaned-up with 1:0.4 SPRI bead mix.

Nanopore sequencing

The prepared 16S rRNA gene library was mixed with the sequencing buffer (SQB) and loading beads (LB) from library loading kit (Oxford Nanopore Technologies, New York, USA) and loaded to a quality checked and primed SpotON flowcell plugged on the MinION device in a dropwise manner (Oxford Nanopore Technologies, New York, USA). Sequencing was monitored using the MinION control software, MinKNOW (v18.07.18) for 48 h and 1D reads were base-called simultaneously by Albacore (v 2.3.1).

Analysis of sequence data

The obtained Fastq reads were demultiplexed and cleared of both primer and barcode sequences using minibar python code (v 0.21) (Krehenwinkel et al., 2019). Epi2me 16S workflow (v 3.1) was used to quality filter reads (quality score >7) with its QScore Filter component (v. 3.9.3) and assign taxonomy by aligning (horizontal coverage >30%, accuracy >77%) to NCBI bacterial 16S rRNA RefSeq database (BioProject: PRJNA33175) (Tatusova et al., 2016) using the 16S classification component (v. 2.1.1). The identified sequence data was exported in tsv format for visualization and further analysis using MicrobiomeAnalyst (Dhariwal et al., 2017) as described in Chapter 2. Briefly, data was decontaminated by removal of singletons, taxa with low count (10% of samples each contain ≥ 2 reads), and taxa with low variance (10%) using data filtration functions of MicrobiomeAnalyst. When the sequencing depth between samples was >10X, samples were rarefied to lowest sample depth per group. Samples with less than 1000 reads were excluded from the analysis. Rarefaction curves and Good's coverage of the included samples were calculated (Appendix II). At the feature level, each of Chao1 richness index, Shannon's diversity index (*H*), and principal coordinate analysis (PCoA) based on Jensen-Shannon divergence metric (Koren et al., 2013) were calculated with phyloseq R package v.1.32.0 (McMurdie and Holmes, 2013). Heatmaps were produced using ggplot2 v.3.3.2 (Wickham, 2016) and viridis v.0.5.1 (Garnier, 2018) to visualize the top species clustered by Ward algorithm based on Euclidean distance measure as implemented by MicrobiomeAnalyst (Dhariwal et al., 2017). LefSe model was used to predict classifier

taxa at the genus level (Segata et al., 2011) in each diet group regardless of genotype. The relative abundance of the gut microbial phyla, families, and genera was exported from MicrobiomeAnalyst and visualized using GraphPad Prism v.8.2.1 (GraphPad Software Inc., CA, USA).

Short-chain fatty acids

Plasma SCFAs were analyzed as described in Chapter 2. Briefly, plasma samples were mixed 1:2 with methanol and centrifuged at 14,000 g for 60 min. Supernatant was collected and injected (1 µl) into an Agilent gas chromatograph system 7890A, with flame ionization detector (Agilent Technologies, Wilmington, DE, USA) and 19091N-133 Agilent capillary column. Oven temperature was set to 100 °C for 10 min and increased to 220 °C over 25 min, with Helium as the carrier gas at a flow rate of 1.0 mL/min. Calibration curves were constructed using SCFAs standard solution (Supelco, 46975-U, Bellefonte, PA, USA) for determining the concentration.

Gene expression analysis

Total RNA from mouse colons was extracted by single step acid guanidinium thiocyanate-phenol-chloroform method of Chomczyński and Sacchi (Chomczynski and Sacchi, 1987; Chomczynski and Sacchi, 2006). RNA integrity was assessed by gel electrophoresis and its quantity was estimated spectrophotometrically by measuring the absorbance at 260 nm. Total RNA (1 µg) was used to synthesize cDNA by reverse transcription using M-MLV reverse transcriptase (Invitrogen, Carlsbad, CA) and random primers. Quantitative analysis of mRNA abundance of each of glucose-regulated protein 78kDa (*Grp78*), spliced X-box binding protein 1 (*sXbp1*), activating transcription factor 4 (*Atf4*), and glucose-regulated protein 94kDa (*Grp94*) genes was carried out by real-time quantitative polymerase chain reaction (qPCR), against the average mRNA abundance of each of Hypoxanthine-guanine phosphoribosyl transferase (*Hprt)* and Glyceraldehyde 3-phosphate dehydrogenase (*Gapdh)*. Samples were assayed in duplicates using a BioRad CFX96 detection system based on SYBR Green chemistry. The thermal profile for the qPCR reactions was 95 °C for 3 min, then 35 cycles of 95 °C for 10 s and 30 s at annealing temperature. A melt curve generated by a gradual

increase of temperature (5 °C/ 5 s) from 65 to 95 to confirm the specificity of the reaction. The fold change of target gene expression was calculated using the taking-difference linear regression method of Rao et al. (2013). The sequences of the primers used are listed in Appendix II.

Statistical analysis

Statistical analysis was performed with GraphPad Prism v.8.2.1 (GraphPad Software Inc., CA, USA) and RStudio v.1.1.463 with R v. 4.0 (R Core Team, 2020). Statistical tests were applied to males and females separately. Data was presented as mean and standard error. Means denoted by different superscript letters indicate a significant difference by one-way ANOVA accompanied with Fisher's LSD test or Kruskal-Wallis test accompanied with Dunn's test based on data normality verified using Shapiro-Wilk's test. The differences were considered significant when $p<0.05$, and trends of $p=0.05$-0.1 were discussed. Permutational analysis of variance (PERMANOVA) of PCoA was performed using Adonis function from VEGAN package v.2.5-6 (Dixon, 2003). The 95% level of confidence ellipses of PCoA based on *t* distribution were plotted using the implementation of ggplot2 package v.3.3.2 (Wickham, 2016) in MicrobiomeAnalyst. Pairwise PERMANOVAs with FDR correction were calculated using RVAideMemoire package v.0.9-75 (Hervé, 2020).

3.3. Results

3.3.1. PRPE supplementation of WSD prevents adiposity in both male and female mice

Previously, PRPE supplementation was shown to prevent diet-induced obesity in mice (Kubow et al., 2014). To confirm the ability of PRPE to reduce adiposity on WSD, we fed mice PRPE-supplemented WSD for 7 weeks. In agreement with previous work, PRPE supplementation of WSD effectively reduced adiposity in both male and female mice (Fig. 3-1A to Fig. 3-1C). Since PRPE contains additional compounds such as polysaccharides and peptides (Kubow et al., 2014), we further purified PRPE (hereafter referred to as PPP) to exclude the possible bioactive effects of these components. Supplementation of WSD with PPP tended (p = 0.08) to reduce the body weight gain of male mice and but not female mice (Fig. 3-1D and Fig. 3-1E).

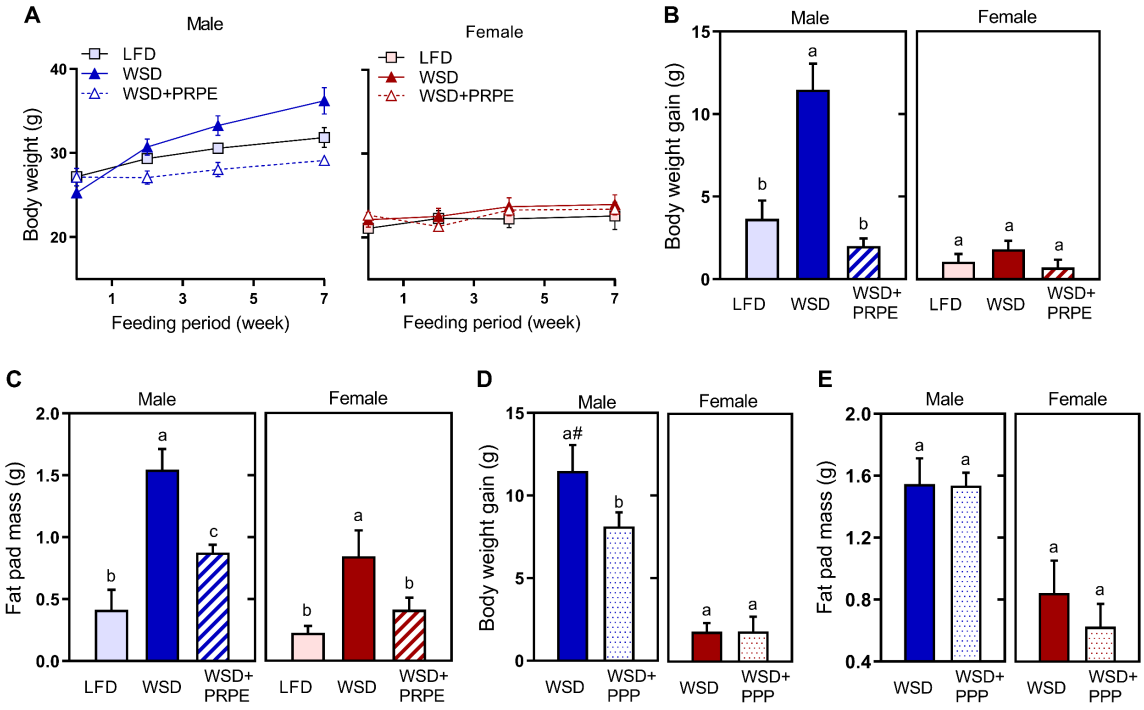

Figure 3-1. PRPE supplementation of WSD reduces body weight gain in mice. (A) Growth curve, (B and D) body weight gain, and (C and E) gonadal fat pad mass of mice, n= 5, except for PPP: n= 3, mean ± SEM. Means denoted by different superscript letters (a and b) indicate $p<0.05$, (#) symbol indicate $p=0.05$-0.1 by one-way ANOVA accompanied with Fisher's LSD test, males and females analyzed in separate models. Blue and red indicate male and female mice. LFD: Low fat diet, WSD: Western-style diet, WSD+PRPE: Western-style diet supplemented with polyphenolic-rich potato extract, WSD+PPP: Western-style diet supplemented with purified PRPE.

To detemine if PRPE supplementation reduced the food intake of mice or altered their metabolic rate, we measured food intake, physical activity and energy expenditure using indirect calorimetry. Both male and female mice fed PRPE-supplemented WSD consumed similar amounts of food (mean± SEM) (g/day): males 3.6±0.06, females 4.1±0.53 compared to their counterparts on WSD (mean± SEM) (g/day): males 3.3±0.38, females 2.8±0.74 (males: $p = 0.49$ and females: $p = 0.14$). As anticipated, on LFD, mice displayed increased activity level during the dark phase compared to the light phase, and feeding WSD reduced the activity of the mice during the dark phase (Fig. 3-2A). Both male and female mice fed PRPE-supplemented WSD showed similar activity level in the dark phase compared to that of their respective counterparts on WSD (Fig. 3-2A). Feeding WSD reduced the respiratory quotient (RQ) of both mice sexes (Fig. 3-2B). While male mice on PRPE-supplemented WSD showed similar RQ value to their counterparts on WSD (Fig. 3-2B, left), the RQ value of female mice on PRPE-supplemented WSD was lower than that observed for their counterparts on WSD in the dark phase (Fig. 3-2B, right). Furthermore, WSD reduced the energy expenditure (EE) of mice in the dark phase, but PRPE supplementation prevented WSD-induced reduction in EE in both sexes of the mice (Fig. 3-2C). Together, these results demonstrate that PRPE supplemetation of WSD increased the energy ependiture in both male and female mice, but altered the respiratory quotient in a sex dimorphic maner without altering the food intake or physical activity.

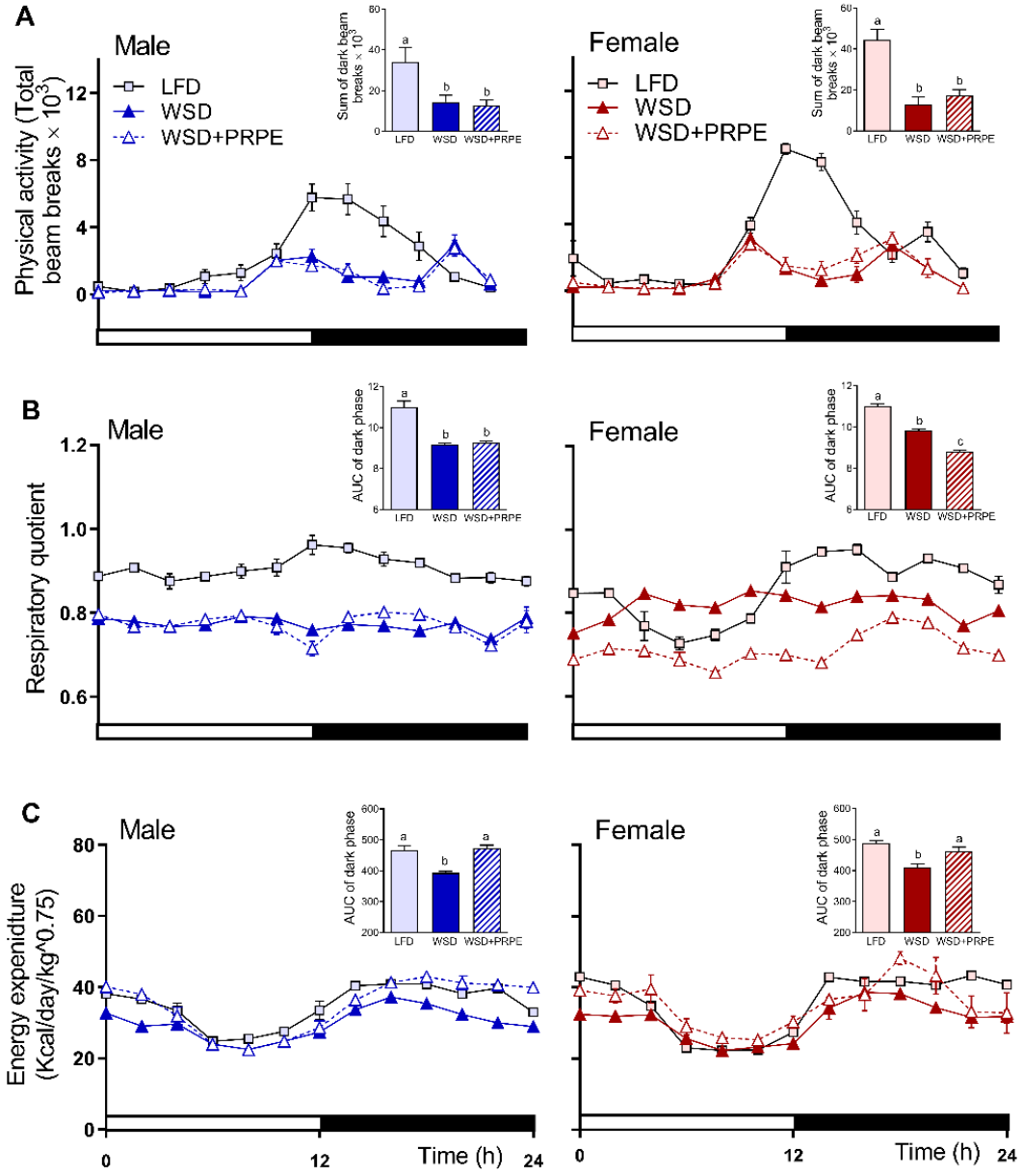
A
Male
LFD
WSD
WSD+PRPE
Physical activity (Total beam breaks × 10^3)
Sum of dark beam breaks × 10^3
Female
B
Respiratory quotient
AUC of dark phase
C
Energy expenidture (Kcal/day/kg^0.75)
Time (h)

Figure 3-2. PRPE supplementation enhances energy expenditure in male and female mice on WSD. (A) Rate of physical activity, (B) respiratory quotient, and (C) energy expenditure, n=3 mice per group of 2-3 dark phases, data represent mean/ 2 h± SEM. Insets represent the summation of total beam breaks (in A) or area under the curve (AUC) (in B and C) of the dark phases, data represented as mean ± SEM. Means denoted by different superscript letters (a, b, and c) indicate data statistically different with $p<0.05$ by one-way ANOVA accompanied with Fisher's LSD test, males and females analyzed in separate models. The white bar represents the light period (12 h) and the black bar represents the dark period (12 h). LFD is represented by square symbols, WSD is represented by closed and PRPE-supplemented WSD by open tringle symbols. Blue and red indicate male and female mice, respectively. LFD: Low fat diet, WSD: Western-style diet, WSD+PRPE: Western-style diet supplemented with poly-phenolic rich potato extract.

3.3.2. Prevention of gut microbial diversity loss by PRPE supplementation of WSD in male mice

Gut microbiota plays an important role in regulating host metabolism (Hooper and Gordon, 2001; Musso et al., 2011). To characterize the gut microbial modification associated with the reduced adiposity status and altered metabolic rate in mice fed PRPE-supplemented WSD, we sequenced the full 16S rRNA gene of DNA purified from mouse stool samples. Results showed that WSD feeding led to a decrease in the gut microbial richness of male mice, which was prevented by PRPE supplementation of WSD (Fig. 3-3A, left). No difference was detected in the gut microbial richness of female mice (Fig. 3-3A, right). Similarly, Shannon's diversity was reduced in response to WSD feeding in both male and female mice (Fig. 3-3B). PRPE supplementation of WSD tended ($p = 0.06$) to prevent this reduction in male mice (Fig. 3-3B, left), but it further reduced the Shannon's diversity in female mice (Fig. 3-3B, right). The heatmap of species abundance showed a loss in gut microbial species following WSD feeding and displayed distinct patterns of gut microbial structure between groups consuming WSD or WSD+PRPE in both sexes. (Fig. 3-3C). Principal coordinate analysis (PCoA) between samples was used to estimate the β-diversity of the gut microbial communities. Both male and female mice on LFD showed clustering between samples in the same diet group and separation from other diet groups (Fig. 3-3D). The separation of samples of mice fed WSD from those of mice fed PRPE-supplemented WSD was more obvious in male compared to female mice (Fig. 3-3D).

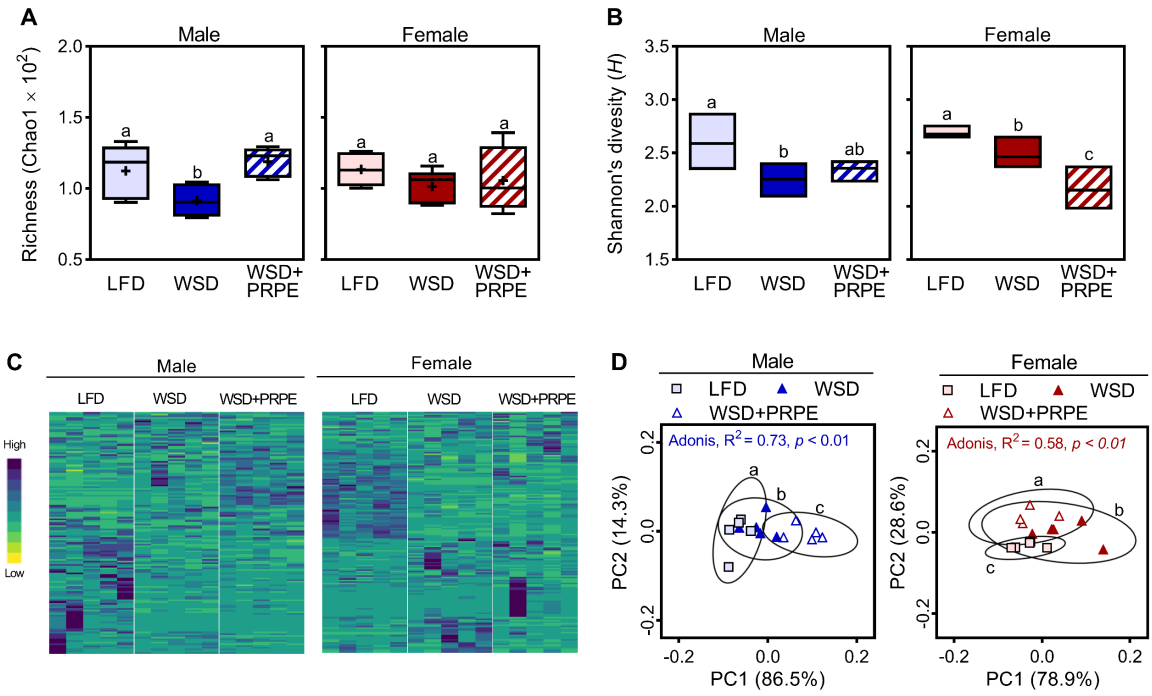

Figure 3-3. Differences in gut microbial diversity of male and female mice fed PRPE supplemented WSD. (A) Taxonomic richness of the gut microbiota estimated by Chao1 index, and (B) Shannon's diversity *H*-index; (+) represent mean and whiskers represent range, means denoted by different superscript letters (a, b, c) indicate $p<0.05$ by one-way ANOVA accompanied with Fisher's LSD test. (C) Heatmaps of the gut microbial species abundance, second female sample on WSD+PRPE was excluded from other analyses as it included <1000 reads. (D) Principal coordinate analysis of the gut microbial samples based on Jensen-Shannon distances, sample clusters denoted by different superscript letters indicate significant clustering ($p<0.05$) by Adonis PERMANOVA accompanied with FDR corrected pairwise comparisons, ellipses indicate 95% confidence assuming *t* distribution. n=5, except female on WSD+PRPE n=4, males and females analyzed in separate models. Blue and red indicate male and female mice, respectively. LFD: Low fat diet, WSD: Western-style diet, WSD+PRPE: Western-style diet supplemented with polyphenolic-rich potato extract.

Due to the coprophagic nature of mice and since mice in this experiment were housed in one cage per diet group, differences in the gut microbial communities between mice in different diet groups may be triggered by co-housing (Ericsson and Franklin, 2015). To exclude this possibility, a second feeding experiment was carried out and mice were housed in 2-3 different cages per treatment. In the second experiment, male and female mice of both wild-type and fatty acid binding protein 6 (Fabp6)-deficient genotypes were used (*Fabp6*$^{+/+}$ and *Fabp6*$^{-/-}$, respectively). *Fabp6*$^{-/-}$ mice were used since they exhibited enhanced state of adiposity on WSD associated gut microbial dysbiosis (Appendix I and Chapter 2). The ability of PRPE supplementation to counteract WSD-induced adiposity in *Fabp6*$^{-/-}$ mice and whether this is associated with desirable remodeling of gut microbiota were evaluated. Both male and female *Fabp6*$^{+/+}$ mice exhibited reduced body weight gain on PRPE-supplemented WSD compared to their counterparts on WSD (Fig. 3-4A). Likewise, male *Fabp6*$^{-/-}$ mice gained significantly less body weight on PRPE-supplemented WSD compared to their counterparts on WSD (Fig. 3-4B, left), however, no statistical differences were observed among female *Fabp6*$^{-/-}$ mice (Fig. 3-4B, right). Thus, the ability of PRPE supplementation to reduce body weight gain on WSD was reproducible in both *Fabp6*$^{+/+}$ and *Fabp6*$^{-/-}$ mice.

Similar to male C57BL/6J mice, the gut microbiota of male *Fabp6*$^{+/+}$ mice showed a reduction in the taxonomic richness and diversity in response to WSD feeding, which was prevented by PRPE supplementation of WSD (Fig. 3-5A, left and 3-5B, left). Female *Fabp6*$^{+/+}$ mice showed an increase in the gut microbial richness in response to both WSD and PRPE supplemented WSD (Fig. 3-5A, right). This was accompanied by a reduction in diversity in response to WSD, which was prevented by PRPE supplementation (Fig. 3-5B, right). PCoA analysis showed clustering of the gut microbiota of male and female *Fabp6*$^{+/+}$ mice fed WSD from the gut microbiota of their respective counterpart mice fed either LFD or PRPE supplemented WSD, however, this clustering was not statistically significant (Fig. 3-5C).

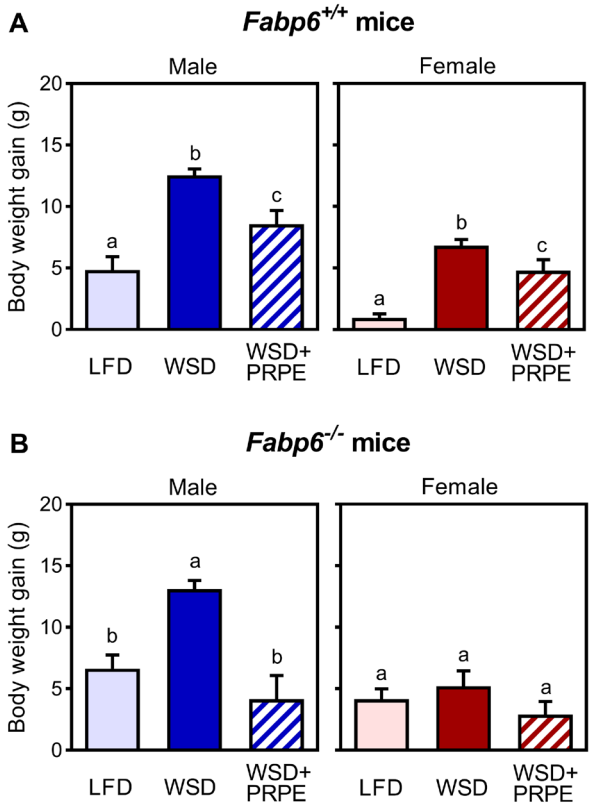

Figure 3-4. PRPE supplementation reduces body weight gain of *Fabp6*$^{+/+}$ and *Fabp6*$^{-/-}$ mice on WSD. Body weight gain of (A) *Fabp6*$^{+/+}$, and (B) *Fabp6*$^{-/-}$ mice, n= 4-6, mean ± SEM, means denoted by different superscript letters (a and b) indicate $p<0.05$, (#) indicate $p= 0.5$-0.1 by one-way ANOVA accompanied with Fisher's LSD test, males and females analyzed in separate models. Blue and red indicate male and female mice. LFD: Low fat diet, WSD: Western-style diet, WSD+PRPE: Western-style diet supplemented with polyphenolic-rich potato extract.

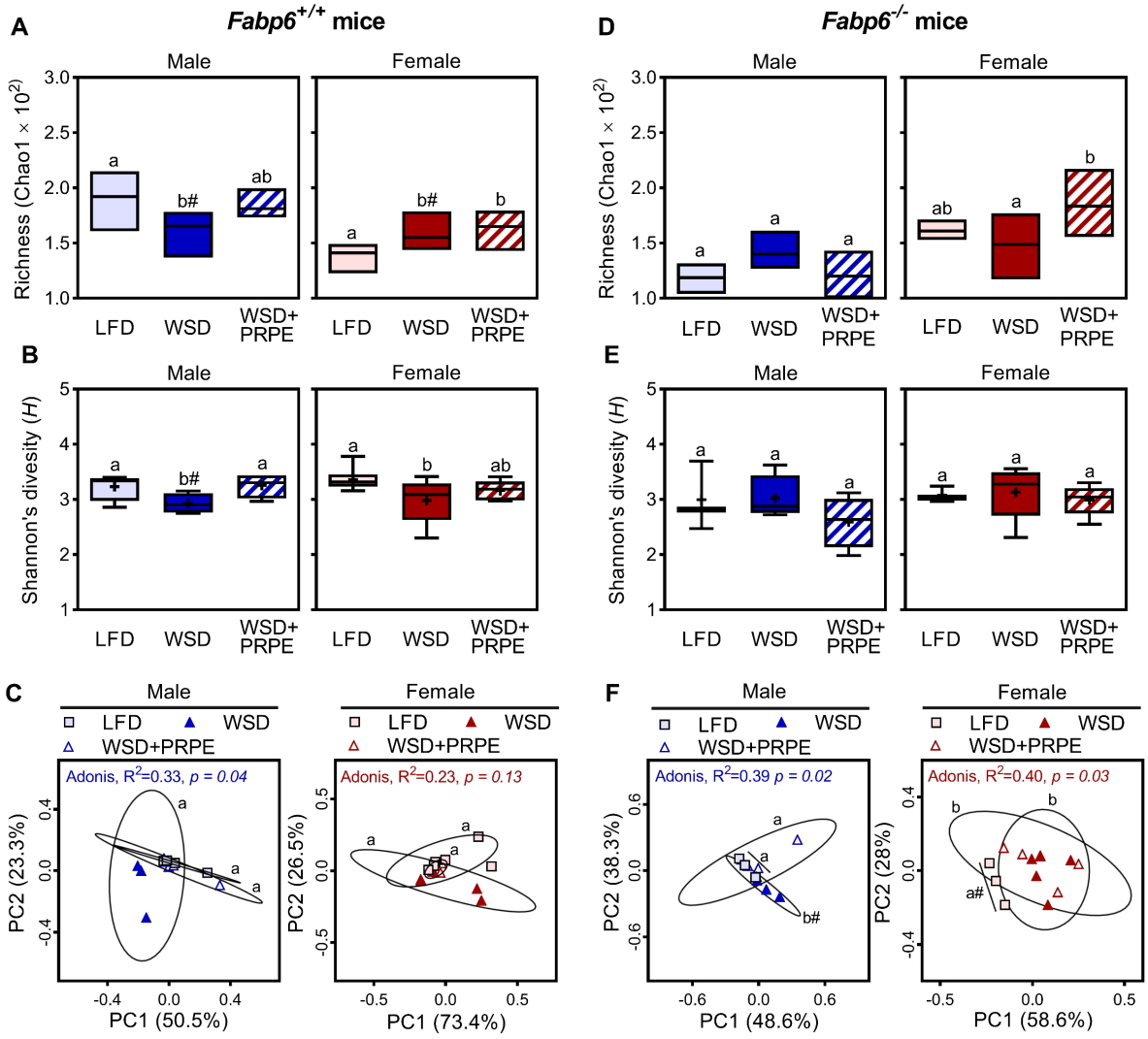

Figure 3-5. The gut microbial diversity of *Fabp6*$^{+/+}$ and *Fabp6*$^{-/-}$ mice on PRPE-supplemented WSD. (A and D) Taxonomic richness estimated by Chao1 index, (B and E) Shannon's diversity *H*-index of the gut microbiota of *Fabp6*$^{+/+}$ (n=4-6) and *Fabp6*$^{-/-}$ (n=3-5), respectively; (+) represent mean and whiskers represent range, means denoted by different superscript letters (a, b, c) indicate $p<0.05$, (#) symbol indicate $p=0.05$-0.1 by one-way ANOVA accompanied with Fisher's LSD test. (C and F) Principal coordinate analysis of the gut microbial samples based on Jensen-Shannon distances in *Fabp6*$^{+/+}$ and *Fabp6*$^{-/-}$, respectively, sample clusters denoted by different superscript letters indicate significant clustering ($p<0.05$), (#) symbol indicate $p=0.05$-0.1 by Adonis PERMANOVA accompanied with FDR corrected pairwise comparisons, ellipses indicate 95% confidence assuming *t* distribution. males and females analyzed in separate models. Fabp6: Fatty acid binding protein 6, PC: principal coordinate, Low LFD: low fat diet, WSD: Western-style diet, WSD+PRPE: Western-style diet supplemented with polyphenolic-rich potato extract.

The analysis of the gut microbiota of *Fabp6*$^{-/-}$ mice showed no significant differences in the gut microbial richness of male mice (Fig. 3-5D, left). However, the gut microbial richness of female *Fabp6*$^{-/-}$ mice fed PRPE-supplemented WSD was higher compared to their counterparts on WSD (Fig. 3-5D, right). In both male and female *Fabp6*$^{-/-}$ mice, no difference in the gut microbial diversity among different diet groups where noticed (Fig. 3-5E). PCoA showed clustering of male *Fabp6*$^{-/-}$ mice samples of both LFD and PRPE-supplemented WSD diet groups (Fig. 3-5F, left), but not in females (Fig. 3-5F, right). Overall, in addition to prevention of WSD-induced adiposity, PRPE supplementation also altered the gut microbial diversity in both *Fabp6*$^{+/+}$ and *Fabp6*$^{-/-}$ mice in a sex dimorphic manner.

3.3.3. Sex dimorphic modulation of gut microbial composition in mice in response to PRPE supplementation of WSD.

To determine the compositional modifications in the gut microbiota of mice in response to PRPE supplementation, the proportions of gut microbiota at phylum, family, and genus taxonomic levels were investigated. At the phylum level, WSD increased the ratio of Firmicutes:Bacteroidetes in both male and female mice (Males: Fig. 3-6A, left; females: Fig. 3-6A, right). Feeding PRPE-supplemented WSD induced further increase in the ratio of Firmicutes:Bacteroidetes in male mice compared to their counterparts on WSD (Fig. 3-6A, left). However, in female mice, PRPE-supplemented WSD feeding reduced the ratio of Firmicutes:Bacteroidetes compared that of mice on WSD (Fig. 3-6A, right). In addition to the main phyla, Bacteroidetes and Firmicutes, mice showed elevated proportion of phylum Verrucomicrobia, which is a distinctive gut microbial feature of mice from Jackson Labs (Rosshart et al., 2017). Verrucomicrobia abundance was similar among the male groups, but it increased in both female fed WSD and PRPE-supplemented WSD compared to their counterparts on LFD (Males: Fig. 3-6A, left; females: Fig. 3-6A, right).

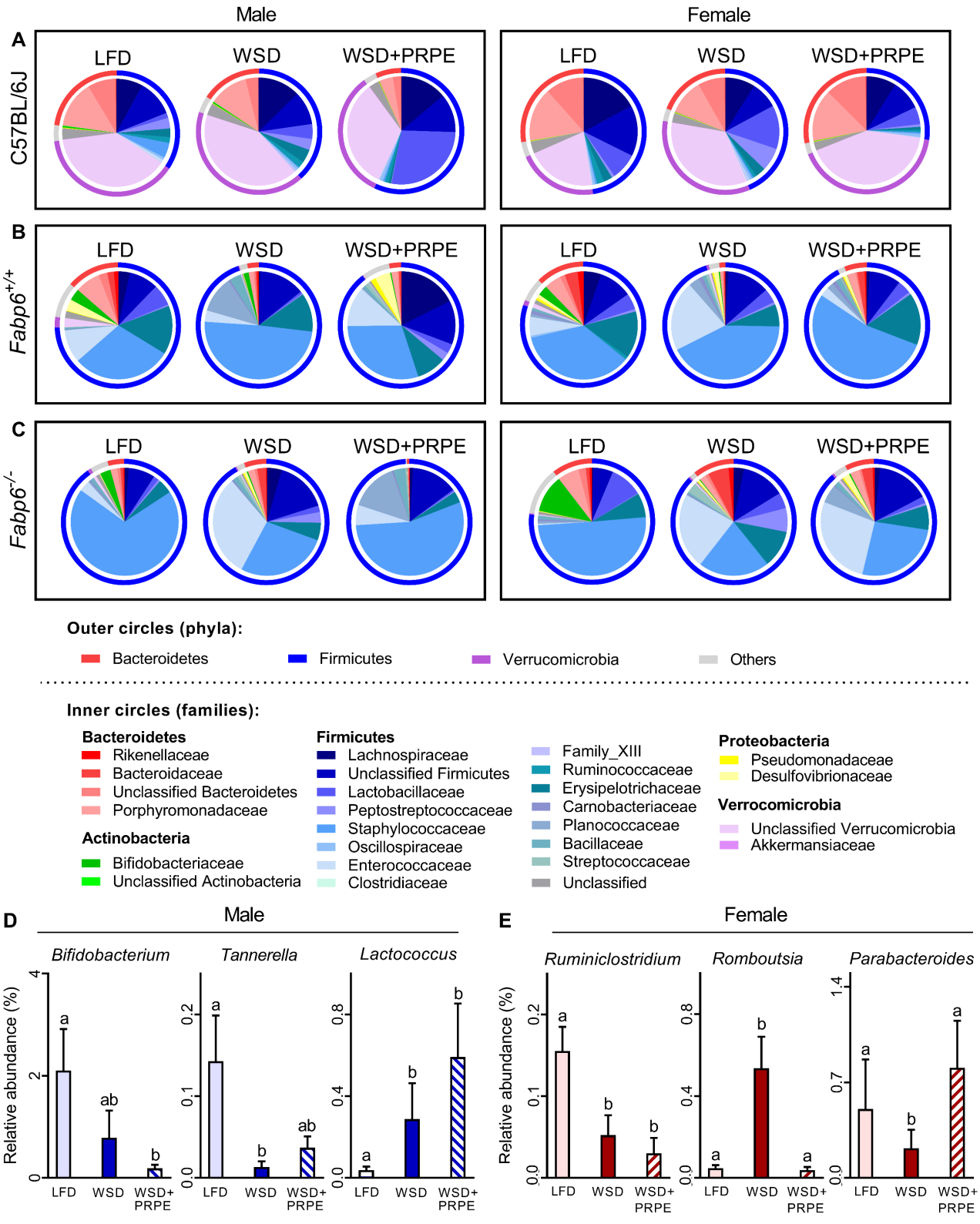
Male
Female
A
C57BL/6J
B
Fabp6+/+
C
Fabp6-/-
LFD
WSD
WSD+PRPE
Outer circles (phyla):
Bacteroidetes
Firmicutes
Verrucomicrobia
Others
Inner circles (families):
Bacteroidetes
Rikenellaceae
Bacteroidaceae
Unclassified Bacteroidetes
Porphyromonadaceae
Actinobacteria
Bifidobacteriaceae
Unclassified Actinobacteria
Firmicutes
Lachnospiraceae
Unclassified Firmicutes
Lactobacillaceae
Peptostreptococcaceae
Staphylococcaceae
Oscillospiraceae
Enterococcaceae
Clostridiaceae
Family_XIII
Ruminococcaceae
Erysipelotrichaceae
Carnobacteriaceae
Planococcaceae
Bacillaceae
Streptococcaceae
Unclassified
Proteobacteria
Pseudomonadaceae
Desulfovibrionaceae
Verrocomicrobia
Unclassified Verrucomicrobia
Akkermansiaceae
D
Male
Bifidobacterium
Tannerella
Lactococcus
E
Female
Ruminiclostridium
Romboutsia
Parabacteroides
Relative abundance (%)
LFD
WSD
WSD+ PRPE

Figure 3-6. PRPE supplementation modifies the gut microbial composition in a sex dimorphic manner. Gut microbial composition, outer circles: relative abundance of the gut microbiota at the phylum level, inner circles: relative abundance of the top 20 gut microbial families in (A) C57Bl/6J mice n=4-5, (B) *Fabp6*$^{+/+}$ mice n=4-6, and (C) *Fabp6*$^{-/-}$ n=3-5. Relative abundance of classifier genera estimated by the LefSe model in pooled samples for (D) male and (E) female mice; n=12-16, mean ± SEM, means denoted by different superscript letters (a and b) indicate $p<0.05$ by Kruskal-Wallis test accompanied with Dunn's test, males and females analyzed in separate models. Fabp6: Fatty acid binding protein 6, LFD: low fat diet, WSD: Western-style diet, WSD+PRPE: Western-style diet supplemented with polyphenolic-rich potato extract.

Male and female *Fabp6*$^{+/+}$ mice, also, showed higher ratio of Firmicutes:Bacteroidetes in response to WSD feeding, which was reduced by PRPE-supplementation of WSD (male: Fig. 3-6B, left; females: Fig. 3-6B, right). This reduction was accompanied with increased Proteobacteria proportion in males, and Bacteroidetes proportion in females (male: Fig. 3-6B, left; females: Fig. 3-6B, right). Conversely, male *Fabp6*$^{-/-}$ mice showed lower ratio of Firmicutes:Bacteroidetes in response to WSD feeding, however PRPE supplementation of WSD resulted in a vast increase of the Firmicutes proportion; as 99% of phylum composition was comprised of Firmicutes (Fig. 3-6C, left). Similar to their *Fabp6*$^{+/+}$ counterparts, female *Fabp6*$^{-/-}$ mice showed higher Firmicutes:Bacteroidetes in response to WSD feeding, and PRPE supplementation further increased this ratio along with the proportion of Proteobacteria (Fig. 3-6C, right).

At the family level, the analysis showed that feeding PRPE-supplemented WSD increased the proportion of Lactobacillaceae but reduced Porphyromonadaceae in male mice compared to their counterparts on WSD (Fig. 3-6A, left). In contrast, female mice fed PRPE-supplemented WSD showed increased Porphyromonadaceae but reduced Lactobacillaceae compared to their counterparts on WSD (Fig. 3-6A, right). Similarly, compared to their respective counterparts on WSD, *Fabp6*$^{+/+}$ male mice fed PRPE-supplemented WSD showed higher proportion of Lactobacillaceae with no difference in Porphyromonadaceae (Fig. 3-6B, left), and *Fabp6*$^{+/+}$ female mice fed PRPE-supplemented WSD showed higher proportion of Porphyromonadaceae, with no difference in Lactobacillaceae (Fig. 3-6B, right). *Fabp6*$^{-/-}$ mice did not show major changes in the proportions of Lactobacillaceae and Porphyromonadaceae in response to PRPE supplementation, however both male and female *Fabp6*$^{-/-}$ mice fed PRPE-supplemented WSD showed increased proportion of Planococcaceae and reduced proportions of each of Lachnospiraceae, Erysipelotrichaceae, and Peptostreptococcaceae compared to their counterparts on WSD (Males: Fig. 3-6C, left; females: Fig. 3-6C, right). Thus, PRPE supplementation of WSD promoted the expansion of distinct gut microbial families in wild-type males and females, whereas it induced multiple consistent changes among gut microbial families in *Fabp6*$^{-/-}$ mice.

LefSe model was used to discover classifier genera among the gut microbial communities in each diet group, for this purpose, mice were pooled into diet groups regardless of their genotype to enhance the model performance. In male mice, the genera *Bifidobacterium*, *Tannerella*, and *Lactococcus* were the top classifiers of the LFD, WSD, and PRPE-supplemented WSD groups respectively (Fig. 3-6D). In female mice, *Ruminiclostridium*, *Rombutsia*, and *Parabacteroides* were the top classifiers of the LFD, WSD, and PRPE-supplemented WSD groups respectively (Fig. 3-E). Thus, the discovered biomarker gut microbial genera where also distinct in male and female mice. Together, these results illustrate the sex dimorphic response of the gut microbial composition to PRPE supplementation.

3.3.4. PRPE supplementation of WSD increases plasma SCFAs concentrations and prevents UPR pathway activation in the colons of male mice

SCFAs are among the most important gut microbial metabolites that impact the health status of the host. The most abundant SCFAs are acetic, propionic and butyric acids, which together compose 95% of the total SCFAs in the colon (Cummings et al., 1987). Thus, we determined whether the above gut microbial modifications were associated with altered plasma SCFAs concentrations. Male mice on WSD showed significantly lower concentration of total SCFAs, and particularly of acetic acid, compared to their counterparts on LFD. PRPE supplementation of WSD increased the concentration of total SCFAs, and acetic acid, to a level comparable to that of mice on LFD (Fig. 3-7A, left). Male *Fabp6*$^{+/+}$ mice showed a similar pattern in response to PRPE supplementation of WSD (Fig. 3-7A, middle). Male *Fabp6*$^{-/-}$ mice showed superior concentrations of total plasma SCFAs in response to PRPE-supplemented WSD compared to their counterparts on either LFD or WSD (Fig. 3-7A, right). In female mice, no difference in the total SCFAs concentration in the diet groups were noticed (Fig. 3-7B, left). A tendency (p = 0.07) to increased total SCFAs in female *Fabp6*$^{+/+}$ mice fed WSD compared to their counterparts fed PRPE-supplemented WSD was noticed, which was, mainly, due to higher propionic acid concentration (Fig. 3-7B, middle). Similar to male *Fabp6*$^{-/-}$ mice, female *Fabp6*$^{-/-}$ mice also exhibited increased concentration of SCFAs in response to PRPE-supplemented WSD (Fig. 3-7B, right).

SCFAs and their metabolites have been shown to promote proteostasis and alleviate endoplasmic reticular stress (Vega et al., 2016; Huang et al., 2017; Hu et al., 2018). The exact mechanism is still unknown, but SCFAs may modify the endoplasmic reticulum environment to facilitate protein folding (Hu et al., 2018). Since colonocytes metabolize the major part of the SCFAs produced by the gut microbiota (Ríos-Covián et al., 2016), we assayed markers of unfolded protein response (UPR) in the colons of a sample of mice. WSD feeding increased the mRNA abundance of *Grp78*, as well as *sXbp1*, *Atf4*, and *Grp94* in male mice (Fig. 3-7C, left), which indicates the activation of the 3 arms of the UPR pathway, inositol-requiring enzyme 1 α (IRE1α), the protein kinase R-like endoplasmic reticulum kinase (PERK), and activating transcription factor-6 (ATF6), respectively (Wang and Kaufman, 2016; Hetz and Papa, 2018). Feeding PRPE-supplemented WSD reduced the mRNA abundance of each of the assayed UPR markers compared to that in mice fed WSD (Fig. 3-7C, left). Only a trend ($p = 0.09$) toward increased *sXbp1* mRNA abundance in female mice fed WSD was noticed, however feeding PRPE-supplemented WSD did not reduce it (Fig. 3-7C, right). Together, these results indicate that supplementing WSD with PRPE attenuates UPR activation in the colon of male mice.

3.4. Discussion

Previously, PRPE was shown to prevent adiposity in mice fed an obesity-inducing high fat diet (Kubow et al., 2014). Similarly, here in this study PRPE prevented WSD-induced adiposity in both wild-type and *Fabp6*$^{-/-}$ mice. On the other hand, PPP, a preparation that contains only the polyphenolic compounds of PRPE, only tended to attenuate the body weight gain of mice fed WSD. This might be due to a loss of some species of polyphenol compounds or other components during the purification process, which impacted the biological activity of the preparation. Thus, optimization of the purification procedure is necessary to ensure the preservation of potency. Nevertheless, the results obtained demonstrate the ability of potato polyphenols to prevent metabolic dysfunction induced by adiposity-inducing high fat diets.

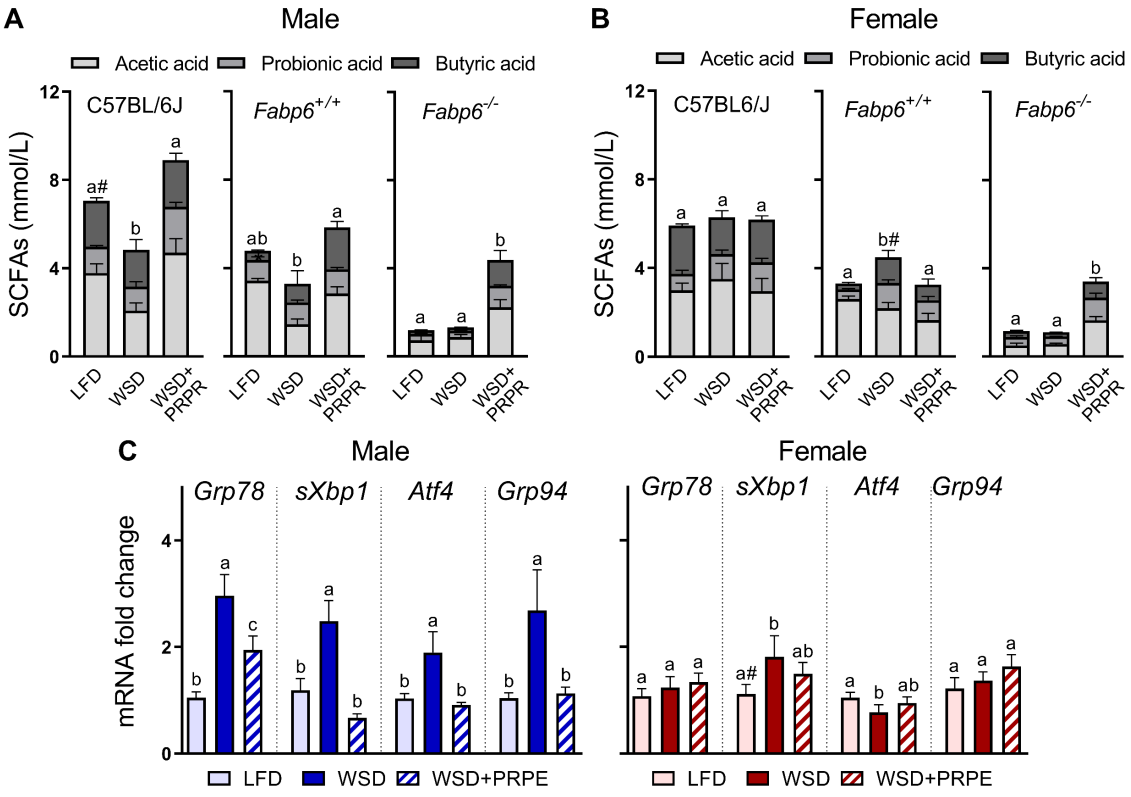

Figure 3-7. PRPE supplementation increases plasma SCFAs and prevents UPR pathway activation in mice fed WSD. SCFAs concentrations in the plasma of (A) male and (B) female mice, n=3-5, (C) markers of unfolded protein response pathway in the colon of male and female C57BL/6J mice, n=5. Mean ± SEM, means denoted by different superscript letters (a, b, c) indicate $p<0.05$, (#) symbol indicate $p=0.05$-0.1 by one-way ANOVA accompanied with Fisher's LSD test, males and females analyzed in separate models. Grp78: Glucose-regulated protein 78kDa, sXbp1: Spliced X-box binding protein 1, Atf4: Activating transcription factor 4, Grp94: Glucose-regulated protein 94kDa, SCFAs: Short chain fatty acids, Low fat diet, WSD: Western-style diet, WSD+PRPE: Western-style diet supplemented with polyphenolic-rich potato extract.

A key finding of this study was the ability of PRPE to counteract the loss of gut microbial diversity which was an undesirable feature of WSD-induced gut microbial dysbiosis. This might be attributable to a prebiotic activity of polyphenols which leads to the enrichment of particular classes of beneficial gut microbiota (Hervert-Hernandez et al., 2009; Bialonska et al., 2010; Etxeberria et al., 2013). In addition, PRPE may modify the gut luminal environment, or enrich the growth of specific gut microbial species whose metabolites modify the gut environment thereby creating conditions suitable for the expansion of non-abundant species (Etxeberria et al., 2013). Polyphenols are also well-known for their ability to inhibit carbohydrate digestion and reduce intestinal abundance of glucose transporters leading to decreased glucose absorption by the host (Hanhineva et al., 2010). On one side this would increase the availability of nutrients to gut microbiota which enhances their diversity, on the other side it may explain the reduced respiratory quotient of female mice in response to PRPE supplementation.

Male and female mice fed PRPE-supplemented WSD showed increased abundance of bacteria belonging to Lactobacillaceae and Bacteroides families, respectively. The enrichment of Lactobacillaceae, many species of which are regularly used as probiotics, by polyphenols extracted from other plants has been observed previously (Hervert-Hernandez et al., 2009; Fogliano et al., 2011). On the other hand, Bacteroides are known for their health promoting effects and have been recently considered as next-generation probiotics. In fact, some Bacteroides spp. have been authorized for use as probiotics by the European Commission (Tan et al., 2019). PRPE therefore may facilitate recovery from dysbiosis by enriching the growth of eubiosis-promoting gut microbial species.

Another important observation of this study was the sex dimorphic response of the gut microbiota to PRPE supplementation, which was associated with sex differences in adiposity, glucose tolerance and UPR pathway activation. Sex differences in the metabolic activity of the host are typically attributed to host factors, such as genes and hormones (Sugiyama and Agellon, 2012). However, it is becoming more apparent that gut microbiota itself may contribute to the sex dimorphic metabolic

response. For example, female nonobese diabetic (NOD) mouse show higher risk to develop type 1 diabetes but transplantation of gut microbiota from adult male NOD mouse to immature germ-free female NOD has been shown to result in significant protection of these mice from type 1 diabetes (Markle et al., 2013). This indicates the importance of gut microbiota in driving the sex dimorphic risk to metabolic dysfunction.

An interesting finding of this study was the mitigation of UPR activation by PRPE supplementation of WSD in male mice. WSD is high in saturated fatty acids such as palmitate, which is a potent inducer of ER stress (Karaskov et al., 2006). Palmitate induces overproduction of reactive oxygen species (ROS) resulting in a loss of redox homeostasis and triggering ER stress (Ly et al., 2017; Chong et al., 2017). Given the antioxidant properties of polyphenols, certain polyphenols of PRPE may act directly to prevent the accumulation of ROS and prevent ER stress. Therefore, the reduced levels of UPR markers in PRPE-supplemented WSD fed mice may indicate low level of ER stress in these mice. On the other hand, mice fed PRPE-supplemented WSD showed increased concentration of plasma SCFAs. Some species of SCFAs and their metabolites can also promote ER proteostasis by facilitating protein folding (Hu et al., 2018). For example, a butyric acid metabolite 4-phenylbutyrate is a potent UPR mitigator and suppressor of oxidative stress associated with type 2 diabetes and colitis in mice (Özcan et al., 2006; Cao et al., 2013; Vega et al., 2016). Interestingly, 4-phenylbutyrate shares similar structure with ferulic acid (Masuzaki et al., 2019), the second major polyphenolic compound found in PRPE (Kubow et al., 2014).

The increased SCFAs concentrations by PRPE supplementation in male wildtype mice, in this study, could be attributed to their higher gut microbial abundance of SCFA-producing microbiota such as *Lactobacillaceae*, *Lachnospiraceae*, and *Clostridiaceae*. It has been also shown that probiotics mixtures included *Lactobacillus* spp. increased the levels of fecal SCFAs and promoted the growth of other SCFA producing microbiota such as Clostridia (Nagpal et al., 2018b; Markowiak-Kopeć and Śliżewska, 2020). Indeed, the growth medium of gut microbiota grown *in vitro* in the presence of synthetic mixtures of polyphenols similar to those found in PRPE showed two- to five-fold increase in the SCFAs concentrations (Sadeghi Ekbatan et al., 2016).

Although the increase of fecal SCFAs in obese subjects could be suggestive of enhanced energy extraction (Turnbaugh et al., 2006; Murphy et al., 2010), the higher concentration of SCFAs in PRPE-supplemented WSD fed mice in this study was associated with reduced adiposity. This effect can be explained, in part, by the increased energy expenditure in these mice as measured by indirect calorimetry. In fact, certain polyphenols were shown to potently reduce body weight gain by activating thyroid hormone and enhancing energy expenditure (da-Silva et al., 2007; Most et al., 2014; Karen Jesus et al., 2019). Moreover, the higher propionic acid levels found in PRPE-supplemented WSD fed mice may also contribute to their increased energy expenditure, as the administration of propionic was previously shown to increase physical activity and reduce lipogenesis (Shultz et al., 2008; Heimann et al., 2014; den Besten et al., 2015).

Several outcomes of the *Fabp6*$^{+/+}$ mouse experiment were in agreement with the outcomes of the first mouse experiment that included mice housed in one cage per group. Examples of these outcomes include the ability of PRPE supplementation to reduce body weight gain on WSD in both mice sexes, the reduction in the taxonomic richness and diversity in response to WSD feeding, which was prevented by PRPE supplementation of WSD in male mice, and the higher ratio of Firmicutes:Bacteroidetes in response to WSD feeding, which was reduced by PRPE-supplementation of WSD. These results provide an evidence that the detected gut microbial changes were related to PRPE supplementation and not primarily an effect of housing the mice in one cage.

Feeding PRPE-supplemented WSD to *Fabp6*$^{-/-}$ mice, a mouse model of bile malabsorption, also prevented features of gut microbial dysbiosis. Interestingly, the response of major gut microbial families that belong to both Firmicutes and Bacteroidetes in male and female mice were similar, as well as the response of plasma SCFAs concentration in both sexes. The reduction of both major Firmicutes families, such as Erysipelotrichaceae and Peptostreptococcaceae, in *Fabp6*$^{-/-}$ mice fed PRPE-supplemented WSD was consistent with that of wild-type mice fed the same diet. However, the increase of Planococcaceae was exclusive to *Fabp6*$^{-/-}$ mice. A positive correlation between the concentration of polyphenols and Planococcaceae growth has

been reported before (Huang et al., 2019). Yet, the similarities in the gut microbial composition between male and female *Fabp6*$^{-/-}$ mice induced by PRPE supplementation may be attributed to an additive effect of the antibacterial properties of both bile acids and polyphenols which was more potent in inhibiting certain classes of gut microbiota or promoting the growth of other classes, compared to the impact of each metabolite individually.

Given that our experimental approach in housing mice during the controlled feeding period was not based on single housing, this may allowed the exchange of some microbes between cage mates due to mice behaviors such as coprophagy and grooming (Ericsson and Franklin, 2015; Robertson et al., 2019). Although individualized housing of mice is recommended for future studies, the effect of PRPE supplementation on gut microbial features such as preventing the loss of diversity and enriching lactic acid bacteria was reproducible in *Fabp6*$^{+/+}$ and *Fabp6*$^{-/-}$ mouse models. This indicates the suitability of PRPE to be further considered in future research as a potential nutraceutical supplement to individuals with conditions associated with loss in gut microbial diversity such as following the intake of antibiotics or the exposure to gut infections. Follow up studies should target determining the main polyphenolic metabolites produced by the gut microbiota using metabolomic profiling, which would provide important clues on the role of the gut microbiota in triggering the observed phenotypes. Moreover, it would be interesting to investigate the specific effects of PRPE on host metabolism and gut microbiota devoid of WSD by feeding PRPE on a low fat diet background.

In summary, supplementation of WSD with PRPE counteracted WSD-induced adiposity and gut microbial dysbiosis in both wild-type and Fabp6-deficient mice. The gut microbial composition of mice fed PRPE-supplemented WSD was associated with enhanced plasma SCFAs concentration and prevented UPR pathway activation. Markedly, differences between male and female mice in their metabolic rate and gut microbial composition in response to PRPE supplementation were evident.

Acknowledgment

This study was supported by grants (to LBA and to SK) from the Natural Sciences and Engineering Research Council of Canada. Thanks to A. Swaby, Y. Chen, and D. Lee for their help in gut microbial sequencing experiment and to M. Iskandar for her help in the preparation of the potato polyphenolic extracts.

3.5. References

Bialonska, D., Ramnani, P., Kasimsetty, S.G.*, et al.* (2010). The influence of pomegranate by-product and punicalagins on selected groups of human intestinal microbiota. *Int J Food Microbiol, 140* (2-3), 175-182.

Cao, S.S., Zimmermann, E.M., Chuang, B.M.*, et al.* (2013). The unfolded protein response and chemical chaperones reduce protein misfolding and colitis in mice. *Gastroenterology, 144* (5), 989-1000.e1006.

Castro-Barquero, S., Lamuela-Raventós, M.R., Doménech, M.*, et al.* (2018). Relationship between Mediterranean dietary polyphenol intake and obesity. *Nutrients, 10* (10).

Chen, Y., Michalak, M. and Agellon, L.B. (2018). Importance of nutrients and nutrient metabolism on human health. *Yale J Biol Med, 91* (2), 95-103.

Chomczynski, P. and Sacchi, N. (1987). Single-step method of RNA isolation by acid guanidinium thiocyanate-phenol-chloroform extraction. *Anal Biochem, 162* (1), 156-159.

Chomczynski, P. and Sacchi, N. (2006). The single-step method of RNA isolation by acid guanidinium thiocyanate-phenol-chloroform extraction: Twenty-something years on. *Nat Protoc, 1* (2), 581-585.

Chong, W.C., Shastri, M.D. and Eri, R. (2017). Endoplasmic reticulum stress and oxidative stress: A vicious nexus implicated in bowel disease pathophysiology. *Int J Mol Sci, 18* (4), 771.

Cummings, J.H., Pomare, E.W., Branch, W.J.*, et al.* (1987). Short chain fatty acids in human large intestine, portal, hepatic and venous blood. *Gut, 28* (10), 1221-1227.

da-Silva, W.S., Harney, J.W., Kim, B.W., *et al.* (2007). The small polyphenolic molecule kaempferol increases cellular energy expenditure and thyroid hormone activation. *Diabetes, 56* (3), 767.

Del Rio, D., Rodriguez-Mateos, A., Spencer, J.P., *et al.* (2013). Dietary polyphenolics in human health: Structures, bioavailability, and evidence of protective effects against chronic diseases. *Antioxid Redox Signal, 18* (14), 1818-1892.

den Besten, G., Bleeker, A., Gerding, A., *et al.* (2015). Short-chain fatty acids protect against high-fat diet–induced obesity via a PPARγ-dependent switch from lipogenesis to fat oxidation. *Diabetes, 64* (7), 2398-2408.

Dhariwal, A., Chong, J., Habib, S., *et al.* (2017). Microbiomeanalyst - A web-based tool for comprehensive statistical, visual and meta-analysis of microbiome data *Nucleic Acids Res, 45* (W1), W180–W188.

Dhouafli, Z., Cuanalo-Contreras, K., Hayouni, E.A., *et al.* (2018). Inhibition of protein misfolding and aggregation by natural phenolic compounds. *Cell Mol Life Sci, 75* (19), 3521-3538.

Dixon, P. (2003). Vegan, a package of R functions for community ecology. *Journal of Vegetation Science, 14* (6), 927-930.

Ericsson, A.C. and Franklin, C.L. (2015). Manipulating the gut microbiota: Methods and challenges. *ILAR Journal, 56* (2), 205-217.

Etxeberria, U., Fernandez-Quintela, A., Milagro, F.I., *et al.* (2013). Impact of polyphenols and polyphenol-rich dietary sources on gut microbiota composition. *J Agric Food Chem, 61* (40), 9517-9533.

Fogliano, V., Corollaro, M.L., Vitaglione, P., *et al.* (2011). In vitro bioaccessibility and gut biotransformation of polyphenols present in the water-insoluble cocoa fraction. *Mol Nutr Food Res, 55 Suppl 1*, S44-55.

Freyssin, A., Page, G., Fauconneau, B., *et al.* (2018). Natural polyphenols effects on protein aggregates in Alzheimer's and Parkinson's prion-like diseases. *Neural Regen Res, 13* (6), 955-961.

Garnier, S. (2018). Viridis: Default color maps from 'matplotlib': R package version 0.5.1. Retrieved from https://CRAN.R-project.org/package=viridis

Groenendyk, J., Agellon, L.B. and Michalak, M. (2013). Coping with endoplasmic reticulum stress in the cardiovascular system. *Annu Rev Physiol, 75* (1), 49-67.

Hanhineva, K., Torronen, R., Bondia-Pons, I.*, et al.* (2010). Impact of dietary polyphenols on carbohydrate metabolism. *Int J Mol Sci, 11* (4), 1365-1402.

Heimann, E., Nyman, M. and Degerman, E. (2014). Propionic acid and butyric acid inhibit lipolysis and de novo lipogenesis and increase insulin-stimulated glucose uptake in primary rat adipocytes. *Adipocyte, 4* (2), 81-88.

Hervé, M. (2020). RVAideMemoire: Testing and plotting procedures for biostatistics: R package version 0.9-75. Retrieved from https://CRAN.R-project.org/package=RVAideMemoire

Hervert-Hernandez, D., Pintado, C., Rotger, R.*, et al.* (2009). Stimulatory role of grape pomace polyphenols on *Lactobacillus acidophilus* growth. *Int J Food Microbiol, 136* (1), 119-122.

Hetz, C. and Papa, F.R. (2018). The unfolded protein response and cell fate control. *Mol Cell, 69* (2), 169-181.

Hooper, L.V. and Gordon, J.I. (2001). Commensal host-bacterial relationships in the gut. *Science, 292* (5519), 1115.

Hu, Y., Liu, J., Yuan, Y.*, et al.* (2018). Sodium butyrate mitigates type 2 diabetes by inhibiting PERK-CHOP pathway of endoplasmic reticulum stress. *Environ Toxicol Pharmacol, 64*, 112-121.

Huang, A., Young, T.L., Dang, V.T.*, et al.* (2017). 4-phenylbutyrate and valproate treatment attenuates the progression of atherosclerosis and stabilizes existing plaques. *Atherosclerosis, 266*, 103-112.

Huang, Y., L, D., Shah, G.M.*, et al.* (2019). Hyperthermophilic pretreatment composting significantly accelerates humic substances formation by regulating precursors production and microbial communities. *Waste Manage, 92*, 89-96.

Jolivet, P. and Foley, J. (2015). Solutions for purifying nucleic acids by solidphase reversible immobilization (SPRI). Retrieved from https://openwetware.org/mediawiki/index.php?title=SPRI_bead_mix&oldid=992125

Karaskov, E., Scott, C., Zhang, L.*, et al.* (2006). Chronic palmitate but not oleate exposure induces endoplasmic reticulum stress, which may contribute to INS-1 pancreatic β-cell apoptosis. *Endocrinology, 147* (7), 3398-3407.

Karen Jesus, O., Maria Isabel, C., Gisele, G.*, et al.* (2019). Thyroid function disruptors: From nature to chemicals. *J Mol Endocrinol, 62* (1), R1-R19.

Kawabata, K., Yoshioka, Y. and Terao, J. (2019). Role of intestinal microbiota in the bioavailability and physiological functions of dietary polyphenols. *Molecules, 24* (2).

Kim, Y., Keogh, J.B. and Clifton, P.M. (2016). Polyphenols and glycemic control. *Nutrients, 8* (1), 17.

Klindworth, A., Pruesse, E., Schweer, T.*, et al.* (2012). Evaluation of general 16S ribosomal RNA gene PCR primers for classical and next-generation sequencing-based diversity studies. *Nucleic Acids Res, 41* (1), e1-e1.

Koren, O., Knights, D., Gonzalez, A.*, et al.* (2013). A guide to enterotypes across the human body: Meta-analysis of microbial community structures in human microbiome datasets. *PLoS Comp Biol, 9* (1), e1002863-e1002863.

Krehenwinkel, H., Pomerantz, A., Henderson, J.B.*, et al.* (2019). Nanopore sequencing of long ribosomal DNA amplicons enables portable and simple biodiversity assessments with high phylogenetic resolution across broad taxonomic scale. *GigaScience, 8* (5).

Kubow, S., Hobson, L., Iskandar, M.M.*, et al.* (2014). Extract of Irish potatoes (*Solanum tuberosum* L.) decreases body weight gain and adiposity and improves glucose control in the mouse model of diet-induced obesity. *Mol Nutr Food Res, 58* (11), 2235-2238.

Lee, Y.M., Yoon, Y., Yoon, H.*, et al.* (2017). Dietary anthocyanins against obesity and inflammation. *Nutrients, 9* (10).

Ly, L.D., Xu, S., Choi, S.-K.*, et al.* (2017). Oxidative stress and calcium dysregulation by palmitate in type 2 diabetes. *Exp Mol Med, 49* (2), e291-e291.

Manach, C., Scalbert, A., Morand, C.*, et al.* (2004). Polyphenols: Food sources and bioavailability. *Am J Clin Nutr, 79* (5), 727-747.

Marin, L., Miguelez, E.M., Villar, C.J.*, et al.* (2015). Bioavailability of dietary polyphenols and gut microbiota metabolism: Antimicrobial properties. *Biomed Res Int, 2015*, 905215.

Markle, J.G., Frank, D.N., Mortin-Toth, S.*, et al.* (2013). Sex differences in the gut microbiome drive hormone-dependent regulation of autoimmunity. *Science, 339* (6123), 1084-1088.

Markowiak-Kopeć, P. and Śliżewska, K. (2020). The effect of probiotics on the production of short-chain fatty acids by human intestinal microbiome. *Nutrients, 12* (4), 1107.

Masuzaki, H., Kozuka, C., Okamoto, S.*, et al.* (2019). Brown rice-specific γ-oryzanol as a promising prophylactic avenue to protect against diabetes mellitus and obesity in humans. *J Diabetes Investig, 10* (1), 18-25.

McMurdie, P.J. and Holmes, S. (2013). Phyloseq: An R package for reproducible interactive analysis and graphics of microbiome census data. *PLoS One, 8* (4), e61217.

Most, J., Goossens, G.H., Jocken, J.W.E.*, et al.* (2014). Short-term supplementation with a specific combination of dietary polyphenols increases energy expenditure and alters substrate metabolism in overweight subjects. *Int J Obesity, 38* (5), 698-706.

Murphy, E.F., Cotter, P.D., Healy, S.*, et al.* (2010). Composition and energy harvesting capacity of the gut microbiota: Relationship to diet, obesity and time in mouse models. *Gut, 59* (12), 1635-1642.

Musso, G., Gambino, R. and Cassader, M. (2011). Interactions between gut microbiota and host metabolism predisposing to obesity and diabetes. *Annu Rev Med, 62*, 361-380.

Nagpal, R., Shively, C.A., Appt, S.A.*, et al.* (2018a). Gut microbiome composition in non-human primates consuming a Western or Mediterranean diet. *Front Nutr, 5*, 28-28.

Nagpal, R., Wang, S., Ahmadi, S.*, et al.* (2018b). Human-origin probiotic cocktail increases short-chain fatty acid production via modulation of mice and human gut microbiome. *Sci Rep, 8* (1), 12649.

Nohynek, L.J., Alakomi, H.L., Kahkonen, M.P.*, et al.* (2006). Berry phenolics: Antimicrobial properties and mechanisms of action against severe human pathogens. *Nutr Cancer, 54* (1), 18-32.

Özcan, U., Yilmaz, E., Özcan, L.*, et al.* (2006). Chemical chaperones reduce ER stress and restore glucose homeostasis in a mouse model of type 2 diabetes. *Science, 313* (5790), 1137.

Pardo, V., Gonzalez-Rodriguez, A., Muntane, J.*, et al.* (2015). Role of hepatocyte S6K1 in palmitic acid-induced endoplasmic reticulum stress, lipotoxicity, insulin resistance and in oleic acid-induced protection. *Food Chem Toxicol, 80*, 298-309.

Popkin, B.M. (2001). The nutrition transition and obesity in the developing world. *J Nutr, 131* (3), 871S-873S.

R Core Team. (2020). R: A language and environment for statistical computing. Vienna, Austria: R Foundation for Statistical Computing. Retrieved from https://www.R-project.org/

Rao, X., Huang, X., Zhou, Z.*, et al.* (2013). An improvement of the 2ˆ(-delta delta CT) method for quantitative real-time polymerase chain reaction data analysis. *Biostat Bioinforma Biomath, 3* (3), 71-85.

Ríos-Covián, D., Ruas-Madiedo, P., Margolles, A.*, et al.* (2016). Intestinal short chain fatty acids and their link with diet and human health. *Front Microbiol, 7*, 185-185.

Robertson, S.J., Lemire, P., Maughan, H.*, et al.* (2019). Comparison of co-housing and littermate methods for microbiota standardization in mouse models. *Cell Rep, 27* (6), 1910-1919.

Rosshart, S.P., Vassallo, B.G., Angeletti, D.*, et al.* (2017). Wild mouse gut microbiota promotes host fitness and improves disease resistance. *Cell, 171* (5), 1015-1028.

Sadeghi Ekbatan, S., Sleno, L., Sabally, K.*, et al.* (2016). Biotransformation of polyphenols in a dynamic multistage gastrointestinal model. *Food Chem, 204*, 453-462.

Segata, N., Izard, J., Waldron, L.*, et al.* (2011). Metagenomic biomarker discovery and explanation. *Genome Biol, 12* (6), R60.

Serino, A. and Salazar, G. (2018). Protective role of polyphenols against vascular inflammation, aging and cardiovascular disease. *Nutrients, 11* (1).

Shah, D., Romero, F., Guo, Z.*, et al.* (2017). Obesity-induced endoplasmic reticulum stress causes lung endothelial dysfunction and promotes acute lung injury. *Am J Respir Cell Mol Biol, 57* (2), 204-215.

Shultz, S.R., MacFabe, D.F., Ossenkopp, K.P.*, et al.* (2008). Intracerebroventricular injection of propionic acid, an enteric bacterial metabolic end-product, impairs social behavior in the rat: Implications for an animal model of autism. *Neuropharmacology, 54* (6), 901-911.

Singh, R.K., Chang, H.W., Yan, D.*, et al.* (2017). Influence of diet on the gut microbiome and implications for human health. *J Transl Med, 15* (1), 73.

Srivathsan, A., Baloğlu, B., Wang, W.*, et al.* (2018). A MinION-based pipeline for fast and cost-effective DNA barcoding. *Mol Ecol Resour*, published online: 2018 Apr 2019.

Suganya, N., Bhakkiyalakshmi, E., Sarada, D.V.*, et al.* (2016). Reversibility of endothelial dysfunction in diabetes: Role of polyphenols. *Br J Nutr, 116* (2), 223-246.

Sugiyama, M.G. and Agellon, L.B. (2012). Sex differences in lipid metabolism and metabolic disease risk. *Biochem Cell Biol, 90* (2), 124-141.

Tan, H., Zhai, Q. and Chen, W. (2019). Investigations of *Bacteroides* spp. towards next-generation probiotics. *Food Res Int, 116*, 637-644.

Tatusova, T., DiCuccio, M., Badretdin, A.*, et al.* (2016). NCBI prokaryotic genome annotation pipeline. *Nucleic Acids Res, 44* (14), 6614-6624.

Tresserra-Rimbau, A., Guasch-Ferre, M., Salas-Salvado, J.*, et al.* (2016). Intake of total polyphenols and some classes of polyphenols is inversely associated with diabetes in elderly people at high cardiovascular disease risk. *J Nutr, 146* (4), 767-777.

Tsai, Y.L. and Olson, B.H. (1992). Detection of low numbers of bacterial cells in soils and sediments by polymerase chain reaction. *Appl Environ Microbiol, 58* (2), 754-757.

Turnbaugh, P.J., Ley, R.E., Mahowald, M.A.*, et al.* (2006). An obesity-associated gut microbiome with increased capacity for energy harvest. *Nature, 444* (7122), 1027-1131.

Vega, H., Agellon, L.B. and Michalak, M. (2016). The rise of proteostasis promoters. *IUBMB Life, 68* (12), 943-954.

Wang, B., Ge, S., Xiong, W.*, et al.* (2018). Effects of resveratrol pretreatment on endoplasmic reticulum stress and cognitive function after surgery in aged mice. *BMC Anesthesiol, 18* (1), 141.

Wang, M. and Kaufman, R.J. (2016). Protein misfolding in the endoplasmic reticulum as a conduit to human disease. *Nature, 529* (7586), 326-335.

Wickham, H. (2016). *ggplot2: Elegant graphics for data analysis*: Springer-Verlag New York. Retrieved from https://ggplot2.tidyverse.org

Williamson, G. and Manach, C. (2005). Bioavailability and bioefficacy of polyphenols in humans. II. Review of 93 intervention studies. *Am J Clin Nutr, 81* (1 Suppl), 243s-255s.

Connecting statement to Chapter 4

In the Chapter 3, I showed that certain kinds of extrinsic metabolites, notably plant-derived PRPE, prevented both dysbiosis of gut microbiota and activation of colonocyte endoplasmic reticulum stress that were induced by WSD in a sex dimorphic manner. In addition, PRPE was efficient in attenuating features of WSD-induced gut microbial dysbiosis in Fabp6-deficient mice (which exhibit bile malabsorption) and induced similar gut microbial responses in male and female mice. In Chapter 4, I investigate the interaction between intrinsic and extrinsic factors in modifying the gut microbiota using a mouse model with two genetic modifications of intestinal Fabps (intrinsic factor) metabolically challenged with WSD (extrinsic factor). This mouse model was developed by crossing *Fabp2*$^{-/-}$ and *Fabp6*$^{-/-}$ mice (Vassileva et al., 2000) (Praslickova et al., 2012), and thus represents a disease model resulting from genetically determined deficiency of both Fabp2 and Fabp6 proteins in the small intestine.

Both Fabp2-deficient and Fabp6-deficient mice exhibit sex dimorphic metabolic responses to targeted gene deletions (Vassileva et al., 2000; Agellon et al., 2007) and (Appendix I). Particularly, while wild-type male and female mice show distinct intestinal gene expression programs, male and female mice deficient in both Fabp2 and Fabp6 show greater similarity in intestinal gene expression programs (Chen and Agellon, 2019) but distinct from either male or female wild-type mice. The aim of the study presented in Chapter 4 was to identify the gut microbial modification in response to combined deficiency of Fabp2 and Fabp6 and to determine if the loss of these intestinal fatty acid binding proteins influence the response of the gut microbiota to diet.

Chapter 4

Intestinal fatty acid binding proteins 2 and 6 are involved in mediating the sex dimorphic response of gut microbiota to dietary perturbation

Salam M. Habib, Luis B. Agellon*

School of Human Nutrition, McGill University, QC, Canada

*Corresponding author at: McGill University School of Human Nutrition, 21111 Lakeshore Road, Ste. Anne de Bellevue, QC H9X 3V9 Canada

Email: luis.agellon@mcgill.ca (L.B. Agellon)

Author contribution: SMH designed and conducted the experiments, analyzed the data, and wrote the manuscript. LBA was involved in the conception of the experimental design.

A version of this manuscript is in preparation for submission to Gut Microbes Journal.

Abstract

Background: Three members of fatty acid binding proteins, namely the liver fatty acid binding protein (Fabp1), the intestinal fatty acid binding protein (Fabp2) and the ileal lipid binding protein (Fabp6) are abundant in the small intestine. Mice deficient in any of these proteins display sex dimorphic metabolic response to a high fat dietary challenge. The objective of this study was to identify the gut microbial modification in response to combined deficiency of Fabp2 and Fabp6 and to determine if the loss of these intestinal fatty acid binding proteins influence the response of the gut microbiota to diet. **Methods**: Mice of both sexes were fed a low fat diet (LFD) or a Western-style diet (WSD) for 10 weeks. Gut microbial composition was investigated using amplicon sequencing of the full 16S rRNA gene in samples of DNA extracted from mouse stools. Short-chain fatty acids (SCFAs) in plasma, markers of unfolded protein response (UPR) status in the large intestine and glucose tolerance were also assayed. **Results**: *Fabp2*$^{-/-}$*;Fabp6*$^{-/-}$ mice gained less body weight on both LFD and WSD compared to their wild-type counterparts and female mice were more affected than males. The combined deficiency of Fabp2 and Fabp6 reduced the proportion of gut microbial families belong to Actinobacteria and increased the proportion of gut microbial families belong to Firmicutes in both male and female mice fed the LFD. On WSD, *Fabp2*$^{-/-}$*;Fabp6*$^{-/-}$ male mice showed increased proportions of Lactobacillaceae, increased plasma SCFAs concentrations, reduced UPR activation and improved glucose tolerance compared to *Fabp2*$^{-/-}$*;Fabp6*$^{-/-}$ female mice on the same diet. **Conclusion**: Fatty acids binding proteins 2 and 6 are involved in regulating the sex dimorphism in dietary lipid assimilation which may mediate the sex dimorphic response of the gut microbiota to WSD.

4.1. Introduction

Dietary fats are digested and absorbed efficiently in the small intestine. Abundant small molecular-weight and soluble intracellular proteins termed fatty acid binding proteins (Fabps) help in transporting fatty acids and other lipid compounds to specific organelles and regulate cellular activity (Agellon et al., 2002; Furuhashi and Hotamisligil, 2008). In intestinal enterocytes for example, Fabps may shuttle lipids to the endoplasmic reticulum for chylomicron synthesis, to the mitochondria and peroxisome for β-oxidation or to the nucleus to regulate gene transcription (Storch and Thumser, 2010; Gajda and Storch, 2015). Enterocytes contain three distinct types of Fabps. The liver fatty acid binding protein (Fabp1) found mainly in the proximal small intestine, the ileal lipid binding protein (Fabp6) found abundantly in the ileum, and the intestinal fatty acid protein (Fabp2) distributed throughout the entire small intestine (Agellon et al., 2002). Although they share similarities in their primary and tertiary structures, these three Fabps show heterogeneity in their affinity to lipids (Agellon et al., 2002; Gajda and Storch, 2015). Fabp1 has high affinity for long-chain unsaturated fatty acids, bile acids, fatty acyl-CoAs, lysophosphatidic acids, prostaglandins and endocannabinoids (Storch and McDermott, 2009; Huang et al., 2016), while Fabp2 bind different types of fatty acids, and Fabp6 has high affinity for bile acids but can also bind fatty acids (Agellon et al., 2002; Labonté et al., 2003).

In mice, deficiency of either Fabp1 (Newberry et al., 2003; Martin et al., 2003) or Fabp2 (Vassileva et al., 2000) impairs fatty acid absorption, while the deficiency of Fabp6 causes bile acid malabsorption (Praslickova et al., 2012). A mouse model deficient in both Fabp2 and Fabp6, and thus exhibits only the fatty acid binding protein Fabp1 in the small intestine, shows an increase in gene expression programs related to fatty acid and lipoprotein metabolism in the small intestine compared to a mouse model deficient in either Fabp2 or Fabp6 (Chen and Agellon, 2019). Although Fabp1 binds both fatty acids and bile acids, it is not evident that it can completely compensate for the lack of either Fabp2 or Fabp6 in *Fabp2*$^{-/-}$ mice or *Fabp6*$^{-/-}$ mice, respectively (Vassileva et al., 2000; Praslickova et al., 2012). Based on this, *Fabp2*$^{-/-}$;*Fabp6*$^{-/-}$ mice exhibit increased excretion of both bile acids and dietary fat. Sex differences in the

degree of bile acid or fat excretion were evident in mice deficient in any one of three intestinal Fabps. Interestingly, when fed a high fat diet, these mice displayed sex dimorphic phenotypes, particularly in terms of adiposity (Vassileva et al., 2000; Agellon et al., 2007; McIntosh et al., 2013; Zwicker, 2013; Gajda et al., 2013) and (Appendix I).

Gut microbiota plays a fundamental role in host metabolism. In lipid metabolism, for example, studies have shown the involvement of gut microbiota through the production of metabolites such as short-chain fatty acids (SCFAs) and secondary bile acids (Ghazalpour et al., 2016; Schoeler and Caesar, 2019). Differences in the assimilation, transport and subcellular metabolism of dietary fats and lipid compounds are associated with sex-specific phenotypes and contribute to metabolic disease risk in the host (Sugiyama and Agellon, 2012). Recently, the presence of gut microbiota was suggested to contribute to sex dimorphism in lipid metabolism (Baars et al., 2018; Weger et al., 2019). Interestingly, while wild-type male and female mice show distinct gene expression programs in the small intestine, male and female *Fabp2*$^{-/-}$;*Fabp6*$^{-/-}$ mice show greater similarity in intestinal gene expression programs (Chen and Agellon, 2019). The objective of this study was to determine if the loss of both Fabp2 and Fabp6 also result in distinct changes in the gut microbial composition of male and female mice and whether the combined loss of these two proteins modify the susceptibility to WSD-induced gut microbial dysbiosis.

4.2. Materials and methods

Mice and diets

Fabp2$^{-/-}$*;Fabp6*$^{-/-}$ mice were produced by interbreeding *Fabp6*$^{-/-}$ mice (Praslickova et al., 2012) and *Fabp2*$^{-/-}$ (Vassileva et al., 2000). C57BL/6J mice (Jackson Laboratory, Bar Harbor, Maine, USA) were inbred to yield the required wild-type (WT) mice. Genotypes of mice were identified by PCR as described in Appendix I and (Vassileva et al., 2000). Mice were housed in animal facility with a climate control and a 12-h light/dark photoperiod. Prior to the controlled feeding period, all mice were fed the Teklad 2020X diet (Teklad-Envigo, Lachine, QC), which was used as a reference low fat diet (LFD) in the feeding experiment. Age matched *Fabp2*$^{-/-}$*;Fabp6*$^{-/-}$ and wild-type

mice (n = 4-5 mice per treatment housed in 2-3 cages per treatment, males and females in separate groups) were *ad libitum* fed the Western-style diet (D12079B, Research Diets, New Brunswick, NJ) or the LFD for 10 weeks. By the end of controlled feeding period, individual stool samples were collected, mice were fasted for 16 h then euthanatized by isoflurane/CO_2, and whole blood was collected through cardiac puncture. The collected plasma and tissue samples were stored at -70°C until processed and analyzed. The reported use of animals was approved by the animal care committee at McGill University and the Canadian Council on Animal Care.

DNA extraction and amplicon sequencing

DNA extraction from stool samples and amplicon sequencing were carried out as described in Chapter 3. Briefly, extracted, purified and quality checked DNA (1 µg) was used to amplify the full 16S rRNA gene by PCR using previously described primers (Klindworth et al., 2012), which we specifically tagged to allow for dual multiplexing (Srivathsan et al., 2018). Primer and tag sequences are provided in Appendix II. Amplicons were purified using solid phase reversible immobilization (SPRI) and their concentration was measured using Qubit fluorometer 2.0 (Thermo Fisher Scientific, Waltham, USA). Equal DNA masses from each sample were mixed to form a pool of amplicons. A quantity of 300 ng of this pool was used for MinION library preparation using SQK-LSK109 ligation kit (Oxford Nanopore Technologies, New York, USA) according to the manufacturer's protocol (v.109, rev_C). Prepared library was mixed with sequencing buffer and loading beads (Library loading kit; Oxford Nanopore Technologies, New York, USA) and loaded to a previously checked and primed SpotON flowcell connected to the MinION device and sequenced for 48 hrs. Sequencing progress was tracked by MinKNOW software (v18.07.18), and 1D reads were base called at the same time using Albacore (v 2.3.1).

Analysis of sequence data

Fastq reads were demultiplexed and trimmed of both primer and barcode sequences using Minibar python code (Krehenwinkel et al., 2019). Epi2me 16S workflow (v 2.61) was used to check the quality of sequence reads and assign

taxonomy by aligning to NCBI bacterial 16S rRNA RefSeq database (Tatusova et al., 2016). The generated data was analyzed by MicrobiomeAnalyst (Dhariwal et al., 2017) as described in Chapter 2. First, data was decontaminated of singletons, taxa with low count (10% of samples each contain ≥ 2 reads), and taxa with low variance (10%) using MicrobiomeAnalyst data filtration functions (Dhariwal et al., 2017). No rarefaction was applied since the sequence depth among samples was <10X. Rarefaction curves and Good's coverage are listed in Appendix II. Each of Chao1 richness and Shannon's diversity (*H*) indices and principal coordinate analysis (PCoA) based on Bray-Curtis dissimilarity were calculated at the lowest taxonomic feature level using phyloseq R package v.1.32.0 (McMurdie and Holmes, 2013) as implemented by MicrobiomeAnalyst (Dhariwal et al., 2017). Top gut microbial species were clustered by Ward algorithm and based on Euclidean distance matrix then plotted in a heatmap using ggplot2 v.3.3.2 (Wickham, 2016) and viridis v.0.5.1 (Garnier, 2018) in MicrobiomeAnalyst (Dhariwal et al., 2017). Classifier taxa at the genus level were predicted using LefSe model (Segata et al., 2011) in each treatment group. The gut microbial relative abundance data was exported from MicrobiomeAnalyst and plotted using GraphPad Prism v.8.2.1 (GraphPad Software Inc., CA, USA).

Short-chain fatty acids

SCFAs of plasma were assayed as described in Chapter 2 and 3. Briefly, plasma samples previously stored at -70°C were diluted with GC grade methanol (1:2) and centrifuged at 14,000 g / 60 min. Supernatant (1 µl) was injected into an Agilent gas chromatograph system 7890A with a flame ionization detector (Agilent Technologies, Wilmington, DE, USA), and equipped with 19091N-133 Agilent capillary column. The flow rate of the carrier gas (Helium) was 1.0 mL/min, and the oven temperature was set to 100 °C for 10 min then gradually raised to 220 °C in 25 min. SCFAs standard (Supelco, 46975-U, Bellefonte, PA, USA) was used for peak identification and concentration determination.

Gene expression analysis

Purification of total RNA from mouse colon samples and the synthesis of cDNA templates were carried out as described in Chapter 3. The fold change of the mRNA abundance of each of glucose-regulated protein 78kDa (*Grp78*), spliced X-box binding protein 1 (*sXbp1*), activating transcription factor 4 (*Atf4*), and glucose-regulated protein 94kDa (*Grp94*) genes was calculated using the method of Rao et al. (2013) in relative to the average mRNA abundance of each of hypoxanthine-guanine phosphoribosyl transferase (*Hprt*) and Glyceraldehyde 3-phosphate dehydrogenase (*Gapdh*) genes by quantitative polymerase chain reaction (qPCR) using the BioRad CFX96 detection system and based on SYBR Green chemistry. The qPCR thermal program included 95 °C for 3 min, then 35 cycles of 95 °C for 10 s and 30 s at annealing temperature, followed by a melt curve generation. The sequences of primer pairs used in this assay are listed in Appendix II.

Oral glucose tolerance test (OGTT)

Prior to OGTT, mice were fasted for four hours to prevent body weight loss and to reduce stress and discomfort (Heijboer et al., 2005; Jensen et al., 2013). Glucose (2 g/kg body weight) was orally gavaged, and blood glucose level was monitored over the next 2 h using OneTouch UltraMini glucometer (LifeScan Inc., Milpitas, CA, USA) in samples collected from the tail vein.

Statistical analysis

All statistical analyses were performed with GraphPad Prism v.8.2.1 (GraphPad Software Inc., CA, USA) except those related to PCoA analysis, which were calculated by R v. 4.0 (R Core Team, 2020) in RStudio v.1.1.463. Based on the normality of the data, evaluated by Shapiro–Wilk's test, either one-way ANOVA accompanied with Fisher's LSD test or Kruskal-Wallis test accompanied with Dunn’s test were used to evaluate the differences in the means of data among treatment groups. Statistical tests were applied to males and females separately. The differences between means were regarded significant when $p<0.05$. Adonis function of VEGAN package v.2.5-6 (Dixon, 2003) was used to calculate the permutational analysis of variance (PERMANOVA) of

PCoA plots, and pairwise PERMANOVAs with FDR correction were calculated using RVAideMemoire package v.0.9-75 (Hervé, 2020). Ellipses of PCoA that reflect 95% level of confidence based on *t* distribution were plotted using ggplot2 package v.3.3.2 (Wickham, 2016) as implemented in MicrobiomeAnalyst (Dhariwal et al., 2017).

4.3. Results

4.3.1. Reduced body weight gain in Fabp2$^{-/-}$;Fabp6$^{-/-}$ mice on both LFD and WSD

Previous studies on *Fabp2*$^{-/-}$ and *Fabp6*$^{-/-}$ mice showed enhanced adiposity of males but not females on high fat diets (Vassileva et al., 2000; Agellon et al., 2006; Agellon et al., 2007) and (Appendix I). To determine if the combined deficiency of Fabp2 and Fabp6 also alters the body weight gain of mice, male and female wild-type and *Fabp2*$^{-/-}$;*Fabp6*$^{-/-}$ mice were fed with either LFD or WSD for 10 weeks. On both diets, male *Fabp2*$^{-/-}$;*Fabp6*$^{-/-}$ mice gained less body weight compared to male wild-type mice, although did not reach statistical significance, while female *Fabp2*$^{-/-}$;*Fabp6*$^{-/-}$ mice gained significantly less body weight compared to female wild-type mice on both diets (Fig. 4-1A). Both male and female *Fabp2*$^{-/-}$;*Fabp6*$^{-/-}$ mice showed similar gonadal fat pad mass compared to their respective wild-type counterparts on both diets (Fig. 4-1B). Male *Fabp2*$^{-/-}$;*Fabp6*$^{-/-}$ mice on WSD and LFD did not show an obvious difference in their gonadal fat pad mass (Fig. 4-1B, left). Interestingly, feeding WSD did not increase the concentration of total triacylglycerols in the livers of both male and female *Fabp2*$^{-/-}$;*Fabp6*$^{-/-}$ mice compared to their respective wild-type counterparts (Fig. 4-1C). Thus, combined deficiency of Fabp2 and Fabp6 induces reduced adiposity in mice.

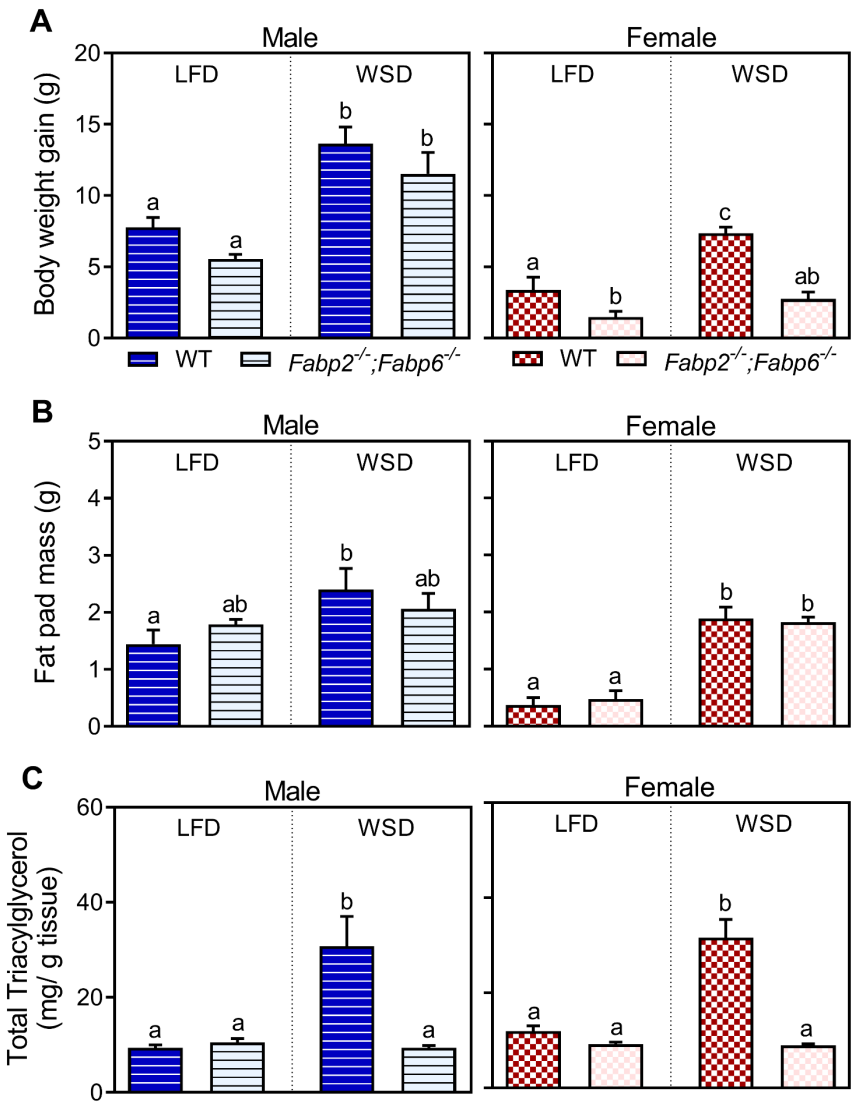

Figure 4-1. Reduced body weight gain in *Fabp2*$^{-/-}$;*Fabp6*$^{-/-}$ mice on both LFD and WSD and female mice are more affected. (A) Body weight gain, (B) gonadal fat pad mass, and (C) liver fat of male and female mice; n= 4-5. Data presented as mean ± SEM, means denoted by different superscript letters indicate $p<0.05$ by one-way ANOVA accompanied with Fisher's LSD test in A and B, and by Kruskal-Wallis test accompanied with Dunne's test in C. Males and females analyzed in separate models. Blue and red indicate LFD and WSD, respectively. Dark color and light color indicate wildtype and *Fabp2*$^{-/-}$;*Fabp6*$^{-/-}$ mice, respectively. WT: Wild-type, Fabp: Fatty acid binding protein, LFD: low fat diet, WSD: Western-style diet.

4.3.2. Combined deficiency of Fabp2 and Fabp6 alters the gut microbial diversity in a sex dimorphic manner

To characterize the changes in the gut microbial community in response to combined deficiency of Fabp2 and Fabp6, the full 16S rRNA gene was sequenced in DNA samples purified from mouse stools using Oxford Nanopore technology. In respect to α-diversity metrics of the gut microbial communities (Koh, 2018), no difference in the gut microbial richness between *Fabp2*$^{-/-}$;*Fabp6*$^{-/-}$ mice and their respective wild-type counterparts was detected on both LFD and WSD (Fig. 4-2A). Shannon's diversity index also showed no difference in the gut microbial diversity of male *Fabp2*$^{-/-}$;*Fabp6*$^{-/-}$ mice and their wild-type counterparts, however, female *Fabp2*$^{-/-}$;*Fabp6*$^{-/-}$ mice showed a tendency (LFD: p=0.07; WSD: p=0.06) for lower gut microbial diversity compared to their wild-type counterpart on both diets (Fig. 4-2B, right). Thus, combined deficiency of Fabp2 and Fabp6 induce a sex dimorphic response of gut microbial diversity to diet.

The analysis of the gut microbial β-diversity using PCoA showed sample clustering in response to diet in both wild-type male and female samples (Fig. 4-3A and 4-3B). Male *Fabp2*$^{-/-}$;*Fabp6*$^{-/-}$ mice also showed distinct clustering on LFD and WSD, however only female *Fabp2*$^{-/-}$;*Fabp6*$^{-/-}$ mice showed no clustering between gut microbial samples of mice fed LFD and WSD (Males: Fig. 4-3A; females: Fig. 4-3B). Moreover, the heatmap of the gut microbial abundance, at the species level, showed differential abundance patterns between male and female *Fabp2*$^{-/-}$;*Fabp6*$^{-/-}$ mice gut microbiota in response to WSD (Males: Fig. 4-3C; females: Fig. 4-3D). Thus, combined deficiency of Fabp2 and Fabp6 in mice was associated with a sex dimorphic gut microbial structure on WSD.

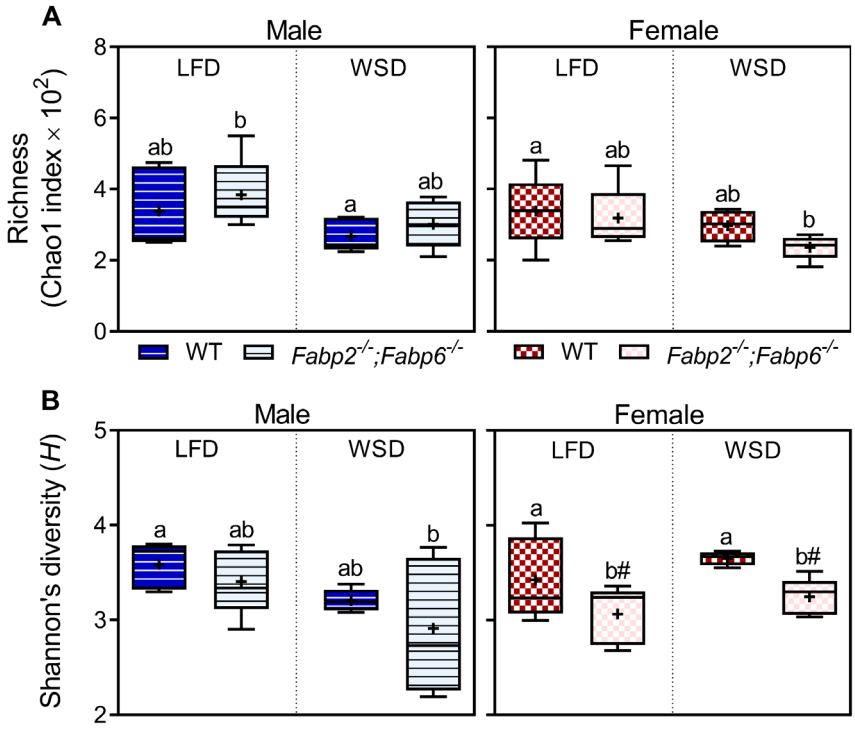

Figure 4-2. Reduced gut microbial diversity in response to the combined deficiency of Fabp2 and Fabp6. (A) Taxonomic richness estimated by Chao1 index and (B) Shannon's diversity index in male and female mice; n= 4-5. Data represent median and interquartile range, (+) represent mean and whiskers represent range, means denoted by different superscript letters indicate $p<0.05$ by one-way ANOVA accompanied with Fisher's LSD test, (#) indicate $p=0.5$-0.1. Males and females analyzed in separate models. Blue and red indicate male and female, respectively. Dark color and light color indicate wildtype and *Fabp2*$^{-/-}$;*Fabp6*$^{-/-}$ mice, respectively. WT: Wild-type, Fabp: Fatty acid binding protein, LFD: low fat diet, WSD: Western-style diet.

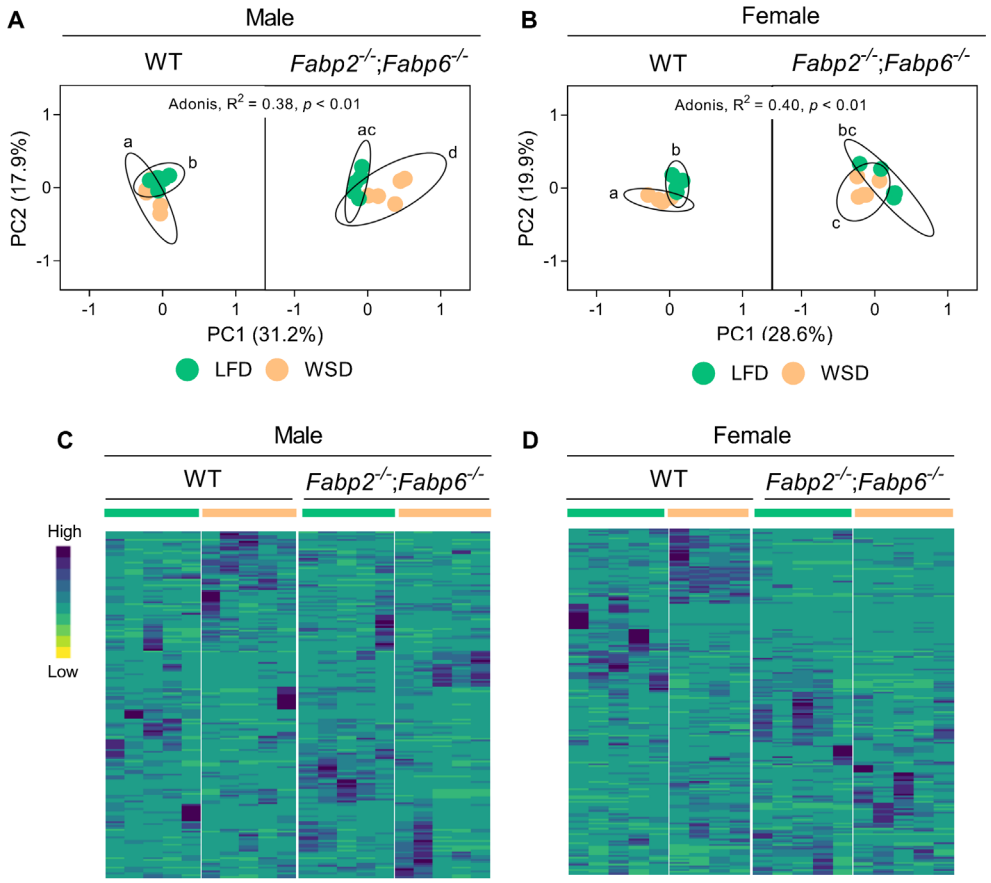

Figure 4-3. Combined deficiency Fabp2 and Fabp6 influence the gut microbial diversity on WSD in a sex dimorphic manner. (A and B) Principal coordinate analysis (PCoA) of gut microbiota samples, same PCoA included wild-type and *Fabp2*$^{-/-}$;*Fabp6*$^{-/-}$ mice, but two plots were used for visualization, (n=4-5) clusters denoted by different letters in one panel indicate significant clustering (p<0.05) by Adonis PERMANOVA accompanied with FDR corrected pairwise comparisons, ellipses indicate 95% level of confidence assuming *t* distribution in males and females, respectively. (C and D) Heatmap of gut microbial species abundance, (n=4-5) Ward algorithm clustering based on Euclidean distance measure in male and female mice, respectively. Males and females analyzed in separate models. Green and orange indicate LFD and WSD, respectively. WT: Wild-type, Fabp: Fatty acid binding protein, LFD: low fat diet, WSD: Western-style diet.

4.3.3. Distinct enrichment of Firmicutes phylum in male Fabp2$^{-/-}$;Fabp6$^{-/-}$ mice fed WSD

In Chapter 2, mice deficient in Fabp6 showed sex dimorphic gut microbial dysbiosis in response to WSD. Since the combined deficiency of Fabp6 and Fabp2 of increases the excretion of both bile acids and dietary fat, we determined if the combined deficiency of Fabp2 and Fabp6 induces similar gut microbial composition to that of Fabp6-deficient mice on WSD. At the phylum level, WSD reduced the proportion of Actinobacteria, but increased the proportion of Firmicutes in both male and female wild-type mice (Males: Fig. 4-4A; females: Fig. 4-4B). The combined deficiency of Fabp2 and Fabp6 also reduced the proportion of Actinobacteria and increased the proportion of Firmicutes in both male and female mice fed LFD (Males: Fig. 4-4A; females: Fig. 4-4B). In addition, the proportion of Bacteroidetes was increased in male mice, but decreased in female mice in response to combined deficiency of Fabp2 and Fabp6 compared to their respective wild-type counterparts on LFD (Males: Fig. 4-4A; females: Fig. 4-4B). Feeding WSD to *Fabp2*$^{-/-}$;*Fabp6*$^{-/-}$ mice further increased the proportion of Firmicutes and reduced the proportion of Bacteroidetes in male mice compared to their wild-type counterparts on the same diet (Fig. 4-4A). In contrast, WSD induced similar Firmicutes and Bacteroidetes proportions in both female *Fabp2*$^{-/-}$;*Fabp6*$^{-/-}$ and wild-type mice (Fig. 4-4B).

At the family level, both male and female *Fabp2*$^{-/-}$;*Fabp6*$^{-/-}$ mice showed reduced proportions of each of Bifidobacteriaceae, Dermabacteracece, and unclassified Verrucomicrobia family, but increased proportion of both unclassified Firmicutes family and Lachnospiraceae compared to their respective wild-type counterparts on LFD (Males: Fig. 4-4A; females: Fig. 4-4B). On WSD, combined deficiency of Fabp2 and Fabp6 increased the proportion of Lactobacillaceae in both male and female mice compared to their wild-type counterparts on the same diet. This increase of Lactobacillaceae proportion in male *Fabp2*$^{-/-}$;*Fabp6*$^{-/-}$ mice on WSD was higher compared to that of their female counterparts (Males: Fig. 4-4A; females: Fig. 4-4B). Thus, while WSD reduces the proportions of gut microbial families belonging to Actinobacteria and increases proportions of families belonging to Firmicutes in both

sexes, combined deficiency of Fabp2 and Fabp6 induces greater expansion of Lactobacillaceae in male compared to female mice.

At the genus level, LefSe model was used to predict classifier gut microbial genera in both male and female mice in response to their diet and genotype. On LFD, the genera *Brachybacterium* and *Bifidobacterium* were classifiers of wild-type male and female gut microbiota respectively, whereas *Ruminiclostridium* and unclassified Firmicutes genus were classifiers of the gut microbiota of male and female *Fabp2*$^{-/-}$;*Fabp6*$^{-/-}$ mice respectively (Males: Fig. 4-5A; females: Fig. 4-5B). On WSD, *Pseudomonas* and *Staphylococcus* were markers of the gut microbiota of male and female wild-type mice respectively, while *Lactobacillus* and *Lactococcus* were markers of male and female *Fabp2*$^{-/-}$;*Fabp6*$^{-/-}$ gut microbiota respectively (Males: Fig. 4-5A; females: Fig. 4-5B). Thus, the gut microbial classifiers of male and female mice at the genus level are distinct in response to diet and genotype.

4.3.4. Combined deficiency of Fabp2 and Fabp6 increases SCFAs concentrations and prevents UPR activation

SCFAs are major and bioactive gut microbial metabolites (Morrison and Preston, 2016; Ríos-Covián et al., 2016). To determine if the gut microbial changes in response to combined deficiency of Fabp2 and Fabp6 influence host metabolism, first we measured plasma acetic, propionic and butyric acids since together they represent the major proportion of SCFAs (Cummings et al., 1987). Both male and female *Fabp2*$^{-/-}$;*Fabp6*$^{-/-}$ mice showed significantly higher plasma acetic acid, propionic acid, and butyric acid, compared to their wild-type counterparts on both diets (Males: Fig. 4-6A; females: Fig. 4-6B). Interestingly, on both diets, male *Fabp2*$^{-/-}$;*Fabp6*$^{-/-}$ mice showed higher total plasma SCFAs levels compared to their female counterparts (Males: Fig. 4-6A; females: Fig. 4-6B). Components of WSD, such as palmitic acid, are known to activate endoplasmic reticulum UPR (Karaskov et al., 2006; Volmer et al., 2013). In contrast, SCFAs and their metabolites are associated with promotion of cellular proteostasis (Vega et al., 2016; Huang et al., 2017; Hu et al., 2018). Therefore, the impact of increased SCFAs levels in *Fabp2*$^{-/-}$;*Fabp6*$^{-/-}$ mice on the large intestinal UPR

status was determined. Feeding WSD in male wild-type mice increased the mRNA abundance of *Grp94* and a higher trend (p = 0.07) in *sXbp1* was noticed compared to their counterparts on LFD. In female wild-type mice, WSD feeding increased the mRNA abundance of *Atf4* compared to their counterparts on LFD. Interestingly, male *Fabp2*$^{-/-}$;*Fabp6*$^{-/-}$ mice on WSD showed lower mRNA abundance of each of the assayed UPR markers compared to their wild-type counterparts, while female *Fabp2*$^{-/-}$;*Fabp6*$^{-/-}$ mice showed lower mRNA abundance of only *Atf4* and *Grp94* compared to their wild-type mice on the same diet (Males: Fig. 4-6C; females: Fig. 4-6D).

Liver plays a crucial role in glucose metabolism and fatty liver has been shown to induce glucose intolerance (Michael et al., 2000). Given that both male and female *Fabp2*$^{-/-}$;*Fabp6*$^{-/-}$ mice exhibited a lower degree of liver fat deposition, we examined their glucose tolerance using OGTT. WSD induced elevated blood glucose levels over 2 h following the glucose challenge in both male and female wild-type mice compared to their counterparts on LFD (Males: Fig. 4-6E, left; females: Fig. 4-6F, left). Remarkably, WSD did not induce elevated glucose levels in male *Fabp2*$^{-/-}$;*Fabp6*$^{-/-}$ mice compared to their wild-type counterparts throughout the OGTT duration (Fig. 4-6E). There was no difference in the glucose levels of female *Fabp2*$^{-/-}$;*Fabp6*$^{-/-}$ mice and their wild-type counterparts on the WSD (4-6F). Together, these results indicate that combined deficiency of Fabp2 and Fabp6 mitigates WSD-induced UPR activation and glucose intolerance to a larger extent in male compared to female mice.

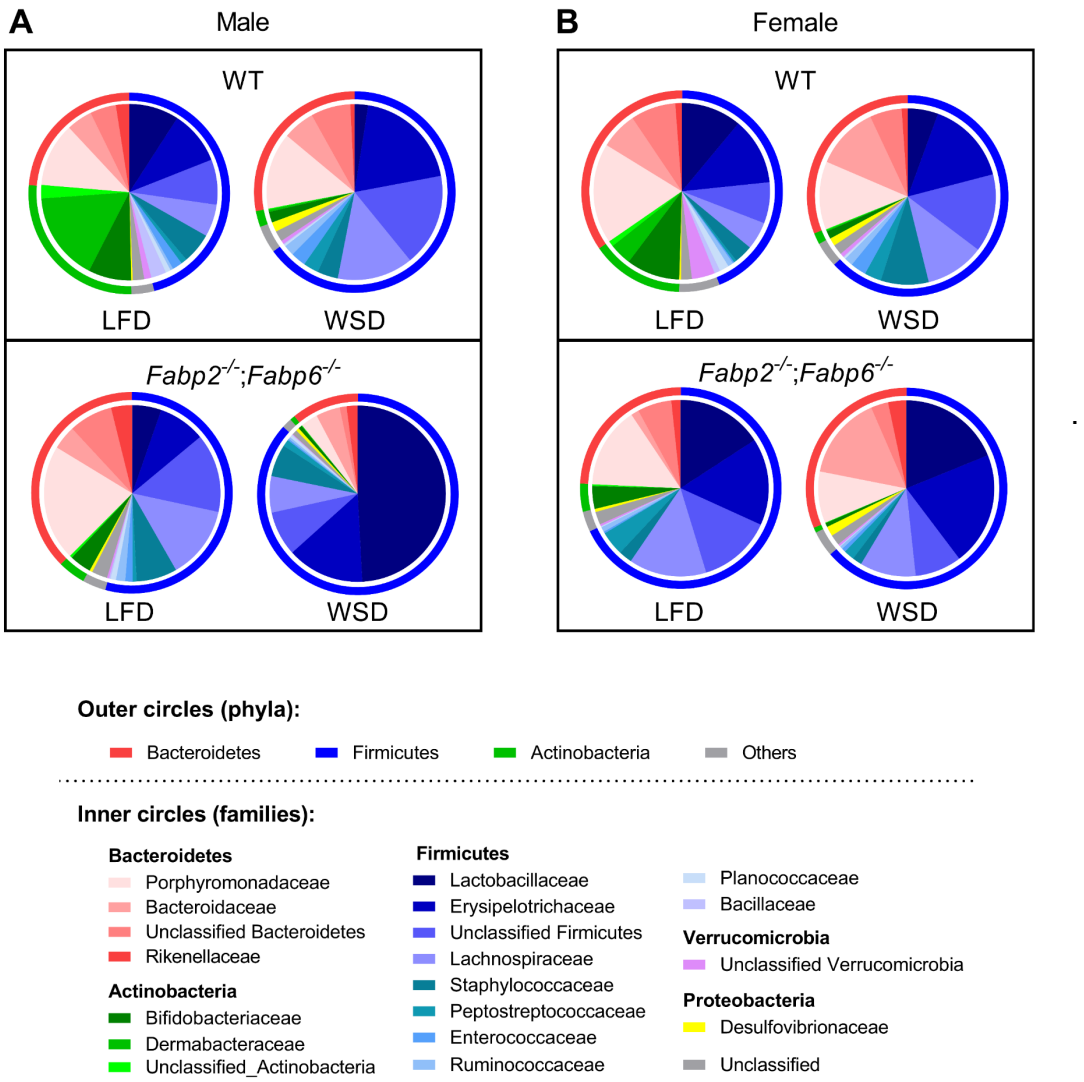

Figure 4-4. Combined deficiency Fabp2 and Fabp6 provokes excessive Firmicutes abundance in male mice fed WSD. (A and B) Gut microbial composition, outer circles represent relative abundance of the gut microbiota at the phylum level, inner circles represent relative abundance of the top 20 gut microbial families of the male and female mice, respectively. n= 4-5. WT: Wild-type, Fabp: Fatty acid binding protein, LFD: low fat diet, WSD: Western-style diet.

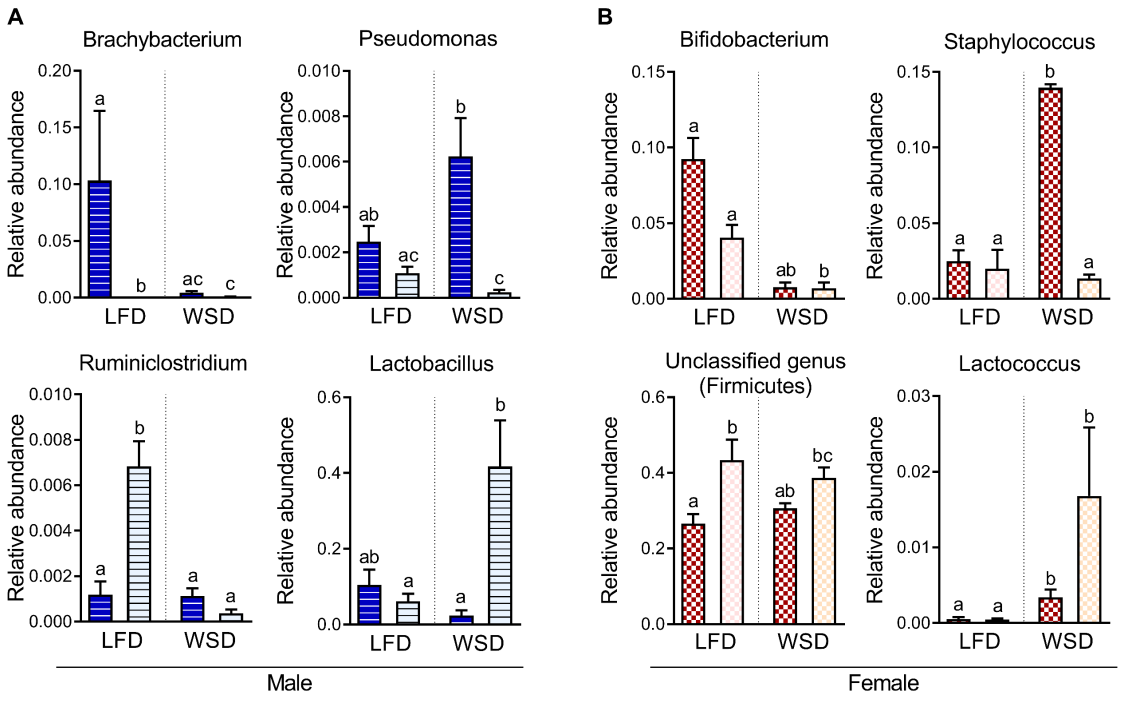

Figure 4-5. Classifier gut microbial genera discovered by LefSe model. (A) Male, (B) female; n=4-5, data represent mean ± SEM, means denoted by different superscript letters indicate $p<0.05$ by Kruskal-Wallis test accompanied with Dunne's test. Males and females analyzed in separate models. Blue and red indicate male and female, respectively. Dark color and light color indicate wildtype and *Fabp2*$^{-/-}$;*Fabp6*$^{-/-}$ mice, respectively. WT: Wild-type, Fabp: Fatty acid binding protein, LFD: low fat diet, WSD: Western-style diet.

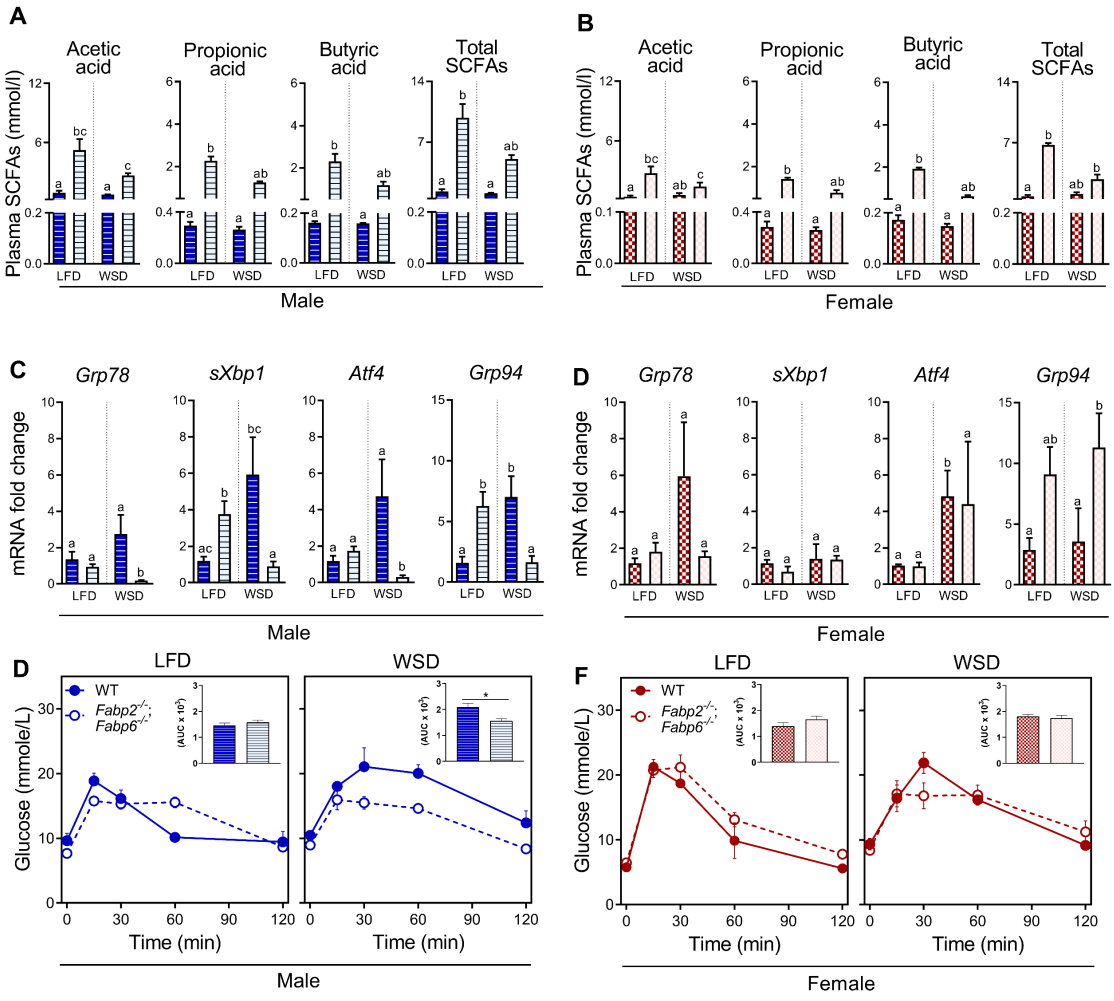

Figure 4-6. Higher plasma SCFAs and sex dimorphic stress coping response and glucose tolerance in *Fabp2*$^{-/-}$;*Fabp6*$^{-/-}$ mice fed WSD. (A and B) Plasma SCFAs, (C and D) markers of unfolded protein response in the colon, and (E and F) blood glucose levels during OGTT of male and female mice, respectively; n=4-5, data represent mean ± SEM, means denoted by different superscript letters indicate significant difference (p<0.05) by Kruskal-Wallis test accompanied with Dunne's test. Insets represent the mean AUC and (*) indicate significant difference by unpaired *t*-test. Males and females analyzed in separate models. Blue and red indicate male and female, respectively. Dark color and light color indicate wildtype and *Fabp2*$^{-/-}$;*Fabp6*$^{-/-}$ mice, respectively. Grp78: Glucose-regulated protein 78kDa, sXbp1: Spliced X-box binding protein 1, Atf4: Activating transcription factor 4, Grp94: Glucose-regulated protein 94kDa, SCFAs: Short chain fatty acids, OGTT: Oral glucose tolerance test, WT: Wild-type, Fabp: Fatty acid binding protein, LFD: low fat diet, WSD: Western-style diet.

4.4. Discussion

Previous studies have shown that mice deficient in one of the intestinal Fabps, namely Fabp1, Fabp2, or Fabp6, exhibit sex dimorphic adiposity in response to high fat diets (Vassileva et al., 2000; Agellon et al., 2007; McIntosh et al., 2013; Zwicker, 2013; Gajda et al., 2013) and (Appendix I). In this study, deficiency of Fabp2 and Fabp6 induced several sex dimorphic responses to WSD. While female *Fabp2*$^{-/-}$;*Fabp6*$^{-/-}$ mice gained lower body weight on both LFD and WSD, male *Fabp2*$^{-/-}$;*Fabp6*$^{-/-}$ mice showed only a trend for lower body weight gain. This response might be explained partly by the increased susceptibility of both male Fabp6-difiecnt and Fabp2-deficient mice to adiposity on high fat diets (Vassileva et al., 2000; Agellon et al., 2007) and (Appendix I). Similarly, the response of female *Fabp2*$^{-/-}$;*Fabp6*$^{-/-}$ mice to WSD was comparable to that of female *Fabp2*$^{-/-}$ mice which were not as vulnerable to WSD-induced adiposity as male *Fabp2*$^{-/-}$ mice (Vassileva et al., 2000; Agellon et al., 2007). However, while the differences between male and female mice deficient in either Fabp2 or Fabp6 were only evident following a challenge with high fat diets, the sex differences in body weight gain by *Fabp2*$^{-/-}$;*Fabp6*$^{-/-}$ mice were evident on LFD. This indicate the involvement of intestinal Fabps in dietary lipid assimilation and in mediating the sex dimorphic adiposity in murine species.

This study showed similar gut microbial richness between female *Fabp2*$^{-/-}$;*Fabp6*$^{-/-}$ mice and wild-type mice on LFD, but lower Shannon's diversity index. Since Chao1 index accounts for species richness while Shannon's index accounts for both richness and evenness (Shannon, 1948; Chao, 1984), this indicates lower evenness in the gut microbial composition; probably due to a higher number of rare gut microbial classes in response to the combined deficiency of Fabp2 and Fabp6 in female mice. Interestingly, female mice have been shown to exhibit a greater degree of dietary fat malabsorption and bile malabsorption in response to the loss of Fabp2 and Fabp6, respectively (Vassileva et al., 2000; Praslickova et al., 2012), which might explain their lower gut microbial diversity. Bile acids have a detergent-like effect on bacteria (Begley et al., 2005), and bile acid malabsorption has been shown to reduce gut microbial diversity (Chapter 2). The reduction of gut microbial diversity has also been reported to

be associated with fat malabsorption on high fat diets (Kriss et al., 2018). Therefore, the effect of fat malabsorption as a result of Fabp2 deficiency may mirror that of fat malabsorption condition associated with high fat diets.

This study demonstrated that gut microbiota of male *Fabp2*$^{-/-}$;*Fabp6*$^{-/-}$ mice fed LFD and WSD diverged completely, whereas that of female *Fabp2*$^{-/-}$;*Fabp6*$^{-/-}$ mice fed LFD and WSD remained similar. Since Fabp2 and Fabp6 bind fatty acids and bile acids respectively, this gut microbial response may be attributed to differences in the intestinal lumen concentrations of bile acids and dietary fats in male mice between LFD and WSD, while these differences may not be significant in female mice. Indeed, the intestinal mRNA abundance of Fabp1 was increased only in female, but not male, Fabp2-deficenct mice in response to high fat diet feeding (Jamaluddine, 2015), which suggests it as a compensatory mechanism in females to handle increased load and trafficking of fatty acids. These findings imply that intestinal Fabps have a substantial role in mediating the sex dimorphic remodeling of the gut microbiota to in response to WSD. Moreover, on LFD, combined deficiency of Fabp2 and Fabp6 induced increase in the Bacteroidetes phylum in male mice, and the Firmicutes phylum in female mice, which might contribute to their distinct susceptibility to diet-induced metabolic dysfunction. Similarly, the increase of Firmicutes in *Fabp2*$^{-/-}$;*Fabp6*$^{-/-}$ female mice fed the LFD could be due to the high degree of fat malabsorption as compared to that of *Fabp2*$^{-/-}$;*Fabp6*$^{-/-}$ male mice on the same diet and thus induce remodeling of the gut microbiota to a profile resembling the gut microbiota of mice on a high fat diet.

Despite that the combined deficiency of Fabp2 and Fabp6 induced greater similarity in intestinal gene expression programs between male and female mice compared that of wild-type mice (Chen and Agellon, 2019), WSD feeding in this mouse model induced sex dimorphic gut microbial composition. Although some gut microbial changes were similar in both sexes, as observed with the reduced abundance of gut microbial families belong to Actinobacteria and Verrucomicrobia, differences in the degree of the change were evident. For example, male and female *Fabp2*$^{-/-}$;*Fabp6*$^{-/-}$ mice on WSD showed enrichment of gut microbial families belonging to Firmicutes, particularly in Lactobacillaceae family. However, the enrichment of Lactobacillaceae

was more prominent in male, compared to female, *Fabp2*$^{-/-}$;*Fabp6*$^{-/-}$ mice. The expansion of Lactobacillaceae in male *Fabp2*$^{-/-}$;*Fabp6*$^{-/-}$ mice was consistent with that of male *Fabp6*$^{-/-}$ mice observed after WSD feeding (Chapter 2). Most *Lactobacillus* spp. exhibit bile salt hydrolase activity which renders them tolerant to bile acids compared to other bacteria (Begley et al., 2006). In addition, *Lactobacillus* spp. have also been reported to tolerate high fat growth media cultures (Haque et al., 1997). The tolerance of species of Lactobacillaceae to both high bile acid and fat levels may explain partly their enrichment in the gut of *Fabp2*$^{-/-}$;*Fabp6*$^{-/-}$ mice.

A key finding of this study was UPR activation by the combined deficiency of Fabp2 and Fabp6 in male but not female mice. This may be attributed to a lack of a compensatory buffering mechanism to handle the increased cellular concentration of free fatty acids in male *Fabp2*$^{-/-}$;*Fabp6*$^{-/-}$ mice, which, in turn, induces lipotoxicity and triggers colonocyte endoplasmic reticulum (ER) stress (Ly et al., 2017; Chong et al., 2017). In contrast, the ability of female *Fabp2*$^{-/-}$;*Fabp6*$^{-/-}$ mice to increase the expression of Fabp1 in response to high fat diet (Jamaluddine, 2015), may provide a protective mechanism from lipotoxicity-induced ER stress. In fact, after 10 weeks of WSD feeding, a reduction in the UPR activity was noticed in male *Fabp2*$^{-/-}$;*Fabp6*$^{-/-}$ mice, but a selective activation of ATF6 arm was noticed in female *Fabp2*$^{-/-}$;*Fabp6*$^{-/-}$ mice. While selective activation of the ATF6 arm may indicate early stage of adaptation, turning off UPR activation upon prolonged ER stress may be indicative of the transition from the adaptive to the pro-apoptotic phase (Yoshida et al., 2003; Lin et al., 2009; Hetz, 2012). A transition to the pro-apoptotic phase upon prolonged consumption of WSD may provide an explanation to a brittle colonic tissue noticed during necropsy in male *Fabp2*$^{-/-}$;*Fabp6*$^{-/-}$ mice. Together, these findings suggest a key role of intestinal Fabps in driving the sex dimorphic phenotype in response to WSD feeding.

Although this study was limited by the low number of mice and the low number of cages per experimental group, the enhancement of glucose tolerance in male *Fabp2*$^{-/-}$;*Fabp6*$^{-/-}$ mice fed WSD was evident. This finding could not be solely attributed to the reduced degree of hepatic fat deposition in these mice, since female *Fabp2*$^{-/-}$;*Fabp6*$^{-/-}$ mice also showed reduced degree of hepatic fat deposition on WSD, but no

improvement in their glucose tolerance were detected. In fact, the sex dimorphic effect of glucose tolerance may be accounted for by the distinct gut microbial composition between male and female *Fabp2*$^{-/-}$;*Fabp6*$^{-/-}$ mice on WSD. Gut microbial metabolites such as SCFAs and secondary bile acids may favorably impact glucose homeostasis by signaling specific intestinal G-protein coupled receptors, such as GPR41/42 and TGR5 respectively, to induce GLP-1 production, stimulate insulin secretion, and regulate liver and intestinal gluconeogenesis (Tolhurst et al., 2012; De Vadder et al., 2014; Psichas et al., 2014; Shapiro et al., 2018). Future research could fruitfully use this mice model in investigating the gut microbiota-glucose homeostasis axis with larger sample size and higher number of cages per group.

In summary, the combined deficiency of the intestinal Fabps, Fabp2 and Fabp6, reduced the body weight gain of mice on both LFD and WSD. The combined deficiency of Fabp2 and Fabp6 also induced distinct gut microbial response to WSD in male and female mice. Overall, the use of this mouse model indicated that Fabp2 and Fabp6 proteins are inherently important in processing of dietary lipids, and consequently affect the composition of the gut microbiota as well as the nutritional status of the host.

Acknowledgment

This study was supported by grants (to LBA) from the Natural Sciences and Engineering Research Council of Canada.

4.5. References

Agellon, L.B., Drozdowski, L., Li, L.*, et al.* (2007). Loss of intestinal fatty acid binding protein increases the susceptibility of male mice to high fat diet-induced fatty liver. *Biochim Biophys Acta, 1771* (10), 1283-1288.

Agellon, L.B., Li, L., Luong, L.*, et al.* (2006). Adaptations to the loss of intestinal fatty acid binding protein in mice. *Mol Cell Biochem, 284* (1), 159-166.

Agellon, L.B., Toth, M.J. and Thomson, A.B. (2002). Intracellular lipid binding proteins of the small intestine. *Mol Cell Biochem, 239* (1-2), 79-82.

Baars, A., Oosting, A., Lohuis, M.*, et al.* (2018). Sex differences in lipid metabolism are affected by presence of the gut microbiota. *Sci Rep, 8* (1), 13426-13426.

Begley, M., Gahan, C.G. and Hill, C. (2005). The interaction between bacteria and bile. *FEMS Microbiol Rev, 29* (4), 625-651.

Begley, M., Hill, C. and Gahan, C.G.M. (2006). Bile salt hydrolase activity in probiotics. *Appl Environ Microbiol, 72* (3), 1729.

Chao, A. (1984). Nonparametric estimation of the number of classes in a population. *Scand J Stat, 11* (4), 265-270.

Chen, Y. and Agellon, L.B. (2019). Distinct alteration of gene expression programs in the small intestine of male and female mice in response to ablation of intestinal fabp genes. *Genes (Basel), 11* (8), 943.

Chong, W.C., Shastri, M.D. and Eri, R. (2017). Endoplasmic reticulum stress and oxidative stress: A vicious nexus implicated in bowel disease pathophysiology. *Int J Mol Sci, 18* (4), 771.

Cummings, J.H., Pomare, E.W., Branch, W.J.*, et al.* (1987). Short chain fatty acids in human large intestine, portal, hepatic and venous blood. *Gut, 28* (10), 1221-1227.

De Vadder, F., Kovatcheva-Datchary, P., Goncalves, D.*, et al.* (2014). Microbiota-generated metabolites promote metabolic benefits via gut-brain neural circuits. *Cell, 156* (1-2), 84-96.

Dhariwal, A., Chong, J., Habib, S., *et al.* (2017). Microbiomeanalyst - A web-based tool for comprehensive statistical, visual and meta-analysis of microbiome data *Nucleic Acids Res, 45* (W1), W180–W188.

Dixon, P. (2003). Vegan, a package of R functions for community ecology. *Journal of Vegetation Science, 14* (6), 927-930.

Furuhashi, M. and Hotamisligil, G.S. (2008). Fatty acid-binding proteins: Role in metabolic diseases and potential as drug targets. *Nat Rev Drug Discov, 7* (6), 489-503.

Gajda, A.M. and Storch, J. (2015). Enterocyte fatty acid-binding proteins (FABPs): Different functions of liver and intestinal FABPs in the intestine. *Prostaglandins Leukot Essent Fatty Acids, 93*, 9-16.

Gajda, A.M., Zhou, Y.X., Agellon, L.B., *et al.* (2013). Direct comparison of mice null for liver or intestinal fatty acid-binding proteins reveals highly divergent phenotypic responses to high fat feeding. *J Biol Chem, 288* (42), 30330-30344.

Garnier, S. (2018). Viridis: Default color maps from 'matplotlib': R package version 0.5.1. Retrieved from https://CRAN.R-project.org/package=viridis

Ghazalpour, A., Cespedes, I., Bennett, B.J., *et al.* (2016). Expanding role of gut microbiota in lipid metabolism. *Curr Opin Lipidol, 27* (2), 141-147.

Haque, Z.U., Kucukoner, E. and Aryana, K.J. (1997). Aging-induced changes in populations of lactococci, lactobacilli, and aerobic microorganisms in low-fat and full-fat cheddar cheese. *J Food Prot, 60* (9), 1095-1098.

Heijboer, A.C., Donga, E., Voshol, P.J., *et al.* (2005). Sixteen hours of fasting differentially affects hepatic and muscle insulin sensitivity in mice. *J Lipid Res, 46* (3), 582-588.

Hervé, M. (2020). RVAideMemoire: Testing and plotting procedures for biostatistics: R package version 0.9-75. Retrieved from https://CRAN.R-project.org/package=RVAideMemoire

Hetz, C. (2012). The unfolded protein response: Controlling cell fate decisions under ER stress and beyond. *Nat Rev Mol Cell Biol, 13* (2), 89-102.

Hu, Y., Liu, J., Yuan, Y.*, et al.* (2018). Sodium butyrate mitigates type 2 diabetes by inhibiting PERK-CHOP pathway of endoplasmic reticulum stress. *Environ Toxicol Pharmacol, 64*, 112-121.

Huang, A., Young, T.L., Dang, V.T.*, et al.* (2017). 4-phenylbutyrate and valproate treatment attenuates the progression of atherosclerosis and stabilizes existing plaques. *Atherosclerosis, 266*, 103-112.

Huang, H., McIntosh, A.L., Martin, G.G.*, et al.* (2016). FABP1: A novel hepatic endocannabinoid and cannabinoid binding protein. *Biochemistry, 55* (37), 5243-5255.

Jamaluddine, Z. (2015). *Fatty acid binding protein 2 protects the small intestine from dietary saturated fatty acid-induced endoplasmic reticulum stress.* (Master of Science), McGill University, Montreal, Canada.

Jensen, T.L., Kiersgaard, M.K., Sørensen, D.B.*, et al.* (2013). Fasting of mice: A review. *Lab Anim, 47* (4), 225-240.

Karaskov, E., Scott, C., Zhang, L.*, et al.* (2006). Chronic palmitate but not oleate exposure induces endoplasmic reticulum stress, which may contribute to INS-1 pancreatic β-cell apoptosis. *Endocrinology, 147* (7), 3398-3407.

Klindworth, A., Pruesse, E., Schweer, T.*, et al.* (2012). Evaluation of general 16S ribosomal RNA gene PCR primers for classical and next-generation sequencing-based diversity studies. *Nucleic Acids Res, 41* (1), e1-e1.

Koh, H. (2018). An adaptive microbiome α-diversity-based association analysis method. *Sci Rep, 8* (1), 18026.

Krehenwinkel, H., Pomerantz, A., Henderson, J.B.*, et al.* (2019). Nanopore sequencing of long ribosomal DNA amplicons enables portable and simple biodiversity assessments with high phylogenetic resolution across broad taxonomic scale. *GigaScience, 8* (5).

Kriss, M., Hazleton, K.Z., Nusbacher, N.M.*, et al.* (2018). Low diversity gut microbiota dysbiosis: Drivers, functional implications and recovery. *Curr Opin Microbiol, 44*, 34-40.

Labonté, E.D., Li, Q., Kay, C.M.*, et al.* (2003). The relative ligand binding preference of the murine ileal lipid binding protein. *Protein Expr Purif, 28* (1), 25-33.

Lin, J.H., Li, H., Zhang, Y., *et al.* (2009). Divergent effects of PERK and IRE1 signaling on cell viability. *PLoS One, 4* (1), e4170.

Ly, L.D., Xu, S., Choi, S.-K., *et al.* (2017). Oxidative stress and calcium dysregulation by palmitate in type 2 diabetes. *Exp Mol Med, 49* (2), e291-e291.

Martin, G.G., Danneberg, H., Kumar, L.S., *et al.* (2003). Decreased liver fatty acid binding capacity and altered liver lipid distribution in mice lacking the liver fatty acid-binding protein gene. *J Biol Chem, 278* (24), 21429-21438.

McIntosh, A.L., Atshaves, B.P., Landrock, D., *et al.* (2013). Liver fatty acid binding protein gene-ablation exacerbates weight gain in high-fat fed female mice. *Lipids, 48* (5), 435-448.

McMurdie, P.J. and Holmes, S. (2013). Phyloseq: An R package for reproducible interactive analysis and graphics of microbiome census data. *PLoS One, 8* (4), e61217.

Michael, M.D., Kulkarni, R.N., Postic, C., *et al.* (2000). Loss of insulin signaling in hepatocytes leads to severe insulin resistance and progressive hepatic dysfunction. *Mol Cell, 6* (1), 87-97.

Morrison, D.J. and Preston, T. (2016). Formation of short chain fatty acids by the gut microbiota and their impact on human metabolism. *Gut Microbes, 7* (3), 189-200.

Newberry, E.P., Xie, Y., Kennedy, S., *et al.* (2003). Decreased hepatic triglyceride accumulation and altered fatty acid uptake in mice with deletion of the liver fatty acid-binding protein gene. *J Biol Chem, 278* (51), 51664-51672.

Praslickova, D., Torchia, E.C., Sugiyama, M.G., *et al.* (2012). The ileal lipid binding protein is required for efficient absorption and transport of bile acids in the distal portion of the murine small intestine. *PLoS One, 7* (12), 1.

Psichas, A., Sleeth, M.L., Murphy, K.G., *et al.* (2014). The short chain fatty acid propionate stimulates GLP-1 and PYY secretion via free fatty acid receptor 2 in rodents. *Int J Obesity, 39*, 424.

R Core Team. (2020). R: A language and environment for statistical computing. Vienna, Austria: R Foundation for Statistical Computing. Retrieved from https://www.R-project.org/

Rao, X., Huang, X., Zhou, Z.*, et al.* (2013). An improvement of the 2ˆ(-delta delta CT) method for quantitative real-time polymerase chain reaction data analysis. *Biostat Bioinforma Biomath, 3* (3), 71-85.

Ríos-Covián, D., Ruas-Madiedo, P., Margolles, A.*, et al.* (2016). Intestinal short chain fatty acids and their link with diet and human health. *Front Microbiol, 7*, 185-185.

Schoeler, M. and Caesar, R. (2019). Dietary lipids, gut microbiota and lipid metabolism. *Reviews in Endocrine and Metabolic Disorders*, published online: 09 November 2019.

Segata, N., Izard, J., Waldron, L.*, et al.* (2011). Metagenomic biomarker discovery and explanation. *Genome Biol, 12* (6), R60.

Shannon, C.E. (1948). A mathematical theory of communication. *Bell Syst Tech J, 27* (3), 379-423.

Shapiro, H., Kolodziejczyk, A.A., Halstuch, D.*, et al.* (2018). Bile acids in glucose metabolism in health and disease. *J Exp Med, 215* (2), 383–396.

Srivathsan, A., Baloğlu, B., Wang, W.*, et al.* (2018). A MinION-based pipeline for fast and cost-effective DNA barcoding. *Mol Ecol Resour*, published online: 2018 Apr 2019.

Storch, J. and McDermott, L. (2009). Structural and functional analysis of fatty acid-binding proteins. *J Lipid Res, 50 Suppl* (Suppl), S126-S131.

Storch, J. and Thumser, A.E. (2010). Tissue-specific functions in the fatty acid-binding protein family. *J Biol Chem, 285* (43), 32679-32683.

Sugiyama, M.G. and Agellon, L.B. (2012). Sex differences in lipid metabolism and metabolic disease risk. *Biochem Cell Biol, 90* (2), 124-141.

Tatusova, T., DiCuccio, M., Badretdin, A.*, et al.* (2016). NCBI prokaryotic genome annotation pipeline. *Nucleic Acids Res, 44* (14), 6614-6624.

Tolhurst, G., Heffron, H., Lam, Y.S.*, et al.* (2012). Short-chain fatty acids stimulate glucagon-like peptide-1 secretion via the G-protein-coupled receptor FFAR2. *Diabetes, 61* (2), 364-371.

Vassileva, G., Huwyler, L., Poirier, K.*, et al.* (2000). The intestinal fatty acid binding protein is not essential for dietary fat absorption in mice. *FASEB J, 14* (13), 2040-2046.

Vega, H., Agellon, L.B. and Michalak, M. (2016). The rise of proteostasis promoters. *IUBMB Life, 68* (12), 943-954.

Volmer, R., van der Ploeg, K. and Ron, D. (2013). Membrane lipid saturation activates endoplasmic reticulum unfolded protein response transducers through their transmembrane domains. *Proc Natl Acad Sci USA, 110* (12), 4628.

Weger, B.D., Gobet, C., Yeung, J.*, et al.* (2019). The mouse microbiome is required for sex-specific diurnal rhythms of gene expression and metabolism. *Cell Metab, 29* (2), 362-382.e368.

Wickham, H. (2016). *ggplot2: Elegant graphics for data analysis*: Springer-Verlag New York. Retrieved from https://ggplot2.tidyverse.org

Yoshida, H., Matsui, T., Hosokawa, N.*, et al.* (2003). A time-dependent phase shift in the mammalian unfolded protein response. *Dev Cell, 4* (2), 265-271.

Zwicker, B. (2013). *Importance of bile acid metabolism in the absorption of nutrients in the Western-type diet.* (Master of Science), McGill University, Montreal, Canada.

Connecting statement to Chapter 5

In Chapters 2-4, I showed the ability of intrinsic (e.g. bile acids) and extrinsic (e.g. potato polyphenols) metabolites to modify the composition of gut microbiota and alter the metabolic status of the host using different mouse models. The use of animal models in gut microbial research is invaluable, since they share physiological features with humans and reflect overall responses as living subjects. Despite their physiological relevance, *in vivo* models are characterized by a complex and interacting host-gut microbial co-metabolism (Lederberg and McCray, 2001) which make it difficult to evaluate the individual host and gut microbial responses to experimental variables. Thus, it is necessary to generate a new framework of research that employs both *in vivo* and *in vitro* models to distinguish the effects of intrinsic and extrinsic factors on each of the host and its gut microbiota.

In vitro gut models are useful to determine the impact of a particular metabolite on the growth, behavior, and function of a particular class of gut microbiota. For example, bile acids may inhibit the growth, trigger transition from vegetative to dormant state, or enrich species capable of modifying bile acids and reducing their toxicity. However, such shifts in the gut microbial structure may be detrimental to the host. An illustration of this is the response of gut microbiota to trehalose, a sugar commonly used in food processing since 2000. This sugar activates the virulence of *Clostridium difficile,* which may explain the increase in the prevalence of infections caused by this microbe lately. Interestingly, determining the degree of virulence and the specific genetic responses of this microbe to trehalose was not possible without the use of an *in vitro* gut model (Eyre et al., 2019). Yet, the currently available *in vitro* gut models suffer from several issues which prevent their efficient use in gut microbial research. These issues include inflexibility in terms of culture size, bulkiness in terms of physical dimensions, and complexity in terms of operating and use (Minekus et al., 1999; Payne et al., 2012; von Martels et al., 2017). The aim of the study presented in Chapter 5 was to develop a modular, scalable, and dynamic *in vitro* gut model to facilitate studying of the gut microbiota in the absence of the host inherent variables.

Chapter 5

Development of simple, scalable, dynamic and modular bioreactors for simulating the digestive tract

Salam Habib, Anikka Swaby, Stan Kubow, Luis B. Agellon*

School of Human Nutrition, McGill University, Ste. Anne de Bellevue, QC, H9X 3V9 Canada

*Corresponding author:
Tel: 514-398-7862
Email: luis.agellon@mcgill.ca

Author contribution: SMH built the model, designed, and conducted evaluation experiments, analyzed the data, and wrote the manuscript. AMS, added the time server, conducted the functionality experiment, helped in evaluation experiments, helped in writing, and editing the manuscript. SK and LBA were involved in the conception, experimental design, interpretation of results and editing of the manuscript.

A version of this manuscript is in preparation to be submitted to Bioengineering Journal.

Abstract

In vitro gut model systems permit the growth of gut microbes outside their natural habitat and are essential to the study of gut microbiota. Systems available today are limited by lack of scalability and flexibility in mode of operation. Here we describe the development of a versatile bioreactor module capable of sensing and controlling of environmental parameters such as pH control of culture medium, and rate of influx and efflux of the culture medium. Modules can be linked in series to construct a model of the digestive tract to allow the growth of gut microbiota *in vitro*. We tested the growth of a simplified gut microbial community in a simulated mammalian gut model. The model attained and maintained a stable bacterial community that metabolized bile acids suggesting the ability of the model to recapitulate biological activities that occur *in vivo*.

5.1. Introduction

The gut microbiota is a diverse and complex community of bacteria, archaea, fungi, and viruses. The characteristics of its species composition and function have garnered great interest of researchers in recent years. The microbial community is an integral part of the gastrointestinal tract as it provides the host with an extended set of metabolic, structural and protective functions (O'Hara and Shanahan, 2006). In recent times, dysbiosis of the gut microbiota has been associated with a variety of diseases, such as inflammatory bowel diseases (Manichanh et al., 2012), diabetes, obesity (Musso et al., 2011), cancers (Zhu et al., 2013) and even some behavioral disorders (Vuong et al., 2017). It is now accepted that the gut microbiota has a strong influence on host health.

Due to the complex nature of the host-microbial interaction, it is challenging to infer specific mechanistic aspects of this interaction using conventional *in vivo* models and thus highlights the need for facile *in vitro* systems to help understand the complex interactions between the host and its gut microbiota (de Vos and de Vos, 2012). The currently available *in vitro* gut models vary in their complexity (Payne et al., 2012). Batch culture models are simple closed fermentation systems, that usually operate for less than two days. In continuous culture models, which might be single or multi-stage in design, fresh culture medium, supplemental growth factors or any other additives, are added continuously, while wastes and toxic byproducts are prevented from accumulating excessively by continuous dilution of the spent medium with fresh culture medium (Moon et al., 2016). The addition of fresh medium can be scheduled at specified time intervals as in the semi-continuous model EnteroMix (Makivuokko and Nurminen, 2006), or continuously supplied as in the Simulator of the Human Intestinal Microbial Ecosystem (SHIME) model (Molly et al., 1993). Some models, such as the TIM1 and TIM2 systems (Minekus et al., 1999), permit simulation of intestinal tract processes like digestion and absorption. Other models permit incorporation of intestinal tissues by employing co-culturing techniques (von Martels et al., 2017). Different gut models have been developed to simulate particular physiological and pathological

states, or the digestive tracts of infants as well as that of animals (Tanner et al., 2014; Card et al., 2017).

Since most of the *in vitro* gut models in existence were designed to simulate a specific digestive tract or condition, their designs inherently make it difficult to study different conditions or applications using the same device. Here we describe the design and implementation of a modular bioreactor, which serves as a new *in vitro* gut model platform that features functional flexibility and allows for static as well as dynamic culturing of gut bacteria.

5.2. Materials and methods

System design

The basic component of the gut model is a standardized bioreactor module (Fig. 5-1). The growth chamber (clear or brown media bottles with GL45 caps; Corning Incorporated) is placed in a jacketed reaction beaker (Chemglass) that serves as the temperature control vessel and is set on top of a stir plate. The temperature control vessel is attached to a recirculating heater/chiller with Prestone® antifreeze/engine coolant as the heat transfer fluid. The growth chamber is equipped with a stir bar and the caps are drilled to accommodate dedicated ports for a pH sensor (Atlas Scientific, Long Island City, NY), inlet and outlet ports for transfer of culture medium, inlet ports for acid and base, inlet port for nitrogen gas, outlet port for venting excess gas, and a valved outlet port for culture sampling. Brown bottles offer protection of light sensitive metabolites from photodamage. The space between the growth chamber and the temperature control vessel is filled with Prestone® antifreeze/coolant to ensure efficient heat transfer. The nitrogen gas inlet can be adapted to permit either an aerobic (port open to the room atmosphere) or anaerobic (constant flow of nitrogen gas) culture environment as required. Mini-peristaltic pumps (Kamoer KPP-DH-B03W), which convey acid and base to the growth chamber, and larger peristaltic pumps (New Era NE-9000), which drive the transfer of culture medium from one growth chamber to the next, are controlled by a Raspberry Pi computer version B-R2 (Raspberry Pi Foundation) running the system control software (Fig. 5-2) written in Python

programming language (Python Software Foundation). All the computers controlling each of the modules are connected *via* an ethernet router. The pH probe is connected to the Raspberry Pi computer through an EZO™ pH circuit stamp (Atlas Scientific, Long Island City, NY). A time server running on a dedicated Raspberry Pi computer fitted with a real-time clock module synchronizes the clocks across all network devices. The number of bioreactor modules operated at a time is flexible (Fig. 5-3). Batch culture mode (growth medium In/Out ports sealed), continuous mode (single bioreactor with growth medium In/Out ports operational) and series mode can be selected at the start of the experiment and the system parameters are supplied to each control computer through a configuration file.

Starter culture and culture conditions

The model gut microbiota in this study was prepared from dehydrated bacterial cultures of *Lactobacillus acidophilus*, *Lactobacillus delbrueckii* subsp. bulgaricus, *Lactobacillus casei*, *Lactobacillus rhamnosus*, *Bifidobacterium bifidum*, *Bifidobacterium breve*, *Bifidobacterium longum* and *Streptococcus salivarius* subsp. thermophilus. Some experiments used monocultures of *Escherichia coli* BL21 or *Bifidobacterium longum* subsp. infantis 35624 (Bifantis™ Align). To establish working bacterial cultures, the dehydrated bacteria were first reconstituted in peptone water (Oxoid). A 1 mL aliquot of the reconstituted bacteria was then added to 9 mL of de Man Rogosa and Sharpe (MRS) medium (Oxoid) supplemented with 0.05 % w/v L-cysteine (Amresco). The starter culture was grown at 37 °C anaerobically until the optical density at 600 nm reached ≥ 1.5 before being used in experiments.

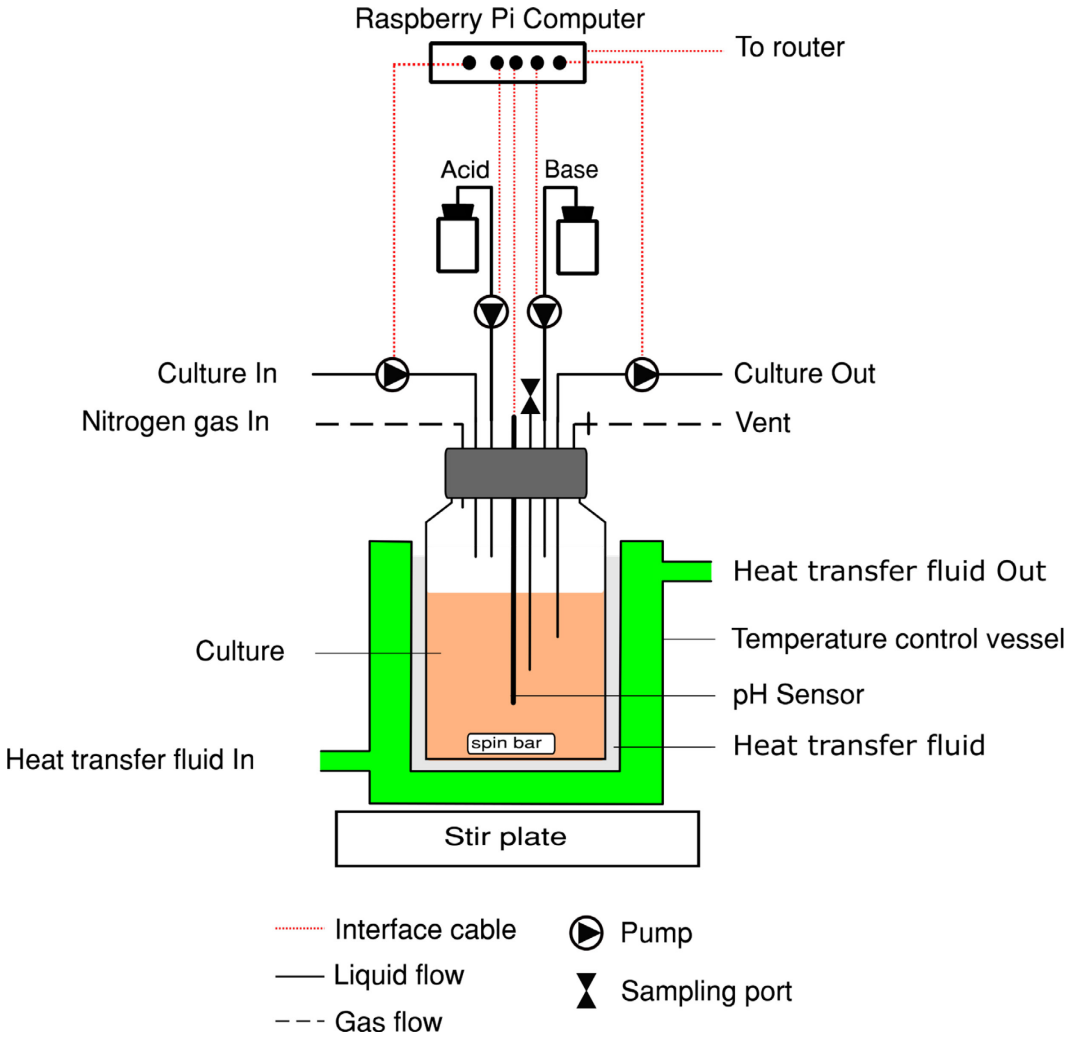

Figure 5-1. Schematic representation of a bioreactor module.

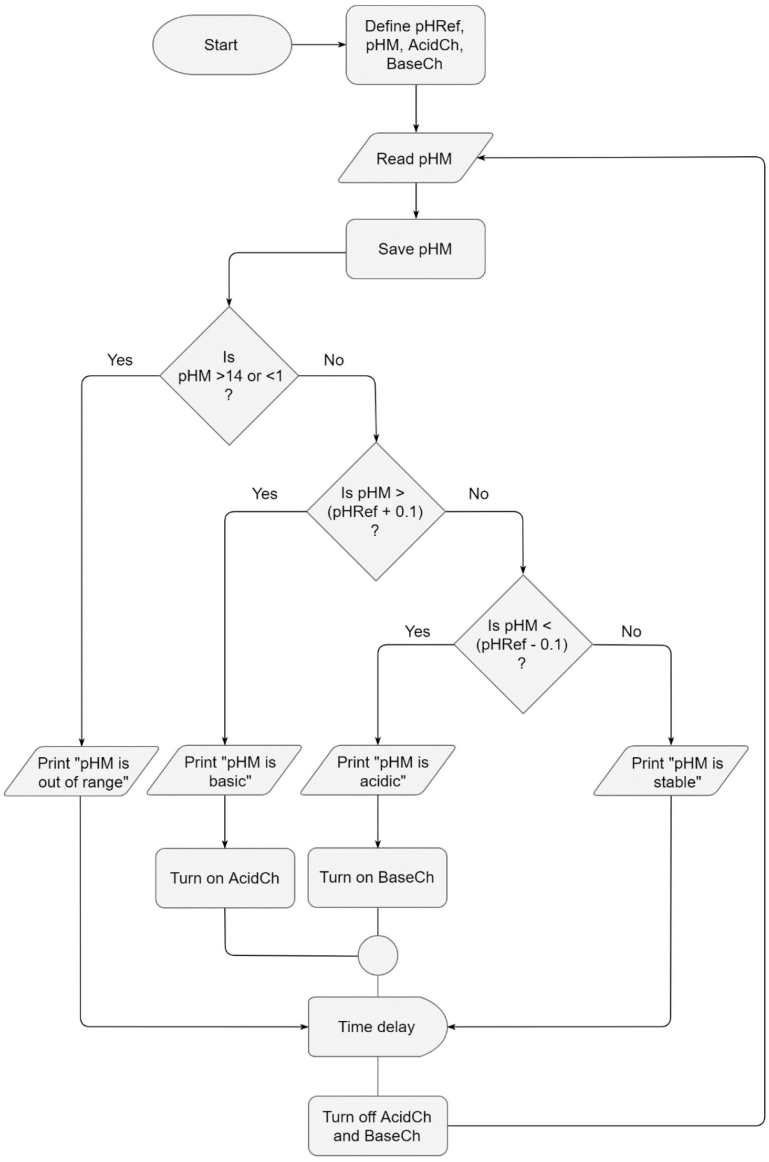

Figure 5-2. The flowchart of the bioreactor pH control.

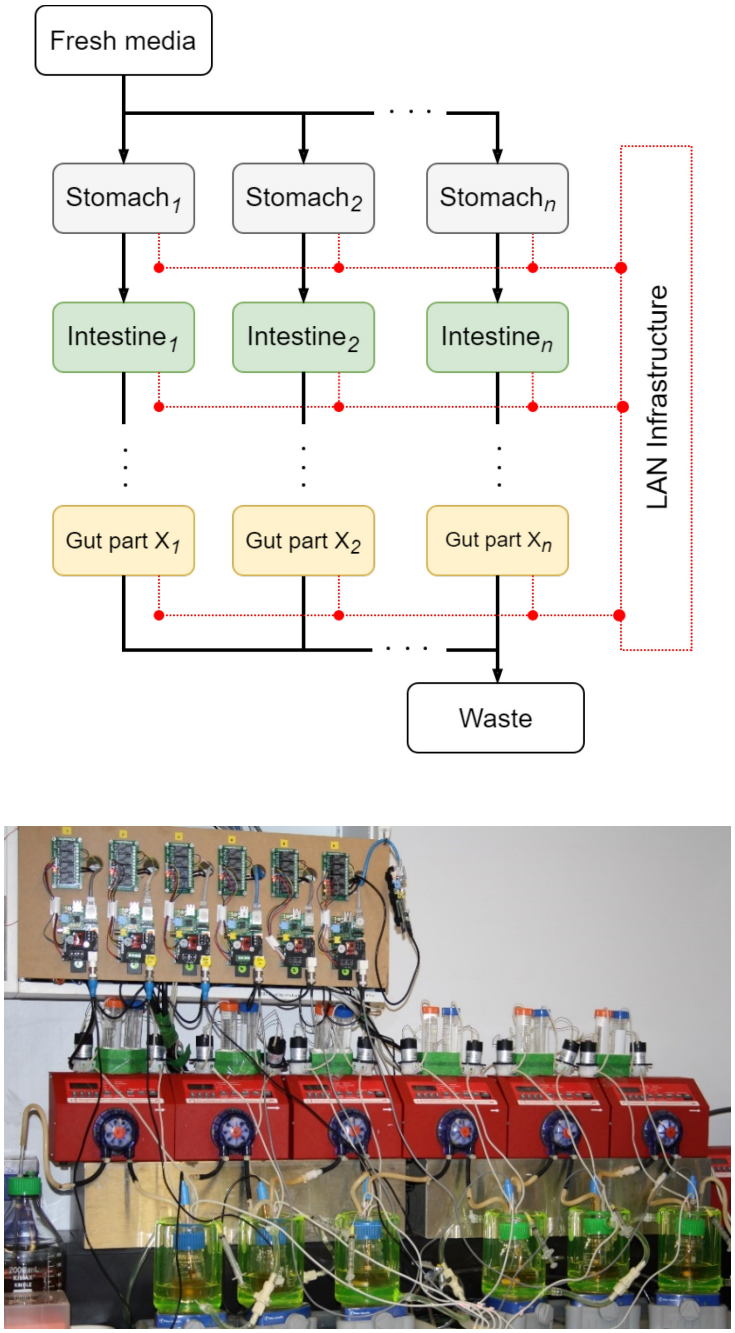

Figure 5-3. Connected bioreactor modules. (A) General connection scheme, (B) A sample of bioreactor module connection.

DNA extraction and quantification

Bacterial cells were sedimented from 1 mL cultures by centrifugation. The pellet was resuspended in buffer containing 0.2 M NaCl, 0.1 M EDTA and 15 mg/mL lysozyme and then incubated at 37 °C for 60 min. SST solution (20% sarkosyl, 0.2 M NaCl, 0.5 M Tris-HCl pH 8.0, 1 mg/mL proteinase K and 4 mM dithiothreitol) was then added and samples incubated at 55 °C for 60 min. Nucleic acids were extracted with an equal volume of phenol:chloroform (1:1) solvent. The aqueous phase was recovered, and nucleic acids were precipitated with 2 volumes of cold absolute ethanol in the presence of 0.3 M sodium acetate, washed with cold 70 % ethanol, dried and then finally dissolved in buffer containing 5 mM Tris-HCl (pH 8.0) and 0.1 mM ethylenediaminetetraacetic acid. The concentration of DNA was determined using the Qubit® dsDNA BR Assay Kit (Invitrogen). The integrity of the isolated DNA was assessed by agarose gel electrophoresis.

Biochemical analyses

Quantitative real-time PCR (qPCR) reactions were carried out using a Bio-Rad CFX96 real-time system operated by CFX Manager software (version 3.1) to determine the relative quantity of bacterial species in each sample. The standard reaction mixture consisted of 80 mM Tris-HCl pH 8.3, 100 mM KCl, 6 mM $MgCl_2$, 300 mM trehalose, 200 mM betaine-HCl, 0.2 mg/mL bovine serum albumin, 0.2 % (v/v) Tween-20, 1 X SYBR Green I, 2 mM dNTP mix, 0.4 U/µL Taq polymerase, 5 µM each of forward and reverse primers and 1 µg/mL DNA template in a total volume reaction volume of 10 µL. The sequences of the primers used in this study are shown in Appendix II. The standard PCR reaction included an initial denaturation step of 95 °C for 5 min and 40 cycles of 95 °C for 10 s and annealing and extension at 65 °C for 30 s, followed by melt curve analysis from 65 °C to 95 °C in 0.5 °C increments. Results were expressed as proportions of the copy number determined for each target within the sample, and each sample was represented as a percentage of the culture with the highest bacterial density which was assigned an arbitrary value of 100 %. Bile acids were separated by HPLC as described previously (Torchia et al., 2001). Bile acid species were identified based on retention times of certified bile acid standards (Steraloids) and quantified

against known amounts of the bile acid standards using area under the curve (AUC) method.

Statistical analyses

Differences between means were evaluated by Student's *t*-test using GraphPad Prism software version 8.2.1 for Windows (GraphPad Software, San Diego, California USA). Differences were considered significant when $p<0.05$.

5.3. Results and discussion

Here we describe a design of a modular bioreactor that can be assembled and operated under various configurations to create an *in vitro* model of a digestive tract. Each module can sense and control the pH of its culture medium and can be set to operate in static or dynamic culturing mode to serve a specific application.

5.3.1. Aerobic and anaerobic environment

To evaluate the ability of the bioreactors to maintain aerobic and anaerobic conditions, two bioreactor modules were inoculated with a monoculture of the anaerobe *Bifidobacterium longum subsp. infantis (B. longum infantis)* and operated in the batch culture mode. This bacterium was able to grow and thrive as indicated by the increase in the optical density of the culture after 24 h (Fig. 5-4A). Analysis of the composition of the culture by qPCR confirmed that the increase in bacterial density over the 24 h of culture was due to the growth of *B. longum infantis* (Fig. 5-4B). In a separate experiment, a set of bioreactor modules were inoculated with a mixed bacterial culture containing different species of bifidobacteria along with other bacterial species from two of the major phyla (Firmicutes and Actinobacteria) of the human gut microbiota (Kostic et al., 2013) to enable us to assess the growth dynamics of bifidobacteria within a mixed bacterial community. In this experiment, the MRS culture medium (Lee and Lee, 2008; Süle et al., 2014) was used and the bioreactor modules were operated in the continuous culture mode. As shown in Fig. 5-4C, the mixed culture maintained under anaerobic condition showed higher growth rates compared to that maintained under

aerobic condition. The increase in the optical density of the culture medium was attributed to the growth of both the *Bifidobacterium spp*. and the *Lactobacillus spp.* at the expense of *Streptococcus spp.* (Fig. 5-4D). These results demonstrate the ability of the bioreactor modules to maintain anaerobic culture conditions and support the growth of anaerobic bacteria such as bifidobacteria.

5.3.2. pH control

To assess the efficacy of pH control, six bioreactor modules were operated independently in batch culture mode. All bioreactor modules were inoculated with an active *E. coli* BL21 culture. One group had no pH control (Fig. 5-5A) and the other group was set to maintain pH 7 (Fig. 5-5B). The pH of the cultures was monitored for 24 h and samples of the cultures were collected for assessment of optical density at regular intervals over the course of the experiment. The cultures of *E. coli* maintained at pH 7 showed enhanced growth during the exponential growth phase compared to the cultures with no pH control. The volume of acid and base added to the growth medium to maintain pH 7 are shown in Fig. 5-5C. These results demonstrate the ability of the bioreactor modules to maintain a steady pH of the culture at a predetermined value.

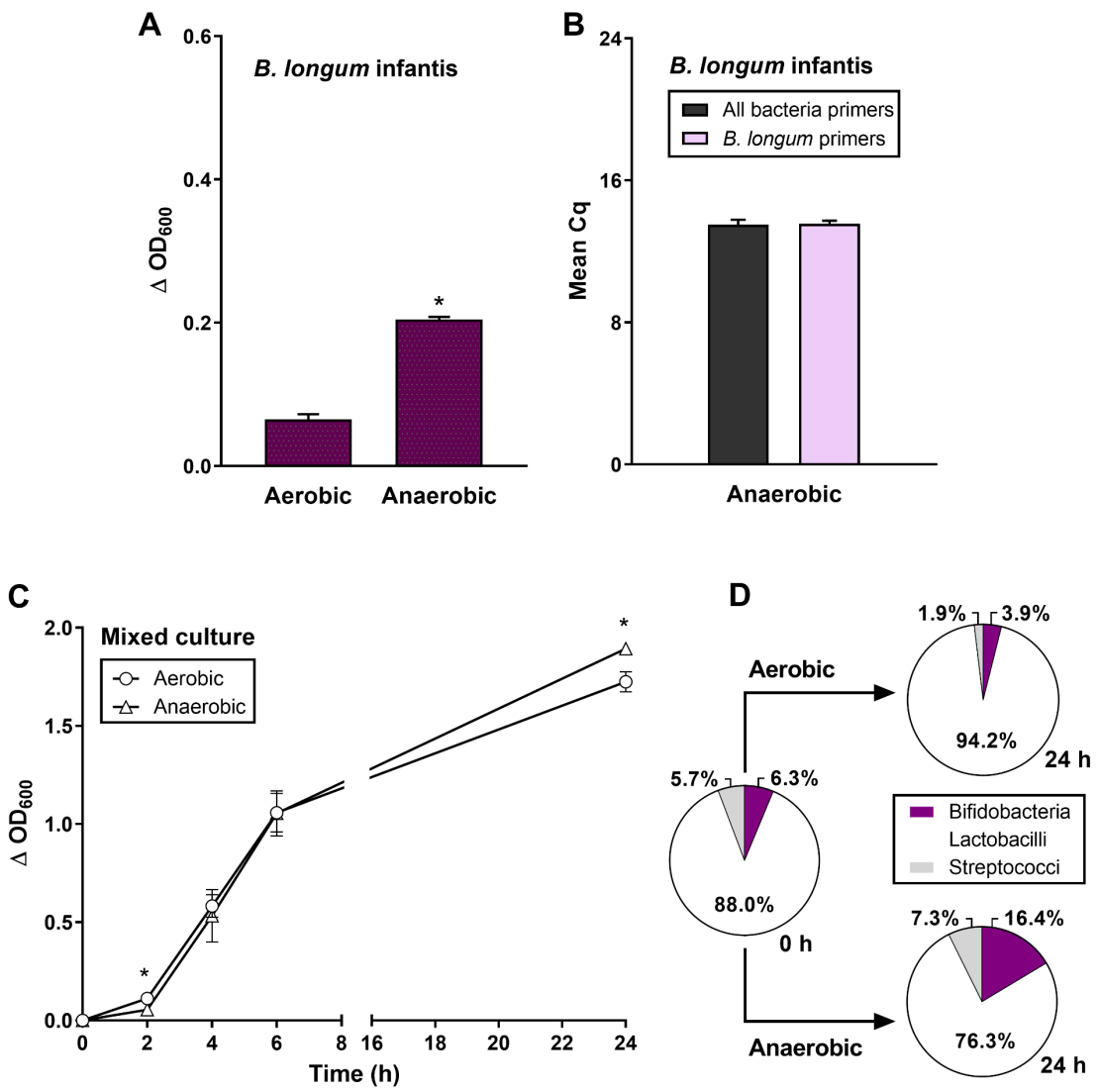

Figure 5-4. Aerobic and anaerobic growth of a gut bacteria. (A) Growth of *Bifidobacterium longum* subsp. *infantis* monocultures under anaerobic conditions at pH 5.8. Data shown is the average of two trials with n=4 replicates. (B) Abundance of bacteria detected by the bacterial 16S rDNA universal primers and 16S rDNA primers specific for *B. longum infantis* in equivalent masses of input template DNA extracted from the monocultures in (A). Data shown is the average of two trials with n=4 replicates. (C) Growth of a model gut microbiota (mixed bacterial cultures) over time in aerobic and anaerobic conditions maintained at pH 5.8. Data shown is the average of two trials with n=2 replicates. (D) Proportions of bacterial genera present in the starter culture (0 h) and after 24 h of growth in aerobic and anaerobic cultures (C). *p<0.05.

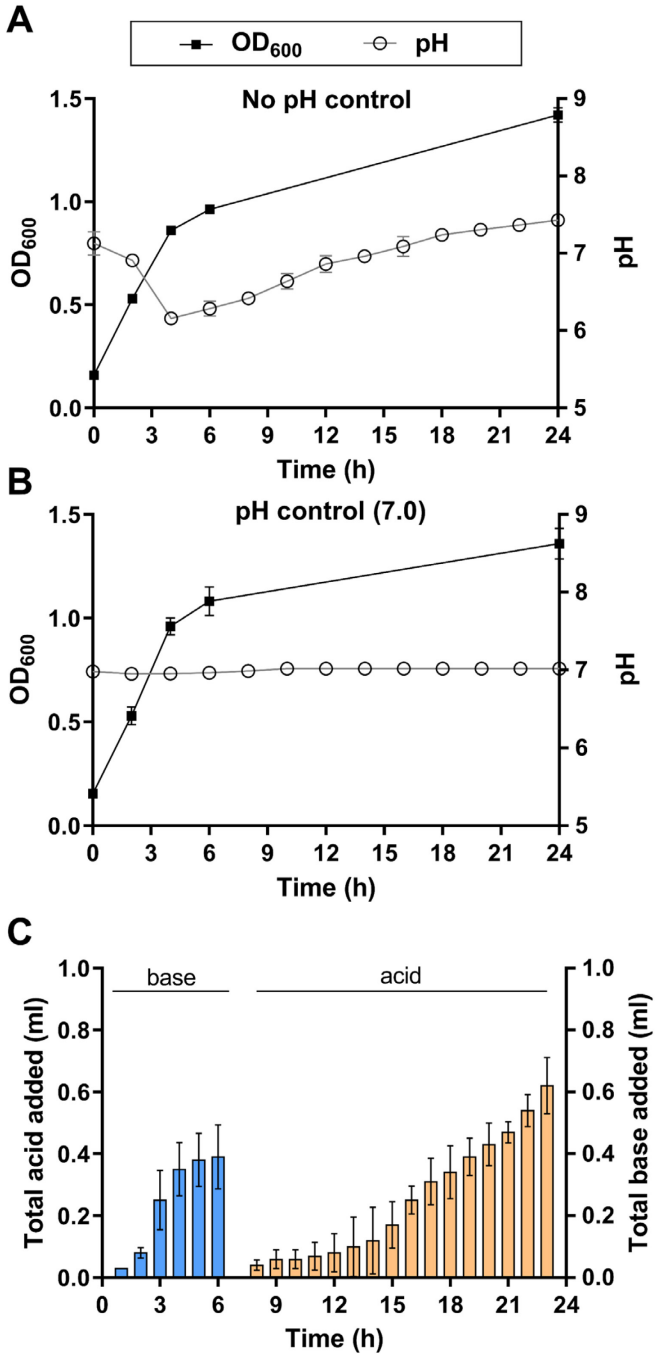

Figure 5-5. Growth of a bacterial monocultures with and without pH control. Growth of an E. coli monocultures over time (A) without pH control and (B) at pH 7.0. (C) Total volume of acid and base added to the pH-controlled culture (B) over time. Data shown is the average of 2 trials with n=3 replicates.

5.3.3. Genetic stability of bacterial community

To assess the genetic stability of the bacterial community in long-term culture, the bioreactors were connected in series to create a dynamic model of the human digestive tract. In this experiment, six bioreactor modules were connected in a series, each set to maintain a specific pH and held under anaerobic conditions to simulate a segment of the human gastrointestinal tract (Fig. 5-6A). The pH values used in the stomach, small intestine, and large intestine compartments were based on the pH values reported for these regions of the human digestive tract (Khutoryanskiy, 2015). At the start of the experiment, Module 1 (representing the stomach) was inoculated with the model microbiota as described earlier (Fig. 5-6B) and the system was operated continuously for 120 h. As shown in Fig. 5-6C to 5-6H, bacterial density in Module 1 decreased (Fig. 5-6C), while the bacterial density in Modules 2 and 3 (representing the proximal and distal small intestine, respectively; Fig. 5-6D and 5-6E) as well as Modules 4-6 (representing the ascending colon, transverse colon and descending colon of the large intestine, respectively; Fig. 5-6F to 5-6H) increased over the duration of the experiment. Modules 4-6 exhibited the greatest bacterial density. At the end of the experiment, genetic composition of the bacterial community in Module 6, which simulates the most distal large intestine compartment (Fig. 5-6H), closely resembled that of the initial inoculum (Fig. 5-6B) at the genus level. The specific bacterial species and their abundance in each of the bioreactor modules in the series were also determined. The composition of the bacterial community was distinct at different pH represented by the different segments of the digestive tract (Fig. 5-6A). *B. bifidum* was not detectable after 24 h of culture, suggesting that specific nutritional or structural substrate requirements of this species that may have not been met by the culture conditions. In contrast, *L. casei*, *L. rhamnosus*, *B. longum*, and *S. thermophilus* remained easily detectable throughout the entire duration of the experiment (Fig. 5-7).

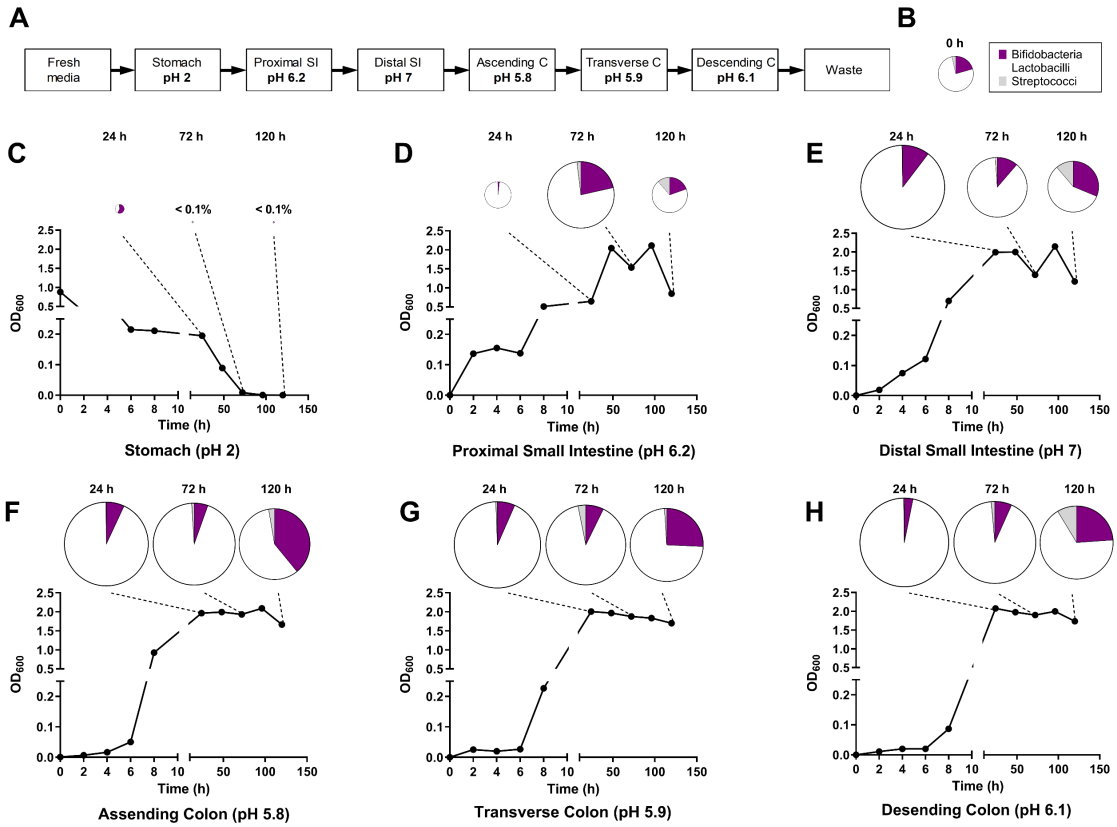

Figure 5-6. Stability of the genotype of a model gut microbiota in a dynamic simulation of the human digestive tract. (A) The pH setpoint of the culture medium representing segments of the simulated digestive tract. The rate of influx and efflux of culture medium into and out of each bioreactor was set to 0.1 mL/min. (B) Proportions of bacterial genera of the starter culture. The growth of the model gut microbiota over 5 days and the proportions of bacterial genera assayed at 24, 72, 120 h in modules representing (C) Stomach, (D) Proximal small intestine, (E) Distal small intestine, (F) Ascending colon, (G) Transverse colon and (H) Descending colon. Data shown is the average of 2 trials with n=2 replicates.

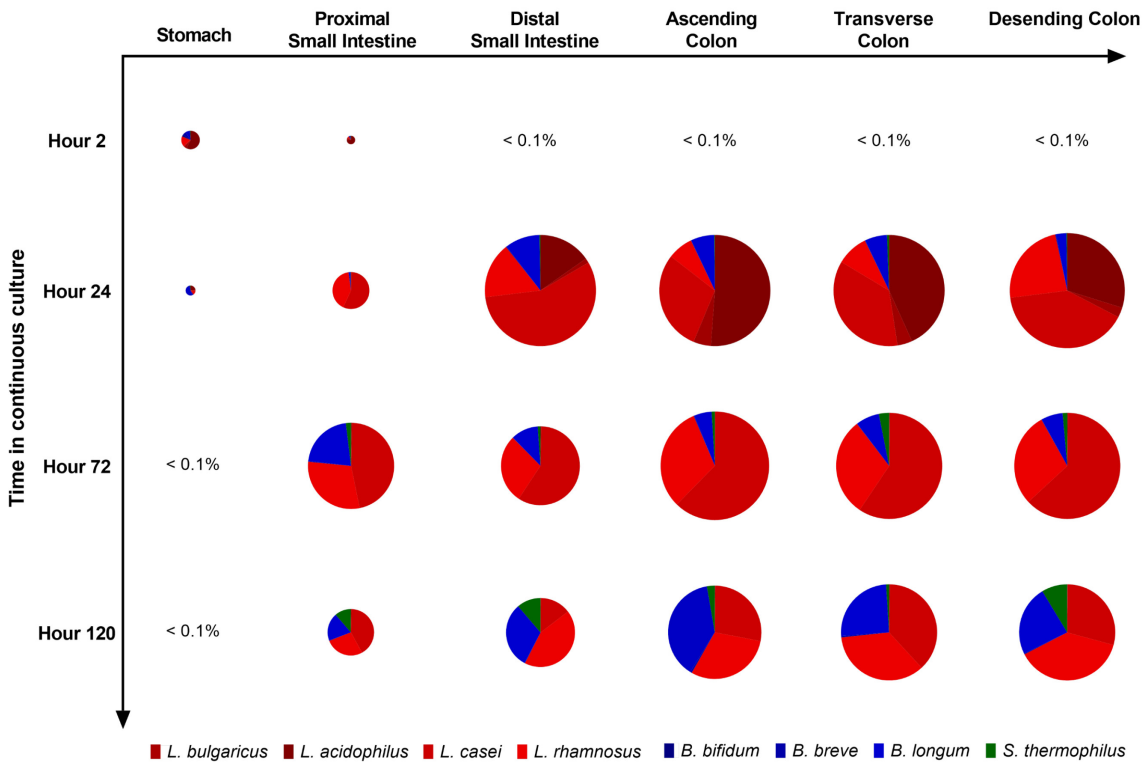

Figure 5-7. Stability of the genotype of a model gut microbiota at the species level. The growth of the model gut microbiota over five days and the proportions of bacterial genera assayed at 2, 72, 120 h in modules represented stomach, proximal small intestine, distal small intestine, ascending colon, transverse colon, and descending colon.

5.3.4. Assessment of biological activity of the model gut microbial community

To test if the model gut microbial community grown in the *in vitro* gut model exhibited selected biological activities associated with gut microbiota *in vivo*, the ability of the culture to metabolize bile acids was assayed. In the first experiment, six bioreactor modules operating in the batch culture mode with pH control were inoculated with the model microbiota. Taurocholic acid (TCA), a common conjugated bile acid, was added to the culture medium either at 0, 10, or 100 mM concentrations. The growth of the model microbiota treated with TCA was substantially less compared to the untreated model microbiota. Nevertheless, bacterial growth was observed even at the highest TCA concentration used in the experiment (Fig. 5-8A). At 10 mM TCA treatment, the proportion of Streptobacteria spp. in the community was reduced while that of *Lactobacillus* spp. was increased (Fig. 5-8B), which is likely due to its ability to metabolize TCA (Gilliland and Speck, 1977). HPLC analysis of the bile acid species in the culture medium showed the appearance of cholic acid, a product of TCA deconjugation by bacteria, after 24 h of culture (Fig. 5-8C). In the second experiment, the model microbiota was treated with chenodeoxycholic acid (CDCA), an unconjugated bile acid. CDCA was more potent than TCA in inhibiting the growth of the model microbiota (Fig. 5-8D). As shown in Fig. 5-8E, ursodeoxycholic acid, the 7β-hydroxyl group epimer of the 7α-hydroxyl group-containing CDCA produced by bacterial metabolism, was present in the culture after 24 h. These results demonstrate that the model microbiota grown in the *in vitro* digestive tract model was capable of exhibiting biological activities normally associated with gut microbiota *in vivo*.

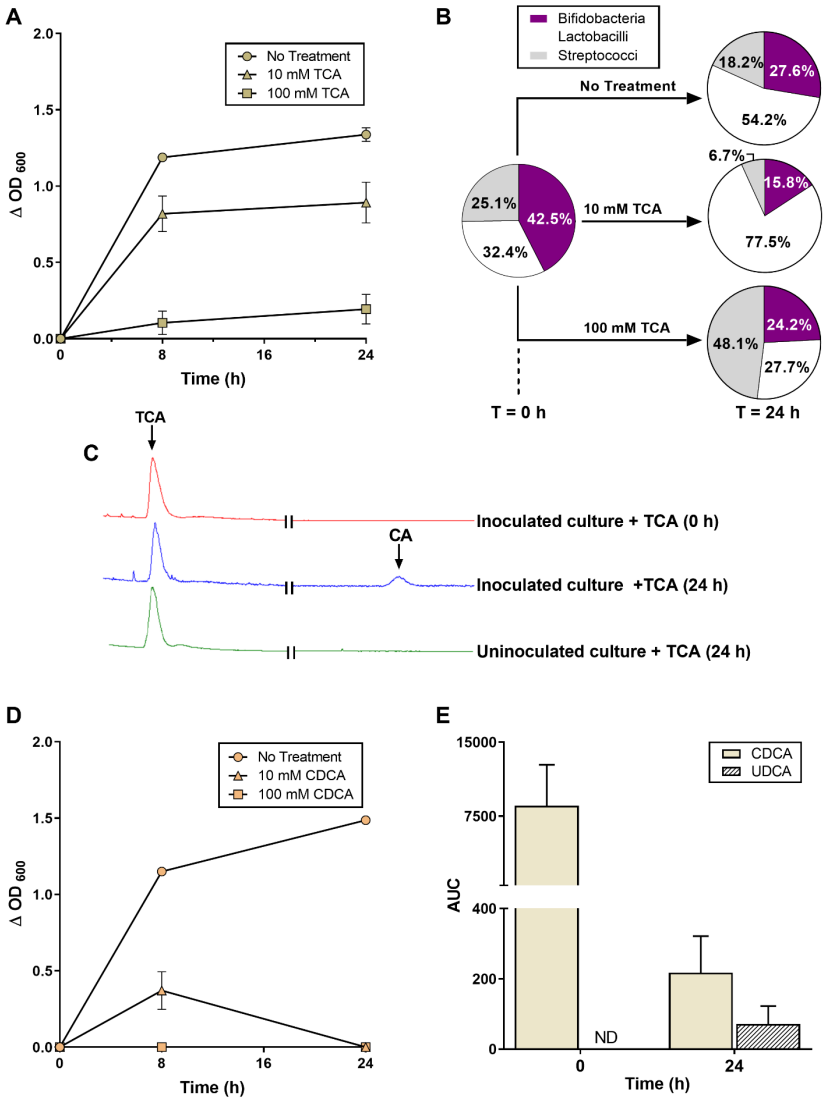

Figure 5-8. Functionality of a model gut microbiota in response to bile acid treatment. (A) Growth of a model gut microbiota in the anaerobic conditions at pH 5.8 in the absence or presence of taurocholic acid (TCA). Data shown is the average of two trials with n=2 replicates. (B) Proportions of bacterial genera present at inoculation (0 h) and after 24 h of culture (A). (C) Representative chromatogram showing bile acids detected in the growth medium of inoculated cultures at 0 h and 24 h, and uninoculated culture (no bacteria) at 24 h. (D) Growth of a model gut microbiota in the presence of chenodeoxycholic acid (CDCA). Data shown is the mean of 2 trials with n=4x replicates. (E) Detection of CDCA and ursodeoxycholic acid (UDCA) in the growth medium at inoculation (0 h) and after 24 h of culture. ND: not detected.

5.4. Summary

The modular bioreactor design described here offers flexibility in terms of culture size, aerobic/anaerobic atmosphere, and static/dynamic culture. Specifically, the modular design enables the creation of simple or complex models of digestive tracts. These models are comprised of independently controlled bioreactor modules of desired culture. Each of the modules that make up the simulated digestive tract can independently control the pH of its culture medium as well as the rate of influx and efflux of the microbial culture. Finally, the system described serves as a new *in vitro* gut model platform to enable the study of gut microbial growth in the absence of host immune surveillance and under controlled availability of metabolites that are normally secreted by the host into the digestive tract. Future work will concentrate on inoculating the gut model with samples of gut microbiota taken from mice and humans to investigate certain mechanistic aspects that would help in explaining the role of gut microbiota in influencing host metabolism.

Acknowledgment

This work was supported by the grants from the Natural Sciences and Engineering Council of Canada to LBA and to SK.

5.5. References

Card, R.M., Cawthraw, S.A., Nunez-Garcia, J.*, et al.* (2017). An in vitro chicken gut model demonstrates transfer of a multidrug resistance plasmid from Salmonella to commensal *Escherichia coli*. *mBio, 8* (4).

de Vos, W.M. and de Vos, E.A. (2012). Role of the intestinal microbiome in health and disease: From correlation to causation. *Nutr Rev, 70*, S45-56.

Eyre, D.W., Didelot, X., Buckley, A.M.*, et al.* (2019). *Clostridium difficile* trehalose metabolism variants are common and not associated with adverse patient outcomes when variably present in the same lineage. *EBioMedicine, 43*, 347-355.

Gilliland, S.E. and Speck, M.L. (1977). Deconjugation of bile acids by intestinal lactobacilli. *Appl Environ Microbiol, 33* (1), 15-18.

Khutoryanskiy, V.V. (2015). Longer and safer gastric residence. *Nat Mater, 14*, 963.

Kostic, A.D., Howitt, M.R. and Garrett, W.S. (2013). Exploring host–microbiota interactions in animal models and humans. *Genes Dev, 27* (7), 701-718.

Lederberg, J. and McCray, A.T.J. (2001). Ome sweet omics - A genealogical treasury of words. *Scientist, 15* (7), 8.

Lee, H.M. and Lee, Y. (2008). A differential medium for lactic acid-producing bacteria in a mixed culture. *Lett Appl Microbiol, 46* (6), 676-681.

Makivuokko, H. and Nurminen, P. (2006). In vitro methods to model the gastrointestinal tract. In A. Ouwehand & E. Vaughan (Eds.), *Gastrointestinal microbiology*. Boca Raton, FL: Taylor & Francis Group.

Manichanh, C., Borruel, N., Casellas, F.*, et al.* (2012). The gut microbiota in IBD. *Nat Rev Gastroenterol Hepatol, 9* (10), 599-608.

Minekus, M., Smeets-Peeters, M., Havenaar, R.*, et al.* (1999). A computer-controlled system to simulate conditions of the large intestine with peristaltic mixing, water absorption and absorption of fermentation products. *Appl Microbiol Biotechnol, 53* (1), 108-114.

Molly, K., Vande Woestyne, M. and Verstraete, W. (1993). Development of a 5-step multi-chamber reactor as a simulation of the human intestinal microbial ecosystem. *Appl Microbiol Biotechnol, 39* (2), 254-258.

Moon, J.S., Li, L., Bang, J.*, et al.* (2016). Application of in vitro gut fermentation models to food components: A review. *Food Sci Biotechnol, 25*, 1-7.

Musso, G., Gambino, R. and Cassader, M. (2011). Interactions between gut microbiota and host metabolism predisposing to obesity and diabetes. *Annu Rev Med, 62*, 361-380.

O'Hara, A.M. and Shanahan, F. (2006). The gut flora as a forgotten organ. *EMBO Rep, 7* (7), 688-693.

Payne, A.N., Zihler, A., Chassard, C.*, et al.* (2012). Advances and perspectives in *in vitro* human gut fermentation modeling. *Trends Biotechnol, 30* (1), 17-25.

Süle, J., Kõrösi, T., Hucker, A.*, et al.* (2014). Evaluation of culture media for selective enumeration of bifidobacteria and lactic acid bacteria. *Braz J Microbiol, 45* (3), 1023-1030.

Tanner, S.A., Zihler Berner, A., Rigozzi, E.*, et al.* (2014). In vitro continuous fermentation model (PolyFermS) of the swine proximal colon for simultaneous testing on the same gut microbiota. *PLoS One, 9* (4), e94123.

Torchia, E.C., Labonté, E.D. and Agellon, L.B. (2001). Separation and quantitation of bile acids using an isocratic solvent system for high performance liquid chromatography coupled to an evaporative light scattering detector. *Anal Biochem, 298* (2), 293-298.

von Martels, J.Z.H., Sadaghian Sadabad, M., Bourgonje, A.R.*, et al.* (2017). The role of gut microbiota in health and disease: In vitro modeling of host-microbe interactions at the aerobe-anaerobe interphase of the human gut. *Anaerobe, 44* (Supplement C), 3-12.

Vuong, H.E., Yano, J.M., Fung, T.C.*, et al.* (2017). The microbiome and host behavior. *Annu Rev Neurosci, 40*, 21-49.

Zhu, Q., Gao, R., Wu, W.*, et al.* (2013). The role of gut microbiota in the pathogenesis of colorectal cancer. *Tumour Biol, 34* (3), 1285-1300.

Chapter 6

General discussion and conclusion

This thesis aimed to address the modification of the gut microbiota by intrinsic and extrinsic metabolites and their impact on the metabolic status of the organism. The results demonstrated that an intrinsic metabolite, such as bile acids, induced gut microbial dysbiosis distinctly in male and female Fabp6-deficient mice, and the change in gut microbial composition was associated with differential predicted capacity of gut microbiome in carbohydrate metabolism by the two sexes (Chapter 2). On the other hand, certain kinds of extrinsic metabolites, such as the plant derived PRPE, prevented both dysbiosis of gut microbiota and activation of colonocyte endoplasmic reticulum stress that were induced by WSD in a sex dimorphic manner (Chapter 3). Moreover, a metabolic challenge such as WSD, amplified the sex differences in gut microbiota in response to the loss of intestinal fatty acids binding proteins (Chapter 4). Together, these results indicate the involvement of gut microbiota in regulating the sex dimorphic response to various metabolic challenges.

Gut microbiota is involved in mediating sex dimorphism

Differences between males and females in the metabolic profile and disease risk are highly influenced by their genetic factors and sex hormones (Sugiyama and Agellon, 2012). Recently, gut microbiota was suggested to be involved in mediating sex differences in metabolism (Mueller et al., 2006; Markle et al., 2013; Dominianni et al., 2015; Haro et al., 2016; Takagi et al., 2019). The findings of this thesis reveal an association between the sex dimorphic gut microbial composition and the distinct metabolic phenotypes in male and female mice in response to high fat diet. For example, when challenged with WSD, male *Fabp6*$^{-/-}$ mice showed enhanced adiposity and distinct gut microbial dysbiosis compared to their female counterparts (Chapter 2). Similarly, female *Fabp2*$^{-/-}$; *Fabp6*$^{-/-}$ mice gained less body weight on both LFD and WSD compared to their male counterparts, and this effect was associated with lower gut microbial diversity and abundance (Chapter 4). In fact, it has been also shown that

mice deficient in any of the three intestinal Fabps (Fabp1, Fabp2, and Fabp6) displayed sex dimorphic phenotypes on high fat diets, particularly in terms of adiposity (Vassileva et al., 2000; Agellon et al., 2007; McIntosh et al., 2013; Gajda et al., 2013) and (Appendix I). Moreover, the analysis of gene expression programs in the small intestine showed that wild-type male and female intestinal transcriptome were distinct, while that of male and female *Fabp2*$^{-/-}$; *Fabp6*$^{-/-}$ or *Fabp2*$^{-/-}$ mice show greater similarity (Sugiyama et al., 2012; Chen and Agellon, 2019). Together, these studies suggest that intestinal Fabps are involved in mediating the sex dimorphic response of the gut microbiota to metabolic challenges.

It has been recently described that male germ-free mice reveal “feminization” by downregulation of male-specific gene expression programs in the liver, and that female germ-free mice reveal “masculinization” by upregulation of male-specific gene expression programs, and both of them were accompanied with altered sex-biased metabolite profiles (Baars et al., 2018; Weger et al., 2019). This line of research indicates the direct involvement of the gut microbiota in the development of distinct metabolic profiles in males and females. In this thesis, *Fabp6*$^{-/-}$ mice depicted distinct gut microbial composition (Chapter 2), this finding is interesting when set in context with a previous study that demonstrated lower ovulation rate and fertility among female *Fabp6*$^{-/-}$ mice compared to normal mice (Duggavathi et al., 2015). Similar findings were also reported in another mouse model of bile acid disrupted metabolism (Martinot et al., 2017). Looking forward, the development of germ-free mouse models deficient in one or more of the intestinal Fabps would greatly facilitate defining the specific role of both the gut microbiota and the intestinal Fabps in driving the reported sex-biased metabolic responses. The role of gut microbiota in mediating the sex dimorphic metabolic responses is important to human research as well, since it may explain, in part, the increased susceptibility of specific sexes to certain types of metabolic disorders (Nedungadi and Clegg, 2009; Sugiyama and Agellon, 2012; Molodecky et al., 2012). For example, differences in gut microbiota between males and females may underlie the changing risk to coronary heart diseases before and after menopause and to the higher risk to inflammatory bowel diseases in women (Nedungadi and Clegg, 2009; Molodecky et al., 2012). In respect to the thesis context, investigating the role of the gut

microbiota in developing other acquired metabolic syndromes such as obesity and type 2 diabetes in women with FAPB2 polymorphism A54T may prove significant.

Gut microbial diversity and nutrient availability

Rich microbial communities characterize the gut microbiota of healthy individuals, whereas the loss of gut microbial diversity has been associated with disease (DeGruttola et al., 2016; Kriss et al., 2018). As the diversity of the gut microbiota implies diversity of functional capacity, reduced gut microbial functionality is expected to be associated with metabolic dysfunction in the host (Larsen and Claassen, 2018). Despite the fact that dynamic changes in the gut microbial diversity are expected (Gerber, 2014), the bile acid malabsorption caused by the loss of Fabp6 in upper gut of *Fabp6*$^{-/-}$ mice results in an inherent decreased gut microbial diversity (Chapter 2). While studies have suggested functional redundancy in the gut microbiome (Lozupone et al., 2012), in certain cases, the loss of gut microbial diversity may result in loss of functions that may not be compensated for, which renders both the gut microbial community and the host vulnerable to dietary perturbations. For example, following WSD-induced dietary perturbation, the gut microbial community of male *Fabp6*$^{-/-}$ mice was shifted toward the expansion of gut microbiota known for its preference to saccharolysis over proteolysis (Chapter 2).

A key determinant of gut microbial diversity may be in the wide assortment of the available nutrients, and since the greater variety of nutrients available may stimulate the growth of diverse bacteria leading to richer diversity of gut microbiota (Holmes et al., 2017). In fact, dietary choices represent bias toward particular substrates that enrich specific types of bacteria and give competency over others (Heiman and Greenway, 2016). The amount of nutrients available for the gut microbiota are not only influenced by host dietary choices, but also by its capacity to digest and assimilate the nutrients that make up chosen food items. Indeed, the increased gut microbial diversity in both Fabp6-deficient and Fabp2- and Fabp6- deficient mice on WSD indicate greater dietary fat availability for gut microbiota implies the integral roles of the intestinal fatty acids binding protein in fat assimilation (Chapter 2 and Chapter 4). Similarly, nutrient assimilation may be altered by PRPE supplementation as this clearly influenced gut

microbial diversity (Chapter 3). In particular, certain plant polyphenols have been shown to improve glycemic control of the host by altering the secretion of carbohydrate digestive enzymes and by reducing the abundance of intestinal sugar transporters (Hanhineva et al., 2010). Moreover, plant polyphenols have the ability to bind minerals such as iron and zinc, which could reduce the bioavailability of these nutrients to host (Ma et al., 2011; Kim et al., 2011). Thus, PRPE may reduce the bioavailability of nutrients to the host but increase the assortment of nutrients available to the gut microbiota and enhance their diversity even on WSD.

Yet, the importance of gut microbial diversity on the health status of the host in early life is evident. For example, the gut microbial diversity of children before the introduction of solid foods is limited and studies have shown that it increases vastly after the introduction of solid foods (Laursen et al., 2017). Similarly, bottle-feeding of infant formula may offer limited sources of nutrients available for the development of the gut microbiota in newborns compared to that of breast-fed infants by mothers with adequate nutritional status (Ho et al., 2018). Certainly, insuring a healthy and diverse gut microbial community early in life is associated with both short- and long-term health benefits (Mulligan and Friedman, 2017; Ho et al., 2018).

The role of intestinal Fabps in dietary lipid assimilation

Fatty acid binding proteins were first reported more than 50 years ago, however, to date their exact functions remain elusive (Levi et al., 1969; Ockner et al., 1972). The presence of more than 10 member proteins of the Fabps family, and the co-expression of multiple Fabps family members in the same tissue suggest unique cellular specific functions (Ockner et al., 1972; Agellon et al., 2002). As implied by their localization, intestinal Fabps are expected to mediate integral role in dietary lipid assimilation. In this thesis, when challenged with WSD, male mice deficient in both Fabp2 and Fabp6 exhibited increased Firmicutes:Bacteroidetes ratio and adiposity along with reduced liver fat deposition, and improved glucose tolerance (Chapter 4). Similarly, male Fabp6-deficient mice on WSD showed increased Firmicutes:Bacteroidetes ratio, enhanced adiposity, and improved glucose tolerance, however, this was accompanied by increased liver fat deposition (Appendix I and Chapter 2). Male Fabp2-deficent mice

also showed enhanced adiposity and increased liver fat deposition on high fat diet, but in contrast, they were hyperinsulinemic and exhibited glucose intolerance (Vassileva et al., 2000). Therefore, these studies suggest an important role of intestinal Fabps in processing of dietary lipids, and consequently the nutritional status of the host as well as the composition of the gut microbiota.

Interestingly, only female Fabp2-deficient mice showed increase in Fabp1 mRNA abundance on high fat diet, which may indicate a female sex-specific buffering capacity of Fabp1 and a protective mechanism against high fat diet induced adiposity (Jamaluddine, 2015). Since the loss of Fabp2 is suggested to alter fatty acid trafficking toward chylomicron production in the enterocytes of female mice, in male mice an increased flux of fatty acids into the portal vein is hypothesized to induce adiposity and glucose intolerance (Agellon et al., 2002). On the other hand, the loss of Fabp6 appears to induce favorable effects on glucose metabolism as indicated by the enhanced glucose tolerance in both Fabp6-dificient and Fabp2 and 6-deficient mouse models (Chapter 2 and Chapter 4).

While bile acids have been long recognized for their role in lipid digestion and transport, it has been more recently demonstrated that bile acids are biologically active compounds that bind several nuclear and cell surface receptors. Nuclear receptors activated by bile acids include farnesoid X receptor (FXR), liver X receptor α (LXRα), vitamin D receptor (VDR), pregnane X receptor (PXR), and constitutive androstane receptor (CAR) (Makishima et al., 1999; Song et al., 2000; Staudinger et al., 2001; Makishima et al., 2002; Saini et al., 2004). Bile acids also activate cell surface G-protein coupled receptors such as Takeda G protein receptor 5 (TGR5), sphingosine1-phosphate receptor (S1PR2), and the muscarinic receptors M2 and M3 (Kawamata et al., 2003; Khurana et al., 2005; Sheikh Abdul Kadir et al., 2010; Studer et al., 2012). The ubiquitous expression of these receptors in different body tissues indicates the ability of bile acids to influence several aspects of body metabolism. In the intestine, the activation of FXR induces the secretion of fibroblast growth factor 19 (FGF19) which has been shown to reduce both food intake and body weight gain and improve glucose tolerance in rats (Holt et al., 2003; Ryan et al., 2013). Specifically, in the

enteroendocrine L cells the activation of TGR5 induces glucagon-like peptide-1 (GLP-1) synthesis and secretion which stimulates insulin secretion, suppresses appetite, and slows down gastrointestinal transit (Katsuma et al., 2005; Shapiro et al., 2018).The loss of Fabp6 restrains bile acid reabsorption which increases the luminal bile acids concentrations (Praslickova et al., 2012). The possibility of stimulating FXR and TGR5 receptors by secondary bile acids produced *via* specific gut microbial classes which were enriched in intestinal Fabps mouse models is certainly interesting and warrants further investigation.

Polymorphisms in human *FABP2* gene, such as A54T variant, are relatively prevalent in certain populations and is associated with sex-specific obesity and insulin resistance (Pratley et al., 2000; Martinez-Lopez et al., 2007; Csep et al., 2007; Liu et al., 2019; Han and So, 2019). Interestingly, the T79M polymorphism in human *FABP6* is associated with improved glucose tolerance in obese population (Fisher et al., 2009). Due to the similarity in the phenotype associated with polymorphism and that of Fabp6-deficient mice, where Fabp6 is absent, T79M polymorphism might be mimicking Fabp6 deficiency. The elucidated impact of intestinal Fabps deficiency on the gut microbiota in presented in this thesis might be extended to human subjects with intestinal Fabps polymorphisms. However, since the results of this thesis were discovered using mouse species, there is a need to explore the same question in other species to evaluate if the effect is universal.

In addition, while the results of this thesis demonstrate an evident association between gut microbial composition and metabolic phenotypes, it is limited by a number of factors. First, due to the small number of mice and cages per treatment, there is a need to replicate these studies in future research using larger mouse numbers and considering individualized housing during the controlled feeding experiments. Moreover, developing germ-free models deficient in the intestinal Fabps of interest and carrying out fecal microbial transplantation is essential to confirm the relationship with the associated phenotypes. Likewise, conducting targeted transcriptome and metabolome profiling to the plasma of the intestinal Fabps deficient mice models would be helpful in finding new gut microbial clues to explain the increased vulnerability of these mice

models to adiposity. Finally, although the observed gut microbial and metabolic responses to intrinsic and extrinsic metabolites were only studied in the high dietary fat context, the long-term exposure to these factors in terms of low-fat diets should be considered in future research.

In conclusion, this is the first study that employed mouse models of genetically induced malfunction in intestinal Fabps to evaluate the ability of intrinsic and extrinsic factors in modifying the gut microbial composition and provided evidence on the ability of intrinsic and extrinsic factors to modify the gut microbiota and impact the metabolic and health status of the host. Future work could trace the capacity of the modified gut microbial composition to produce SCFAs and secondary bile acids and define their exact contribution inducing the observed phenotypes. Since gut microbial dysbiosis is correlated with several acquired metabolic disorders such as, obesity, diabetes, and cardiovascular diseases, an ability to alter the gut microbial composition by dietary interventions, through specific nutrient and non-nutrient components of the diet, may be crucial for managing metabolic disease risk. When applied to human conditions, the knowledge generated from this work emphasizes the need for sex-specific nutritional approaches and guidelines in promoting health.

References

Agellon, L.B., Drozdowski, L., Li, L.*, et al.* (2007). Loss of intestinal fatty acid binding protein increases the susceptibility of male mice to high fat diet-induced fatty liver. *Biochim Biophys Acta, 1771* (10), 1283-1288.

Agellon, L.B., Toth, M.J. and Thomson, A.B. (2002). Intracellular lipid binding proteins of the small intestine. *Mol Cell Biochem, 239* (1-2), 79-82.

Baars, A., Oosting, A., Lohuis, M.*, et al.* (2018). Sex differences in lipid metabolism are affected by presence of the gut microbiota. *Sci Rep, 8* (1), 13426-13426.

Chen, Y. and Agellon, L.B. (2019). Distinct alteration of gene expression programs in the small intestine of male and female mice in response to ablation of intestinal fabp genes. *Genes (Basel), 11* (8), 943.

Csep, K., Vitay, M., Dudutz, G.*, et al.* (2007). [correlation of FABP2-a54t polymorphism and the metabolic syndrome in maros county of romania]. *Orv Hetil, 148* (13), 597-602.

DeGruttola, A.K., Low, D., Mizoguchi, A.*, et al.* (2016). Current understanding of dysbiosis in disease in human and animal models. *J Inflamm Bowel Dis Disord, 22* (5), 1137-1150.

Dominianni, C., Sinha, R., Goedert, J.J.*, et al.* (2015). Sex, body mass index, and dietary fiber intake influence the human gut microbiome. *PLoS One, 10* (4), e0124599.

Duggavathi, R., Siddappa, D., Schuermann, Y.*, et al.* (2015). The fatty acid binding protein 6 gene (Fabp6) is expressed in murine granulosa cells and is involved in ovulatory response to superstimulation. *J Reprod Dev, 61* (3), 237-240.

Fisher, E., Grallert, H., Klapper, M.*, et al.* (2009). Evidence for the Thr79Met polymorphism of the ileal fatty acid binding protein (FABP6) to be associated with type 2 diabetes in obese individuals. *Mol Genet Metab, 98* (4), 400-405.

Gajda, A.M., Zhou, Y.X., Agellon, L.B.*, et al.* (2013). Direct comparison of mice null for liver or intestinal fatty acid-binding proteins reveals highly divergent phenotypic responses to high fat feeding. *J Biol Chem, 288* (42), 30330-30344.

Gerber, G.K. (2014). The dynamic microbiome. *FEBS Lett, 588* (22), 4131-4139.

Han, T.K. and So, W.Y. (2019). Effects of FABP2 Ala54Thr gene polymorphism on obesity and metabolic syndrome in middle-aged Korean women with abdominal obesity. *Cent Eur J Public Health, 27* (1), 37-43.

Hanhineva, K., Torronen, R., Bondia-Pons, I.*, et al.* (2010). Impact of dietary polyphenols on carbohydrate metabolism. *Int J Mol Sci, 11* (4), 1365-1402.

Haro, C., Rangel-Zuniga, O.A., Alcala-Diaz, J.F.*, et al.* (2016). Intestinal microbiota is influenced by gender and body mass index. *PLoS One, 11* (5), e0154090.

Heiman, M.L. and Greenway, F.L. (2016). A healthy gastrointestinal microbiome is dependent on dietary diversity. *Molecular Metabolism, 5* (5), 317-320.

Ho, N.T., Li, F., Lee-Sarwar, K.A.*, et al.* (2018). Meta-analysis of effects of exclusive breastfeeding on infant gut microbiota across populations. *Nature communications, 9* (1), 4169-4169.

Holmes, A.J., Chew, Y.V., Colakoglu, F.*, et al.* (2017). Diet-microbiome interactions in health are controlled by intestinal nitrogen source constraints. *Cell Metab, 25* (1), 140-151.

Holt, J.A., Luo, G., Billin, A.N.*, et al.* (2003). Definition of a novel growth factor-dependent signal cascade for the suppression of bile acid biosynthesis. *Genes Dev, 17* (13), 1581-1591.

Jamaluddine, Z. (2015). *Fatty acid binding protein 2 protects the small intestine from dietary saturated fatty acid-induced endoplasmic reticulum stress.* (Master of Science), McGill University, Montreal, Canada.

Katsuma, S., Hirasawa, A. and Tsujimoto, G. (2005). Bile acids promote glucagon-like peptide-1 secretion through TGR5 in a murine enteroendocrine cell line STC-1. *Biochem Biophys Res Commun, 329*, 386-390.

Kawamata, Y., Fujii, R., Hosoya, M.*, et al.* (2003). A G protein-coupled receptor responsive to bile acids. *J Biol Chem, 278* (11), 9435-9440.

Khurana, S., Yamada, M., Wess, J.*, et al.* (2005). Deoxycholyltaurine-induced vasodilation of rodent aorta is nitric oxide- and muscarinic M(3) receptor-dependent. *Eur J Pharmacol, 517* (1-2), 103-110.

Kim, E.-Y., Pai, T.-K. and Han, O. (2011). Effect of bioactive dietary polyphenols on zinc transport across the intestinal Caco-2 cell monolayers. *J Agric Food Chem, 59* (8), 3606-3612.

Kriss, M., Hazleton, K.Z., Nusbacher, N.M.*, et al.* (2018). Low diversity gut microbiota dysbiosis: Drivers, functional implications and recovery. *Curr Opin Microbiol, 44*, 34-40.

Larsen, O.F.A. and Claassen, E. (2018). The mechanistic link between health and gut microbiota diversity. *Sci Rep, 8* (1), 2183.

Laursen, M.F., Bahl, M.I., Michaelsen, K.F.*, et al.* (2017). First foods and gut microbes. *Front Microbiol, 8*, 356-356.

Levi, A.J., Gatmaitan, Z. and Arias, I.M. (1969). Two hepatic cytoplasmic protein fractions, Y and Z, and their possible role in the hepatic uptake of bilirubin, sulfobromophthalein, and other anions. *The Journal of clinical investigation, 48* (11), 2156-2167.

Liu, P.J., Liu, Y.P., Qin, H.K.*, et al.* (2019). Effects of polymorphism in FABP2 Ala54Thr on serum lipids and glycemic control in low glycemic index diets are associated with gender among Han Chinese with type 2 diabetes mellitus. *Diabetes Metab Syndr Obes, 12*, 413-421.

Lozupone, C.A., Stombaugh, J.I., Gordon, J.I.*, et al.* (2012). Diversity, stability and resilience of the human gut microbiota. *Nature, 489* (7415), 220-230.

Ma, Q., Kim, E.Y., Lindsay, E.A.*, et al.* (2011). Bioactive dietary polyphenols inhibit heme iron absorption in a dose-dependent manner in human intestinal Caco-2 cells. *J Food Sci, 76* (5), H143-150.

Makishima, M., Lu, T.T., Xie, W.*, et al.* (2002). Vitamin D receptor as an intestinal bile acid sensor. *Science, 296* (5571), 1313-1316.

Makishima, M., Okamoto, A.Y., Repa, J.J.*, et al.* (1999). Identification of a nuclear receptor for bile acids. *Science, 284* (5418), 1362-1365.

Markle, J.G.M., Frank, D.N., Mortin-Toth, S.*, et al.* (2013). Sex differences in the gut microbiome drive hormone-dependent regulation of autoimmunity. *Science, 339* (6123), 1084.

Martinez-Lopez, E., Ruiz-Madrigal, B., Hernandez-Canaveral, I.*, et al.* (2007). Association of the t54 allele of the FABP2 gene with cardiovascular risk factors in obese mexican subjects. *Diab Vasc Dis Res, 4* (3), 235-236.

Martinot, E., Baptissart, M., Vega, A.*, et al.* (2017). Bile acid homeostasis controls CAR signaling pathways in mouse testis through FXRalpha. *Sci Rep, 7*, 42182.

McIntosh, A.L., Atshaves, B.P., Landrock, D.*, et al.* (2013). Liver fatty acid binding protein gene-ablation exacerbates weight gain in high-fat fed female mice. *Lipids, 48* (5), 435-448.

Molodecky, N.A., Soon, I.S., Rabi, D.M.*, et al.* (2012). Increasing incidence and prevalence of the inflammatory bowel diseases with time, based on systematic review. *Gastroenterology, 142* (1), 46-54.e42.

Mueller, S., Saunier, K., Hanisch, C.*, et al.* (2006). Differences in fecal microbiota in different european study populations in relation to age, gender, and country: A cross-sectional study. *Appl Environ Microbiol, 72* (2), 1027-1033.

Mulligan, C.M. and Friedman, J.E. (2017). Maternal modifiers of the infant gut microbiota: Metabolic consequences. *J Endocrinol, 235* (1), R1-R12.

Nedungadi, T.P. and Clegg, D.J. (2009). Sexual dimorphism in body fat distribution and risk for cardiovascular diseases. *J Cardiovasc Transl Res, 2* (3), 321-327.

Ockner, R.K., Manning, J.A., Poppenhausen, R.B.*, et al.* (1972). A binding protein for fatty acids in cytosol of intestinal mucosa, liver, myocardium, and other tissues. *Science, 177* (4043), 56-58.

Praslickova, D., Torchia, E.C., Sugiyama, M.G.*, et al.* (2012). The ileal lipid binding protein is required for efficient absorption and transport of bile acids in the distal portion of the murine small intestine. *PLoS One, 7* (12), 1.

Pratley, R.E., Baier, L., Pan, D.A.*, et al.* (2000). Effects of an Ala54Thr polymorphism in the intestinal fatty acid-binding protein on responses to dietary fat in humans. *J Lipid Res, 41* (12), 2002-2008.

Ryan, K.K., Kohli, R., Gutierrez-Aguilar, R.*, et al.* (2013). Fibroblast growth factor-19 action in the brain reduces food intake and body weight and improves glucose tolerance in male rats. *Endocrinology, 154* (1), 9-15.

Saini, S.P., Sonoda, J., Xu, L.*, et al.* (2004). A novel constitutive androstane receptor-mediated and CYP3A-independent pathway of bile acid detoxification. *Mol Pharmacol, 65* (2), 292-300.

Shapiro, H., Kolodziejczyk, A.A., Halstuch, D.*, et al.* (2018). Bile acids in glucose metabolism in health and disease. *J Exp Med, 215* (2), 383–396.

Sheikh Abdul Kadir, S.H., Miragoli, M., Abu-Hayyeh, S.*, et al.* (2010). Bile acid-induced arrhythmia is mediated by muscarinic M2 receptors in neonatal rat cardiomyocytes. *PLoS One, 5* (3), e9689-e9689.

Song, C., Hiipakka, R.A. and Liao, S. (2000). Selective activation of liver X receptor alpha by 6alpha-hydroxy bile acids and analogs. *Steroids, 65* (8), 423-427.

Staudinger, J.L., Goodwin, B., Jones, S.A.*, et al.* (2001). The nuclear receptor PXR is a lithocholic acid sensor that protects against liver toxicity. *Proc Natl Acad Sci USA, 98* (6), 3369-3374.

Studer, E., Zhou, X., Zhao, R.*, et al.* (2012). Conjugated bile acids activate the sphingosine-1-phosphate receptor 2 in primary rodent hepatocytes. *Hepatology, 55* (1), 267-276.

Sugiyama, M.G. and Agellon, L.B. (2012). Sex differences in lipid metabolism and metabolic disease risk. *Biochem Cell Biol, 90* (2), 124-141.

Sugiyama, M.G., Hobson, L., Agellon, A.B.*, et al.* (2012). Visualization of sex-dimorphic changes in the intestinal transcriptome of fabp2 gene-ablated mice. *J Nutrigenet Nutrigenomics, 5* (1), 45-55.

Takagi, T., Naito, Y., Inoue, R.*, et al.* (2019). Differences in gut microbiota associated with age, sex, and stool consistency in healthy Japanese subjects. *J Gastroenterol, 54* (1), 53-63.

Vassileva, G., Huwyler, L., Poirier, K.*, et al.* (2000). The intestinal fatty acid binding protein is not essential for dietary fat absorption in mice. *FASEB J, 14* (13), 2040-2046.

Weger, B.D., Gobet, C., Yeung, J.*, et al.* (2019). The mouse microbiome is required for sex-specific diurnal rhythms of gene expression and metabolism. *Cell Metab, 29* (2), 362-382.e368.

Appendices

Appendix I. Bile malabsorption causes fat malabsorption

Note: the concepts presented in the following manuscript appeared previously in the thesis of BLZ, 2013, McGill University. SMH replicated all mice experiments, combined, and reanalyzed the data, conducted the tracer experiments and wrote the manuscript. LW provided training, facility, and reagents for the tracer experiments, LBA developed the overall study design, wrote, and edited the manuscript.

Sexually dimorphic response of mice to the Western-style diet caused by deficiency of fatty acid binding protein 6 (Fabp6)

Salam M. Habib[1], Brittnee L. Zwicker[1,2], Linda Wykes, Luis B. Agellon*

School of Human Nutrition, McGill University, Ste. Anne de Bellevue, QC, Canada

*Corresponding author at: McGill University School of Human Nutrition, 21111 Lakeshore Road, Ste. Anne de Bellevue, QC H9X 3V9 Canada
Email: luis.agellon@mcgill.ca (L.B. Agellon)

[1]Contributed equally to this work.
[2]Present address: McGill University Health Centre, Montreal, QC H4A 3J1 Canada

This manuscript was accepted for publication in Physiological Reports Journal on January 4th ,2021.

Abstract

Bile acids are natural detergents that aid in the absorption of dietary lipids. Fatty acid binding protein 6 (Fabp6) is a component of the bile acid recovery system that operates in the small intestine. The aim of this study was to determine if Fabp6 deficiency causes dietary fat malabsorption. Wild-type and Fabp6-deficient mice were fed a Western-style diet (WSD) or a reference low fat diet (LFD) for 10 weeks. The body weight gain, bile acid excretion, fat excretion, energy metabolism and major gut microbial phyla of the mice were assessed at the end of the controlled diet period. *Fabp6*$^{-/-}$ mice exhibited enhanced excretion of both bile acids and fat on the WSD but not on the LFD diet. Paradoxically, male *Fabp6*$^{-/-}$ mice, but not female *Fabp6*$^{-/-}$ mice, had greater adiposity despite increased fat excretion. Analysis of energy intake and of expenditure by indirect calorimetry revealed sex differences in physical activity level and respiratory quotient, but these did not account for the enhanced adiposity displayed by male *Fabp6*$^{-/-}$ mice. Analysis of stool DNA showed sex-specific changes in the abundance of major phyla of bacteria in response to Fabp6 deficiency and WSD feeding. The results obtained indicate that the malabsorption of bile acids that occurs in *Fabp6*$^{-/-}$ mice is associated with dietary fat malabsorption on the high fat diet but not on the low fat diet. The WSD induced a sexually dimorphic increase in adiposity displayed by *Fabp6*$^{-/-}$ mice and sexually distinct pattern of change in gut microbiota composition.

Keywords: bile acid malabsorption, fat malabsorption, fatty acid binding protein, gut microbiota, obesity, sexual dimorphism.

1. Introduction

Bile acids are important in facilitating the digestion and absorption of dietary lipids and lipid-soluble molecules (Agellon, 2008). Bile acids are produced in the liver from cholesterol and released into the lumen of the small intestine upon meal ingestion. Gut bacteria are capable of metabolizing bile acids, transforming them into metabolites known as secondary and tertiary bile acids. The majority of bile acids are reabsorbed by the ileum, returned to the liver via the portal vein, and then stored in the gallbladder or resecreted into the small intestine as needed (Agellon, 2008). Bile acids that are not recovered by the ileum are passed to the large intestine and eventually excreted.

In ileal enterocytes, the mechanism for the recovery of bile acids consists of three main components: the apical sodium-dependent bile acid transporter (Asbt; murine gene symbol Slc10a2), the heteromeric basolateral efflux transporter organic solute transporter (comprised of Ostα and Ostβ; murine gene symbols Slc51a and Slc51b, respectively), and the intracellular bile acid binding protein Fabp6 (Fabp6, also known as ileal lipid binding protein; murine gene symbol Fabp6) (Zwicker and Agellon, 2013). In mice, gene variations that cause loss-of-function of any of these components result in bile acid malabsorption (BAM) (Oelkers et al., 1997; Dawson et al., 2003; Rao et al., 2008; Ballatori et al., 2008; Praslickova et al., 2012).

In humans, mutations in the SLC10A2 gene cause primary BAM (Oelkers et al., 1997). BAM can be also result from ileal resection, or secondary to digestive tract disorders such as irritable bowel syndrome, pancreatic insufficiency and celiac disease (Watson et al., 2015). In general, BAM is characterized by excessive amounts of bile acids passed into the colon, where it causes enhanced electrolyte and water excretion and chronic steatorrhea. Fat malabsorption was not previously observed in mice lacking Asbt (Dawson et al., 2003), however this may be due to efficient intestinal fat absorption in this species. In the present study, we evaluated the relationship between bile acid malabsorption and fat excretion in the context of dietary fat content in mice with and without Fapb6.

2. Materials and methods

Mice and diets

C57BL/6J mice (Jackson Laboratory, Bar Harbor, Maine, USA) were crossed with *Fabp6*$^{-/-}$ mice (Praslickova et al., 2012) to produce an F1 generation of heterozygotes which were then inbred to yield *Fabp6*$^{+/+}$ and *Fabp6*$^{-/-}$ mice that were used in this study. Genotypes were confirmed by PCR using the primers described in Appendix II (Table II-5). The age of mice used in the study ranged from 12 to 28 weeks. Mice were housed (n ≤ 5 mice per cage) in a climate-controlled facility with a 12-h light/dark photoperiod. Mice were maintained on the Teklad 2020X diet (Teklad-Envigo, Lachine, QC), which was used as the reference low fat diet (LFD). Age matched, *Fabp6*$^{+/+}$ and *Fabp6*$^{-/-}$ sibling mice (n = 8-12 per group; males and females in separate groups) were placed on the Western-style diet (D12079B, Research Diets, New Brunswick, NJ) for 10 weeks. For the LFD, the percentage of protein mass, total carbohydrate mass and fat mass were 19.1 %, 62 % (47 % available carbohydrates + 15 % fiber) and 6.5 %, respectively. For the WSD, the percentage of protein mass, total carbohydrate mass and fat mass were 19.8 %, 55 % (50 % available carbohydrates + 5 % fiber), and 21 %, respectively. Mice had free access to food and water. At the end of controlled diet period, mice were fasted for 16 h prior to euthanasia by isoflurane/CO_2 inhalation. Blood was collected by cardiac puncture into EDTA-containing tubes and plasma was separated by centrifugation then stored at -70 °C along with the tissues and gallbladder bile collected at necropsy. The use of animals in this study was approved by the animal care committee at McGill University in accordance with the Canadian Council of Animal Care guidelines.

Biochemical Assays

Total triacylglycerols and total cholesterol concentrations in the plasma were measured using commercial diagnostic assay kits (Wako Chemicals USA, VA). Plasma lipid profile was determined by size exclusion chromatography using a Superose 6 column (GE Healthcare Life Sciences) attached to a Beckman System Gold HPLC system. For measurement of bile acid and fat excretion rates, mice were placed in

individual cages and stools were collected daily then dried in a fume hood. Stools were pulverized into a fine powder in a Mini-Beadbeater apparatus (BioSpec Products, Bartlesville, OK) using 2.3 mm stainless steel ball bearings as the grinding medium. Total bile acids were extracted from known mass of powdered stool samples using 50 % *t*-butanol (Van der Meer et al., 1985); and then quantitated using a commercial colorimetric enzymatic assay kit (Diazyme Bile Acids, Diazyme, CA). Bile acids in gallbladder bile were identified and quantitated by HPLC as described previously (Torchia et al., 2001). Total lipids were extracted from a known mass of liver and powdered stool samples using previously described methods (Folch et al., 1957; Kraus et al., 2015).

Tracer experiments

In the first experiment, male and female mice (n=3) of both genotypes, wild-type and *Fabp6*$^{-/-}$, were orally gavaged with olive oil containing 0.05g/ml of [1-^{13}C]palmitic acid (Sigma Chemical Co., St. Louis, MO) at 6 mL/kg body weight, housed individually with free access to LFD and water. Stools were collected after 24 h and then stored at -20 °C until analysis. In the second experiment, WSD with [U-^{13}C]palmitic acid (CCLM409, Cambridge Isotope Laboratories, Tewksbury, MA) (10 µmol/g diet) and was fed over 3 days to individually housed wild-type and *Fabp6*$^{-/-}$ mice (n=3) of both sexes. Stools were collected every 24 h and stored at -20 °C until analysis. Pentadecanoic acid (1 µmol) was added to each stool sample and fat was extracted as described above. Extracted fat was derivatized with pentafluorobenzyl bromide and N,N-diisopropylethylamine overnight at 4 °C. The derivatized fatty acids were extracted and reconstituted in hexane before gas chromatography mass spectrometry analysis (Agilent 5975C, Palo Alto, CA) using methane negative chemical ionization and select-ion monitoring at m/z 256.4, m/z 257.4 and m/z 241.4 for the first experiment, and m/z 256.4, m/z 271.4 and m/z 241.4 for the second experiment.

Indirect Calorimetry

Physical activity, energy expenditure, respiratory quotient and food intake were measured using the Oxylet Metabolic Monitoring System (Panlab-Harvard Apparatus,

Barcelona, Spain). At the start of Week 9 of the controlled diet period, mice from each group were transferred to individual Physiocage apparatus for monitoring over three days, then returned to group housing after measurements. The total number of beam breaks in all axes (x, y and z dimensions) represented the total physical activity. For both the energy expenditure and respiratory quotient, the areas under the curves were used to calculate statistics. The fat intake was estimated from food intake based on the fat content of each diet. Data was analyzed using GraphPad Prism version 8.21 (GraphPad Software Inc., CA, USA).

Analysis of Stool DNA

DNA was extracted from powdered stool samples following a previously published method Tsai and Olson (1992). DNA concentration was determined fluorometrically using the DNA Qubit assay (Invitrogen, CA). The number of total bacteria and bacteria belonging to Bacteroidetes, Firmicutes and Proteobacteria phyla were estimated by quantitative PCR (Guo et al., 2008; Yang et al., 2015). The data are presented as relative bacterial load which is the ratio between each phylum and the total copy number (Navidshad et al., 2012). The murine single copy *Mos* gene (Gene ID: 17451) was used to measure the amount of murine DNA in the stool samples. In general, the extent of murine genomic DNA contamination in the stool samples was approximately 30 pg/µg of total stool DNA and was accounted for in the calculation of the gut microbial composition. The sequences of the primers used for this study are described in Appendix II (Table II-5).

Statistics

Statistical analyses were performed using GraphPad Prism version 8.21 (GraphPad Software Inc., CA, USA). Parametric and non-parametric tests were applied where appropriate. Data presented as mean ± SEM and means were compared using a two-tailed unpaired Student's t-test unless indicated otherwise. Differences were considered significant when $p<0.05$.

3. Results

3.1 Fat malabsorption is associated with bile malabsorption

We previously showed that *Fabp6*$^{-/-}$ mice exhibit BAM on a diet with low fat content (Praslickova et al., 2012). To determine whether BAM causes fat malabsorption under high dietary fat diet intake, we fed wild-type and *Fabp6*$^{-/-}$ mice the WSD for 10 weeks. Both male and female *Fabp6*$^{-/-}$ mice showed increased rate of bile acid excretion compared to wild-type mice on both the LFD (Fig. I-1A) and the WSD (Fig. I-1C). Concurrently, both male and female *Fabp6*$^{-/-}$ mice showed higher total fat excretion rate compared to their wild-type counterparts on the WSD (Fig. I-1D), but not on the LFD (Fig. I-1B). On both diets, fat intakes of male and female wild-type and *Fabp6*$^{-/-}$ mice were comparable (Fig. I-S1A and I-S1B). We also compared the total amount of fat excreted in stool and the total amount of dietary fat ingested. On the LFD, the total fat mass excreted, expressed as a percentage of total fat mass ingested, by both male and female *Fabp6*$^{-/-}$ mice was similar to that of wild-type mice (Fig. I-S1C). In contrast, on the WSD, it was higher for both male and female *Fabp6*$^{-/-}$ mice compared to that of their wild-type counterparts (4- and 2-fold higher, respectively) (Fig. I-S1D).

To confirm the correlation between bile acid malabsorption and fat malabsorption in *Fabp6*$^{-/-}$ mice we measured the amount of [1-^{13}C]palmitic acid excreted in stool during the 24 h following the delivery of the label by oral gavage, however no change in excretion of the label by both male and female *Fabp6*$^{-/-}$ mice compared to wild-type mice was observed (Fig. I-S2A). Since differences in fat excretion between both mice genotypes were evident on WSD, we fed mice WSD mixed with [U-^{13}C]palmitic acid and measured the excretion of this label in stool over three days. Male *Fabp6*$^{-/-}$ mice excreted more label in the stool compared to male wild-type mice ($P < 0.05$) (Fig. I-S2B, left) however no difference was observed between female *Fabp6*$^{-/-}$ and female wild-type mice ($P = 0.06$) (Fig. I-S2B, right). Over time, the amount of excreted label in the stool of male and female *Fabp6*$^{-/-}$ mice increased whereas it decreased in both male and female wild-type mice (Fig. I-S2C). Based on these results, we concluded that the loss of Fabp6, which causes bile acid malabsorption (Praslickova et al., 2012) in both male and female mice, was associated with fat malabsorption when mice were fed a diet with a high dietary fat content.

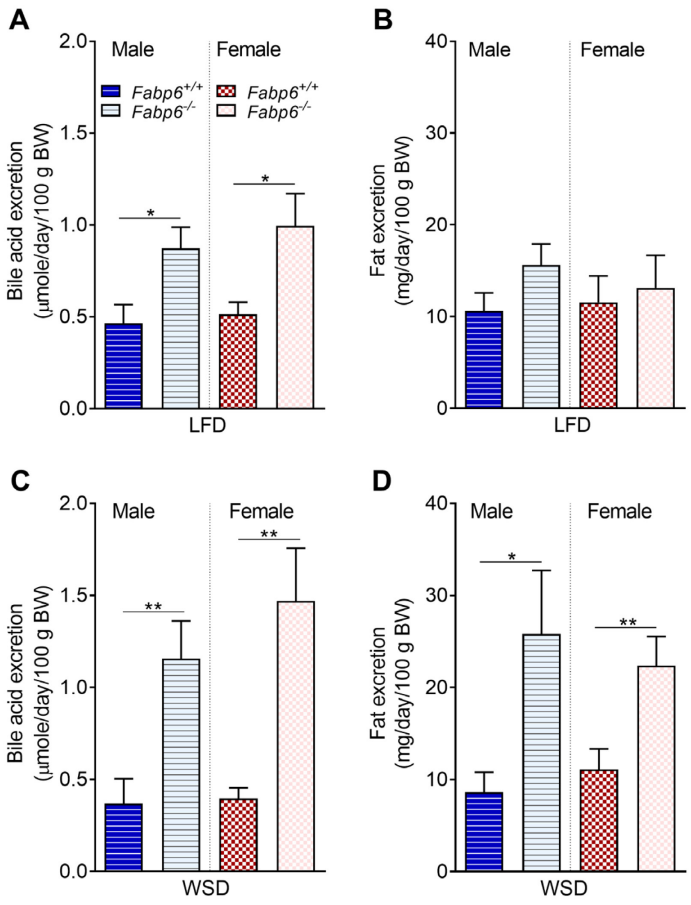

Figure 0-1. Fat malabsorption is associated with bile acid malabsorption. (A and C) Stool bile acid excretion (A and C), stool fat excretion (B and D) on the low fat diet (LFD) and Western-style diet (WSD), respectively. The plot shows the combined data of two independent experiments. Dark and light bars indicate *Fabp6*$^{+/+}$ and *Fabp6*$^{-/-}$ mice, respectively. Mean ± SEM (n=8-12 mice per group). Means were compared using Student's t-test. *P<0.05 and **P<0.01.

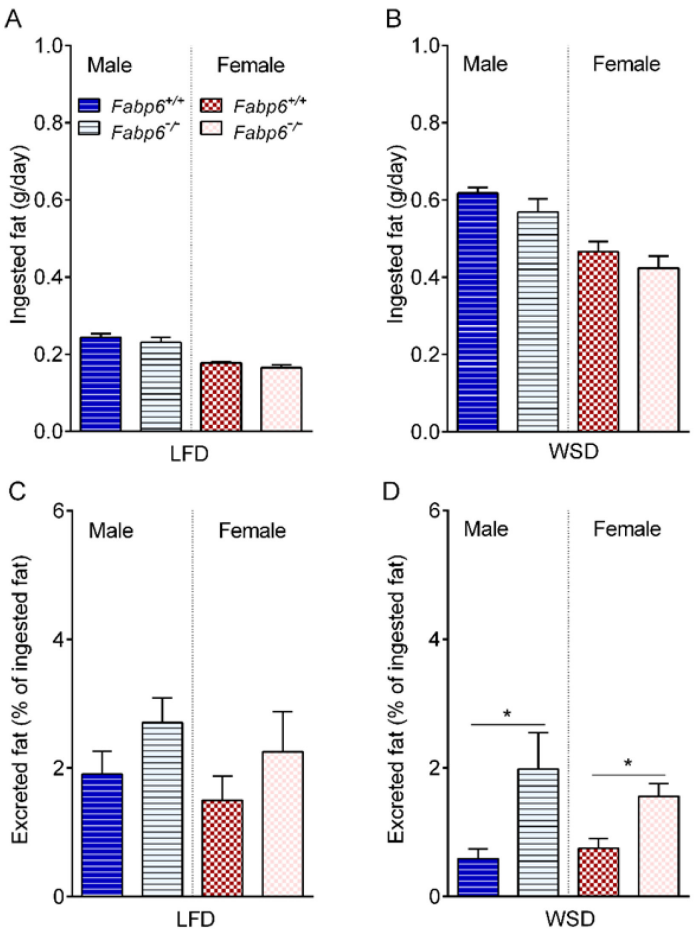

Figure I-S1. Ingested fat and excreted fat. (A) and (B), mass of fat ingested per day (24 h) (C) and (D), mass of fat excreted into stool expressed as a percentage of mass of fat ingested. The mass of ingested fat (mean± SEM) was based on the mass of ingested food measured using the Oxylet Metabolic Monitoring System. Blue and red bars depict male and female mice, respectively. Dark and light bars indicate *Fabp6*$^{+/+}$ and *Fabp6*$^{-/-}$ mice (n=3 mice per group), respectively. Means were compared using Student's t-test and differences were considered statistically significant when *P<0.05. LFD, reference low fat diet. WSD, Western-style diet.

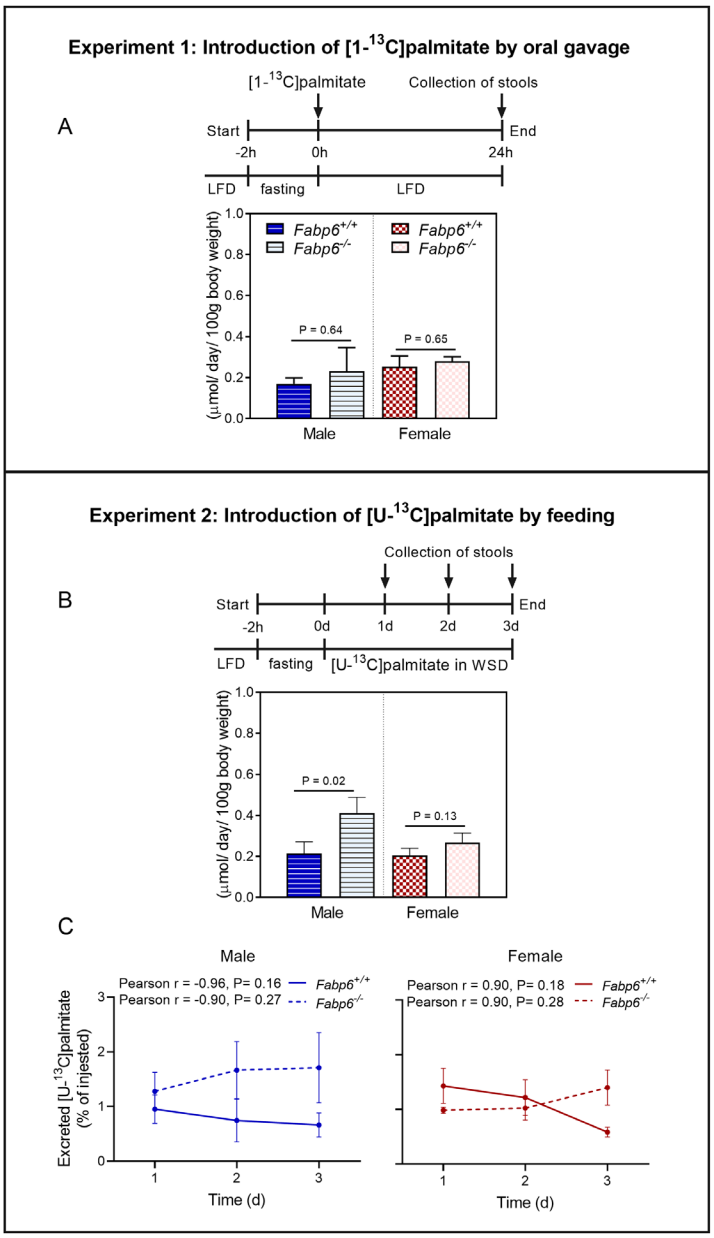

Figure I-S2. Fate of orally administered palmitic acid. The experimental design and amount of (A) [1-^{13}C]palmitate and (B) [U-^{13}C]palmitate excreted into stool expressed as micromole per day per 100 g body weight (mean ±SEM, n=3 mice per group). Blue and red bars depict male and female mice, respectively. Dark and light bars indicate *Fabp6*$^{+/+}$ and *Fabp6*$^{-/-}$ mice, respectively. (C) Mass of [U-^{13}C]palmitate excreted in stool over 3 days expressed as a percentage of mass of [U-^{13}C]palmitate ingested (mean ± SEM, n=3 mice per group). *Fabp6*$^{+/+}$ mice are represented by the solid lines, and *Fabp6*$^{-/-}$ mice are represented by broken lines. Blue and red lines depict male and female mice, respectively LFD, reference low fat diet. WSD, Western-style diet.

3.2 The WSD induces greater adiposity in male Fabp6$^{-/-}$ mice

Interestingly, at necropsy we noticed a higher degree of fat deposition in the viscera of male *Fabp6*$^{-/-}$ mice on the WSD compared to male wild-type mice on the same diet while female *Fabp6*$^{-/-}$ mice did not show an obvious difference in the degree of fat deposition in the viscera compared to the female wild-type mice. Comparison of gonadal fat pads revealed that male *Fabp6*$^{-/-}$ mice had greater increment in fat mass than female *Fabp6*$^{-/-}$ mice in response to the WSD (Fig. I-2D, right), a pattern that mirrored the increment in their body weights (Fig. I-2C, right). There was no difference between male and female wild-type mice body weight or gonadal fat mass increments (Fig. I-2A and I-2B, right). Thus, while male and female wild-type mice had similar weight gain to their wild-type counterparts in response to WSD, the deficiency of Fabp6 caused greater adiposity in male mice than in female mice.

Since both male and female *Fabp6*$^{-/-}$ mice on WSD exhibited increased rate of fat excretion compared to wild-type mice, it seemed paradoxical that male *Fabp6*$^{-/-}$ mice gained more body weight and had greater adiposity than female *Fabp6*$^{-/-}$ mice. To gain insight into the metabolic response of male and female *Fabp6*$^{-/-}$ mice to the WSD, we first examined the plasma lipid concentrations of the mice. Total plasma cholesterol was higher in all mice on WSD compared to mice on the LFD (Table I-1). Lipoprotein profile analysis showed higher low density lipoprotein cholesterol content in the plasma of male *Fabp6*$^{-/-}$ mice on WSD as compared to their female counterparts (Fig. I-S3A and I-S3B, top). Male wild-type and *Fabp6*$^{-/-}$ mice, but not female wild-type and *Fabp6*$^{-/-}$ mice, showed higher total plasma triacylglycerol concentrations on the WSD compared to the LFD (Table I-1). Male *Fabp6*$^{-/-}$ mice had higher very low density lipoprotein triacylglycerol on the WSD compared to the female mice (Fig. I-S3A and I-S3B, bottom).

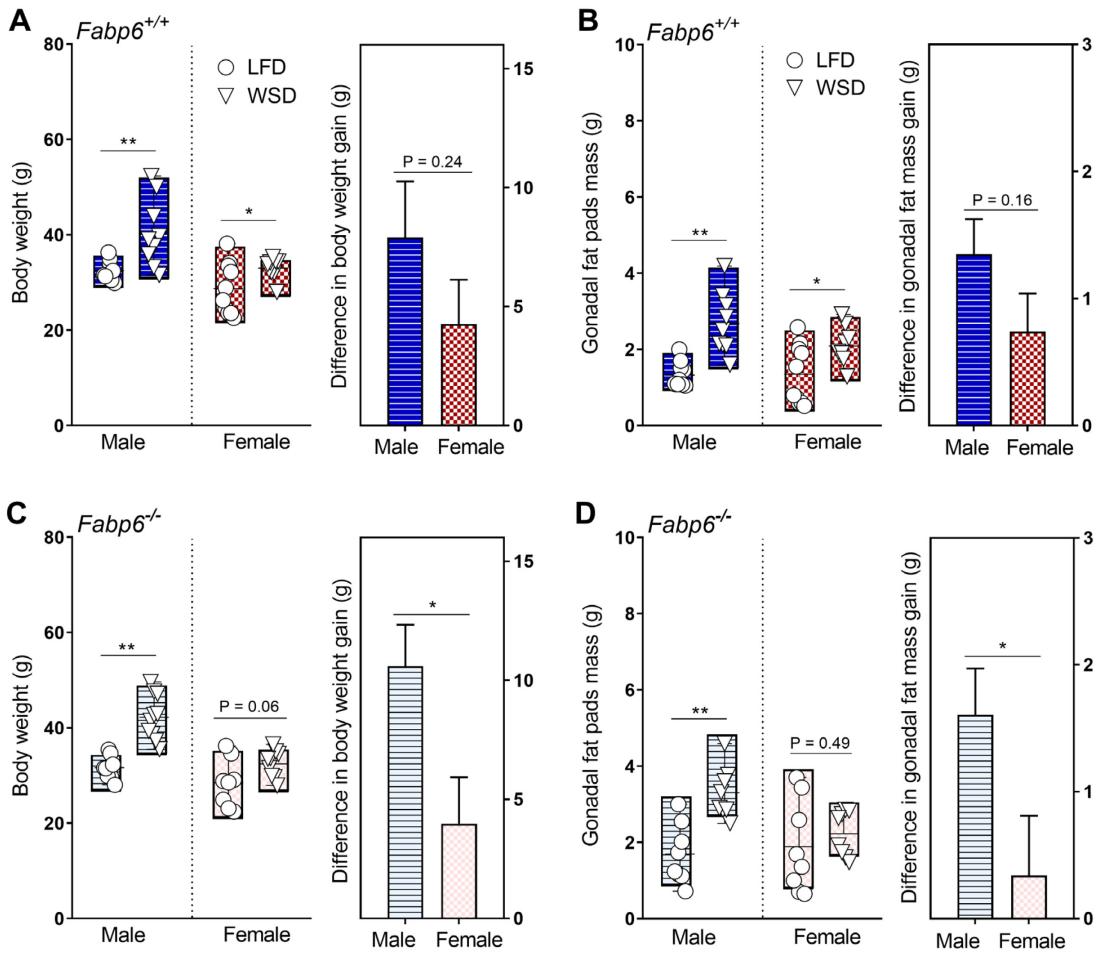

Figure 0-2. Greater adiposity in male *Fabp6*$^{-/-}$ mice on WSD. (A and C) Left, body weight; Right, the difference in body weight gain of *Fabp6*$^{+/+}$ and *Fabp6*$^{-/-}$ mice on the low fat diet (LFD) and Western-style diet (WSD), respectively. (B and D) Left, gonadal fat pads mass; Right, the difference in gonadal fat mass gain of *Fabp6*$^{+/+}$ and *Fabp6*$^{-/-}$ mice on LFD and WSD, respectively. The plot shows the combined data of two independent experiments. Dark and light bars indicate *Fabp6*$^{+/+}$ and *Fabp6*$^{-/-}$ mice, respectively. Mean ± SEM (n=8-12 mice per group). Means were compared using Student's t-test. *P<0.05, **P<0.01.

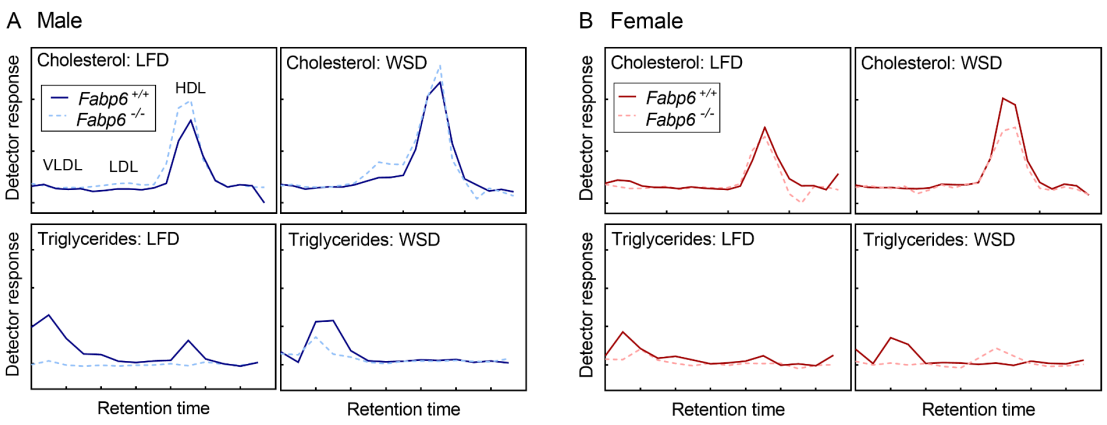

Figure 0-S3. Lipid profiles of plasma from (A) male and (B) female mice, respectively. The top and bottom panels depict cholesterol and triacylglycerol profiles, respectively. Samples from *Fabp6*$^{+/+}$ and *Fabp6*$^{-/-}$ mice are represented by solid and broken lines, respectively. LFD: low fat diet. WSD: Western-style diet.

Table I-1. Total cholesterol and triacylglycerol in plasma and liver.

	Male				Female			
	Fabp6$^{+/+}$		*Fabp6*$^{-/-}$		*Fabp6*$^{+/+}$		*Fabp6*$^{-/-}$	
	LFD	WSD	LFD	WSD	LFD	WSD	LFD	WSD
Plasma								
Total cholesterol (mmol/L)	1.95 ± 0.07	3.80 ± 0.27*	2.04 ± 0.12	3.69 ± 0.32*	2.09 ± 0.09	2.97 ± 0.16*	1.74 ± 0.14	2.77 ± 0.33*
Total triacylglycerol (mmol/L)	2.02 ± 0.04	3.22 ± 0.22*	1.87 ± 0.13	2.75 ± 0.14*	1.89 ± 0.14	2.19 ± 0.13	1.82 ± 0.10	2.12 ± 0.10
Liver								
Total cholesterol (mmol/L)	1.40 ± 0.04	1.64 ± 0.05*	1.39 ± 0.06	1.86 ± 0.13*	1.82 ± 0.07	2.11 ± 0.05*	2.15 ± 0.05	2.33 ± 0.04*
Total triacylglycerol (mmol/L)	4.73 ± 0.44	19.76 ± 5.1*	4.59 ± 0.24	23.23 ± 2.3*	5.55 ± 0.48	17.85 ± 2.9*	4.90 ± 0.67	15.57 ± 1.4*

Data presented as mean ± SEM (n=4-8). Comparison between diets by unpaired Student's t-test, *P<0.05.

Next, we measured total triacylglycerols and cholesterol concentrations in the liver. The WSD increased total liver cholesterol and triacylglycerols concentrations of male mice regardless of genotype (Table I-1). Female wild-type mice, but not female *Fabp6*$^{-/-}$ mice, had increased total liver cholesterol and triacylglycerols concentrations on the WSD (Table I-1). Thus, the plasma and liver lipid profiles showed a sexually dimorphic response where male *Fabp6*$^{-/-}$ mice, but not female *Fabp6*$^{-/-}$ mice, showed elevations in plasma and liver cholesterol and triacylglycerols concentrations on the WSD. Taken together, the data demonstrated that the greater sensitivity of male *Fabp6*$^{-/-}$ mice to the WSD was associated with increased body weight gain and enhanced adiposity.

3.3 Male Fabp6$^{-/-}$ *mice are physically and metabolically active on WSD*

To determine if the enhanced adiposity of male *Fabp6*$^{-/-}$ mice induced by the WSD was associated with altered metabolic rate, we measured the rate of physical activity and energy expenditure by indirect calorimetry. On the LFD, wild-type mice displayed increased activity level during the dark phase compared to the light phase as expected (Fig. I-3A). On the WSD, male wild-type mice showed a 60 % reduction of activity level in the dark phase compared to wild-type mice on the LFD (Fig. I-3A and I-3B). In contrast, the physical activity level of male *Fabp6*$^{-/-}$ mice on the WSD was unchanged and remained comparable to that of wild-type mice on the LFD (Fig. I-3A and I-3B). Female wild-type mice had similar levels of physical activity on both diets during the light and dark phases. In contrast, female *Fabp6*$^{-/-}$ mice had lower activity level in the dark phase on the WSD compared to mice on the LFD (Fig. I-3A and I-3B). Thus, the loss of Fabp6 in mice also caused a sexually dimorphic effect on physical activity level, as male *Fabp6*$^{-/-}$ mice, but not female *Fabp6*$^{-/-}$ mice, remained physically active in response to the WSD.

Energy expenditure (EE) is a function of both physical activity and metabolic rate (Weir, 1949). Wild-type mice had lower EE (40 % lower in males; 20 % lower in females) on the WSD compared to mice on the LFD regardless of sex in the dark phase (Fig. I-3C and I-3D). Loss of Fabp6 also caused a reduction of EE on the LFD (Fig. I-3C). On WSD, male *Fabp6*$^{-/-}$ had lower EE (15 %) compared to their wild-type

counterparts, while female *Fabp6*$^{-/-}$ mice had higher EE (15 %) in the dark phase compared to their wild-type counterparts (Fig. I-3D). This reduction of EE in male *Fabp6*$^{-/-}$ mice on WSD was not comparable to that of male wild-type mice on WSD and did not account for the enhanced adiposity displayed by the male *Fabp6*$^{-/-}$ mice.

Respiratory quotient (RQ) reflects the fuel substrate used for energy (Dewar and Newton, 1948). As expected, the RQ value for wild-type mice consuming the WSD was lower than that for mice on the LFD (Fig. I-3E and I-3F) regardless of sex. Interestingly, the RQ value for male *Fabp6*$^{-/-}$ mice on the WSD in the dark phase was greater than that observed for their wild-type counterparts (Fig. I-3F). Female *Fabp6*$^{-/-}$ mice had a lower RQ value in the dark phase than female wild-type mice on both diets (Fig. I-3E and I-3F). Thus, the sex of *Fabp6*$^{-/-}$ mice modified the change in RQ values induced by the WSD, indicating that loss of Fabp6 affects substrate utilization in both male and female mice. Together, these results demonstrate that the metabolic response of *Fabp6*$^{-/-}$ mice to the WSD was highly influenced by sex but the observed changes in physical activity and energy expenditure do not account for the enhanced adiposity in response to WSD feeding of male *Fabp6*$^{-/-}$ mice.

3.4 Alteration of gut microbiota in Fabp6$^{-/-}$ *mice on WSD*

Modulation of gut microbiota has been associated with changes in energy extraction efficiency from diet and consequently affect adiposity (Turnbaugh et al., 2006). Bile acids have bacteriostatic and bactericidal activity (Stacey and Webb, 1947; Watanabe et al., 2017) and thus have the potential to remodel gut microbiota. Since malabsorption of bile acids in the small intestine exposes the colonic bacteria to high concentrations of bile acids, we assayed for changes in the gut microbial community which is composed of the three main phyla, namely Bacteroidetes, Firmicutes, and Proteobacteria (Kostic et al., 2013).

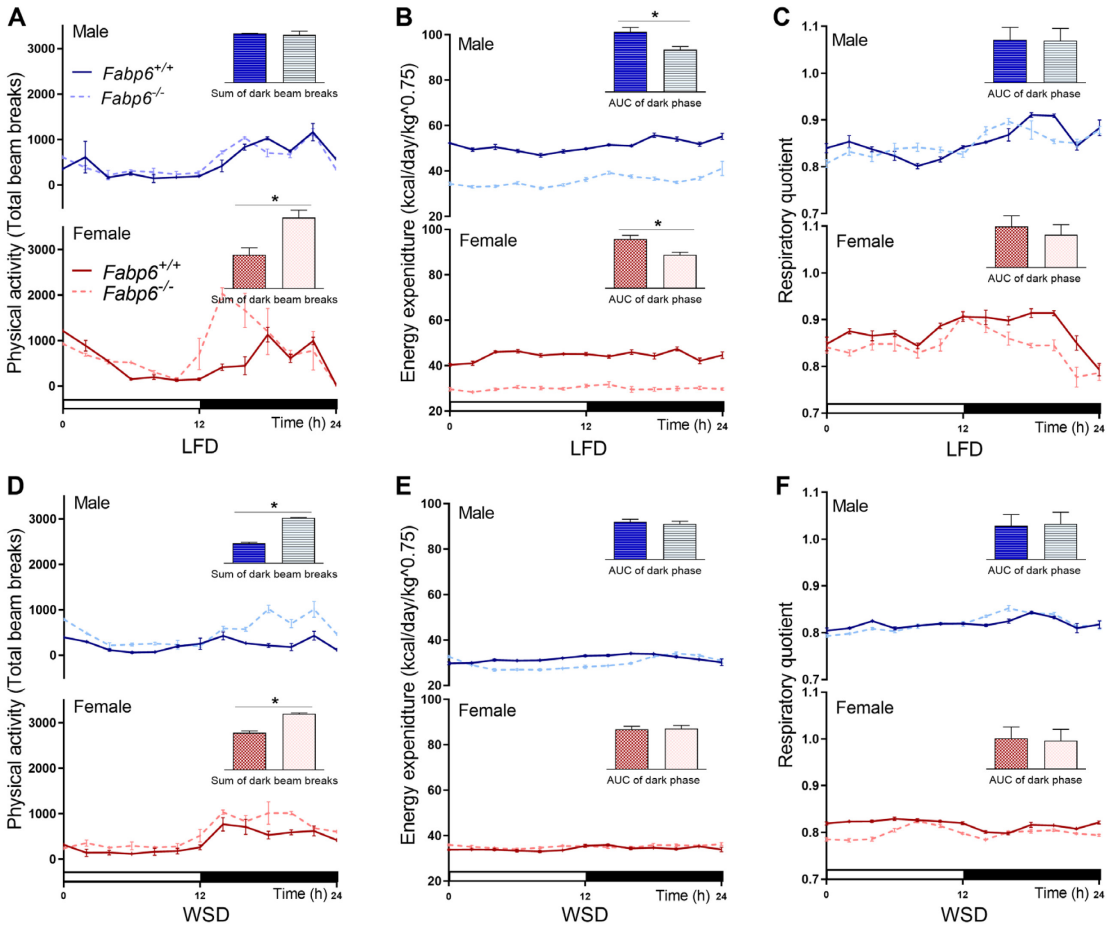

Figure I-3. Enhanced physical activity and metabolic rate of male *Fabp6*$^{-/-}$ mice on WSD. (A and B) Rate of physical activity, (C and D) energy expenditure, (E and F) respiratory quotient on the reference low fat diet (LFD) and Western-style diet (WSD), respectively. Data shown are representative of at least two independent experiments. The white bar represents the light period (12 h) and the black bar represents the dark period (12 h). *Fabp6*$^{+/+}$ mice are represented by the solid lines and dark bars, and *Fabp6*$^{-/-}$ mice are represented by broken lines and light bars. For each panel, top and bottom sections depict data from male and female mice, respectively. Insets represent the sum of beam breaks (x, y, z axes) or area under the curve (AUC) during the dark phases as mean ± SEM (n=6 mice per group) of three dark phases. Means were compared using Student's t-test, *p<0.05.

Fabp6$^{-/-}$ mice on the LFD showed similar total numbers of bacteria and phylum composition compared to wild-type mice on the same diet (Males: Fig. I-4A and I-4C; Females: Fig. I-4B and I-4D). The feeding of the WSD diet decreased the total numbers of gut bacteria in both wild-type male and female mice (by 27 % and 12 %, respectively) (Fig. I-4A, top and I-4B, top), but expanded the Firmicutes and Bacteroidetes phyla at the expense of Proteobacteria phylum in male mice (Fig. I-4A and I-4B) and reduced Bacteroidetes phylum in female mice (Fig. I-4B). In contrast to wild-type mice, only male *Fabp6*$^{-/-}$ mice exhibited a decrease in the total number of gut bacteria in response to WSD, and this change was characterized by the expansion of the Bacteroidetes phylum at the expense of Proteobacteria phylum (Fig. I-4C, bottom).

We also evaluated the speciation of bile acids in the enterohepatic circulation by analyzing the composition of gallbladder bile. On the LFD, the loss of Fabp6 increased the concentration of secondary bile acids taurodeoxycholic acid (TDCA) in males (Fig. I-S4A) and tauroursodeoxycholic (TUDCA) in females (Fig. I-S4C), however the ratio of taurocholic acid (TCA) to tauromuricholic acid (TMCA) was not affected in both sexes (Males: Fig. I-S4A, right; females: I-S4C, right). This indicated that the speciation of bile acids in the enterohepatic circulation was altered by the loss of Fabp6. On the WSD, TDCA was higher in male *Fabp6*$^{-/-}$ mice (Fig. I-S4B) whereas TCDCA, a primary bile acid, was higher in female *Fabp6*$^{-/-}$ mice (Fig. I-S4D). The TCA:TMCA ratio was higher in the bile of male *Fabp6*$^{-/-}$ mice (Fig. I-S4B, right) but not in female *Fabp6*$^{-/-}$ mice (Fig. I-S4D, right). The observed change in bile acid speciation was in support of the observed modification of gut microbial composition. Moreover, the loss of Fabp6 in male mice, but not in female mice, resulted in the remodeling of the gut microbial community in response to the WSD to a pattern that is associated with enhanced adiposity.

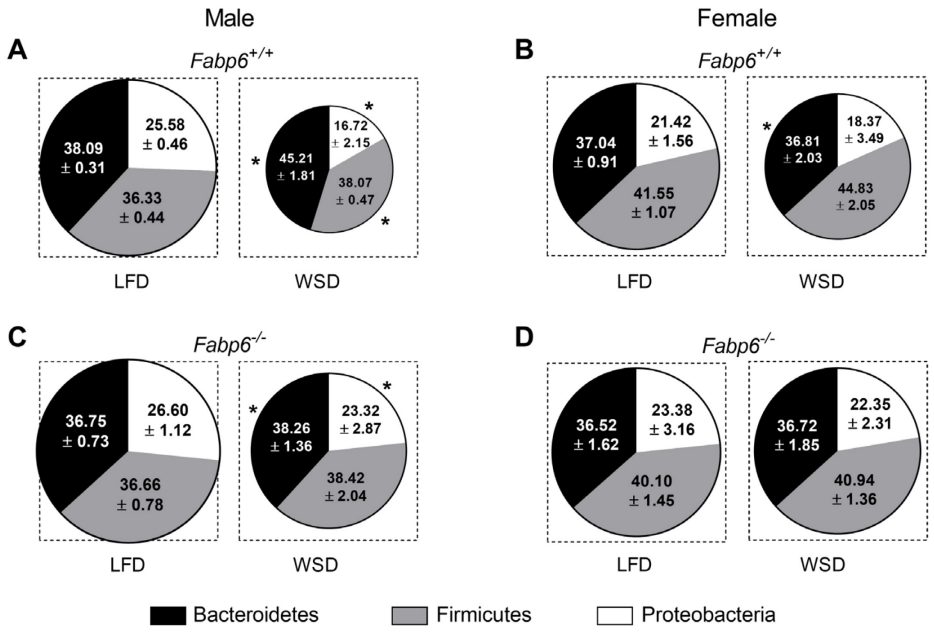

Figure 0-4. Remodeling of gut microbial composition. Gut microbial composition of male (A) and female (B) *Fabp6*$^{+/+}$ and *Fabp6*$^{-/-}$ mice (top and bottom, respectively). The area of the circles represents the percentage of total bacteria normalized to the total number of bacteria determined for male *Fabp6*$^{+/+}$ mice, which was set to 100 %. Data reported are representative of two independent experiments. Data represent the ratio between each phylum and the total copy number as mean ± SEM (n=3-5). The dimensions of the boxes superimposed on the circles are equivalent. Bacteroidetes phylum shown in black, Firmicutes phylum in grey, and Proteobacteria phylum in white. The means of each phylum in the Western-style diet (WSD) diet groups were compared to the corresponding phylum in the low fat diet (LFD) groups using Student's t-test. *P<0.05.

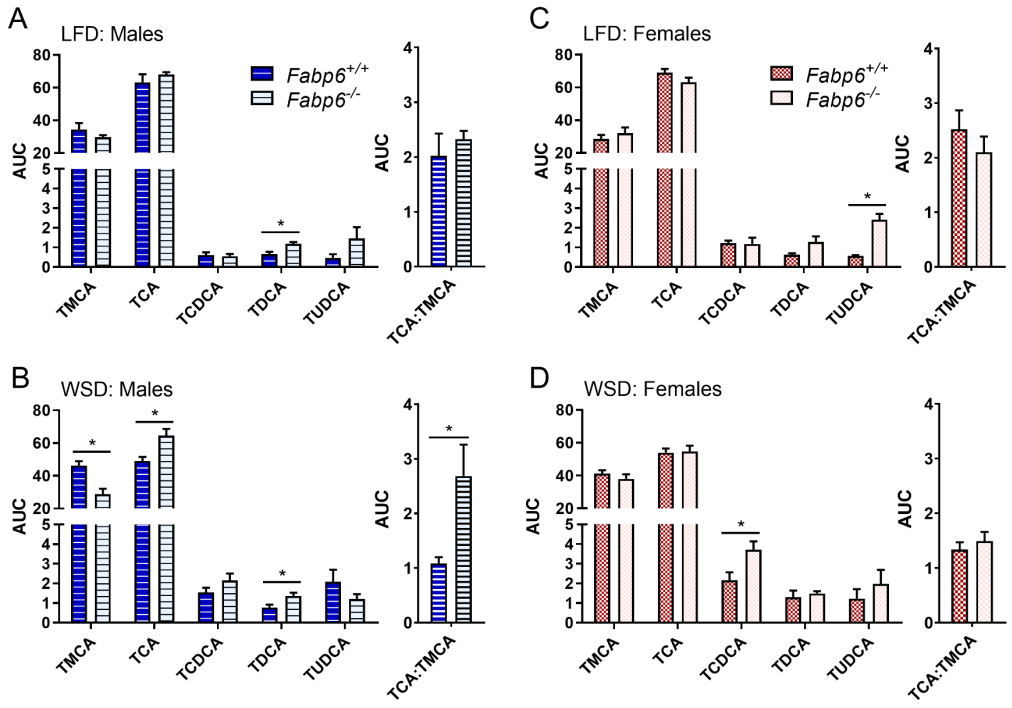

Figure 0-S4. Bile acid profiles of gallbladder bile from male (blue bars) and female (red bars) mice fed the low fat diet (LFD), (A and C), respectively, and the Western-style diet (WSD), (B) and (D), respectively. Mean ± SEM (n=5-6 mice per group). Means were compared using Student's t-test and differences were considered statistically significant when *p<0.05. Dark bars, *Fabp6*$^{+/+}$ mice. Light bars, *Fabp6*$^{-/-}$ mice.

4. Discussion

Bile acids are essential for the digestion and absorption of dietary lipids (Ishibashi et al., 1996; Zwicker and Agellon, 2013). In humans, a mutation in the SLC10A2 gene that encodes defective ASBT causes primary bile acid malabsorption and chronic steatorrhea (Heubi et al., 1982; Oelkers et al., 1997). Mice deficient in Asbt also show BAM, but unlike humans, fat malabsorption was not associated with BAM in this model (Dawson et al., 2003). The dissimilarity in phenotype could be attributable to differences in metabolism of bile acid between humans and mice (Agellon, 2008), or related to other factors that influence the overall efficiency of dietary fat absorption in these two species. We previously showed that deletion of the *Fabp6* gene in mice causes bile acid malabsorption (Praslickova et al., 2012). In the present study, we studied *Fabp6*$^{-/-}$ mice to determine if BAM impacts fat dietary fat absorption. On the LFD, *Fabp6*$^{-/-}$ mice do not exhibit fat malabsorption; however increasing the dietary fat content to a level that is normally found in the WSD provoked the significant reduction in efficiency of dietary fat absorption in both sexes of Fabp6-deficient mice as compared to that of wild-type mice on the same diet. Moreover, while efficiency of fat absorption was increased over time in wild-type mice, it decreased over time in *Fabp6*$^{-/-}$ mice. This indicates the importance of Fabp6 in the regulation of fat absorption on high fat diets.

Unexpectedly, we discovered that male *Fabp6*$^{-/-}$ mice experienced enhanced adiposity in response to the WSD feeding compared to male wild-type mice whereas the extent of adiposity induced by the WSD in female *Fabp6*$^{-/-}$ mice and female wild-type mice was similar. The role of estrogen in regulating energy homeostasis and adiposity has been well established through inactivation of the *Cyp19* (encodes aromatase) and *Esr1* (encodes estrogen receptor α) genes in mice (Jones et al., 2000; Heine et al., 2000). However, an enhanced body weight gain phenomenon was also noticed in male *Slc51a*$^{-/-}$ mice (deficient in Ostα) compared to wild-type mice fed the WSD (Hammond et al., 2015). It is more likely that the enhanced adiposity manifested by male *Fabp6*$^{-/-}$ mice is a consequence of disrupted bile acid metabolism in the gut

caused by the loss of Fabp6, although estrogen may mask this effect since female *Fabp6*$^{-/-}$ mice did not show the same phenotype as male *Fabp6*$^{-/-}$ mice.

In the present study, both the food intake and changes in metabolic rate induced by the WSD feeding did not account for the sex differential fat accretion shown by male *Fabp6*$^{-/-}$ mice. In addition, male *Fabp6*$^{-/-}$ mice fed the WSD, unlike female *Fabp6*$^{-/-}$ mice, maintained a high level of activity and a high rate of energy expenditure. Interestingly, in humans, the consumption of the WSD has been correlated with lower physical activity levels and sedentary behavior (Ekelund et al., 2017; Bibiloni et al., 2017). Our findings therefore suggest the possibility that bile acid metabolism may play a role in determining the level of physical activity.

Several studies have described the association between high Firmicutes to Bacteroidetes ratio and efficiency of energy extraction from the diet, which consequently leads to obesity (Backhed et al., 2004; Ley et al., 2005; Turnbaugh et al., 2006). Our findings suggest that exposure of the gut microbiota in *Fabp6*$^{-/-}$ mice to excess bile acids induced dysbiosis. Indeed, the appearance of secondary bile acids in gallbladder bile is consistent with the change in gut microbial composition. It has been determined that wild-type male and female mice possess distinct gut microbiomes (Org et al., 2016). The expansion of the Firmicutes phylum we observed in male *Fabp6*$^{-/-}$ mice fed the WSD at the expense of other phyla is also distinct from that of female *Fabp6*$^{-/-}$ mice fed the same diet, and this is concordant with the pattern of change known to promote obesity (Musso et al., 2011; Ridaura et al., 2013). The selection of the WSD as the lipid-rich diet in this study also exposed the sexually dimorphic response of *Fabp6*$^{-/-}$ mice to this diet, possibly due to its refined carbohydrate content. However, the specific nature of the taxonomic differences between male and female gut microbiomes that were induced by the exposure of the gut microbiota to the components of the WSD is not apparent from the present study, but this should become evident by analysis of the changes in gut metagenome in future studies.

In summary, our study found that malabsorption of dietary fat in *Fabp6*$^{-/-}$ mice can occur coincidentally with bile acid malabsorption but this is dependent on dietary fat

content. Fortuitously, we uncovered a sexually dimorphic enhancement of adiposity in male *Fabp6*$^{-/-}$ mice as well as sexually distinct remodeling of the gut microbial composition in response to WSD feeding.

Acknowledgment

This study was supported by grants (to LBA) from the Natural Sciences and Engineering Research Council of Canada and the Canadian Institutes of Health Research. SMH was supported by a scholarship from the University of Jordan.

Appendix II. Supplemental data

II.1. Supplemental data to Chapter 2

Table II-1 Good's coverage and number of sequences per sample- Chapter 2

Sample	Sex	Diet	Genotype	Good's Coverage (%)	Number of sequences
g1	Male	LFD	*Fabp6*$^{+/+}$	99.57	5989
g2	Male	LFD	*Fabp6*$^{+/+}$	99.84	8171
g3	Male	LFD	*Fabp6*$^{+/+}$	99.92	3613
g4	Male	LFD	*Fabp6*$^{+/+}$	99.77	4879
g5	Male	LFD	*Fabp6*$^{+/+}$	99.78	6951
g6	Male	LFD	*Fabp6*$^{-/-}$	99.84	5508
g7	Male	LFD	*Fabp6*$^{-/-}$	99.78	4596
g8	Male	LFD	*Fabp6*$^{-/-}$	99.66	2086
g9	Male	LFD	*Fabp6*$^{-/-}$	99.98	5771
g10	Male	LFD	*Fabp6*$^{-/-}$	99.72	4575
g11	Male	WSD	*Fabp6*$^{+/+}$	99.98	11153
g12	Male	WSD	*Fabp6*$^{+/+}$	99.98	6235
g13	Male	WSD	*Fabp6*$^{+/+}$	100.00	4547
g14	Male	WSD	*Fabp6*$^{+/+}$	99.76	3364
g15	Male	WSD	*Fabp6*$^{+/+}$	99.97	7955
g16	Male	WSD	*Fabp6*$^{-/-}$	99.93	10296
g17	Male	WSD	*Fabp6*$^{-/-}$	99.90	7036
g18	Male	WSD	*Fabp6*$^{-/-}$	99.91	5371
g19	Male	WSD	*Fabp6*$^{-/-}$	99.77	3538
g20	Male	WSD	*Fabp6*$^{-/-}$	99.85	5410
g21	Female	LFD	*Fabp6*$^{+/+}$	99.83	7540
g22	Female	LFD	*Fabp6*$^{+/+}$	99.82	5524
g23	Female	LFD	*Fabp6*$^{+/+}$	99.79	4751
g24	Female	LFD	*Fabp6*$^{+/+}$	99.88	4124
g25	Female	LFD	*Fabp6*$^{+/+}$	99.79	6117
g26	Female	LFD	*Fabp6*$^{-/-}$	99.82	9356
g27	Female	LFD	*Fabp6*$^{-/-}$	99.87	6833
g28	Female	LFD	*Fabp6*$^{-/-}$	99.80	4071
g29	Female	LFD	*Fabp6*$^{-/-}$	99.77	4847
g30	Female	LFD	*Fabp6*$^{-/-}$	99.87	7468
g31	Female	WSD	*Fabp6*$^{+/+}$	99.89	9150
g32	Female	WSD	*Fabp6*$^{+/+}$	99.94	6823
g33	Female	WSD	*Fabp6*$^{+/+}$	99.77	4281
g34	Female	WSD	*Fabp6*$^{+/+}$	99.91	4336
g35	Female	WSD	*Fabp6*$^{+/+}$	99.83	5390
g36	Female	WSD	*Fabp6*$^{-/-}$	99.96	7954
g37	Female	WSD	*Fabp6*$^{-/-}$	99.96	9723
g38	Female	WSD	*Fabp6*$^{-/-}$	99.88	5081
g39	Female	WSD	*Fabp6*$^{-/-}$	99.83	5312
g40	Female	WSD	*Fabp6*$^{-/-}$	99.89	8403

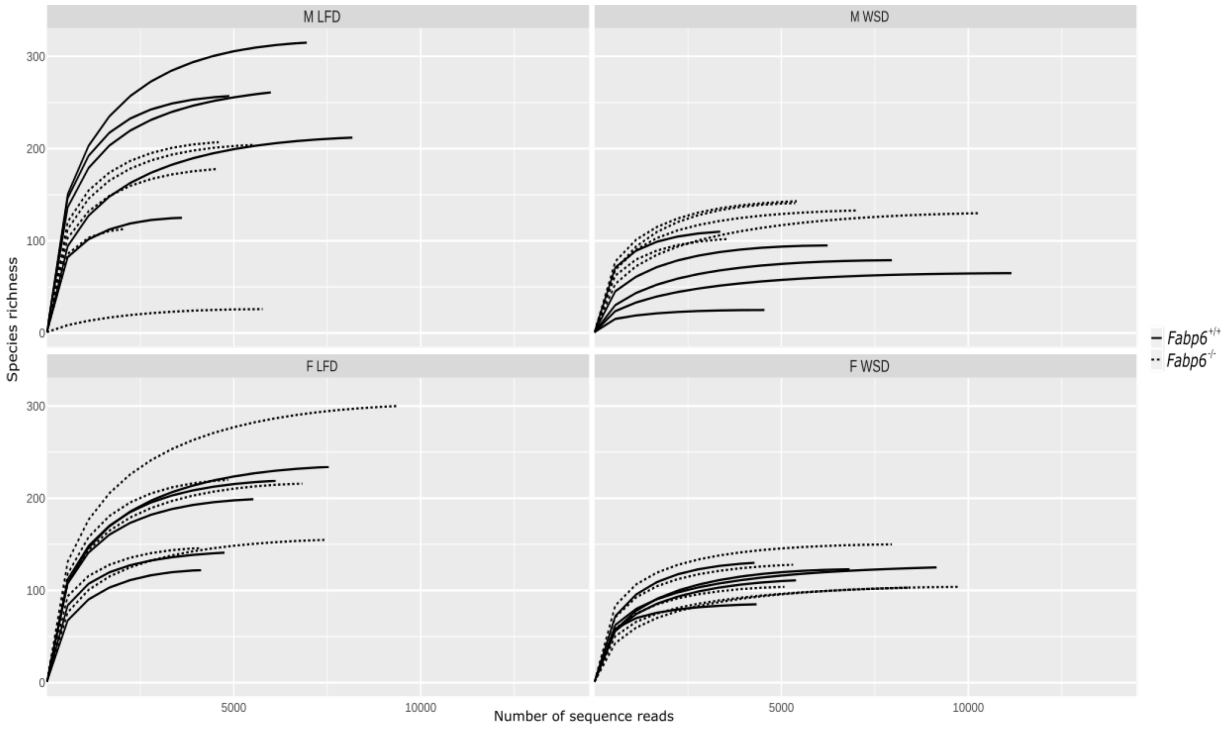

Figure II-1. Rarefaction curves of samples- Chapter 2. M: male, F: female, LFD: low fat diet, WSD: Western-style diet. Solid and dashed lines represent wild-type and *Fabp6*$^{-/-}$mice, respectively.

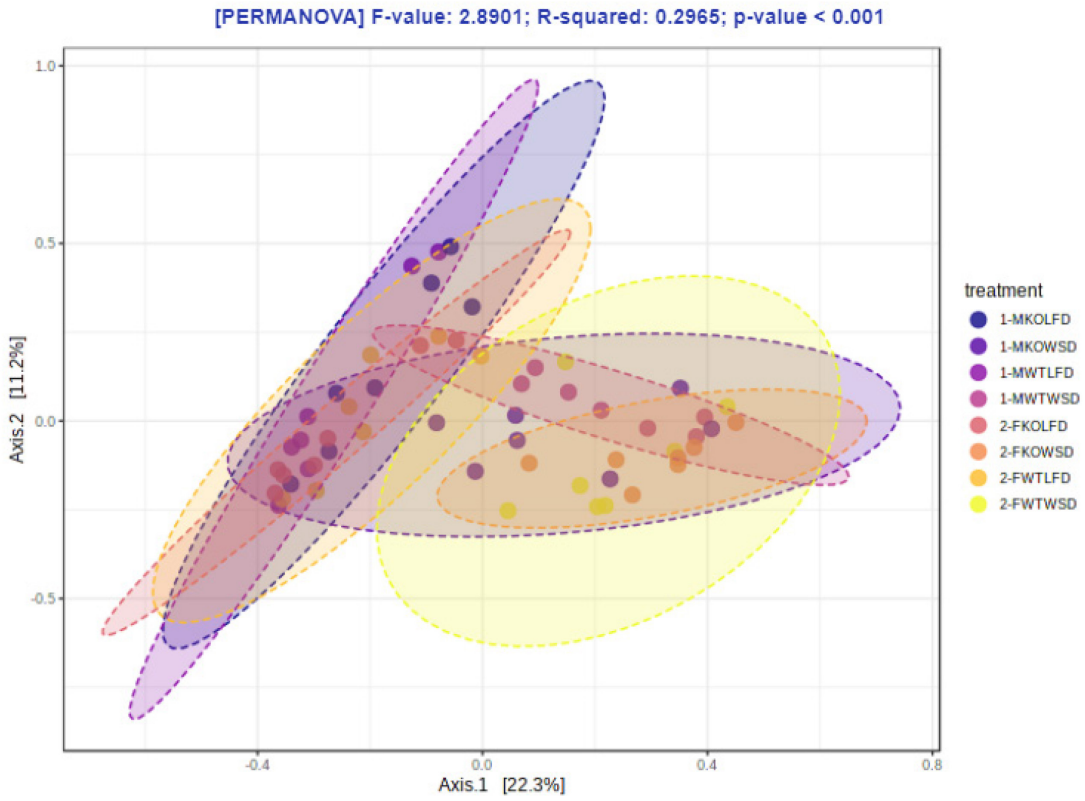

Figure II-2. Principal coordinates analysis of gut microbial species in mice including the samples of all treatments used in Chapter 2. Darker shades indicate male and lighter shades indicate female mice. Permutational analysis of variance (PERMANOVA) was calculated using Adonis function of Vegan implemented with MicrobiomeAnalyst. KO: knockout, WT: wildtype, LFD: low fat diet, WSD: Western-style diet, M: male, F: female.

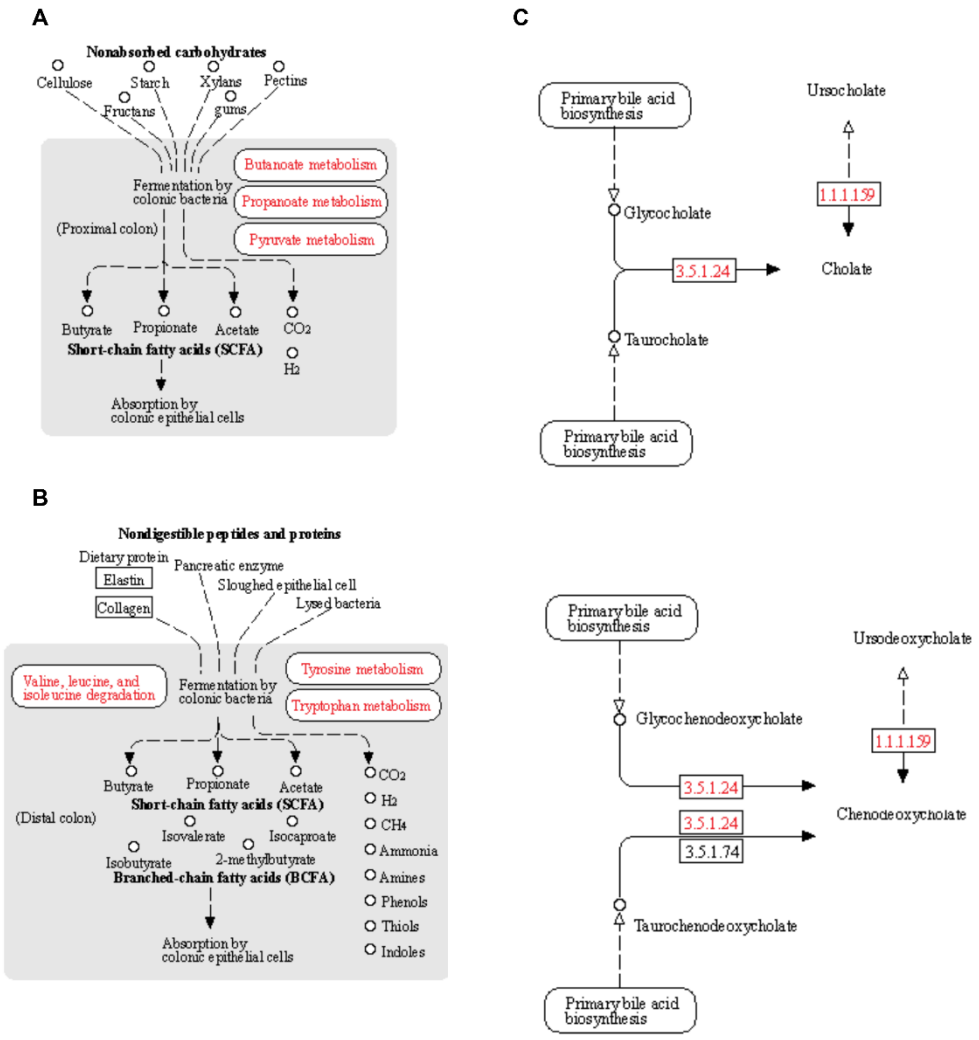

Figure II-3. Gut microbial SCFAs and secondary bile acid biosynthesis pathways inferred from 16S rRNA gene sequence data (A) Fermentation of non-absorbed carbohydrates by colonic bacteria adapted from KEGG pathway (ko04973), (B) Fermentation of non-digestible peptides and proteins by colonic bacteria adapted from KEGG pathway (ko04974), (c) Secondary bile acid biosynthesis by colonic bacteria adapted from KEGG pathway (ko00121), EC 3.5.1.24 represent bile salt hydrolase and EC1.1.1.1.59 represent 7alpha-hydroxysteroid dehydrogenase.

II.2. Supplemental data to Chapter 3

Table II-2 Good's coverage and number of sequences per sample- Chapter 3

Sample	Sex	Diet	Genotype	Before rarefaction		After rarefaction	
				Number of sequences	Good's Coverage (%)	Number of sequences	Good's Coverage (%)
N1	male	LFD	C57BL/6J	4679	98.2	2813	99.2
N2	male	LFD	C57BL/6J	8283	99.1	2813	99.3
N3	male	LFD	C57BL/6J	7205	99.0	2813	99.3
N4	male	LFD	C57BL/6J	2840	98.1	2813	99.3
N5	male	LFD	C57BL/6J	4760	98.2	2813	99.3
N6	male	WSD	C57BL/6J	24646	99.7	2813	99.2
N7	male	WSD	C57BL/6J	5051	98.9	2813	99.4
N8	male	WSD	C57BL/6J	7073	99.2	2813	99.4
N9	male	WSD	C57BL/6J	5613	99.0	2813	99.2
N10	male	WSD	C57BL/6J	5858	99.3	2813	99.1
N11	male	WSD+PRPE	C57BL/6J	16866	99.5	2813	99.0
N12	male	WSD+PRPE	C57BL/6J	15405	99.6	2813	98.6
N13	male	WSD+PRPE	C57BL/6J	8325	99.1	2813	98.8
N14	male	WSD+PRPE	C57BL/6J	10671	99.4	2813	98.9
N15	male	WSD+PRPE	C57BL/6J	7637	99.1	2813	99.1
N16	female	LFD	C57BL/6J	25984	99.9	2509	98.9
N17	female	LFD	C57BL/6J	13953	99.7	2509	98.5
N18	female	LFD	C57BL/6J	14447	99.8	2509	99.0
N19	female	LFD	C57BL/6J	21755	99.8	2509	98.9
N20	female	LFD	C57BL/6J	12968	99.7	2509	98.8
N21	female	WSD	C57BL/6J	9663	99.6	2509	98.9
N22	female	WSD	C57BL/6J	2768	98.6	2509	99.4
N23	female	WSD	C57BL/6J	17271	99.8	2509	98.7
N24	female	WSD	C57BL/6J	14000	99.8	2509	99.0
N25	female	WSD	C57BL/6J	18583	99.8	2509	98.8
N26	female	WSD+PRPE	C57BL/6J	11283	99.6	2509	98.6
N27	female	WSD+PRPE	C57BL/6J	9246	99.6	2509	98.9
N28	female	WSD+PRPE	C57BL/6J	2509	98.3	2509	99.3
N29	female	WSD+PRPE	C57BL/6J	41098	99.9	2509	98.8
N30	male	LFD	*Fabp6*$^{+/+}$	15802	99.3	3462	98.5
N31	male	LFD	*Fabp6*$^{+/+}$	5138	98.3	3462	98.7
N32	male	LFD	*Fabp6*$^{+/+}$	4913	97.8	3462	98.7
N33	male	LFD	*Fabp6*$^{+/+}$	5528	98.4	3462	99.1
N34	male	WSD	*Fabp6*$^{+/+}$	45131	99.7	3462	98.8
N35	male	WSD	*Fabp6*$^{+/+}$	13277	99.1	3462	98.7
N36	male	WSD	*Fabp6*$^{+/+}$	14779	99.3	3462	98.9

N37	male	WSD	*Fabp6*$^{+/+}$	5925	98.9	3462	99.0
N38	male	WSD+PRPE	*Fabp6*$^{+/+}$	7059	98.9	3462	99.2
N39	male	WSD+PRPE	*Fabp6*$^{+/+}$	3500	97.3	3462	99.0
N40	male	WSD+PRPE	*Fabp6*$^{+/+}$	7674	98.7	3462	98.6
N41	male	WSD+PRPE	*Fabp6*$^{+/+}$	25733	99.5	3462	98.3
N42	female	LFD	*Fabp6*$^{+/+}$	3431	97.6	3407	99.1
N43	female	LFD	*Fabp6*$^{+/+}$	4450	97.6	3407	98.6
N44	female	LFD	*Fabp6*$^{+/+}$	11169	98.7	3407	98.4
N45	female	LFD	*Fabp6*$^{+/+}$	9297	98.6	3407	98.4
N46	female	LFD	*Fabp6*$^{+/+}$	4384	97.6	3407	98.9
N47	female	LFD	*Fabp6*$^{+/+}$	7974	98.7	3407	98.9
N48	female	WSD	*Fabp6*$^{+/+}$	47097	99.7	3407	98.4
N49	female	WSD	*Fabp6*$^{+/+}$	18595	99.2	3407	98.5
N50	female	WSD	*Fabp6*$^{+/+}$	9295	98.9	3407	98.8
N51	female	WSD	*Fabp6*$^{+/+}$	14102	99.2	3407	98.4
N52	female	WSD	*Fabp6*$^{+/+}$	4311	97.4	3407	98.7
N53	female	WSD+PRPE	*Fabp6*$^{+/+}$	24785	99.4	3407	98.0
N54	female	WSD+PRPE	*Fabp6*$^{+/+}$	22490	99.2	3407	98.4
N55	female	WSD+PRPE	*Fabp6*$^{+/+}$	19393	99.4	3407	98.1
N56	female	WSD+PRPE	*Fabp6*$^{+/+}$	18892	99.3	3407	98.6
N57	female	WSD+PRPE	*Fabp6*$^{+/+}$	35662	99.5	3407	98.1
N58	male	LFD	*Fabp6*$^{-/-}$	6005	98.9	1500	98.2
N59	male	LFD	*Fabp6*$^{-/-}$	1544	95.5	1500	98.7
N60	male	LFD	*Fabp6*$^{-/-}$	5152	98.7	1500	97.5
N62	male	WSD	*Fabp6*$^{-/-}$	3219	97.5	1500	96.9
N63	male	WSD	*Fabp6*$^{-/-}$	13510	99.0	1500	97.5
N64	male	WSD	*Fabp6*$^{-/-}$	22965	99.5	1500	97.0
N65	male	WSD	*Fabp6*$^{-/-}$	11398	99.0	1500	97.7
N67	male	WSD+PRPE	*Fabp6*$^{-/-}$	17032	99.4	1500	98.2
N68	male	WSD+PRPE	*Fabp6*$^{-/-}$	9145	99.0	1500	97.5
N69	male	WSD+PRPE	*Fabp6*$^{-/-}$	14972	99.5	1500	97.9
N70	male	WSD+PRPE	*Fabp6*$^{-/-}$	21769	99.6	1500	97.7
N72	female	LFD	*Fabp6*$^{-/-}$	7054	98.3	1655	98.4
N73	female	LFD	*Fabp6*$^{-/-}$	13772	99.1	1655	97.4
N74	female	LFD	*Fabp6*$^{-/-}$	8669	98.9	1655	97.6
N75	female	WSD	*Fabp6*$^{-/-}$	2617	97.0	1655	98.2
N76	female	WSD	*Fabp6*$^{-/-}$	1677	95.4	1655	98.4
N77	female	WSD	*Fabp6*$^{-/-}$	8214	98.7	1655	96.4
N78	female	WSD	*Fabp6*$^{-/-}$	15291	99.2	1655	97.7
N79	female	WSD	*Fabp6*$^{-/-}$	3786	97.7	1655	97.4
N80	female	WSD+PRPE	*Fabp6*$^{-/-}$	19416	99.4	1655	97.2
N81	female	WSD+PRPE	*Fabp6*$^{-/-}$	18111	99.3	1655	97.3
N82	female	WSD+PRPE	*Fabp6*$^{-/-}$	31702	99.6	1655	97.1

N83	female	WSD+PRPE	*Fabp6*$^{-/-}$	12513	99.1	1655	97.6
N84	female	WSD+PRPE	*Fabp6*$^{-/-}$	11660	98.8	1655	97.4

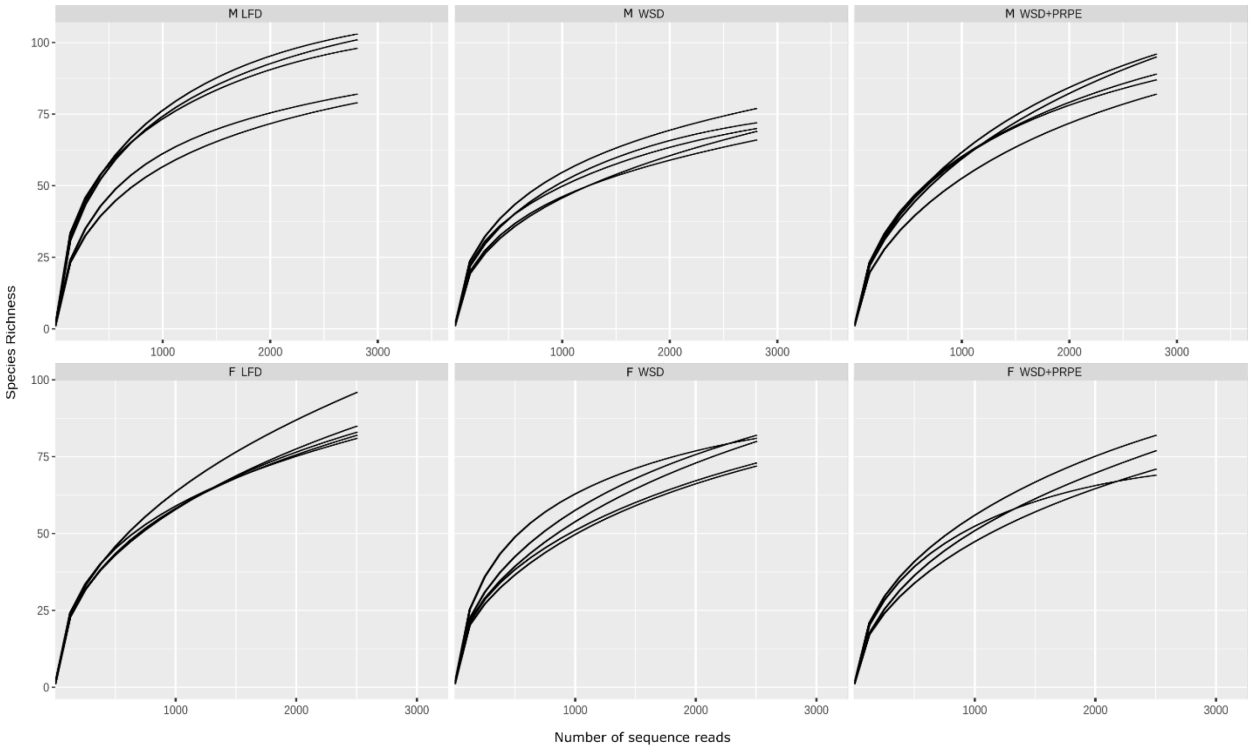

Figure II-4. Rarefaction curves of C57BL/6J mice samples- Chapter 3. M: male, F: female, LFD: low fat diet, WSD: Western-style diet, WSD+PRPE: WSD-supplemented with polyphenolic rich potato extract.

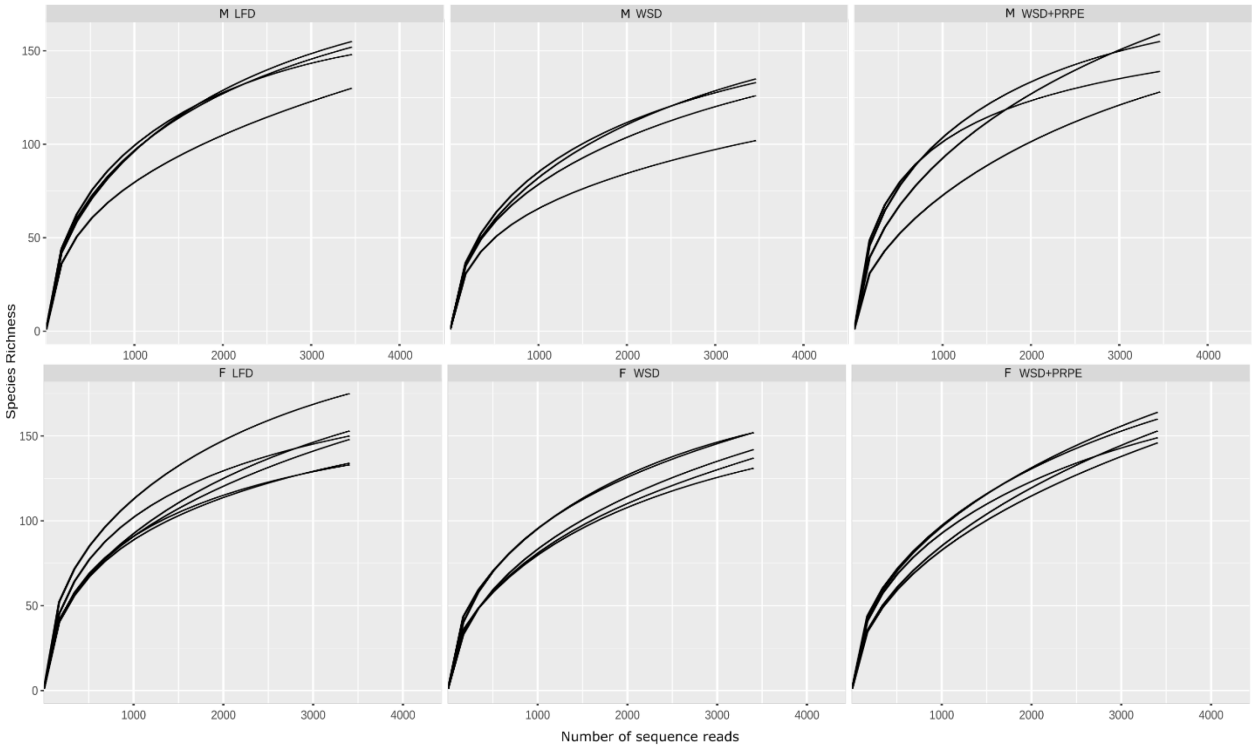

Figure II-5. Rarefaction curves of *Fabp6*$^{+/+}$ mice samples- Chapter 3. M: male, F: female, LFD: low fat diet, WSD: Western-style diet, WSD+PRPE: WSD-supplemented with polyphenolic rich potato extract.

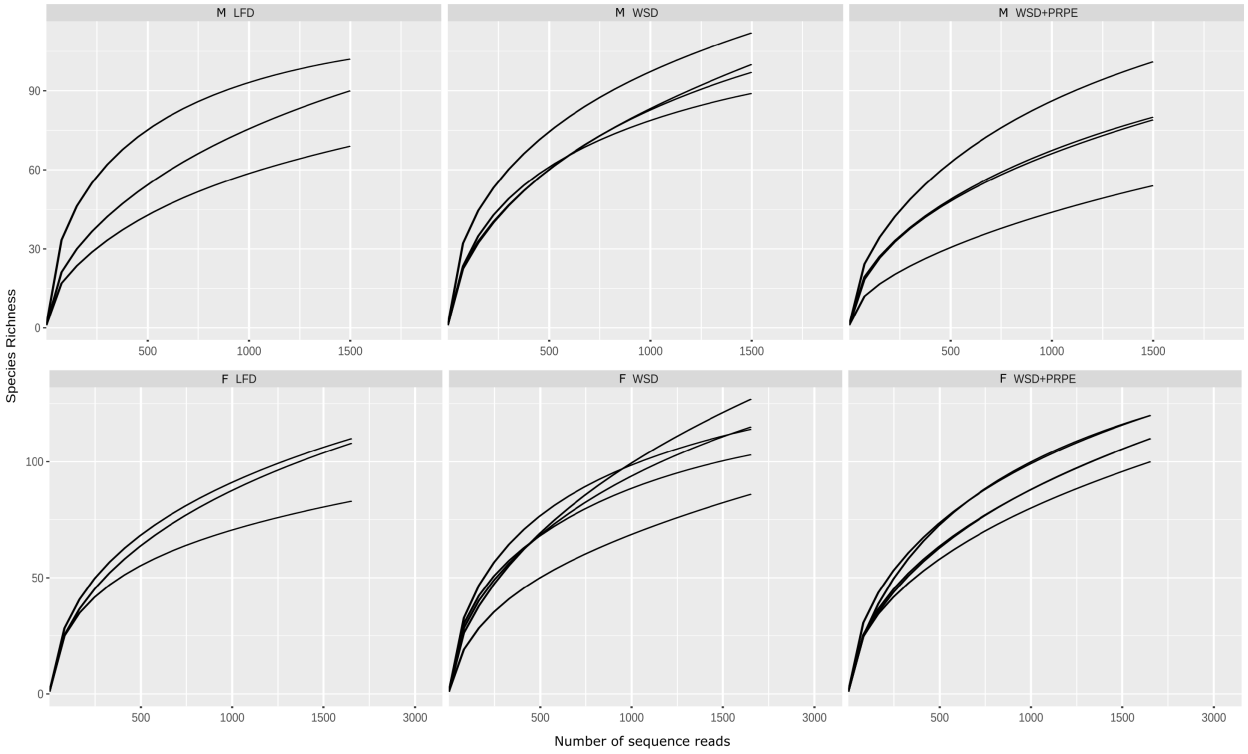

Figure II-6. Rarefaction curves of *Fabp6*$^{-/-}$ mice samples- Chapter 3. M: male, F: female, LFD: low fat diet, WSD: Western-style diet, WSD+PRPE: WSD-supplemented with polyphenolic rich potato extract.

II.3. Supplemental data to Chapter 4

Table II-3 Good's coverage and number of sequences per sample- Chapter 4

Sample	Sex	Diet	Genotype	Number of sequences	Good's Coverage (%)
D1	male	LFD	WT	6116	97.8
D2	male	LFD	WT	7698	98.4
D3	male	LFD	WT	1533	95.6
D4	male	LFD	WT	1395	95.3
D5	male	LFD	WT	1045	93.5
D6	male	WSD	WT	4391	98.3
D7	male	WSD	WT	1785	96.4
D8	male	WSD	WT	2198	96.5
D9	male	WSD	WT	2747	97.7
D10	male	WSD	WT	2227	97.1
D11	male	LFD	DKO	3679	97.2
D12	male	LFD	DKO	7892	98.2
D13	male	LFD	DKO	4751	98.1
D14	male	LFD	DKO	2983	97.4
D15	male	LFD	DKO	7673	98.9
D16	male	WSD	DKO	3279	97.8
D17	male	WSD	DKO	4452	97.8
D18	male	WSD	DKO	8471	99.1
D19	male	WSD	DKO	6463	99.2
D20	male	WSD	DKO	6410	98.5
D21	female	LFD	WT	2577	96.0
D22	female	LFD	WT	2006	96.2
D23	female	LFD	WT	3305	97.1
D24	female	LFD	WT	1995	97.2
D25	female	LFD	WT	5882	98.4
D26	female	WSD	WT	1953	96.3
D27	female	WSD	WT	1610	95.3
D28	female	WSD	WT	2938	96.9
D29	female	WSD	WT	4526	98.1
D30	female	LFD	DKO	5754	98.2
D31	female	LFD	DKO	5041	98.3
D32	female	LFD	DKO	4378	98.2
D33	female	LFD	DKO	3302	98.0
D34	female	LFD	DKO	3818	97.9
D35	female	WSD	DKO	1655	96.6
D36	female	WSD	DKO	2941	98.0
D37	female	WSD	DKO	1481	96.9

D38	female	WSD	DKO	3466	98.1
D39	female	WSD	DKO	2064	96.7

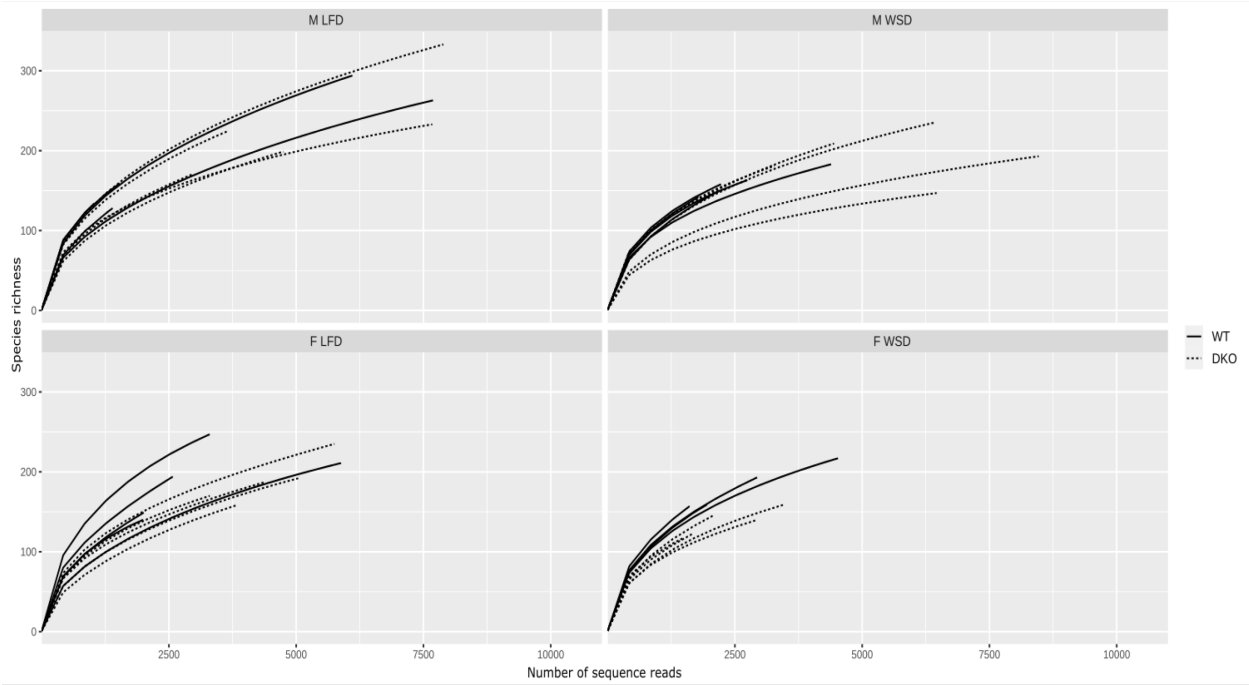

Figure II-7. Rarefaction curves of samples- Chapter 4. M: male, F: female, LFD: low fat diet, WSD: Western-style diet. Solid and dashed lines represent wild-type (WT) and *Fabp2*$^{-/-}$;*Fabp6*$^{-/-}$ (DKO) mice, respectively.

II.4. Supplemental data to manuscript presented in Appendix I

Table II-4. Fatty acid and cholesterol content of the diets.

Criteria (g/Kg diet)	Low fat diet[1]	Western-style diet[2, 3]
Total saturated fatty acids	8	125
Total monounsaturated fatty acids	11	60
Total polyunsaturated fatty acids	29	13
Palmitic acid	6	53
Stearic acid	1	24
Oleic acid	11	53
Linoleic acid	26	10
Linolenic acid	3	3
Cholesterol	--	2

[1]Tecklad global soy-protein free extruded rodent diet (2920X), Teklad-Envigo, Lachine, QC.

[2] Rodent western diet (D12079B), Research Diets, New Brunswick, NJ.

[3] Calculated using FoodData central (FDC ID 173412 and 748323): U.S. Department of Agriculture-Agricultural Research Service. (2019). FoodData central. Retrieved from fdc.nal.usda.gov.

II.5. Primer and barcode sequences

Table II-5 Primer sequences.

Target	Direction: Sequence	Size (bp)	Reference
Fabp6 wildtype allele	F: 5'-ATGTGGAGCAGCAGGTTGTG R: 5'-TTACGCGCTCATAGGTCACA	449	This thesis
Fabp6 disrupted allele	F: 5'-GACTGTGCCTTCTAGTTGCCA R: 5'-TTACGCGCTCATAGGTCACA	228	This thesis
Mouse *Mos* gene	F: 5'-ACATAAAGCATTGAGGTGCTAACAA R: 5'-TCAAAGTTCACCAAACTCCAGGT	102	This thesis
16S rRNA gene: V3-V4	F: 5'-ACTCCTACGGGAGGCAGCAG R: 5'-GGACTACHVGGGTWTCTAAT	488	Fu et al. (2016)
16S rRNA gene	F: 5'-GAGTTTGATCMTGGCTCAG R: 5'-GACGGGCGGTGWGTRCA	1399	Klindworth et al. (2012)
Gapdh	F: 5'-AGCTTGTCATCAACGGGAAG R: 5'-TTTGATGTTAGTGGGGTCTCG	62	Takeshita et al. (2014)
Hprt	F: 5'-TCAGTCAACGGGGGACATAAA R: 5'-GGGGCTGTACTGCTTAACCAG	142	Hamilton et al. (2017)
Grp78	F: 5'-CGATACTGGCCGAGACAAC R: 5'-GACGACGGTTCTGGTCTCA	71	Maehara et al. (2014)
Atf4	F: 5'-GGACAGATTGGATGTTGGAGAAAATG R: 5'-GGAGATGGCCAATTGGGTTCAC	192	Nguyen et al. (2014)
sXbp1	F: 5'-TGCTGAGTCCGCAGCAGGTG R: 5'-GACTAGCAGACTCTGGGGAAG	170	Oñate et al. (2016)
Grp94	F: 5'-CTGGGTCAAGCAGAAAGGAG R: 5'-TGCCAGACCATCCATACTGA	345	Egawa et al. (2011)

All bacteria	F: 5'-GTGSTGCAYGGYYGTCGTCA R: 5'-ACGTCRTCCMCNCCTTCCTC	147	Ramirez-Farias et al. (2009)
Lactobacillus spp.	F: 5'-GAGGCAGCAGTAGGGAATCTTC R: 5'-GGCCAGTTACTACCTCTATCCTTCTTC	126	This thesis
Bifidobacterium spp.	F: 5'-CGCGTCYGGTGTGAAAG R: 5'-CCCCACATCCAGCATCCG	244	This thesis
Lactobacillus acidophilus	F: 5'-CTTTGACTCAGGCAATTGCTCGTGAAGGTATG R: 5'-CAACTTCTTTAGATGCTGAAGAAACAGCAGCTACG	145	Herbel et al. (2013)
Lactobacillus delbrueckii subsp. bulgaricus	F: 5'-GAACTTGATGTTGTTGAAGGGATGCAATTCG R: 5'-GAGCGGCCTTGTTGCACGATTTC	182	Herbel et al. (2013)
Lactobacillus casei	F: 5'-CTTGTCAGTGAATACATAGCTGGCC R: 5'-CTTCCTGCGGGTACTGAGATGT	70	This thesis Haarman and Knol (2005)
Lactobacillus rhamnosus	F: 5'-GTGCTTGCATCTTGATTTAATTTT R: 5'-TGCGGTTCTTGGATCTATGCG	125	Furet et al. (2004)
Bifidobacterium bifidum	F: 5'-CCACATGATCGCATGTGATTG R: 5'-CCGAAGGCTTGCTCCCAAA	278	Matsuki et al. (1999)
Bifidobacterium breve	F: 5'-GTGGTGGCTTGAGAACTGGATAG R: 5'-CAAAACGATCGAAACAAACACTAAA	118	Haarman and Knol (2005)
Bifidobacterium longum	F: 5'-GTATCCGTCCGACCCAGCAG R: 5'-GGTGACGGAGCCCGGCTTG	161	Lawley et al. (2018)
Streptococcus salivarius subsp. thermophilus	F: 5'-ACGCTGAAGAGAGGAGCTTG R: 5'-GCAATTGCCCCTTTCAAATA	157	Tabasco et al. (2007)
Bacteroidetes	F: 5'-GTTTAATTCGATGATACGCGAG R: 5'-TTAASCCGACACCTCACGG	122	Yang et al. (2015)

Firmicutes	F: 5'-GGAGYATGTGGTTTAATTCGAAGCA R: 5'-AGCTGACGACAACCATGCAC	126	Guo et al. (2008)
e-proteobacteria	F: 5'-TAGGCTTGACATTGATAGAATC R: 5'-CTTACGAAGGCAGTCTCCTTA	109	Yang et al. (2015)

Table II-6 Barcode sequences used for sample dual multiplexing in Nanopore library preparation.

Tag ID	Sequence (Srivathsan et al., 2018)
T1	AACTCGTGTCTG
T2	ACAATTCGGCGA
T3	ACCGAGGATGTA
T4	ACGCTCATGTGT
T5	ACGGTATAGCAT
T6	ACGTTAGGTGCC
T14	CAGGCCAGTCTA
T15	CATCCTGCCTTG
T16	CATGCAGTTAGT
T17	CCAGTGCTCTAG
T18	CCTATAGGAGTT
T19	CGCTGTACGTCA
T27	GAAGATCCATCG
T28	GACGGTTCCATA
T29	GATCTGCGTCTT

References

Agellon, L.B. (2008). Metabolism and function of bile acids. In D.E. Vance & J.E. Vance (Eds.), *Biochemistry of lipids, lipoproteins and membranes (5th edition)* (Vol. 36, pp. 423-440). San Diego: Elsevier.

Backhed, F., Ding, H., Wang, T.*, et al.* (2004). The gut microbiota as an environmental factor that regulates fat storage. *Proc Natl Acad Sci USA, 101* (44), 15718-15723.

Ballatori, N., Fang, F., Christian, W.V.*, et al.* (2008). Ostα-Ostβ is required for bile acid and conjugated steroid disposition in the intestine, kidney, and liver. *Am J Physiol Gastrointest Liver Physiol, 295* (1), G179-G186.

Bibiloni, M.D.M., Julibert, A., Argelich, E.*, et al.* (2017). Western and Mediterranean dietary patterns and physical activity and fitness among Spanish older adults. *Nutrients, 9* (7), e704.

Dawson, P.A., Haywood, J., Craddock, A.L.*, et al.* (2003). Targeted deletion of the ileal bile acid transporter eliminates enterohepatic cycling of bile acids in mice. *J Biol Chem, 278* (36), 33920-33927.

Dewar, A.D. and Newton, W.H. (1948). The relationship between food intake and respiratory quotient in mice. *Br J Nutr, 2* (2), 142-145.

Egawa, N., Yamamoto, K., Inoue, H.*, et al.* (2011). The endoplasmic reticulum stress sensor, ATF6alpha, protects against neurotoxin-induced dopaminergic neuronal death. *J Biol Chem, 286* (10), 7947-7957.

Ekelund, U., Kolle, E., Steene-Johannessen, J.*, et al.* (2017). Objectively measured sedentary time and physical activity and associations with body weight gain: Does body weight determine a decline in moderate and vigorous intensity physical activity? *Int J Obesity, 41* (12), 1769-1774.

Folch, J., Lees, M. and Sloane Stanley, G.H. (1957). A simple method for the isolation and purification of total lipides from animal tissues. *J Biol Chem, 226* (1), 497-509.

Fu, J., Lv, H. and Chen, F. (2016). Diversity and variation of bacterial community revealed by MiSeq sequencing in Chinese dark teas. *PLoS One, 11* (9), e0162719-e0162719.

Furet, J.P., Quenee, P. and Tailliez, P. (2004). Molecular quantification of lactic acid bacteria in fermented milk products using real-time quantitative PCR. *Int J Food Microbiol, 97* (2), 197-207.

Guo, X., Xia, X., Tang, R.*, et al.* (2008). Development of a real-time PCR method for Firmicutes and Bacteroidetes in faeces and its application to quantify intestinal population of obese and lean pigs. *Lett Appl Microbiol, 47* (5), 367-373.

Haarman, M. and Knol, J. (2005). Quantitative real-time PCR assays to identify and quantify fecal Bifidobacterium species in infants receiving a prebiotic infant formula. *Appl Environ Microbiol, 71* (5), 2318-2324.

Hamilton, M.K., Ronveaux, C.C., Rust, B.M.*, et al.* (2017). Prebiotic milk oligosaccharides prevent development of obese phenotype, impairment of gut permeability, and microbial dysbiosis in high fat-fed mice. *Am J Physiol Gastrointest Liver Physiol, 312* (5), G474-g487.

Hammond, C.L., Wheeler, S.G., Ballatori, N.*, et al.* (2015). Ostα$^{-/-}$ mice are not protected from Western diet-induced weight gain. *Physiol Rep, 3* (1), e12263.

Heine, P.A., Taylor, J.A., Iwamoto, G.A.*, et al.* (2000). Increased adipose tissue in male and female estrogen receptor-alpha knockout mice. *Proc Natl Acad Sci USA, 97* (23), 12729-12734.

Herbel, S.R., Lauzat, B., von Nickisch-Rosenegk, M.*, et al.* (2013). Species-specific quantification of probiotic lactobacilli in yoghurt by quantitative real-time PCR. *J Appl Microbiol, 115* (6), 1402-1410.

Heubi, J.E., Balistreri, W.F., Fondacaro, J.D.*, et al.* (1982). Primary bile acid malabsorption: Defective in vitro ileal active bile acid transport. *Gastroenterology, 83* (4), 804-811.

Ishibashi, S., Schwarz, M., Frykman, P.K.*, et al.* (1996). Disruption of cholesterol 7α-hydroxylase gene in mice. I. Postnatal lethality reversed by bile acid and vitamin supplementation. *J Biol Chem, 271* (30), 18017-18023.

Jones, M.E., Thorburn, A.W., Britt, K.L.*, et al.* (2000). Aromatase-deficient (ArKO) mice have a phenotype of increased adiposity. *Proc Natl Acad Sci USA, 97* (23), 12735-12740.

Klindworth, A., Pruesse, E., Schweer, T.*, et al.* (2012). Evaluation of general 16S ribosomal RNA gene PCR primers for classical and next-generation sequencing-based diversity studies. *Nucleic Acids Res, 41* (1), e1-e1.

Kostic, A.D., Howitt, M.R. and Garrett, W.S. (2013). Exploring host–microbiota interactions in animal models and humans. *Genes Dev, 27* (7), 701-718.

Kraus, D., Yang, Q. and Kahn, B.B. (2015). Lipid extraction from mouse feces. *Bio Protoc, 5* (1), e1375.

Lawley, B., Centanni, M., Watanabe, J.*, et al.* (2018). Tuf gene sequence variation in *Bifidobacterium longum* subsp. Infantis detected in the fecal microbiota of Chinese infants. *Appl Environ Microbiol, 84* (13), e00336-00318.

Ley, R.E., Backhed, F., Turnbaugh, P.*, et al.* (2005). Obesity alters gut microbial ecology. *Proc Natl Acad Sci USA, 102* (31), 11070-11075.

Maehara, N., Arai, S., Mori, M.*, et al.* (2014). Circulating AIM prevents hepatocellular carcinoma through complement activation. *Cell Rep, 9* (1), 61-74.

Matsuki, T., Watanabe, K., Tanaka, R.*, et al.* (1999). Distribution of bifidobacterial species in human intestinal microflora examined with 16S rRNA-gene-targeted species-specific primers. *Appl Environ Microbiol, 65* (10), 4506-4512.

Musso, G., Gambino, R. and Cassader, M. (2011). Interactions between gut microbiota and host metabolism predisposing to obesity and diabetes. *Annu Rev Med, 62*, 361-380.

Navidshad, B., Liang, J.B. and Jahromi, M.F. (2012). Correlation coefficients between different methods of expressing bacterial quantification using real time PCR. *Int J Mol Sci, 13* (2), 2119-2132.

Nguyen, A., Tao, H., Metrione, M.*, et al.* (2014). Very low density lipoprotein receptor (VLDLR) expression is a determinant factor in adipose tissue inflammation and adipocyte-macrophage interaction. *J Biol Chem, 289* (3), 1688-1703.

Oelkers, P., Kirby, L.C., Heubi, J.E.*, et al.* (1997). Primary bile acid malabsorption caused by mutations in the ileal sodium-dependent bile acid transporter gene (SLC10A2). *J Clin Invest, 99* (8), 1880-1887.

Oñate, M., Catenaccio, A., Martínez, G.*, et al.* (2016). Activation of the unfolded protein response promotes axonal regeneration after peripheral nerve injury. *Sci Rep, 6* (1), 21709.

Org, E., Mehrabian, M., Parks, B.W.*, et al.* (2016). Sex differences and hormonal effects on gut microbiota composition in mice. *Gut Microbes, 7* (4), 313-322.

Praslickova, D., Torchia, E.C., Sugiyama, M.G.*, et al.* (2012). The ileal lipid binding protein is required for efficient absorption and transport of bile acids in the distal portion of the murine small intestine. *PLoS One, 7* (12), 1.

Ramirez-Farias, C., Slezak, K., Fuller, Z.*, et al.* (2009). Effect of inulin on the human gut microbiota: Stimulation of *Bifidobacterium adolescentis* and *faecalibacterium prausnitzii*. *Br J Nutr, 101* (4), 541-550.

Rao, A., Haywood, J., Craddock, A.L.*, et al.* (2008). The organic solute transporter α-β, Ostα-Ostβ, is essential for intestinal bile acid transport and homeostasis. *Proc Natl Acad Sci USA, 105* (10), 3891-3896.

Ridaura, V.K., Faith, J.J., Rey, F.E.*, et al.* (2013). Gut microbiota from twins discordant for obesity modulate metabolism in mice. *Science, 341* (6150), 1241214.

Srivathsan, A., Baloğlu, B., Wang, W.*, et al.* (2018). A MinION-based pipeline for fast and cost-effective DNA barcoding. *Mol Ecol Resour*, published online: 2018 Apr 2019.

Stacey, M. and Webb, M. (1947). Studies on the antibacterial properties of the bile acids and some compounds derived from cholanic acid. *Proc R Soc Med, 134* (877), 523-537.

Tabasco, R., Paarup, T., Janer, C.*, et al.* (2007). Selective enumeration and identification of mixed cultures of *Streptococcus thermophilus*, *Lactobacillus delbrueckii* subsp. Bulgaricus, *L. Acidophilus*, *L. Paracasei* subsp. Paracasei and *Bifidobacterium lactis* in fermented milk. *Int Dairy J, 17* (9), 1107-1114.

Takeshita, S., Fumoto, T., Naoe, Y.*, et al.* (2014). Age-related marrow adipogenesis is linked to increased expression of RANKL. *J Biol Chem, 289* (24), 16699-16710.

Torchia, E.C., Labonté, E.D. and Agellon, L.B. (2001). Separation and quantitation of bile acids using an isocratic solvent system for high performance liquid chromatography coupled to an evaporative light scattering detector. *Anal Biochem, 298* (2), 293-298.

Tsai, Y.L. and Olson, B.H. (1992). Detection of low numbers of bacterial cells in soils and sediments by polymerase chain reaction. *Appl Environ Microbiol, 58* (2), 754-757.

Turnbaugh, P.J., Ley, R.E., Mahowald, M.A.*, et al.* (2006). An obesity-associated gut microbiome with increased capacity for energy harvest. *Nature, 444* (7122), 1027-1131.

Van der Meer, R., de Vries, H. and Glatz, J. (1985). *t*-Butanol extraction of feces: A rapid procedure for enzymic determination of bile acids. In A.C. Beynen (Ed.), *Cholesterol metabolism in health and disease: Studies in the netherlands* (pp. 113–119). Wageningen: Ponsen & Looijen.

Watanabe, M., Fukiya, S. and Yokota, A. (2017). Comprehensive evaluation of the bactericidal activities of free bile acids in the large intestine of humans and rodents. *J Lipid Res, 58* (6), 1143-1152.

Watson, L., Lalji, A., Bodla, S.*, et al.* (2015). Management of bile acid malabsorption using low-fat dietary interventions: A useful strategy applicable to some patients with diarrhoea-predominant irritable bowel syndrome? *Clin Med, 15* (6), 536-540.

Weir, J.B. (1949). New methods for calculating metabolic rate with special reference to protein metabolism. *J Physiol, 109* (1-2), 1-9.

Yang, Y.W., Chen, M.K., Yang, B.Y.*, et al.* (2015). Use of 16S rRNA gene-targeted group-specific primers for real-time PCR analysis of predominant bacteria in mouse feces. *Appl Environ Microbiol, 81* (19), 6749-6756.

Zwicker, B.L. and Agellon, L.B. (2013). Transport and biological activities of bile acids. *Int J Biochem Cell Biol, 45* (7), 1389-1398.